frontiers | Research Topics

Foliar, shoot, stem and rust diseases of trees IUFRO 2022

Edited by
Isabel Alvarez Munck, Julio Javier Diez Casero, Salvatore Moricca, Philippe Tanguay and Pierluigi Bonello

Published in
Frontiers in Forests and Global Change

ISSN 1664-8714
ISBN 978-2-8325-4350-4
DOI 10.3389/978-2-8325-4350-4

About Frontiers

Frontiers is more than just an open access publisher of scholarly articles: it is a pioneering approach to the world of academia, radically improving the way scholarly research is managed. The grand vision of Frontiers is a world where all people have an equal opportunity to seek, share and generate knowledge. Frontiers provides immediate and permanent online open access to all its publications, but this alone is not enough to realize our grand goals.

Frontiers journal series

The Frontiers journal series is a multi-tier and interdisciplinary set of open-access, online journals, promising a paradigm shift from the current review, selection and dissemination processes in academic publishing. All Frontiers journals are driven by researchers for researchers; therefore, they constitute a service to the scholarly community. At the same time, the *Frontiers journal series* operates on a revolutionary invention, the tiered publishing system, initially addressing specific communities of scholars, and gradually climbing up to broader public understanding, thus serving the interests of the lay society, too.

Dedication to quality

Each Frontiers article is a landmark of the highest quality, thanks to genuinely collaborative interactions between authors and review editors, who include some of the world's best academicians. Research must be certified by peers before entering a stream of knowledge that may eventually reach the public - and shape society; therefore, Frontiers only applies the most rigorous and unbiased reviews. Frontiers revolutionizes research publishing by freely delivering the most outstanding research, evaluated with no bias from both the academic and social point of view. By applying the most advanced information technologies, Frontiers is catapulting scholarly publishing into a new generation.

What are Frontiers Research Topics?

Frontiers Research Topics are very popular trademarks of the *Frontiers journals series*: they are collections of at least ten articles, all centered on a particular subject. With their unique mix of varied contributions from Original Research to Review Articles, Frontiers Research Topics unify the most influential researchers, the latest key findings and historical advances in a hot research area.

Find out more on how to host your own Frontiers Research Topic or contribute to one as an author by contacting the Frontiers editorial office: frontiersin.org/about/contact

Foliar, shoot, stem and rust diseases of trees IUFRO 2022

Topic editors

Isabel Alvarez Munck — Forest Health Protection, Forest Service (USDA), United States

Julio Javier Diez Casero — University of Valladolid, Spain

Salvatore Moricca — University of Florence, Italy

Philippe Tanguay — Laurentian Forestry Centre, Natural Resources Canada, Canadian Forest Service, Canada

Pierluigi Bonello — The Ohio State University, United States

Citation

Munck, I. A., Diez Casero, J. J., Moricca, S., Tanguay, P., Bonello, P., eds. (2024). *Foliar, shoot, stem and rust diseases of trees IUFRO 2022*. Lausanne: Frontiers Media SA. doi: 10.3389/978-2-8325-4350-4

Table of contents

frontiers | Frontiers in Forests and Global Change

TYPE Editorial
PUBLISHED 11 January 2024
DOI 10.3389/ffgc.2024.1356533

OPEN ACCESS

EDITED AND REVIEWED BY
Juan A. Martin,
Polytechnic University of Madrid, Spain

*CORRESPONDENCE
Isabel Alvarez Munck
✉ isabel.munck@usda.gov

RECEIVED 15 December 2023
ACCEPTED 03 January 2024
PUBLISHED 11 January 2024

CITATION
Munck IA, Diez-Casero JJ, Moricca S, Tanguay P and Bonello P (2024) Editorial: Foliar, shoot, stem and rust diseases of trees IUFRO 2022.
Front. For. Glob. Change 7:1356533.
doi: 10.3389/ffgc.2024.1356533

Editorial: Foliar, shoot, stem and rust diseases of trees IUFRO 2022

Isabel Alvarez Munck[1]*, Julio Javier Diez-Casero[2], Salvatore Moricca[3], Philippe Tanguay[4] and Pierluigi Bonello[5]

[1]Forest Health Protection, Forest Service (USDA), Durham, NH, United States, [2]Higher Technical School of Agrarian Engineering, University of Valladolid, Palencia, Spain, [3]Department of Agricultural, Food, Environmental, and Forest Sciences and Technologies (DAGRI), Plant Pathology and Entomology Division, University of Florence, Florence, Italy, [4]Laurentian Forestry Centre, Natural Resources Canada, Canadian Forest Service, Quebec, QC, Canada, [5]Department of Plant Pathology, College of Food, Agricultural, and Environmental Sciences, The Ohio State University, Columbus, OH, United States

KEYWORDS

global change, forest health, forest pathology, plant disease, invasive (exotic non-native) species

Editorial on the Research Topic
Foliar, shoot, stem and rust diseases of trees IUFRO 2022

Foliar, shoot, stem and rust diseases can cause devastating damage to their tree hosts through a variety of mechanisms: (1) reduction in photosynthetic capacity, (2) loss of apical dominance leading to stem deformities, (3) lower amounts of soil nutrients and water transported to the crown (wilts) and from the crown to the roots (blights and cankers), and (4) girdling and mechanical failure. Altered precipitation regimes / drought/temperature patterns due to climate change further compound such negative outcomes by often increasing host susceptibility and pathogen virulence.

In this volume, several articles examine several of these diseases with a contemporary as well as global perspective. In Burns et al. we learn that, between 2004 and 2017, the rate of mortality of limber pine (*Pinus flexilis*), surveyed in 106 long-term monitoring plots established in critical high elevation ecosystems in western North America, exceeded the rate of recruitment and growth. They determined that this was due to combined damage by white pine blister rust (WPBR), bark beetles, and climate change. This is important knowledge, because limber pine is a foundational species in those ecosystems. The authors conclude that disease and insect management will be vital to the sustainability of this critical tree species. However, this is easier said than done. As Munck et al. report, management of pests and diseases can be done, but can also be quite challenging. They studied the effects of silvicultural treatments in the eastern U.S. on WPBR, white pine weevil, foliar pathogens and Caliciopsis canker in white pine (*Pinus strobus*) stands, and found that treatments providing partial shading, reduced overstory stem density, and soil scarification to encourage pine regeneration improved the health of residual trees compared to untreated controls. Complete removal of the overstory had the added benefit of creating seral habitat utilized by many songbird species.

WPBR is certainly important, but other pine stem rusts (*Cronartium* and *Peridermium* spp.), *Melampsora* rusts and eucalyptus rust, have also caused economic and ecological losses on continental scales. One more example is provided by the *Melampsora* rust Ramsfield et al. recently reported on laurel

willow (*Salix pentandra*) in Alberta, Canada. The fungus was identified as *Melampsora epitea* and is capable of infecting catkins and stems, in addition to leaves, thus increasing inoculum pressure and potentially affecting regeneration. The authors were able to rapidly identify the species thanks to specimens maintained in a mycological herbarium, highlighting the critical value of such repositories. Anger et al. also report a first rust record, *Melampsoridium asiaticum,* this time on ironwood (*Carpinus caroliniana*) and hophornbeam (*Ostrya virginiana*) in the southeastern Unites States. The authors used morphological and molecular data from field and, once again, herbarium samples to identify the pathogen. The disease is of unknown origin. Because of its recent discovery, the impact of this disease is unknown and merits further monitoring.

In addition to identifying and characterizing novel diseases, this issue also discusses important detection and control strategies. For example, Bourgault et al. developed a DNA-based RPA-CRISPR/Cas12a assay for the detection of *Bretziella fagacearum*, the causal agent of oak wilt. While less sensitive than qPCR, it is specific, field-implementable, and rapid, thus helping democratize and accelerate diagnostics, all invaluable aspects of invasive species management. Meanwhile, Sánchez-Gómez et al. present promising data for the control of pine wood nematode, the causal agent of pine wilt, a disease of global concern. In particular, they demonstrate that the fungal species, *Beauveria* spp. or their mycotoxin, beauvericin, have strong *in vitro* nematicidal effects. Staying with nematodes, McIntire begins to alleviate our lack of knowledge of the physiological effects of *Litylenchus crenatae mccannii* (the causal agent of beech leaf disease - BLD) on American beech (*Fagus grandifolia*). Specifically, this article shows significant relationships between BLD symptom severity and leaf gas exchange and physiological leaf traits that lead to decrease growth, vigor, and long-term survival, all of which will likely compromise the significant ecosystem services provided by diseased American beech.

Pathogens don't act in a vacuum, they are part of a microbial milieu, the phytobiome, which also includes non-pathogenic species, known as endophytes. Endophytes play an important role in disease defense strategies; however, how the plant's health status affects the endophytic communities is not known. Diez-Hermano et al. used metabarcoding to profile the fungal endophytic communities of four declining Mediterranean tree species and found indicator genera that were present only in declining trees. Declining Mediterranean trees are also discussed in Benigno et al., who report known and new harmful fungal and oomycete pathogens that are becoming more aggressive and widespread on *Fraxinus* species (ash) as a likely consequence of climate change, causing tree mortality, loss of natural regeneration and the retreat of some ash species from less favorable sites. This is a stark warning of things to come as climate warming shifts host-parasite interactions in favor of the infectious agent.

Finally, while this Research Topic is all about diseases that affect above ground organs, we cannot forget that trees are unitary systems that are subject to diseases below ground as well, and those can have major effects on how serious above ground diseases can become. Diez-Hermano et al. investigated whether declining tree species in Mediterranean forests were associated with specific rhizosphere fungal communities. They found high overall diversity (674 genera) of fungal species but no evidence of known root pathogens in the declining areas. Paired with the study by Benigno et al., this suggests that, even though the two studies were conducted in different countries, Mediterranean forest decline may be due to a combination of environmental factors and pathogens acting above, rather than below, ground.

Taken together, these articles contribute to many aspects of aboveground tree pathology while advancing our understanding of very critical groups of tree diseases, a body of knowledge that we will need to keep refining as we attempt to deal with an unpredictable world in this age of climate and global changes.

Author contributions

IM: Conceptualization, Writing – original draft, Writing – review & editing. JD-C: Writing – original draft, Writing – review & editing. SM: Writing – original draft, Writing – review & editing. PT: Writing – original draft, Writing – review & editing. PB: Writing – original draft, Writing – review & editing.

Funding

The author(s) declare that no financial support was received for the research, authorship, and/or publication of this article.

Acknowledgments

We are grateful to Foliar, Shoot, Stem and Rust Diseases of Trees IUFRO 2022 participants, organizers and contributors of this Research Topic.

Conflict of interest

The authors declare that the research was conducted in the absence of any commercial or financial relationships that could be construed as a potential conflict of interest.

Publisher's note

frontiers | Frontiers in Forests and Global Change

TYPE Original Research
PUBLISHED 15 December 2022
DOI 10.3389/ffgc.2022.1068135

OPEN ACCESS

EDITED BY
Benoit Marçais,
INRA Centre Nancy-Lorraine, France

REVIEWED BY
Jaime Aguayo,
Agence Nationale de Sécurité Sanitaire de l'Alimentation, de l'Environnement et du Travail (ANSES), France
Luisa Ghelardini,
University of Florence, Italy

*CORRESPONDENCE
Philippe Tanguay
Philippe.Tanguay@nrcan-rncan.gc.ca

†These authors have contributed equally to this work and share first authorship

SPECIALTY SECTION
This article was submitted to Pests, Pathogens and Invasions, a section of the journal Frontiers in Forests and Global Change

RECEIVED 12 October 2022
ACCEPTED 30 November 2022
PUBLISHED 15 December 2022

CITATION
Bourgault É, Gauthier M-K, Potvin A, Stewart D, Chahal K, Sakalidis ML and Tanguay P (2022) Benchmarking a fast and simple on-site detection assay for the oak wilt pathogen *Bretziella fagacearum*. *Front. For. Glob. Change* 5:1068135. doi: 10.3389/ffgc.2022.1068135

Benchmarking a fast and simple on-site detection assay for the oak wilt pathogen *Bretziella fagacearum*

Émilie Bourgault[1†], Marie-Krystel Gauthier[1†], Amélie Potvin[1], Don Stewart[1], Karandeep Chahal[2], Monique L. Sakalidis[2,3] and Philippe Tanguay[1*]

[1]Natural Resources Canada, Canadian Forest Service, Laurentian Forestry Centre, Québec, QC, Canada, [2]Department of Plant, Soil and Microbial Sciences, Michigan State University, East Lansing, MI, United States, [3]Department of Forestry, Michigan State University, East Lansing, MI, United States

Oak wilt is a vascular disease of oak trees caused by the fungus *Bretziella fagacearum*. Once infected, trees may die in a few weeks. Although the disease is currently only found in the United States, it has been reported within just a few hundred meters of the Canada–USA border. To limit the establishment and spread of oak wilt in Canada, the development of an on-site, quick and reliable method to detect *B. fagacearum* is critical. In this study, we developed and validated a new qPCR TaqMan® assay that can detect *B. fagacearum* in a laboratory setting with great specificity and sensitivity. Using this test as a reference, we also developed and validated a new DETECTR assay that can detect *B. fagacearum* under 1 h from a variety of environmental samples, such as mycelium mats and insect vectors, using minimal laboratory equipment. While there are still some limitations to the sensitivity of this assay, we believe that its ease of use, flexibility and accuracy will provide an essential tool in efforts to reduce the spread of oak wilt.

KEYWORDS

DETECTR, molecular detection, oak wilt, *Bretziella fagacearum*, TaqMan® assay

1 Introduction

Oak wilt is a vascular disease of oak trees (*Quercus* spp.) caused by the fungus *Bretziella fagacearum*, previously known as *Ceratocystis fagacearum* (Beer et al., 2017). First described in the 1940's (Henry, 1944; Bretz, 1953), disease symptoms appear after the pathogen enters the sapwood and disrupts the xylem vessels, therefore preventing water and nutrient transport (French and Stienstra, 1980). The affected trees eventually die, sometimes within just a few months of infection. For instance, red oaks (section *Lobatae*) are highly susceptible to the disease and can die in a matter of weeks, forever

altering urban landscapes, plantations, and natural ecosystems (Gibbs and French, 1980).

Dispersion of *B. fagacearum* to healthy trees happens by underground or aboveground transmission. Underground transmission involves the movement of *B. fagacearum* through naturally occurring root grafts and accounts for short distance spread and the creation of expanding oak wilt pockets. The connected xylem vessels of the root grafts allow the fungus to travel from an infected tree to adjacent healthy oaks. Aboveground transmission occurs mainly through spores dissemination *via* insect vectors, mostly by Nitidulidae species (sap beetles) such as *Colopterus truncatus* and *Carpophilus sayi* (Cease and Juzwik, 2001). Sap beetles are attracted to fragrant sporulating fungal mats formed on bark cracks on the trunk of oak wilt killed trees or by mat bearing firewood (Juzwik et al., 2008). They can later transmit spores to wounded healthy trees, up to 600 meters away within a single year (Shelstad et al., 1991).

Currently, oak wilt disease is only found in Texas, midwestern and eastern states in the United States (USDA-Forest Service Northern Research Station, and Forest Health Protection, 2019), where it was potentially introduced many years ago (Juzwik et al., 2008). However, there has been a continuous northward spread of the disease, with an increasing number of infected counties being reported at the Canada–USA border (Jensen-Tracy et al., 2009).

Of the 200 oak species existing in the world, only 10 can be found in Canada, mainly located in Ontario and Eastern Canada (Lacoursière, 2015). They include species from red oaks, white oaks (section *Quercus*) and chestnut oaks (section *Quercus*), all of whom are susceptible to *B. fagacearum* infections to various levels (Gibbs and French, 1980; OWTAC, 2019).

As climate change progresses, insect vectors could possibly carry the fungus across the border and eventually spread to all of Eastern Canada, an area now climatically suitable for *B. fagacearum* and numerous potential vectors. In fact, the climate in southern Ontario has already been found appropriate for *B. fagacearum*, *C. truncatus*, and *C. sayi* (Pedlar et al., 2020). Additionally, despite the regulatory measures already in place, oak wilt could enter Canada through the transportation of contaminated logs (CFIA, 2020). The spread of oak wilt to Canada may lead to large-scale mortality of urban trees, the devastation of natural ecosystems and could cripple the oak log industry, with estimated economic losses of CDN$ 400 million (Pedlar et al., 2020).

Since it is not possible to cure infected trees, management of oak wilt is focused on preventing additional spread and involves the establishment of root graft barriers and trench inserts, removal of potential spore-producing trees, preventive fungicide injections, a ban on firewood transportation between different areas and restricted oak tree wounding activities to certain periods of the year (O'Brien et al., 2000; Wilson, 2001; Koch et al., 2010). The European Union is also tightening its restrictions when trading oak logs with bark from the USA (EFSA et al., 2020). For these efforts to be successful, rapid confirmation of infection is critical.

Diseased trees can tentatively be identified due to wilted leaves and defoliation. Unfortunately, those early symptoms are common among other abiotic and biotic issues, such as oak leaf blister and drought (Natural Resources Canada [NRCAN], 2015; Moore et al., 2022). Therefore, lab-based identification of *B. fagacearum* from symptomatic plant samples is required to confirm oak wilt. The need for a lab confirmation results in delays to the implementation of mitigating measures and increased associated costs. *B. fagacearum* may be present in logs or firewood from oak wilt killed trees, and may also persist in the root system of cut down diseased trees for several years and go unnoticed (Juzwik et al., 2008). The need to develop an on-site, quick and reliable method to detect *B. fagacearum* is now becoming more and more pressing in order to limit the establishment and spread of oak wilt.

Quantitative real-time PCR (qPCR) has become the gold standard in pathogen detection in many fields, including invasive alien tree pathogens, facilitating the detection of infinitesimal amounts of target DNA within a large quantity of environmental material (Heid et al., 1996). However, while qPCR is highly specific and sensitive, it is time-consuming, costly and requires specialized equipment, i.e., real-time PCR machine and technical expertise. Efforts have been made to miniaturize this piece of equipment, and various companies have commercialized portable real-time PCR instruments like the Franklin^{TM} by Biomeme (Biomeme, Philadelphia, PA, USA), facilitating point-of-care detection. In a recent study, the Franklin^{TM} machine, was shown to reliably detect forest pests and pathogens such as *Sphaerulina musiva*, *Phytophthora ramorum*, *Lymantria dispar*, and *Cronartium* sp. in the field (Capron et al., 2020). Other studies have also demonstrated on-site molecular detection using a variety of portable machines and sample types (Brown et al., 2020; Zowawi et al., 2021). These portable machines are robust, allow multiplexing and can also use previously developed lab-validated assays (Capron et al., 2020). However, with a price around US $10 0000, the cost of the portable real-time PCR machine can hamper its deployment.

In recent years, a novel technique called recombinase polymerase amplification (RPA) was developed, which can exponentially amplify a DNA target with a sensitivity, specificity, and a reliability comparable to that of a standard PCR (Piepenburg et al., 2006). The RPA reaction exploits the activity of recombinase proteins that bind to oligonucleotide primers and scan the double stranded DNA for complementary sequence. The recombinase then inserts the primers *via* strand exchange, and a single-strand DNA binding protein binds to the displaced strand to stabilize the loop. A polymerase can then initiate polymerization from the primers if the target sequence is present. Companies like TwistDx have packaged RPA reactions in very convenient lyophilized tubes, making the technology even more accessible (TwistDx, Cambridge, UK). RPA is fast and

works at a constant low temperature, two features making this technology highly desirable for outdoor deployment since the use of a simple thermal block can now be considered. RPA has been used for the rapid detection of viruses (Euler et al., 2012a; Boyle et al., 2013; Yang et al., 2017), bacteria (Euler et al., 2012b; Ahmed et al., 2014) and fungi (Ahmed et al., 2015; Karakkat et al., 2018).

It has recently been shown that RPA can be combined with CRISPR/Cas technologies leading to different detection methods. DNA endonuclease-targeted CRISPR trans reporter (DETECTR) is one of these new detection methods. DETECTR uses RPA enzymes combined with Cas12a enzyme from the clustered regularly interspaced short palindromic repeats (CRISPR) platform (Chen et al., 2018). This innovative detection tool exploits the collateral *trans*-cleavage activity of an activated Cas12a, which will, upon recognition of a dsDNA target sequence, cleave ssDNA non-specifically at multiple random sites. By adding a modified ssDNA reporter in the reaction, a positive signal, i.e., the presence of the original target DNA sequence, can be detected by various methods, such as lateral flow assays or fluorometry (Chen et al., 2018). DETECTR assays have already been used in the detection and/or diagnosis of various pathogens and cancer (Arora et al., 2020; Zhang et al., 2020), most notably for the betacoronavirus severe acute respiratory syndrome (SARS)-CoV-2 (Broughton et al., 2020; Ding et al., 2020; Lucia et al., 2020). Similar assays have also been recently tested, to a lesser extent, on bacterial and viral plant diseases (Luo et al., 2021; Singh et al., 2022).

This study therefore aimed at developing and validating a DETECTR assay targeting the internal transcribed spacer (ITS) gene of *B. fagacearum*. The specificity and sensitivity of this detection test were evaluated and compared to a newly designed qPCR TaqMan® assay for a variety of environmental sample types, namely mycelial mats and insect samples. A panel of participants was also used to optimize the DETECTR assay for on-site deployment. We hope that future implementation of this detection test with phytosanitary inspectors and other end users will effectively limit the spread of oak wilt in Canada and the USA.

2 Materials and methods

2.1 Isolates, DNA extraction and sample preparation

DNA from *B. fagacearum* and closely related species was obtained from a previously published study (Lamarche et al., 2015) and is listed in **Supplementary Table 1**. To confirm the species identity of all samples, the ITS gene, recognized as the universal DNA barcode for fungi (Schoch et al., 2012), was amplified and sequenced. A genus-specific SYBR Green-based qPCR assay (**Table 1**) was designed in a conserved region of the ITS gene to perform an absolute quantification (Rutledge, 2011) of all the strains and to standardize their concentration when necessary.

Fresh cultures of *B. fagacearum* were also isolated from wood tissue of various infected *Quercus* spp. in the Lower Peninsula of Michigan in 2020. Isolates were grown on acidified potato dextrose agar (PDA; Difco™, Sparks, MD, USA) for 2 weeks at room temperature, and hyphal-tip purified. One mL of Lactic acid, 85% (JT Baker, Phillipsburg, NJ, USA) was added into 1L of PDA. Mycelium was then harvested, frozen in liquid nitrogen, and ground with a mortar and pestle. Subsequent DNA extraction followed the protocol described before (Parada-Rojas and Quesada-Ocampo, 2018). All samples were quantified using the SYBR Green assay and are listed in **Supplementary Table 1**.

2.2 Novel target-specific TaqMan®-based real-time PCR assay design

To benchmark the DETECTR assay, we first developed a TaqMan®-based real-time PCR assay. A total of 37 published ITS sequences for *B. fagacearum* and closely related species were aligned (**Supplementary File 2**). A set of primers and a probe were then designed in regions showing *B. fagacearum*-specific nucleotide polymorphisms. All primers were designed using previously described criteria and amplifications were conducted under the conditions described in Lamarche et al. (2015; **Table 1**). Positive (using *B. fagacearum* DNA from pure culture isolate C520, **Supplementary Table 1**) and negative (no DNA template) controls were included in all qPCR runs.

2.3 Novel target-specific DETECTR assay design

The DETECTR assay was performed using RPA to amplify fungal DNA with the TwistAmp Basic Kit (TwistDx, Cambridge, UK), and LbaCas12a (New England Biolabs, MA, USA) for the DETECTR part of the assay. RPA primers (Integrated DNA Technologies Inc., Coralville, IA, USA) were adapted from the TaqMan® qPCR assay following the TwistAmp Basic kit manual and are listed in **Table 1**. Amplification was achieved with a few modifications to the manufacturer's instructions. Briefly, each reaction was prepared using 29.5 μL of TwistAmp Rehydration buffer, 2.75 μL of forward and reverse primers (10 μM) and 10.8 μL of nuclease-free water. The mix was used to resuspend the reaction pellets provided with the TwistAmp Basic kit. Then, 1 μL of DNA template and 3.2 μL of 280 mM magnesium acetate were added in a final volume of 50 μL. Tubes were quickly vortexed and incubated at 37°C for 20 min, followed by inactivation at 65°C for 10 min.

TABLE 1 Primers and probe used for genus-specific qPCR SYBRGreen, species-specific qPCR TaqMan®, and DETECTR assays.

Name	Target gene	Amplicon length (bp)	Sequence (5′ → 3′)	References
Ceratocystis sensu lato				
qPCR SYBR green assay				
Cerat ITS gen F277–301	ITS	120	GCGAAATGCGATAMGTAATGTGAATTG	This study
Cerat Gen ITS R377–397	ITS		CTTGAGTGGTGAAATGACGCT	This study
***B. fagacearum*-specific**				
qPCR TaqMan® assay				
Cfag ITS F 75–97	ITS	168	TAAAACCATTTGTGAACATACCA	This study
Cfag ITS R2 215–43	ITS		TGAAAGTTTTAACTATTTTGTTAAATGCA	This study
Cfag ITS T RC 126–50	ITS		6FAM-AACATCCCCTGAAGAAAGAAGTCC-ZEN	This study
RPA reaction				
Cfag ITS RPA-F1	ITS	170	AACTCTTTAAAACCATTTGTGAACATACCA	This study
Cfag ITS R2 215–43	ITS		TGAAAGTTTTAACTATTTTGTTAAATGCA	This study
DETECTR assay				
Cfag ITS crRNA–2	ITS	—	TGCCAGTAGTATTTACAAACTCTT[a]	This study
FQ-reporter	—	—	/56-FAM/ttatt/3IABkFQ/	Zhang et al., 2020

[a]Targeting sequence of crRNA.

The LbaCas12a (Cas12a from *Lachnospiraceae bacterium ND2006*) *trans*-cleavage assay was performed similarly to those previously described (Chen et al., 2018; Zhang et al., 2020). Cas12a targeting sequence was selected according to the presence of PAM for Lba Cas12a (TTTV) (Zetsche et al., 2015). Guide RNA and ssDNA FQ-reporter are listed in **Table 1** and were designed following recommendations from NEB (New England Biolabs, MA, USA) as well as previous studies (Zetsche et al., 2015; Zhang et al., 2020). Both were ordered from Integrated DNA Technology (IDT Inc., Coralville, IA, USA). To detect the DNA target *via* fluorescence, Cas12a digestion reactions were prepared using 1X NEBuffer 2.1, 50 nM of LbaCas12a, 50 nM guide RNA and 250 nM FQ-reporter in a final volume of 60 μL. The mix was pre-incubated at room temperature for 10 min. Then, 6 μL of unpurified RPA product was added to the reaction and transferred to a 96-well black optical-bottom plate (Thermo Fisher Scientific, MA, USA). Fluorescence was measured at 37°C every 5 min for 1 h (excitation: 485 nm, emission: 535 nm) using the Fluoroskan Ascent plate reader (Labsystems).

2.4 Validating the specificity and sensitivity of the qPCR TaqMan® assay

To validate the specificity of the newly designed qPCR TaqMan® for *B. fagacearum*, we ran the assay in triplicates on 31 *B. fagacearum* strains from pure cultures as well as a panel of closely related species (section "DNA from pure cultures," **Supplementary Table 1**). Closely related species' DNA samples were standardized to approximately 5,000 ITS copies with the SYBR Green assay. Since high DNA concentrations are known to sometimes inhibit amplification, we wanted to ensure that, if samples were not detected, it would be due to the specificity of the assay, and not because of potential inhibition.

In order to evaluate the sensitivity of the qPCR TaqMan® assay, we built standard curves using serial dilutions of *B. fagacearum* ITS synthetic DNA target sequence, and calculated the limit of detection (LOD), which is the smallest amount of target DNA that can be detected 95% of the time with the assay (Bustin et al., 2009). Briefly, 10-fold serial dilutions of *B. fagacearum* ITS copies were made from a gBlocks™ gene fragment (IDT Inc., Coralville, IA, USA) comprising a segment of the *B. fagacearum* ITS sequence, encompassing the two TaqMan® assay primers (**Table 1**) (ref GenBank: KC305152.1). The ITS concentration of each dilution was calculated using the TaqMan® primers and SYBR Green reagents. The qPCR TaqMan® assay was then run in triplicates for each dilution and a standard curve was obtained by plotting the Ct values against the log value of the number of ITS copies. The LOD was determined by running 20 replicates of the smallest dilution of the standard curve giving 3 positive results.

2.5 Efficiency of two DNA extractions methods using the qPCR TaqMan® assay

To assess the efficiency of two DNA extraction methods, standard curves were also built using DNA extracted with 2 protocols from serial dilutions of *B. fagacearum* conidia. A conidial suspension was prepared by growing isolate MIFCC41 on acidified PDA for 2 weeks at room temperature (Chahal et al., 2019). Conidia were harvested by flooding pure cultures with 70% ethanol, followed by two filtrations using a

double layer of Miracloth (Miracloth, EMD Millipore, Billerica, MA, USA). The concentration of conidia in the suspension was determined using a hemocytometer (6.18×10^7 conidia per mL). Conidia were plated onto acidified PDA to confirm their non-viability, sedimented by centrifugation, and then sent to the Tanguay Lab at the Laurentian Forestry Centre, Canada. Conidia were then resuspended in 1 mL of sterile distilled water, disaggregated by repeatedly pushing them through a 24-gauge needle, and counted with a hemocytometer. Concentration was adjusted to 10^E6 conidia per mL, and the stock solution was diluted following a series of 10-fold dilutions in water, down to 1000 conidia per mL. Aliquots of 10 μL from each concentration were dried using a SpeedVac, and then extracted using two different methods. First, to speed-up and facilitate the on-site detection process, samples were immersed in 100 μL of the QuickExtract™ Plant DNA Extraction Solution (Lucigen, WI, USA) and were immediately heated to 65°C for 6 min, followed by 98°C for 2 min. Extracted samples were stored at −20°C until use. As a comparison, we also extracted DNA from the conidia dilutions using the QIAamp DNA micro kit (Qiagen, Valencia, CA, USA) according to the manufacturer's recommendations. The qPCR TaqMan® assay was run in triplicates with both sets of conidia dilutions and standard curves were obtained by plotting the Ct values against the log value of the number of conidia.

2.6 Performance of the DETECTR and TaqMan® qPCR assays on environmental samples

We ran the DETECTR along with the qPCR TaqMan® (in triplicates) on the same samples to see if the source of the material would impact the performance of the assay. The list of all environmental samples, and their origins, used to validate both of our new assays, is shown in **Supplementary Table 1**. DNA from *B. fagacearum* mycelial mat samples, which ranged from development stages 0 to 5 (Chahal et al., 2021) was extracted with 200 μL of QuickExtract™ Plant DNA Extraction Solution (Lucigen, Wisconsin, USA). DNA samples from various insect vectors carrying *B. fagacearum* spores (*Carpophilus sayi*, *Epuraea corticina*, *Glischrochilus sanguinolentus*) were obtained from Lamarche et al. (2015). DNA from other insect samples not carrying *B. fagacearum* spores was also included to ensure the specificity of both tests (Bergeron et al., 2019).

2.7 Adapting DETECTR protocol for on-site deployment

In order to facilitate the on-site deployment of this DETECTR assay, a few modifications were made to simplify its use outside of laboratory settings (**Figure 1**). Most notably, each step of the protocol was carried out in a microtube of a specific color, incubation times were reduced to the minimum and reactions were lyophilized when possible. The DNA extraction step using Lucigen buffer was the same as described above, except that only 100 μL of buffer was prealiquoted in red microtubes. The RPA reaction components (TwistAmp Rehydration buffer, forward and reverse primers, MgOAc and ddH_2O) were aliquoted in green microtubes with the addition of 5% trehalose. Cas12a digestion reactions were assembled in blue microtubes with a few modifications: reactions were prepared in a final volume of 50 μl, FQ-reporter concentration was increased to 500 nM and 5% of trehalose was added. The RPA and Cas12a reactions were lyophilized overnight at −50°C in a FreeZone 2.5 Liter freeze-dryer (Labconco, Kansas City, MO, USA) and stored at −20°C until use.

Just before use, each of the RPA and Cas12a lyophilized reactions tubes were rehydrated with water (approx. 48 μL, or 3 drops) using a 1.5 mL extended fine tip transfer pipette (Samco™ Fine Tip Transfer Pipettes, 231PK, Thermo Fisher Scientific, MA, USA). A small piece of mycelium mat was inserted in red microtubes containing the QuickExtract™ buffer, and samples were then incubated at 65°C for 6 min, followed by 98°C for 2 min in a portable mini16 Thermal cycler (miniPCR Bio, Cambridge, MA, USA). Using the same transfer pipette, the extracted DNA was diluted about 10-fold when transferred to the green microtubes. The entire content of the green microtubes was then used to rehydrate the RPA reaction pellets provided with the TwistAmp Basic Kit (TwistDx, Cambridge, UK). Samples were incubated at 37°C for 10 min without further inactivation. Part of the RPA reactions (approx. 8 μL) was then transferred to the blue microtubes. Samples were incubated at 37°C for 20 min, and fluorescence was visualized with the P51™ Molecular Fluorescence Viewer (miniPCR Bio, Cambridge, MA, USA). Each sample's fluorescence was compared to that of the negative control, which was run along the assay. The complete protocol for the on-site DETECTR assay is illustrated in **Figure 1** and listed in (**Supplementary File 3**).

2.8 Human trial to validate the simplified DETECTR assay

To evaluate the level of difficulty in implementing the DETECTR on-site assay with non-laboratory end users, we organized a trial consisting of 22 volunteers with various backgrounds (from non-scientific to basic/advanced laboratory skills). Each participant was given a detailed version of the on-site protocol to read beforehand (**Supplementary File 3**), from DNA extraction to fluorescence read-out. A demonstration as well as clarifications were offered on the day of the trial. A total of 3 randomized samples (positive fungal mats or negative fungi) as well as a negative (no template) DNA control were given to each volunteer. Participants were told to use the on-site DETECTR assay to detect the presence of *B. fagacearum* in their

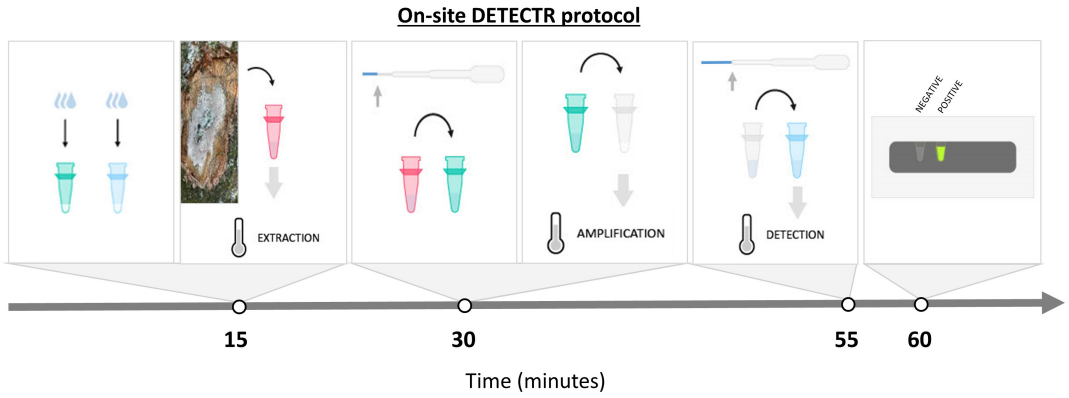

FIGURE 1
Summary of the new and simplified on-site DETECTR assay. Amplification of target DNA by RPA, and detection by *trans*-cleavage release of fluorescence from the ssDNA FQ-reporter following CRISPR/CAS12a recognition of the target DNA. Each step is carried out in a specific colored microtube. All liquid handling is done *via* a simple transfer pipette. Reagents are either stable at room temperature or have been previously lyophilized to facilitate the deployment of the test. The equipment needed to perform the test is minimal and easy to carry into the field. A complete description of the protocol is available in **Supplementary File 3**.

samples. Various parameters were investigated, including time to completion and accuracy of results. Suggested improvements and recommendations from participants were also considered when designing the final written version of the simplified on-site protocol (**Supplementary File 3**).

2.9 Statistical analysis

Analysis was conducted using R (R Core Team, 2014), RStudio (R Studio Team, 2018). The standard curves, that represent the relationships between the outcome (Ct values) and the predictors (either ITS copies or the number of extracted conidia) were evaluated by simple regression using the *lm* function in the R statistical package.

Performance of the DETECTR assay was compared to the qPCR reference by constructing confusion matrices for each type of samples. The python package *pycm* (Haghighi et al., 2018) was used to generate the tables and calculate the accuracy. The statistical comparison was performed using the *mcnemar* function of the *statsmodels* package (Seabold and Perktold, 2010) with default parameters.

3 Results

3.1 Design and validation of a new *B. fagacearum* gold standard qPCR TaqMan® assay

We first designed a new qPCR TaqMan® assay that could specifically detect *B. fagacearum* but also act as a reference for our new molecular DETECTR assay. Using closely related species listed in **Supplementary Table 1** (see section "DNA from pure cultures"), our data shows amplification only for *B. fagacearum* DNA. There was no amplification of any sister species isolates, making this new qPCR TaqMan® assay 100% specific in discriminating *B. fagacearum* among the other closely related species selected here. Of note, some very highly concentrated DNA samples from pure cultures had to be diluted first to be detectable, most probably due to the presence of inhibitors or a DNA concentration too high. Nonetheless, amplification results were proportional to the amount of DNA present in the samples.

We then assessed the sensitivity of the qPCR TaqMan® assay and calculated its LOD. First, we ran the assay in triplicates on serial dilutions of the gBlocks™ ITS gene fragments. The standard curve obtained by plotting the Ct values against the log value of the number of ITS copies shows a square correction coefficient (R^2) of 0.98 and a LOD of 2 ITS copies (**Figure 2A**). The LOD was determined by re-running 20 times the last dilution that gave 3 positive detection results, giving a positive detection 18/20 runs. In all cases, Ct values were proportional to the amount of template DNA used for the qPCR reactions.

3.2 Comparison of DNA extraction methods using the qPCR TaqMan® assay and a previously designed assay

The assay was also run on two series of dilutions of conidia DNA extracted with the QIAamp and Lucigen DNA extraction kits. **Figure 2B** shows the standard curves obtained, with R^2 ranging from 0.93 to 0.95. The difference between the two DNA extraction methods is clearly showed by a 3.4

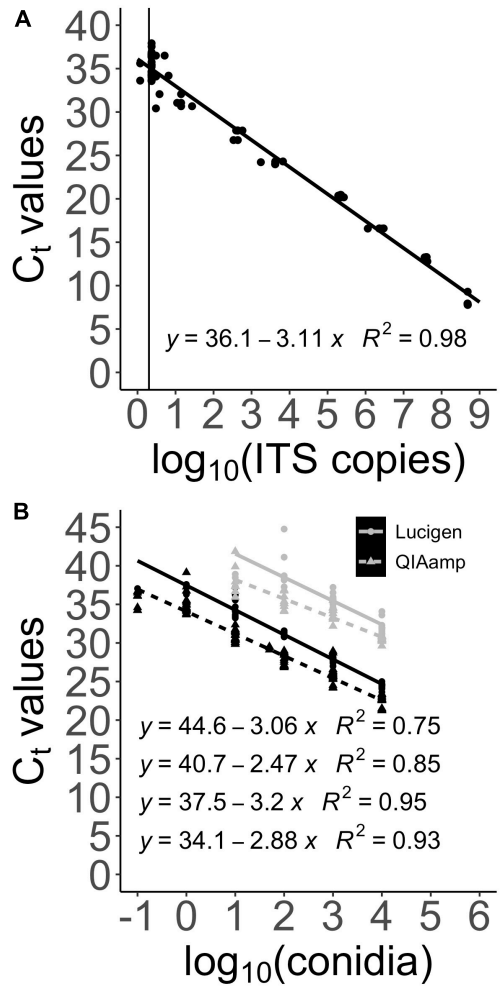

FIGURE 2
Sensitivity of the new qPCR TaqMan® detection test against *B. fagacearum* and comparison of DNA extraction methods. Ct values obtained from running the qPCR TaqMan® assay are plotted against the log value of the number of ITS copies (gBlocks™ gene fragment) and conidia. Equations and coefficients R^2 are displayed on the graphs. **(A)** LOD of the newly designed qPCR TaqMan® assay on ITS copies (gBlocks™ gene fragment) is 2 ITS copies. **(B)** Comparison of the new qPCR TaqMan® detection test (black) and the old qPCR TaqMan® designed in the TEF region (gray) to detect *B. fagacearum* DNA extracted from various amount of conidia using the Lucigen (circle points) and QIAamp (triangle points) procedures.

Ct shift upward with the Lucigen method, making it about 10 times less sensitive than the QIAamp method, but easier to deploy.

In parallel, another goal when designing the *B. fagacearum* ITS qPCR TaqMan® assay was to replace the previous qPCR detection assay that our laboratory had developed and published in 2015 (Lamarche et al., 2015), which, while being specific, lacked in sensitivity. The previous detection assay targeted the transcription elongation factor 1-a (TEF) gene instead of the ITS region. **Figure 2B** shows a comparison between the two detection assays using the two DNA extraction methods above mentioned. As seen clearly on the graph, results confirm that our new *B. fagacearum* qPCR assay allowed us to gain a downshift of 6.6 Ct (with the QIAamp extraction), which corresponds to a 97-fold increase in sensitivity when run on conidia dilutions. This result was expected since TEF is a single copy gene, while the ITS is multi-copy. The increase in sensitivity suggests that the *B. fagacearum* genome possesses about 100 copies of the nuclear ribosomal DNA.

3.3 Design and validation of a new molecular DETECTR assay

The specificity of the DETECTR assay was evaluated with the same sister species isolates used with the qPCR TaqMan® assay (see "DNA from pure cultures," **Supplementary Table 1**). This new molecular test is not meant to be quantitative and therefore only determines if a sample is "positive" or "negative." As for our qPCR TaqMan® assay, the DETECTR test only gave a positive result for *B. fagacearum*, whereas every other closely related species came up negative following a fluorescence reading on a plate reader. The new DETECTR test is therefore 100% specific for *B. fagacearum* according to the panel of species tested.

To estimate the sensitivity of this non-quantitative test, we ran it on various *B. fagacearum* sample types that could be naturally found in the environment, for instance, fungal mats and insect vectors known to carry spores of the pathogen (see samples in **Supplementary Table 1**). We also investigated the conidia dilution set extracted with the Qiagen method, as well as DNA samples from pure cultures (**Supplementary Table 1**). **Figure 3** represents a scatter plot graph comparing the sensitivities of the qPCR TaqMan® and DETECTR assays for all sample types combined. Results show that the DETECTR assay does not span the same detection range as that of the reference qPCR TaqMan® assay. As described by Bustin et al. (2009), sensitivity refers to the minimum number of copies in a sample that can be measured accurately with an assay, and it is typically expressed as the LOD. While we didn't run the DETECTR assay on predefined amounts of copies as we did with the qPCR TaqMan® assay to determine the LOD, plotting all the data from this study as shown in **Figure 3** suggests that the DETECTR test is roughly a 1000 times less sensitive than the qPCR TaqMan® assay. As described above, LOD is only dependant on the target copy number, which we were able to obtain for all types of samples. Sample type and DNA preparation will, however, impact the amount of target copies being present in a sample.

In order to further validate and compare our new DETECTR assay to the qPCR reference, we looked into their respective detection results of these samples. **Supplementary Table 1**

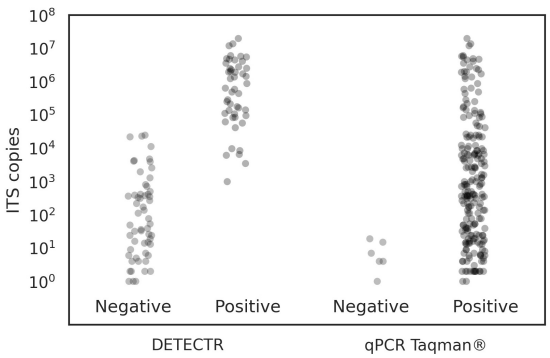

FIGURE 3
Comparison of the qPCR TaqMan® and DETECTR assays sensitivity when detecting various sample types. The scatter plot depicted here suggests that the lower detection limit of the DETECTR test is much higher than that of the qPCR TaqMan®.

shows results obtained with both tests for the same sample, and **Table 2** summarizes the outcome of the comparison using a confusion matrix. Results were exactly the same for both assays when investigating DNA from pure cultures and DNA from insect vectors, with positive and negative results matching perfectly, giving an accuracy of 1 in both circumstances. In a confusion table, the accuracy represents the number of all correct predictions divided by the total number of the dataset. Therefore, the best possible case is an accuracy of 1 and indeed shows here that DETECTR results for pure DNA cultures and insects thoroughly match the qPCR "reference" results. However, while the qPCR TaqMan® assay detected a positive signal for every mycelial mat tested, the DETECTR assay missed 5 of the late-stage samples, therefore giving 5 false-negative results. This slightly lowered the accuracy of the test to 0.84375, but with a negligible difference (McNemar's exact test, $P = 0.0625$). Those mats were also late-stage mats (stages 4A and 5), with the expectation that extracted DNA amount and quality would be lower than fresh mats. SYBR Green quantification of those samples indeed confirmed that very few ITS copies were present. Hence, the DETECTR test can still be considered as a reliable assay when applied to young and fresh mycelial mats.

3.4 Assessing how user friendly the on-site assay is and improving it using a panel of participants

In order to facilitate the deployment of the new DETECTR assay designed here, a few modifications were made to the original protocol, as described in section "2.6 Performance of the DETECTR and TaqMan® qPCR assays on environmental samples." To ensure that every end user with any experience background could handle this novel on-site detection assay, we ran a trial combining 22 participants with or without previous laboratory experience. The average time to completion was 66.6 min, where people with a scientific background fared slightly better regarding the time taken to perform the test. Accuracy of results obtained by these beta participants compared to the qPCR TaqMan® results are shown in the bottom part of the confusion matrix (**Table 2**). The accuracy of the DETECTR assay was calculated at just above 80% when compared to the qPCR reference. However, a total of 12 false-negative and one false-positive results (cross contamination from a manipulation) were recorded, lowering the *P*-value of the McNemar test below 0.05.

The trial was also used to gather feedback from participants in order to make the on-site DETECTR test more user-friendly and easily deployable. Their suggestions and comments strongly shaped the final version of the protocol presented in (**Supplementary File 3**). The factors and challenges most commonly pointed out by the participants were the wording and nomenclature of the protocol (i.e., replace technical terms like "microtube, resuspend, incubation," etc. with non-scientific terms) and the manipulation of the transfer pipette. All participants agreed that performing the protocol a second time would be much easier and that mistakes would most certainly be avoided then.

4 Discussion

In this study, we report a new field detection assay using DETECTR technology that can confirm the presence of *B. fagacearum* on-site within 1 h. We first developed and validated a traditional qPCR TaqMan® assay that could detect specifically *B. fagacearum* and act as a reference when testing the new assay. We then designed and optimized the new DETECTR assay and benchmarked it to our gold standard qPCR TaqMan® assay. In addition, we used a panel of participants from various scientific backgrounds to estimate the ease of deployment of the DETECTR test with different users.

We strongly believe that biosurveillance of invasive forest pests would benefit from on-site DNA testing capability, hence the need to develop deployable, quick and reliable detection tests. Unfortunately, rapid detection is currently hampered by the requirement to send samples to a laboratory for confirmation. With the continued spread of oak wilt in the USA and concern over its introduction into Canada, rapid, on-site detection of *B. fagacearum* is critical.

The qPCR TaqMan® assay developed here is specific to *B. fagacearum,* with no cross-amplification, and is more sensitive than our previously reported assay (Lamarche et al., 2015). Unlike the nested PCR reported by Yang and Juzwik (2017), this assay is quantitative, allowing an estimation of the biomass load of the target species in given samples, and does

TABLE 2 Confusion matrix showing the comparison of both detection tests on various sample types.

Sample type	Number of samples	Confusion matrix		Reference qPCR		Accuracy	McNemar's test *P*-Value
				0	1		
DNA from pure cultures	62	Predicted DETECTR	0	30	0	1	1
			1	0	32		
DNA from insect vectors	40	Predicted DETECTR	0	23	0	1	1
			1	0	17		
Mycelial mat	32	Predicted DETECTR	0	0	5	0.84375	0.0625
			1	0	27		
Beta participants	66	Predicted DETECTR	0	29	12	0.803	0.003418
			1	1	24		

not require a post amplification step to visualize the results. McLaughlin et al. (2022) recently published a very interesting study where Yang's double-nested PCR successfully detected the oak wilt fungus from insects trapped in various locations in New York State, US. However, as mentioned before, this method not only requires sorting the content of the traps beforehand, it also needs more time than our qPCR TaqMan® assay to obtain results. Nonetheless, while this test is highly sensitive and very accurate, it can either be performed in laboratory settings or deployed using expensive and fragile equipment.

The on-site DETECTR assay designed here could detect DNA purified from axenic cultures of *B. fagacearum* with the same specificity as the qPCR TaqMan® assay. We successfully validated the DETECTR assay on environmental samples of mycelial mats, both fresh and older ones, as well as insect vectors. Although the sensitivity of the DETECTR assay was not as good as that of the qPCR TaqMan® test for very old mycelium mats, we still believe it can act as a useful tool to deploy and screen apparent symptoms in the field. Indeed, the current best way to identify *B. fagacearum* on insects is a timely culture-based method requiring 2–4 weeks before *B. fagacearum* can be confirmed. And while confirmation of *B. fagacearum* is straightforward from fresh mats (the only diagnostic sign), it can be difficult from older, decayed mats, also requiring laborious culture work and microscopy. Moreover, since mycelial mats develop once the tree has been killed from a *B. fagacearum* infection, earlier detection in still living plant tissues such as wood and wilted twigs would increase the usefulness of the test and reduce disease spread and tree loss. Work is already underway in our laboratory to assess this possibility.

Additionally, results from insect vectors and serial dilution of spores clearly showed a relationship between spore loads and detection results. We found that target pathogen DNA concentrations that are lower than 10^E4 copies most often yield false negatives detection results when using the DETECTR assay. Efforts to increase the quantity and quality of the DNA extracted might help circumvent this limitation. However, most protocols are lengthy, requiring more time than the Lucigen extraction method used here, and necessitate bulky laboratory equipment, such as a vortex or a centrifuge, which cannot be easily deployed out in the field. A recent study showed that *B. fagacearum* DNA could be detected from oak wilt infected wood chips using a simple alkaline DNA extraction procedure (Moore et al., 2022). The compatibility of other simple and deployable protocols reported for the DNA extraction of pathogens from symptomatic plants (Capron et al., 2020; Paul et al., 2020) with the DETECTR approach developed here is also being tested in our laboratory.

To facilitate the ease and speed of use and reduce costs of the DETECTR test, we simplified the whole process by using color-coded tubes, dehydrated pre-packed reagents, and disposable transfer pipets along with an affordable battery-powered heating block and a simple blue light box (see **Supplementary File 3**). The resulting kit is easily usable in any environment harboring a small flat surface to work on.

The panel of beta participants that had never performed this assay before, the majority of whom lacked laboratory experience, were able to use the kits and correctly identify 80% of samples as either a positive *B. fagacearum* target specimen or as a negative non-target specimen. These results suggest that by providing minimal training to phytosanitary inspectors, they could achieve very accurate on-site detection of the oak wilt pathogen. Previous investigators streamlined detection assays for on-site detection by end users (Capron et al., 2020). However, this study is one of the rare examples where the accuracy of a test is determined with a panel of untrained and inexperienced participants. We found that comments received from the panel improved the assay and the related protocol, mostly by simplifying the wording for non-scientific people and adding a few extra explanations.

Streamlining the assay by reducing the number of steps required would further facilitate the ease of use and time taken, but also potentially increase accuracy (less steps leading to fewer mistakes). Currently, the RPA amplification and Cas12a cleavage of the fluorescent ssDNA probe are being carried sequentially in two different tubes. However, recent publications have successfully combined the reagents of these two reactions into a single tube and performed the two reactions simultaneously (Chen et al., 2020; de Puig et al., 2021). We tested a one-step reaction with pure DNA according to Chen et al. (2020) protocol. In this preliminary work, the fluorescent signal was very weak and required an increased amount of DNA template as well as longer incubation times, which makes this method less suitable for a rapid on-site detection at this time (data not shown).

One major benefit of the DETECTR based detection is the ability to easily design assay components. In fact, in the present paper, primer F1, used for the RPA, consisted of a longer version of the primer used in the TaqMan® assay (primer extended of a few bases in 5′), primer *R*2 was the same for both assays, and the gRNA was straightforwardly designed based on PAM site within the amplified region. Therefore, we believe that relatively little effort would be required to implement DETECTR assays from available TaqMan® assays containing discriminatory nucleotides. This is especially true if primers contain target specific SNPs, and the sequence amplified contains PAM sites with target specific polymorphisms in the 3′ end of the crRNA. On the other hand, and unlike TaqMan® technology, multiplexing multiple assays into one reaction tube is not possible due to the unspecific ssDNA *trans*-nuclease activity of the RNP complex upon binding to the target crRNA site.

In conclusion, we report in this study the development and validation of a new DETECTR assay detecting the presence of *B. fagacearum* in mycelial mats and insect vectors, both common environmental sample types. This reliable and cost-effective test has been optimized to be rapidly deployed on-site. We expect that training front line people such as wood industry workers and phytosanitary inspectors on how to use the DETECTR assay in the field will help prevent the establishment of oak wilt in Canada and reduce its spread in the USA. The qPCR TaqMan® assay designed in parallel is reliable, has a high sensitivity and can confidently be used to confirm results in a laboratory setting.

Data availability statement

The datasets presented in this study can be found in online repositories. The names of the repository/repositories and accession number(s) can be found in the article/**Supplementary material**.

Author contributions

PT, M-KG, and ÉB designed the study. DS performed the bioinformatics analyses. AP, ÉB, and M-KG performed the lab experiments. KC collected the field material. PT and ÉB conducted the statistical analyses. M-KG and PT drafted the initial manuscript with contributions from ÉB, AP, KC, and MS. All authors contributed to the article and approved the submitted version.

Funding

Findings for this project were received through the Natural Resources Canada Expanding Market Opportunities and Pest Risk Management programs. KC was funded through the Michigan Invasive Species Grant Program, Michigan State University Project GREEEN and Forrest Strong endowments. Both KC and MS were supported by HATCH project MICL02505 from the USDA National Institute of Food and Agriculture.

Acknowledgments

We would like to thank all 22 participants of the trial conducted to optimize the on-site DETECTR protocol.

Conflict of interest

The authors declare that the research was conducted in the absence of any commercial or financial relationships that could be construed as a potential conflict of interest.

Publisher's note

Supplementary material

The Supplementary Material for this article can be found online at: https://www.frontiersin.org/articles/10.3389/ffgc.2022.1068135/full#supplementary-material

References

Ahmed, A., Linden van der, H., and Hartskeerl, R. A. (2014). Development of a recombinase polymerase amplification assay for the detection of pathogenic leptospira. *Int. J. Environ. Res.* 11, 4953–4964. doi: 10.3390/ijerph110504953

Ahmed, S. A., Sande, W. W. J., van de, Desnos-Ollivier, M., Fahal, A. H., Mhmoud, N. A., et al. (2015). Application of isothermal amplification techniques for identification of madurella mycetomatis, the prevalent agent of human mycetoma. *J. Clin. Microbiol.* 53, 3280–3285. doi: 10.1128/jcm.01544-15

Arora, R., Gupta, K., Vijaykumar, A., and Krishna, S. (2020). DETECTing merkel cell polyomavirus in merkel tumors. *Front. Mol. Biosci.* 7:10. doi: 10.3389/fmolb.2020.00010

Beer, Z. W., de, Marincowitz, S., Duong, T. A., and Wingfield, M. J. (2017). *Bretziella*, a new genus to accommodate the oak wilt fungus, *Ceratocystis fagacearum* (Microascales, Ascomycota). *Mycokeys* 27, 1–19. doi: 10.3897/mycokeys.27.20657

Bergeron, M.-J., Feau, N., Stewart, D., Tanguay, P., and Hamelin, R. C. (2019). Genome-enhanced detection and identification of fungal pathogens responsible for pine and poplar rust diseases. *PLoS One* 14:e210952. doi: 10.1371/journal.pone.0210952

Boyle, D. S., Lehman, D. A., Lillis, L., Peterson, D., Singhal, M., Armes, N., et al. (2013). Rapid detection of HIV-1 Proviral DNA for early infant diagnosis using recombinase polymerase amplification. *mBio* 4, e135–e113. doi: 10.1128/mbio.00135-13

Bretz, T. W. (1953). Oak wilt, a new threat. *Yearb. Agric.* 1953, 851–855.

Broughton, J. P., Deng, X., Yu, G., Fasching, C. L., Servellita, V., Singh, J., et al. (2020). CRISPR–Cas12-based detection of SARS-CoV-2. *Nat. Biotechnol.* 38, 870–874. doi: 10.1038/s41587-020-0513-4

Brown, A. T., McAloose, D., Calle, P. P., Auer, A., Posautz, A., Slavinski, S., et al. (2020). Development and validation of a portable, point-of-care canine distemper virus qPCR test. *PLoS One* 15:e0232044. doi: 10.1371/journal.pone.0232044

Bustin, S. A., Benes, V., Garson, J. A., Hellemans, J., Huggett, J., Kubista, M., et al. (2009). The MIQE guidelines: Minimum information for publication of quantitative Real-Time PCR experiments. *Clin. Chem.* 55, 611–622. doi: 10.1373/clinchem.2008.112797

Capron, A., Stewart, D., Hrywkiw, K., Allen, K., Feau, N., Bilodeau, G., et al. (2020). In situ processing and efficient environmental detection (iSPEED) of tree pests and pathogens using point-of-use real-time PCR. *PLoS One* 15:e0226863. doi: 10.1371/journal.pone.0226863

Cease, K. R., and Juzwik, J. (2001). Predominant nitidulid species (Coleoptera: Nitidulidae) associated with spring oak wilt mats in Minnesota. *Can. J. For. Res.* 31, 635–643. doi: 10.1139/x00-201

CFIA (2020). *D-99-03: Phytosanitary import requirements to prevent the entry of oak wilt disease (Bretziella fagacearum (Bretz) Hunt) from the Continental United States*. Available online at: https://inspection.canada.ca/plant-health/invasive-species/directives/forest-products/d-99-03/eng/1323852753311/1323852875523 (accessed April 11, 2022).

Chahal, K., Morris, O. R., McCullough, D. G., Cregg, B., and Sakalidis, M. L. (2021). Sporulation timing of the invasive oak wilt fungus, *Bretziella fagacearum* in Michigan, (Abstr.). *Phytopathology* 111:S2.51. doi: 10.1094/PHYTO111-10-S2.1

Chahal, K., Morris, O.,McCullough, D. G., and Sakalidis, M. L. (2019). Biology, epidemiology and detection of oak wilt in Michigan. (Abstr). *Phytopathology* 109:S2.33. doi: 10.1094/PHYTO-109-10-S2.1

Chen, J. S., Ma, E., Harrington, L. B., Costa, M. D., Tian, X., Palefsky, J. M., et al. (2018). CRISPR-Cas12a target binding unleashes indiscriminate single-stranded DNase activity. *Science* 360, 436–439. doi: 10.1126/science.aar6245

Chen, Y., Mei, Y., Zhao, X., and Jiang, X. (2020). Reagents-loaded, automated assay that integrates recombinase-aided amplification and Cas12a nucleic acid detection for a point-of-care test. *Anal. Chem.* 92, 14846–14852. doi: 10.1021/acs.analchem.0c03883

de Puig, H., A., Lee, R., Najjar, D., Tan, X., Soeknsen, L., Angenent-Mari, N., et al. (2021). Minimally instrumented SHERLOCK (miSHERLOCK) for CRISPR-based point-of-care diagnosis of SARS-CoV-2 and emerging variants. *Sci. Adv.* 7:eabh2944.doi: 10.1126/sciadv.abh2944

Ding, X., Yin, K., Li, Z., Lalla, R. V., Ballesteros, E., Sfeir, M. M., et al. (2020). Ultrasensitive and visual detection of SARS-CoV-2 using all-in-one dual CRISPR-Cas12a assay. *Nat. Commun.* 11:4711. doi: 10.1038/s41467-020-18575-6

EFSA, P., On, P. H., Bragard, C., Dehnen-Schmutz, K., Serio, F. D., Jacques, M., et al. (2020). Commodity risk assessment of oak logs with bark from the US for the oak wilt pathogen *Bretziella fagacearum* under an integrated systems approach. *EFSA J.* 18:e06352. doi: 10.2903/j.efsa.2020.6352

Euler, M., Wang, Y., Nentwich, O., Piepenburg, O., Hufert, F. T., and Weidmann, M. (2012a). Recombinase polymerase amplification assay for rapid detection of rift valley fever virus. *J. Clin. Virol.* 54, 308–312. doi: 10.1016/j.jcv.2012.05.006

Euler, M., Wang, Y., Otto, P., Tomaso, H., Escudero, R., Anda, P., et al. (2012b). Recombinase polymerase amplification assay for rapid detection of *Francisella tularensis*. *J. Clin. Microbiol.* 50, 2234–2238. doi: 10.1128/jcm.06504-11

French, D. W., and Stienstra, W. C. (1980). *Oak wilt*. Minneapolis, MN: University of Minnesota.

Gibbs, J. N., and French, D. W. (1980). *The transmission of oak wilt*. St Paul, MN: U.S. Department of Agriculture.

Haghighi, S., Jasemi, M., Hessabi, S., and Zolanvari, A. (2018). PyCM: Multiclass confusion matrix library in Python. *J. Open Source Softw.* 3:729. doi: 10.21105/joss.00729

Heid, C. A., Stevens, J., Livak, K. J., and Williams, P. M. (1996). Real time quantitative PCR. *Genome Res.* 6, 986–994. doi: 10.1101/gr.6.10.986

Henry, B. W. (1944). *Chalara quercina* n. sp., the cause of oak wilt. *Phytopathology* 34, 631–635.

Jensen-Tracy, S., Kenaley, S., Hudler, G., Harrington, T., and Logue, C. (2009). First report of the oak wilt fungus, ceratocystis fagacearum, in New York state. *Plant Dis.* 93, 428–428. doi: 10.1094/pdis-93-4-0428b

Juzwik, J., Harrington, T. C., MacDonald, W. L., and Appel, D. N. (2008). The Origin of *Ceratocystis fagacearum*, the Oak wilt fungus. *Annu. Rev. Phytopathol.* 46, 13–26. doi: 10.1146/annurev.phyto.45.062806.094406

Karakkat, B. B., Hockemeyer, K., Franchett, M., Olson, M., Mullenberg, C., and Koch, P. L. (2018). Detection of root-infecting fungi on cool-season turfgrasses using loop-mediated isothermal amplification and recombinase polymerase amplification. *J. Microbiol. Meth.* 151, 90–98. doi: 10.1016/j.mimet.2018.06.011

Koch, K. A., Quiram, G. L., and Venette, R. C. (2010). A review of oak wilt management: A summary of treatment options and their efficacy. *Urban For. Urban Green.* 9, 1–8. doi: 10.1016/j.ufug.2009.11.004

Lacoursière, E. (2015). *Oak, the Canadian encyclopedia*. Available online at: https://www.thecanadianencyclopedia.ca/en/article/oak (accessed June 15, 2022).

Lamarche, J., Potvin, A., Pelletier, G., Stewart, D., Feau, N., Alayon, D. I. O., et al. (2015). Molecular detection of 10 of the most unwanted alien forest pathogens in Canada using real-time PCR. *PLoS One* 10:e0134265. doi: 10.1371/journal.pone.0134265

Lucia, C., Federico, P.-B., and Alejandra, G. C. (2020). An ultrasensitive, rapid, and portable coronavirus SARS-CoV-2 sequence detection method based on CRISPR-Cas12. *bioRxiv* [Preprint]. doi: 10.1101/2020.02.29.971127

Luo, M., Meng, F.-Z., Tan, Q., Yin, W.-X., and Luo, C.-X. (2021). Recombinase polymerase amplification/Cas12a-Based Identification of *Xanthomonas arboricola* pv. pruni on peach. *Front. Plant Sci.* 12:740177. doi: 10.3389/fpls.2021.740177

McLaughlin, K., Snover-Clift, K., Somers, L., Cancelliere, J., and Cole, R. (2022). Early detection of the oak wilt fungus (*Bretziella fagacearum*) using trapped nitidulid beetle vectors. *For. Pathol.* 52. doi: 10.1111/efp.12767

Moore, M. J., Juzwik, J., Saiapina, O., Ahmed, S., Yang, A., and Abbas, A. (2022). Use of sodium hydroxide DNA extraction methods for nested PCR detection of *Bretziella fagacearum* in the sapwood of Oak Species in Minnesota. *Plant Health Prog.* 23, 132–139. doi: 10.1094/php-03-21-0057-rs

Natural Resources Canada [NRCAN] (2015). *Red oak*. Available online at: https://tidcf.nrcan.gc.ca/en/trees/factsheet/66 (accessed July 21, 2022).

O'Brien, J., Mielke, M., Starkey, D., and Juzwik, J. (2000). *How to identify, prevent and control oak wilt*. St-Paul, MN: USDA Forest Service.

OWTAC (2019). *Oak wilt response framework for Canada*. Available online at: https://inspection.canada.ca/plant-health/invasive-species/plant-diseases/oak-wilt/response-framework/eng/1563898431188/1563898479048 (accessed July 21, 2022).

Parada-Rojas, C. H., and Quesada-Ocampo, L. M. (2018). Analysis of microsatellites from transcriptome sequences of *Phytophthora capsici* and applications for population studies. *Sci. Rep.* 8:5194. doi: 10.1038/s41598-018-23438-8

Paul, R., Ostermann, E., and Wei, Q. (2020). Advances in point-of-care nucleic acid extraction technologies for rapid diagnosis of human and plant

diseases. *Biosens. Bioelectron.* 169, 112592–112592. doi: 10.1016/j.bios.2020.112592

Pedlar, J. H., McKenney, D. W., Hope, E., Reed, S., and Sweeney, J. (2020). Assessing the climate suitability and potential economic impacts of Oak wilt in Canada. *Sci. Rep.* 10:19391. doi: 10.1038/s41598-020-75549-w

Piepenburg, O., Williams, C. H., Stemple, D. L., and Armes, N. A. (2006). DNA detection using recombination proteins. *PLoS Biol.* 4:e204. doi: 10.1371/journal.pbio.0040204

R Core Team (2014). *R: A language and environment for statistical computing*. Vienna: R Core Team.

R Studio Team (2018). *RStudio: Integrated development environment for R*. Boston, MA: R Studio, Inc.

Rutledge, R. G. (2011). A Java program for LRE-based real-time qPCR that enables large-scale absolute quantification. *PLoS One* 6:e17636. doi: 10.1371/journal.pone.0017636

Schoch, C. L., Seifert, K. A., Huhndorf, S., Robert, V., Spouge, J. L., Levesque, C. A., et al. (2012). Nuclear ribosomal internal transcribed spacer (ITS) region as a universal DNA barcode marker for Fungi. *Proc. Natl. Acad. Sci. U.S.A* 109, 6241–6246.

Seabold, S., and Perktold, J. (2010). "Econometric and statistical modeling with Python skipper seabold 1 1," in *Proceedings of the 9th python in science conference*, Austin, TX.

Shelstad, D., Queen, L., French, D., and Fitzpatrick, D. (1991). Describing the spread of Oak Wilt using a geographic information system. *Arboric. J.* 17, 192–199. doi: 10.48044/jauf.1991.047

Singh, M., Bindal, G., Misra, C. S., and Rath, D. (2022). The era of Cas12 and Cas13 CRISPR-based disease diagnosis. *Crit. Rev. Microbiol.* 48, 714–729. doi: 10.1080/1040841x.2021.2025041

USDA-Forest Service Northern Research Station, and Forest Health Protection (2019). *Alien forest pest explorer—Species map*. Available online at: https://www.nrs.fs.fed.us/tools/afpe/maps (accessed April 11, 2022).

Wilson, A. D. (2001). Oak Wilt, a potential threat to southern and western oak forests. *J. For.* 99, 4–11.

Yang, A., and Juzwik, J. (2017). Use of nested and real-time PCR for the detection of ceratocystis fagacearum in the sapwood of diseased oak Species in Minnesota. *Plant Dis.* 101, 480–486. doi: 10.1094/pdis-07-16-0990-re

Yang, Y., Qin, X., Song, Y., Zhang, W., Hu, G., Dou, Y., et al. (2017). Development of real-time and lateral flow strip reverse transcription recombinase polymerase Amplification assays for rapid detection of peste des petits ruminants virus. *Virol. J.* 14:24. doi: 10.1186/s12985-017-0688-6

Zetsche, B., Gootenberg, J. S., Abudayyeh, O. O., Slaymaker, I. M., Makarova, K. S., Essletzbichler, P., et al. (2015). Cpf1 is a single RNA-Guided endonuclease of a class 2 CRISPR-Cas system. *Cell* 163, 759–771. doi: 10.1016/j.cell.2015.09.038

Zhang, Y., Zhang, Y., Zhang, Y., and Xie, K. (2020). Evaluation of CRISPR/Cas12a-based DNA detection for fast pathogen diagnosis and GMO test in rice. *Mol. Breed.* 40, 1–12. doi: 10.1007/s11032-019-1092-2

Zowawi, H. M., Alenazi, T. H., AlOmaim, W. S., Wazzan, A., Alsufayan, A., Hasanain, R. A., et al. (2021). Portable RT-PCR system: A rapid and scalable diagnostic tool for COVID-19 testing. *J. Clin. Microbiol.* 59, e3004–e3020. doi: 10.1128/jcm.03004-20

frontiers | Frontiers in Forests and Global Change

TYPE Original Research
PUBLISHED 22 December 2022
DOI 10.3389/ffgc.2022.1056980

OPEN ACCESS

EDITED BY
Ari Mikko Hietala,
The Norwegian Institute
of Bioeconomy Research (NIBIO),
Norway

REVIEWED BY
Juan A. Martin,
Universidad Politécnica de Madrid,
Spain
Tessa Camenzind,
Freie Universität Berlin, Germany

*CORRESPONDENCE
Julio Javier Diez
✉ JulioJavier.Diez@uva.es
Sergio Diez-Hermano
✉ sergio.diez.hermano@uva.es

SPECIALTY SECTION
This article was submitted to
Pests, Pathogens, and Invasions,
a section of the journal
Frontiers in Forests and Global Change

RECEIVED 29 September 2022
ACCEPTED 06 December 2022
PUBLISHED 22 December 2022

CITATION
Diez-Hermano S, Ahmad F,
Niño-Sanchez J, Benito A, Hidalgo E,
Escudero LM, Morel WA and Diez JJ
(2022) Health condition
and mycobiome diversity
in Mediterranean tree species.
Front. For. Glob. Change 5:1056980.
doi: 10.3389/ffgc.2022.1056980

Health condition and mycobiome diversity in Mediterranean tree species

Sergio Diez-Hermano[1,2]*, Farooq Ahmad[1,2], Jonatan Niño-Sanchez[1,2], Alvaro Benito[1,2], Elena Hidalgo[1,2], Laura Morejón Escudero[2], Wilson Acosta Morel[1,2] and Julio Javier Diez[1,2]*

[1]Sustainable Forest Management Research Institute (iuFOR), University of Valladolid, Palencia, Spain, [2]Department of Plant Production and Forest Resources Higher Technical School of Agricultural Engineering of Palencia (ETSIIAA), University of Valladolid, Palencia, Spain

Introduction: Mediterranean forests are currently facing a surge in abiotic stressors such as droughts and massive fires as a result of climate crisis and human pressure. Susceptibility to biotic stressors has also increased, including a variety of pests and pathogens capable of weakening and potentially killing forest flora. Biodiversity of microbiome protects forests against declines as it increases trees' resilience and adaptability.

Objectives: With the objective of analyzing the relationship between health status and fungal diversity, in the present work the mycobiota of declined and healthy specimens of keystone Mediterranean tree species is described and compared.

Methods: To this end, bark and wood from declining Spanish forests of *Castanea sativa* (chestnut), *Quercus ilex* (holm oak), *Quercus suber* (cork oak), and *Quercus pyrenaica* (pyrenean oak) were sampled and the Internal Transcribed Spacer (ITS1) genomic region was sequenced.

Results: Results showed a predominance of Ascomycota, Basidiomycota, and Mucoromycota in all samples. Alpha diversity at genus level was not affected by health status and was characterized by uneven, poorly distributed fungal communities dominated by a few genera. Differentially abundant (DA) genera between healthy and declined samples were found in chestnut (15), holm oak (6), and pyrenean oak (4) trees, but not in cork oak. Some genera known for their plant protection potential, such as *Trichoderma*, were found exclusively in healthy trees. Functional profiles revealed a predominance of phytopathogens and saprobes in all tree species, irrespective of their health status.

Discussion: This study emphasizes the importance of Mediterranean forests as biodiversity refuges and highlights the value of above-ground tissues as a valid approach to assess shifts in forests' microbiome diversity in response to biotic and abiotic stressors.

KEYWORDS

metabarcoding, biodiversity, forest pathology, *Quercus*, *Castanea*

1 Introduction

Forests are extremely valuable for the ecosystem services they provide. Forests act as biodiversity refuges and serve as important carbon sinks, but are experiencing severe degradation worldwide that threatens their very existence (Trumbore et al., 2015). Forest degradation is usually characterized by destruction of stand structure, dysregulation of functionality, and lowered productivity as a result of damaging human activities (Ghazoul et al., 2015; Vásquez-Grandón et al., 2018). As a result, forest resilience is heavily compromised. Forest decline can be listed as an important factor contributing to forest degradation, and encompasses reduction of growth rate and vigor of individual trees, loss of soil fertility, and ultimately, permanent death of trees (Zhu and Li, 2007).

Several factors contribute to forest decline, making it difficult to pinpoint specific causes. A variety of models of tree mortality have been conceptualized (Houston, 1981; Manion, 1991) and all of them share the idea that forest decline occurs when environmental stress factors interact with various biotic agents in forests at different stages of development. Declining trees often exhibit reduced water transport as a result of reduced radial growth, which creates an imbalance between the water-demanding foliage and the water-providing roots (Manion, 2003). This leads to alterations in carbon balance and systemic homeostasis and ends up increasing tree susceptibility to biotic attacks and other stressors (McDowell et al., 2008; Wang et al., 2012). This physiological disruption, alongside the continuous pressure exerted by human action and climate crisis, triggers a spiral of processes driven by interactions between abiotic and biotic stress factors that predispose, incite and contribute to stand-level decline (Manion, 1991; Amoroso et al., 2017).

Mediterranean forests rank among the terrestrial ecosystems most threatened by climate crisis and loss of biodiversity caused by changes in land use regime (Ochoa-Hueso et al., 2017; Newbold et al., 2020). Meteorological predictions for Iberian and Italian Peninsulas project severe decreases in precipitation, changes in rain patterns and rising temperatures in the following decades, which make the Mediterranean basin particularly prone to long drought periods and large-scale wildfires (Camia and Amatulli, 2009; Batllori et al., 2017; Turco et al., 2017). Post-fire soil is exposed to erosive agents and its recovery might be hindered if other extreme events, such as heavy rainfall, occur within the window of disturbance period (Morán-Ordóñez et al., 2020). Soil in Mediterranean forests is especially vulnerable to this kind of disturbances, as dry summers are followed by rain-intense autumns with 70–80% of the annual precipitation (Shakesby, 2011; Panagos et al., 2015).

Thus, edaphic instability and high frequency of climatic adversities impair the ability of Mediterranean trees to withstand other challenges such as insect pests and fungal diseases, which in turn contribute to the deterioration of tree health status. Inciting factors can also be of biotic origin, such as the *Cerambyx welensii* and *Coraebus undatus* beetles that create tunnels in oak trees and other deciduous species and for which neither preventive nor curative methods exist (Torres-Vila et al., 2013; Tiberi et al., 2016). These stressors not only affect tree health directly but also influence the composition of forest microbiota (Bowd et al., 2022). Compositional changes in the microbiome have a big influence on the severity of diseases affecting the host plant (Wei et al., 2018). Before decline starts, trees with higher microbial diversity pose more resistance against external disturbances. *In vitro* experiments have shown that several microbial communities can decrease the invasion success of pathogens (Jones et al., 2021). Core microbiome assemblies capable of buffering plants from extreme environmental conditions have also been identified (Timm et al., 2018). The relationship between trees and their microbiome is so close that considering them as a holobiont - a 'functional entity formed by a macrobe and its long- and short-term associations with microbes and viruses' (Gordon et al., 2013) - has been proposed as a necessity to combat forest decline (Bettenfeld et al., 2020).

Within plants' microbiome, fungal diversity (mycobiota) is of particular interest in terrestrial ecosystems given that many survival, nutrition, and interaction strategies depend on them. Currently, the international LIFE MycoRestore consortium, focused on Mediterranean forests from Spain, Italy, and Portugal, seeks to utilize mycological biodiversity in order to increase soil and tree health, leading to a greater forest resilience to climate change, drought, forest fires, and pests. However, fungi can also be pathogens responsible for some of the most devastating diseases affecting trees, such as chestnut blight caused by *Cryphonectria parasitica* and ink disease caused by oomycetes of the *Phytophthora* genus. Metabarcoding studies have shown that the diversity and composition of fungal and oomycete soil communities are associated with the severity of symptoms in declining oak dehesas (Ruiz Gómez et al., 2019). In contrast, soil mycobiota of *Castanea sativa* trees affected by *Phytophthora cambivora* have been found to be particularly resilient to the pathogen (Venice et al., 2021). Direct examination of plant material is also of great importance. Root-associated fungi can be affected by pathogens, as shown by the limited diversity of symbiotic ectomycorrhizas found in *Quercus ilex* forests affected by *Phytophthora cinnamomi* (Corcobado et al., 2014). Moreover, analysis of internal tissues of trees allows the study of endophytic fungi, which commonly act as antagonists to pathogens and enhancers of plant immunity response (Busby et al., 2016b; Terhonen et al., 2019). Endophytes can increase tree tolerance to abiotic stressors as well, such as drought (Bae et al., 2009; Khan et al., 2016; Ferus et al., 2019), salinity (Rodriguez et al., 2008), and heat (Redman et al., 2002).

Therefore, the aim of the present work is to shed light on the relationship between diversity of plant mycobiota and health condition of Mediterranean forests, represented by four key species: holm oak, cork oak, and chestnut, that are of great economic importance in Iberian Peninsula ecosystems,

and pyrenean oak, which is endemic to Spain. To this end, wood and bark from healthy and declined specimens was sampled in locations where insect pests and fungal diseases are known to be prevalent. The mycobiota composition was assessed by means of metabarcoding using the ITS1 region of ribosomal DNA.

2 Materials and methods

2.1 Sampling sites and procedure

Bark and wood samples were extracted from healthy and declining trees of *Castanea sativa* (chestnut), *Quercus suber* (cork oak), *Quercus ilex* (holm oak), and *Quercus pyrenaica* (pyrenean oak) from Salamanca (Castile and Leon, Spain) forests (**Table 1** and **Figure 1**). Each site sampled corresponded to a single tree species. Sampling was conducted for all four sites in June and July 2020.

For all sampling sites, declining patches were defined as areas with high percentage of declining trees (presence of canker wounds or stem bleeds, >70% of trees with severe dieback and foliage wilting). Tree diameter was measured at breast height using calipers. Tree height was measured using a Vertex hypsometer. Crown conditions (% mortality and defoliation) were evaluated according to ICP Forests Manual Part IV "Visual Assessment of Crown Condition and Damaging Agents" (Eichhorn et al., 2016). Each sampling site had been previously characterized by the occurrence of a putative biotic stressor (**Table 1**), although sampled trees were not specifically tested for their presence. All selected symptomatic trees were alive at the moment of sampling and had variable although comparable degree of decline. Dead or close-to-death trees were not sampled to ensure that detected fungi belonged to microbial communities present in physiologically active trees. Stands of healthy trees were primarily composed of asymptomatic trees free of dieback or crown transparency.

TABLE 1 Description of sampling sites.

Location	Characteristics	Sampled species	Putative biotic stressor†	Main criteria for decline
La Alamedilla, Spain	Elevation: 756 m Rainfall: 600–854 mm	*Quercus ilex*	*Phytophthora cinnamomi*	Dead trees and exudates
Linares de Riofrío, Spain	Elevation: 956 m Rainfall: 700–900 mm	*Castanea sativa*	*Cryphonectria parasitica*	Dead trees and cankers
Cubo de Don Sancho, Spain	Elevation: 736 m Rainfall: 500–700 mm	*Quercus pyrenaica*	*Cerambyx welensii*	Dead trees, dieback and exit holes
Valdelosa, Spain	Elevation: 842 m Rainfall: 500–700 mm	*Quercus suber*	*Coraebus undatus*	Dieback and crown transparency

†Only well-characterized harmful agents known to be present at sampling sites.

Three plots of healthy trees and three with high degree of decline were selected in each site. Material from five live trees (North orientation) was sampled and pooled per plot. After removing the external bark, one sample was taken per tree from the main trunk at the height of 50 cm over the collar to a depth of 2–3 cm. Only xylem and the internal bark layer (phloem) were considered in the analysis. Six xylem-phloem samples were obtained per tree species (two health conditions × three plots), this totalling 24 samples. Samples were stored at −20°C prior to processing.

2.2 Sample processing

Samples were thawed and washed three times, first with 1 ml of 0.9% NaCl, then with 1 ml of 7% PVP and again with 1 ml of 0.9% NaCl. Following centrifugation for 5 min at 10000 rpm, the supernatant was discarded to remove polyphenols and impurities. Samples were then pulverized by milling during for 5 min at 30 Hz (RETSCH MM 400) with 2 mm tungsten steel beads. DNA was extracted from the wood powder using the EZNA Tissue DNA kit (Omega Bio-tek, Norcross, GA, USA), according to the manufacturer's instructions. The yield and purity of the DNA was measured by Qubit and then stored at −20°C until use.

2.3 Library preparation and sequencing

Samples were sent for molecular analysis to Biome Makers Inc., (West Sacramento, CA, USA). Region 1 of fungal Internal Transcribed Spacer 1 (ITS1) gene was amplified using WineSeq® custom primers according to Patent WO2017096385 (Becares and Fernandez, 2017). After quality control by gel electrophoresis, each library was pooled in equimolar amount and subsequently sequenced on an Illumina MiSeq instrument (Illumina, San Diego, CA, USA) using 2 × 301 paired-end reads. Sequencing data was analyzed through a QIIME-based custom and in-house bioinformatics pipeline (Caporaso et al., 2010; Becares and Fernandez, 2017). Illumina adapters and chimeras were removed (Edgar et al., 2011) and reads were quality-trimmed. ITS1 sequences were clustered into non-singleton operational taxonomic units (OTUs) at a 97% sequence similarity level. Taxonomy assignment and abundance estimation were performed comparing OTUs against UNITE database version 7.2 (Nilsson et al., 2019). Rarefaction curves were used to evaluate the relationship between sequencing depth and the number of OTUs.

2.4 Statistical analysis

Prior to the analysis, taking into consideration that only ITS1 marker was used, OTUs' raw reads were aggregated

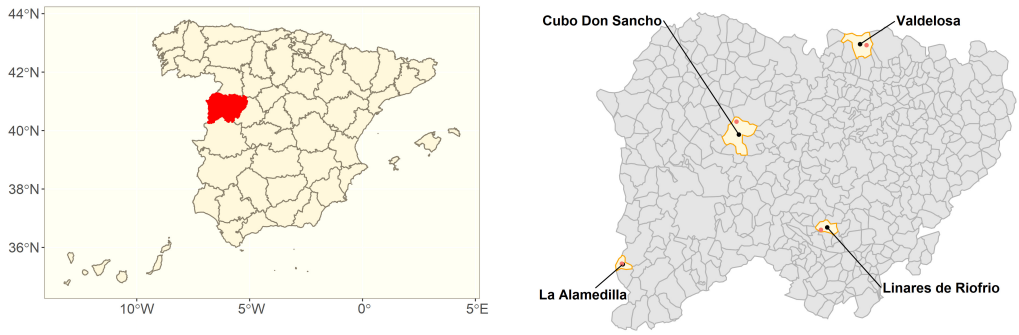

FIGURE 1
Location of sampling sites. **(Left)** Map of Spain's provinces, the sampled Salamanca province is highlighted in red. **(Right)** Close up of Salamanca province. Sampled municipalities are highlighted in yellow. Red dots correspond to sampling sites.

at genus level to have better confidence, and to avoid misidentification of closely-related species (Yang et al., 2018).

Differences in height, diameter, crown mortality, and crown defoliation were assessed using Wilcoxon test (p-value < 0.05 for statistical significance). P-values were adjusted for multiple comparisons by means of Bonferroni correction. Differences between mycobiome communities were evaluated in terms of alpha and beta diversity. Alpha diversity was assessed using Hill diversity indexes according to the equation.

$$D = \left(\sum_{i=1}^{S} p_i (r_i)^l \right)^{1/l}$$

Where D is diversity, S is the number of taxa, p_i is the proportion of all individuals that belong to taxa i, r_i is the rarity of taxa i, defined as $1/p_i$, and l is the exponent that determines the rarity scale and corresponds to richness ($l = 1$) or equivalence-corrected versions of Shannon ($l = 0$) and Simpson indexes ($l = -1$) (Roswell et al., 2021). Differences between health conditions per tree species at $l = [-1, 0, 1]$ were contrasted using Wilcoxon's rank test.

Beta diversity was evaluated in terms of differential abundance taking into account that high-throughput sequencing counts should be considered compositional data (Gloor et al., 2017). Analyses followed anova-like differential expression analysis (ALDEx) technique, which has been shown to produce results very similar to the intersection of multiple independent tools (Soneson and Delorenzi, 2013; Wallen, 2021). Reads were transformed to centered log-ratio (clr) values and per-genus technical variation within each sample was estimated using 1,000 Monte-Carlo instances drawn from the Dirichlet distribution, which returns the posterior probability of observing the counts given the data collected (Fernandes et al., 2013). Effect size was then calculated as the median standardized difference of clr values between groups. A genus was deemed as differentially abundant if the estimated effect was bigger than 1 (absolute value) and the 95% confidence interval (95%CI) didn't include 0.

All fungal genera were included in the functional analysis. Each genus was assigned a functional guild according to the "primary lifestyle" column obtained from FungalTraits database V1.2 (Põlme et al., 2020). Raw read numbers of each guild were summed per tree species and health condition and expressed as $\log_2$ (guild abundance/total abundance).

All analyses were performed in R environment 4.1.3 (R Core Team, 2022). Hill diversity analysis was performed using the package *MeanRarity* (Roswell and Dushoff, 2022). Compositional analysis was performed using the packages *ALDEx2* (Fernandes et al., 2014; Gloor et al., 2016), *CoDaSeq* (Gloor and Reid, 2016), and *zCompositions* (Palarea-Albaladejo and Martin-Fernandez, 2015). Plotting and data cleaning and formatting were performed using the packages *dplyr* (Wickham et al., 2022), *doParallel* (Microsoft Corporation and Weston, 2022), *ggplot2* (Wickham, 2016), *ggplotify* (Guangchuang, 2021), *ggpubr* (Kassambara, 2020), *ggVennDiagram* (Gao, 2021), *openxlsx* (Schauberger and Walker, 2021), and *tidyr* (Wickham and Girlich, 2022).

3 Results

3.1 Characterization of decline

No differences in height and diameter were observed between healthy and declined trees (**Figure 2**). Crown mortality and defoliation were higher in declined samples of cork oak and holm oak, while chestnut showed differences only in crown mortality. Pyrenean oaks showed comparable levels of crown mortality and defoliation regardless of health status.

3.2 Fungal community description

Sequencing after quality control yielded 38,421 (25,817–66,879) reads on average (median and P25–75) and a total

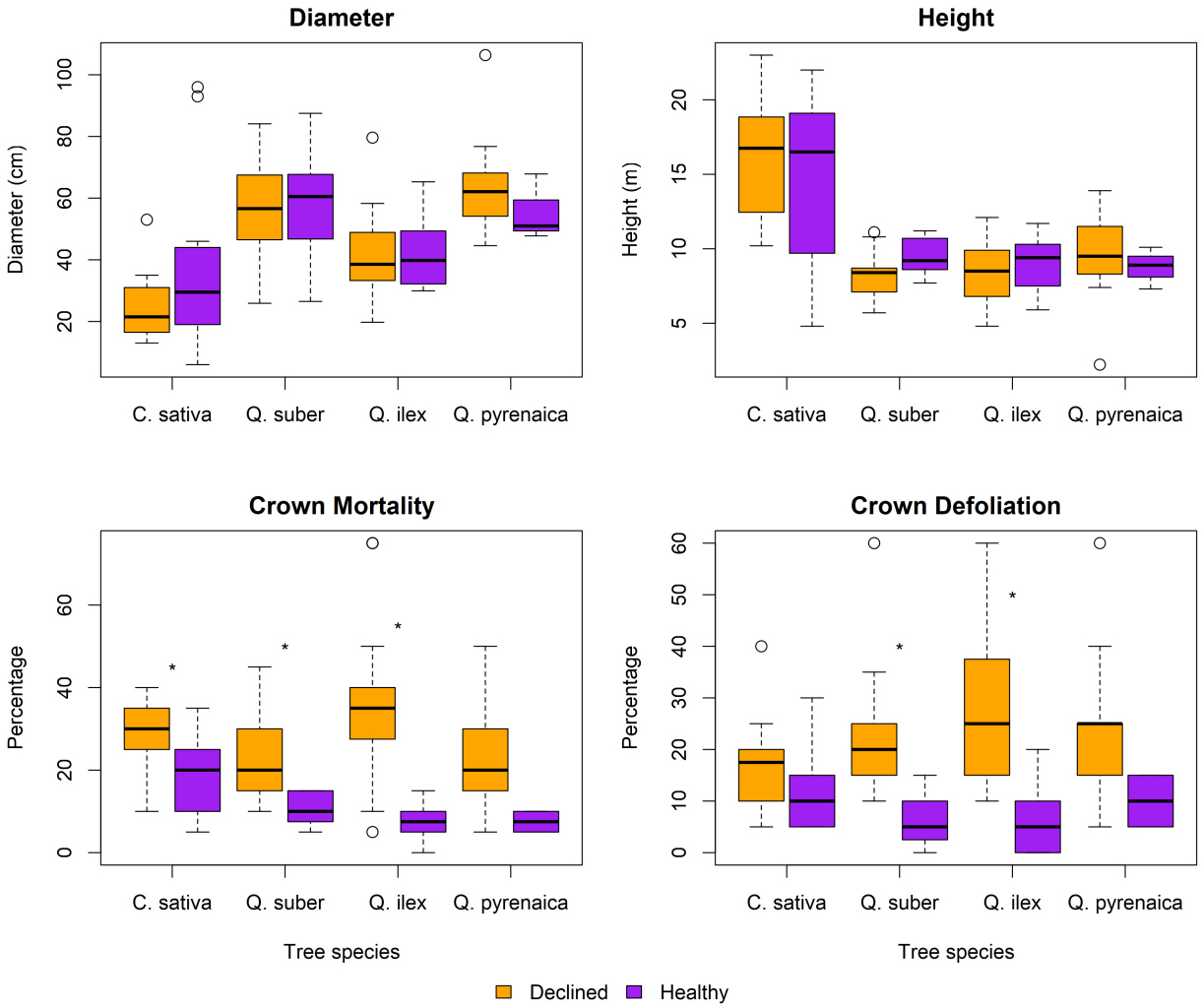

FIGURE 2
Dendrometric measurements. Boxplots correspond to 15 symptomatic and 15 asymptomatic individuals per tree species, later on pooled into 3 replicates of $n = 5$ (per health status) for metabarcoding analysis. Asterisks mark statistically significant differences (Wilcoxon tests, $p < 0.05$ after Bonferroni correction).

of 483 OTUs clustered at genus level (97% similarity) (**Supplementary Tables 1**, **2**). In general, all samples had sufficient reads to capture most of the diversity, as shown by the plateauing rarefaction curves (**Supplementary Figure 1**). The most common phyla corresponded to Ascomycota (~74%), Basidiomycota (~19%), and Mucoromycota (~6%) (**Figure 3**). The same pattern was observed regardless of health condition and ecosystem (**Supplementary Figure 2**).

3.3 Global comparison by health condition

Presence/absence of fungal genera was assessed regardless of tree species as a first approach to find commonalities associated with health status. Some genera were exclusively present in healthy ($n = 8$, ~21.1%) or diseased ($n = 4$, ~10.5%) samples, although most genera were common to both ($n = 26$, ~68.4%) (**Figure 4A**). Dimensionality reduction analysis showed no signs of clustering in terms of health condition or tree species (**Figure 4B**).

3.4 Biodiversity analysis

Effect of health conditions on the biodiversity of fungal communities was assessed separately per tree species. No significant differences were found in terms of alpha diversity (**Figure 5**). On average, healthy and diseased samples had comparable estimators for richness, Hill–Shannon and Hill–Simpson indexes. All samples had uneven, poorly distributed fungal communities and were dominated by a few genera

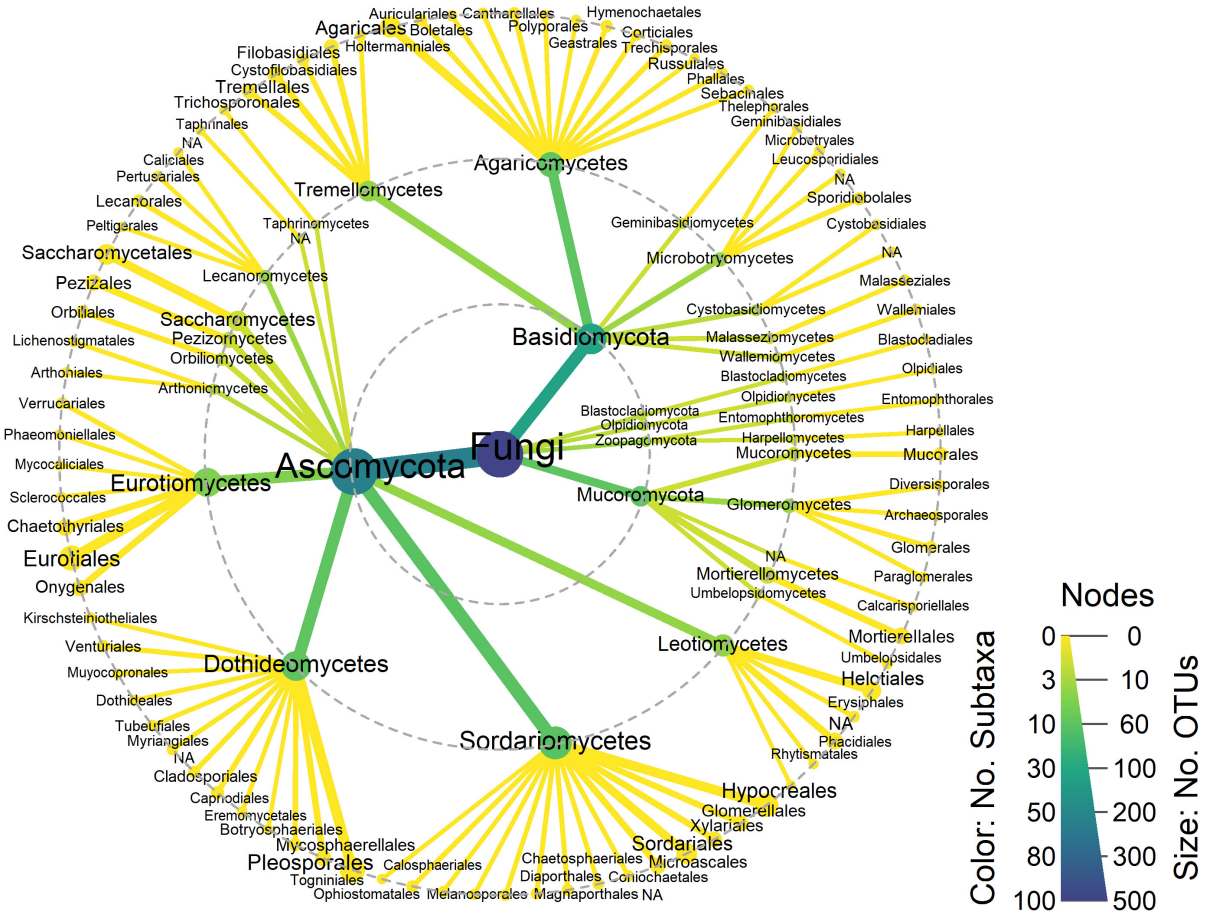

FIGURE 3
Taxonomic heat tree. Node size represents the number of OTUs and color scale represents the number of subtaxa. Dashed gray circles indicate the following taxonomic levels: phylum (inner), class (middle), order (outer). NA, not assigned.

(usually 1 to 3, corresponding with Hill = −1). High variability was found particularly in the richness estimation, as shown by the widening of intervals as Hill's index approaches 1 (with the exception of holm oak samples).

Beta diversity was evaluated in terms of differences in fungal composition using log ratio-transformed values of raw reads. Differentially abundant (DA) genera between healthy and diseased samples were found in chestnut (15), holm oak (6), and pyrenean oak (4) trees, but not in cork oak (Figure 6). Identities of DA genera, alongside the corresponding effect estimator and 95%CI are shown in Figure 7. DA genera were more prominently found in samples from declined trees of chestnut and pyrenean oak, and in samples from healthy trees of holm oak.

3.5 Functional profiles

Assignment of fungal genera to their primary lifestyle was performed per tree species and health status (Figure 8). Although plant pathogens and saprotrophs were the most abundant guilds in all cases, there was no consistent relation with health status. Plant pathogens were more abundant in declined samples of holm oak and healthy samples of chestnut and pyrenean oak, whereas the difference was non-existent in cork oaks. Functional guilds with the biggest differences in abundance per tree species were nectar/tap saprotroph in chestnut, ectomycorrhizas in cork oak, animal parasite in holm oak and wood saprotroph in pyrenean oak. Some guilds couldn't be found in both healthy and declined trees, such as sooty molds (absent from healthy chestnuts, holm oaks and pyrenean oaks, and declined cork oaks), and animal endosymbionts (absent from declined chestnuts, holm oaks and pyrenean oaks, and healthy cork oaks).

4 Discussion

Human action and climate crisis contribute to forest dieback and increase the vulnerability of the surviving plants. That

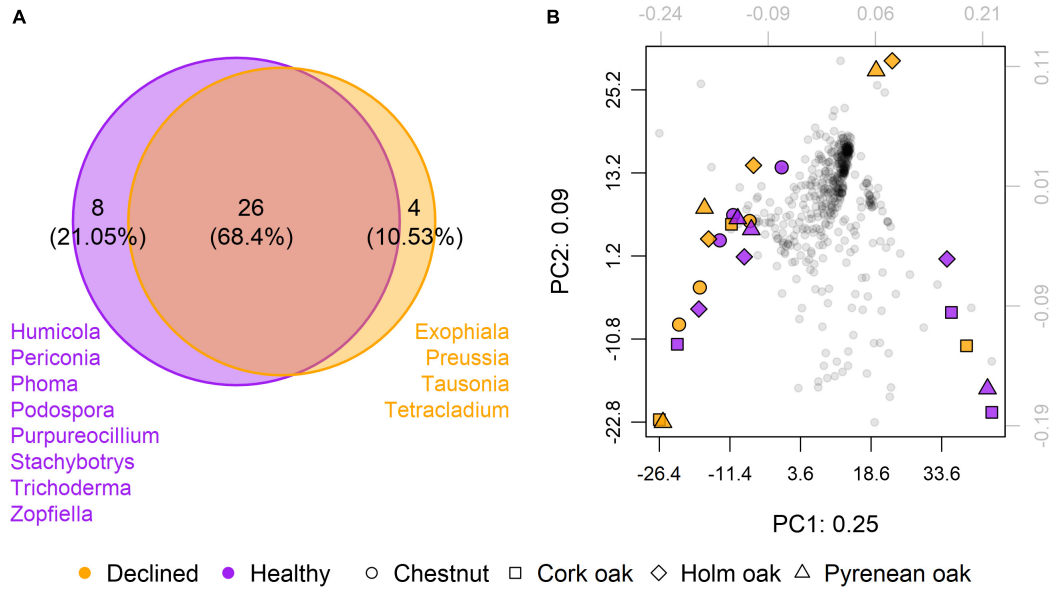

FIGURE 4
Overall effect of health status on mycobiota. **(A)** Venn's diagram showing the number of common and exclusive genera between samples from healthy (n = 12) and diseased (n = 12) trees. Only genera present in at least 10 out of 12 samples per condition are included. **(B)** Principal components analysis (PCA) of presence/absence based on clr-transformed abundances. Gray dots correspond to genera. Colored dots correspond to samples. Total variance explained by the first two dimensions is 35%.

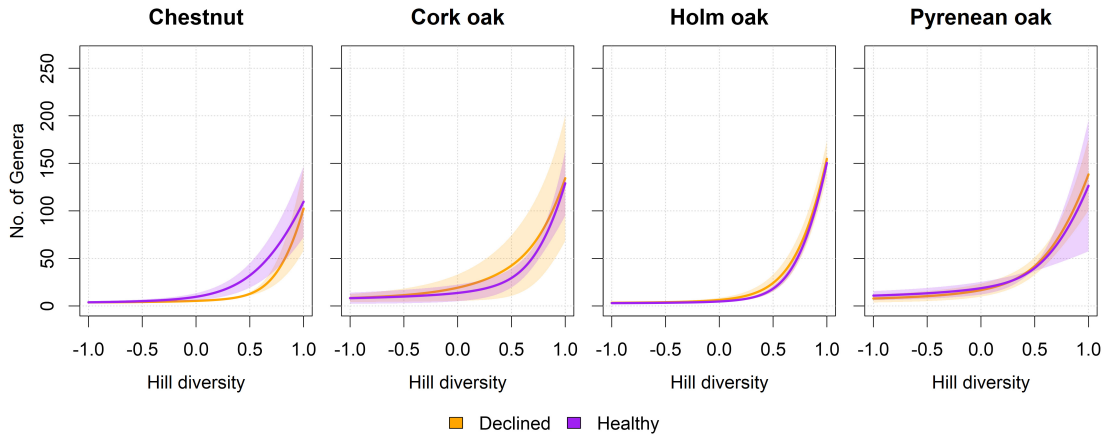

FIGURE 5
Diversity profiles per tree species and health status. Curves represent the average diversity in samples from healthy and declined trees, in terms of an imaginary assemblage with that same diversity, but in which all species are equally abundant (Jost, 2006; Roswell et al., 2021). The horizontal axis represents the exponent l of Hill diversity, which can be interpreted as equivalence-corrected versions for richness (l = 1), Shannon (l = 0), and Simpson (l = −1) diversity estimators. Shadowed intervals correspond to standard error. No significant differences were found at l = [1, 0, −1] (Wilcoxon test, n = 3 per tree species and health condition, $p > 0.05$). Raw curves prior to averaging can be found in **Supplementary Figure 3**.

way forests are led into a spiral of decline in which trees are weakened and become susceptible to other abiotic and biotic stressors, which ultimately places the health and existence of the whole ecosystem at risk. Mycobiota of trees affected by recent wildfires show increases in genetic diversity and shifts in community structure and taxonomic composition (Huang et al., 2016). Imbalances in microbiome diversity have been related to severity of decline, as essential functions of the holobiont might not be guaranteed, reducing its fitness (Moricca et al., 2012; Bettenfeld et al., 2020; Lyu et al., 2021). Therefore, biodiversity acts as a buffer that makes forests more resilient, minimizing the damages caused by disturbances.

However, a majority of metabarcoding studies focus on commercial crops and soil composition, making the studies on

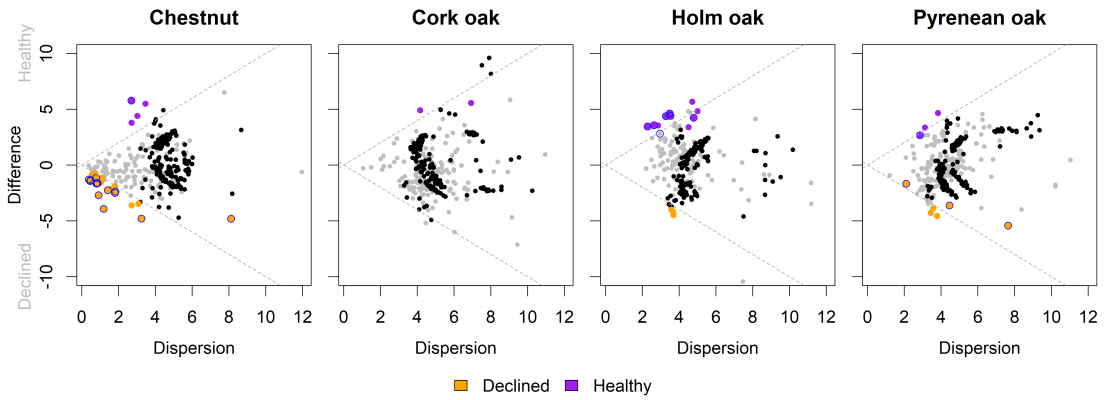

FIGURE 6
Effect plot of ALDEx differential abundance comparisons. Colored dots represent genera with effect size >1 (purple if more abundant in samples from healthy trees and orange if more abundant in samples from declined trees); blue outline indicates differential abundance (zero not included in 95% CI); rare (clr-transformed abundance < 0) non significant genera are shown in black and abundant (clr-transformed abundance > 0) in grey, as represented in the Bland–Altmann plots in **Supplementary Figure 4**. Dotted gray lines show the effect = 1 isopleth. Vertical and horizontal axes represent Median Log_2 transformations of abundances' difference (between samples variability) and dispersion (within samples variability), respectively.

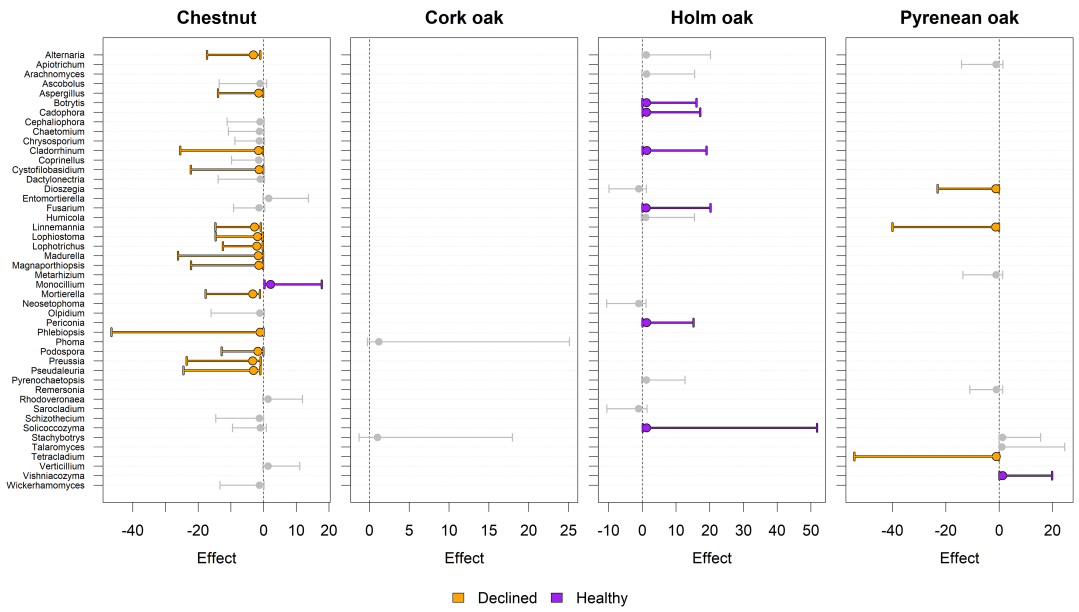

FIGURE 7
Differentially abundant (DA) genera detected by ALDEx analysis. Effect size point estimators and 95%CI are shown. Vertical gray lines indicate no effect. Colored dots and intervals indicate differential abundance (zero line not crossed) for a given tree species. Only genera with effect >1 (absolute value) in at least one tree species are shown to facilitate visual comparisons. Absence of a genus in a plot indicates that its effect was <1 (absolute value). Positive effect size favors healthy status and vice versa. Size of confidence intervals can be interpreted as a proxy of the effect size estimation robustness (the smaller the better).

tree health in forest ecosystems very scarce. Even fewer studies have dealt with above-ground microbiota and its composition in tissues from declined and healthy trees. For example, it has been shown that foliar fungi can decrease disease severity in *Populus trichocarpa* and make the host more resistant against the rust disease (Busby et al., 2016a). In addition, to the best of our knowledge, only a handful of studies have attempted to characterize the microbiota of ecosystems as sensitive to climate change as Mediterranean forests are (Lasa et al., 2019; Maghnia et al., 2019; Ruiz Gómez et al., 2019; Venice et al., 2021; Gómez-Aparicio et al., 2022). These studies, however, only focused on a single tree species or pathosystem, i.e., *Quercus suber* (Maghnia et al., 2019; Gómez-Aparicio et al., 2022), *Quercus pyrenaica* (Lasa et al., 2019), *Quercus ilex* (Ruiz Gómez et al., 2019), and

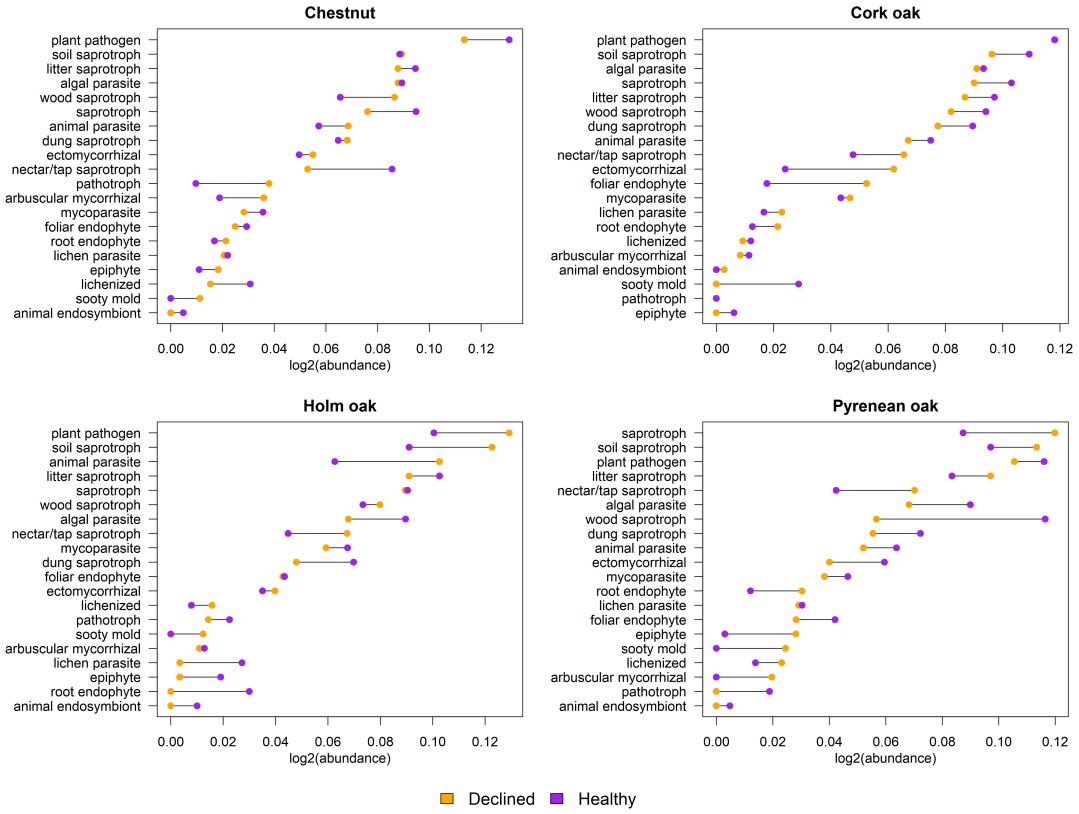

FIGURE 8
Comparison of functional guilds between declined and healthy samples. Horizontal axis represents sum of abundances expressed as $\log_2$ (guild abundance/total abundance). Connecting lines between two dots correspond to the difference between declined and healthy samples.

Castanea sativa (Venice et al., 2021), and none of them dealt with above-ground tissues. Thus, the present work supplements prior studies by describing mycobiota in above-ground tissues of declined and healthy trees, belonging to key species in Mediterranean ecosystems in Spain.

In our study no significant differences between the alpha diversity of declined and healthy trees were found. Contrary to this result, more diverse fungal communities have been found in needles and sapwood of declining *Picea abies* and *Pinus sylvestris* trees, respectively, as compared to tissues from healthy specimens (Giordano et al., 2009; Millberg et al., 2015). Opposite effect was found in ficus trees where a brown root rot fungus decreased their microbial diversity (Liu et al., 2022). Water stress can also reduce diversity of endophytic mycobiota in cork oak (Linaldeddu et al., 2011). Nonetheless, in some cases the correlation between alpha diversity and plant health status has been found to be weak or non-existent as well (Lebreton et al., 2019; Solís-García et al., 2021; Romeralo et al., 2022).

Some genera were only found in either declined or healthy samples and could be identified as indicator genera. The number of indicator genera was slightly higher in healthy trees than in declined trees, as found in other studies (Hossain et al., 2021). On the one hand, regarding genera exclusive to healthy samples, *Phoma* and *Periconia* are known to have a plant-pathogenic lifestyle. Other genera are considered to be primarily saprotrophic, such as *Stachybotrys*, *Humicola*, *Zopfiella*, and *Podospora*. Parasitic genera such as *Trichoderma* (mycoparasite) and *Purpureocillium* (animal parasite) were also only found in healthy samples and have been linked to improved in plant health and resilience (Gong et al., 2017; Dutta et al., 2022). On the other hand, genera exclusive to declined samples were saprotrophs (*Tetracladium, Preussia, Tausonia*) or animal parasites (*Exophiala*), although none of them have been described as detrimental to plant health so far.

Within the genera present in both declined and healthy plants, many were differentially abundant, with few genera having significant differences. The chestnut ecosystem had the highest amount of differentially abundant genera. The healthy chestnuts had 4 differentially abundant genera; one of them, *Monocillium*, was significantly different compared to declined chestnuts and is known for having a saprotrophic lifestyle, with some species being nematode parasites (Ashrafi et al., 2017). Some genera that were more abundant in declined chestnuts also have a saprotrophic lifestyle (*Cystofilobasidium, Cladorrhinum, Lophiostoma, Lophotrichus*), and a few are well known as plant pathogens. For example, *Alternaria* and *Aspergillus* have several

species that are either obligate or facultative pathogens. In cork oak, no significant differences were found between declined and healthy plants, neither in the alpha diversity nor in the differential abundance. In other host species, fewer genera were differentially abundant according to health condition.

Functional profiles revealed a predominance of genera with pathogenic and saprobic primary lifestyles in all tree species. This is in line with previous studies that showed high percentage of endophytes with pathogenic potential in twigs from declining *Quercus* species (Ragazzi et al., 2003). It has been long hypothesized that weak pathogens that have an endophytic state as part of their life cycle might play a role in the rapid decline of stressed oak trees (Petrini and Fisher, 1990; Kehr and Wulf, 1993; Ragazzi et al., 1995). Environmental adversities such as drought can induce switches in the lifestyle of an endophyte from neutral to pathogenic (Gonthier et al., 2006; Moricca and Ragazzi, 2008; Porras-Alfaro and Bayman, 2011). Type and abundance of functional guilds are also coincidental with recent studies performed on soil mycobiota of declining dehesas (Ruiz Gómez et al., 2019). This may be indicative of an increased trafficking of soil-borne fungi to above-ground tissues, taking into account that stressed trees show higher colonization frequencies in comparison to healthy trees (Ragazzi et al., 2003). However, differences in abundance of functional guilds according to health status were not uniform among tree species. It should also be noted that fungi might have different lifestyles when inhabiting tree wood than when observed in soil, which would add to the variability caused by host species and by the different abiotic stressors affecting each sampling site more severely.

There are some limitations to the present work that should be taken into consideration when interpreting the results. First, the study was performed after extracting total DNA and hence it is not possible to check if the microbial communities detected were living or dead. Pathogens are not likely to affect non-active or dead communities present in the ecosystems, and therefore, an RNA sequencing study (for example, studying rRNA instead of rRNA genes) could help to understand how pathogens affect active communities. Second, lack of samples from other latitudes and environmental conditions make it difficult to consider the potential environmental and demographic effects on mycobiomes. It remains to be explored how a combination of biotic and abiotic stress could affect the mycobiome composition. Moreover, although the ITS regions of ribosomal DNA are considered useful DNA barcodes for fungi, in some genera, such as Fusarium, these regions are very conserved across species, complicating OTU identification at species level. We tried to avoid this problem by using data up to the genus level to have better confidence. In turn, this hinders inferences about the functional roles of fungi based on their primary lifestyle because different species within a genus can have very different roles. Nonetheless, the same species can change its role depending on the host, making *in silico* predictions of functional guilds noisy at any taxonomic resolution level. Moreover, databases still offer partial collections of functional traits, rendering functional analysis incomplete at best. Finally, comparison between different ecosystems should be taken with caution, given the limited sample size.

As a conclusion, in this work we show the resilience of above-ground fungal mycobiota in four tree species located in declining Mediterranean forests. Our study indicates that beta diversity but not alpha diversity of fungal communities was significantly affected by health status of the host trees. Some indicator genera that were only present in either diseased or healthy plants were also identified. These genera could be valuable for assessing the plant's health status and could be used as predictors of the onset of declines.

Data availability statement

Data and scripts used in this study are available in the following GitHub repository: https://github.com/serbiodh/2022_FrontiersForests. Raw sequencing data are available at NCBI SRA under BioProject PRJNA885270.

Author contributions

AB and LE collected the data. SD-H and FA analyzed the data. SD-H, FA, JN-S, EH, WM, and JD designed the sampling and wrote the manuscript. All authors contributed to the article and approved the submitted version.

Funding

This work was supported by LIFE project MycoRestore "Innovative use of mycological resources for resilient and productive Mediterranean forests threatened by climate change, LIFE18 CCA/ES/001110", and projects PID2019-110459RB-I00 and PLEC2021-008076 funded by MICINN (Spain) as well as the project VA208P20 funded by JCYL (Spain), both co-financed by FEDER (UE) budget. JN-S was also supported by the European Union's Horizon Europe Research and Innovation Programme under the MSCA agreement No. 101068728.

Acknowledgments

The data analysis has been carried out using the resources from "Centro de Supercomputación de Castilla y León" (SCAYLE) under the valuable technical support of Carmen Calvo and Jesús Lorenzana. We would also like to thank the reviewers for their insightful comments and suggestions, which have helped improving not only the clarity of the manuscript, but also our understanding of the results presented here.

Conflict of interest

The authors declare that the research was conducted in the absence of any commercial or financial relationships that could be construed as a potential conflict of interest.

Publisher's note

All claims expressed in this article are solely those of the authors and do not necessarily represent those of their affiliated organizations, or those of the publisher, the editors and the reviewers. Any product that may be evaluated in this article, or claim that may be made by its manufacturer, is not guaranteed or endorsed by the publisher.

Supplementary material

The Supplementary Material for this article can be found online at: https://www.frontiersin.org/articles/10.3389/ffgc.2022.1056980/full#supplementary-material

References

Amoroso, M. M., Rodríguez-Catón, M., Villalba, R., and Daniels, L. D. (2017). "Forest decline in Northern Patagonia: the role of climatic variability," in *Dendroecology. Ecological Studies*, Vol. 231, eds M. Amoroso, L. Daniels, P. Baker, and J. Camarero (Cham: Springer).

Ashrafi, S., Stadler, M., Dababat, A. A., Richert-Pöggeler, K. R., Finckh, M. R., and Maier, W. (2017). *Monocillium gamsii* sp. nov. and *Monocillium bulbillosum*: two nematode-associated fungi parasitising the eggs of *Heterodera filipjevi*. *MycoKeys* 27, 21–38. doi: 10.3897/mycokeys.27.21254

Bae, H., Sicher, R. C., Kim, M. S., Kim, S. H., Strem, M. D., Melnick, R. L., et al. (2009). The beneficial endophyte *Trichoderma hamatum* isolate DIS 219b promotes growth and delays the onset of the drought response in *Theobroma cacao*. *J. Exp. Bot.* 60, 3279–3295. doi: 10.1093/jxb/erp165

Batllori, E., De Cáceres, M., Brotons, L., Ackerly, D. D., Moritz, M. A., and Lloret, F. (2017). Cumulative effects of fire and drought in Mediterranean ecosystems. *Ecosphere* 8:e01906. doi: 10.1002/ecs2.1906

Becares, A. A., and Fernandez, A. F. (2017). *Microbiome Based Identification, Monitoring and Enhancement of Fermentation Processes and Products*. French Patents: WO2017096385A1. West Sacramento, CA: Biome Makers Inc.

Bettenfeld, P., Fontaine, F., Trouvelot, S., Fernandez, O., and Courty, P. E. (2020). Woody plant declines. What's wrong with the microbiome? *Trends Plant Sci.* 25, 381–394. doi: 10.1016/j.tplants.2019.12.024

Bowd, E. J., Banks, S. C., Bissett, A., May, T. W., and Lindenmayer, D. B. (2022). Disturbance alters the forest soil microbiome. *Mol. Ecol.* 31, 419–447. doi: 10.1111/mec.16242

Busby, P. E., Peay, K. G., and Newcombe, G. (2016a). Common foliar fungi of Populus trichocarpa modify Melampsora rust disease severity. *New Phytol.* 209, 1681–1692. doi: 10.1111/nph.13742

Busby, P. E., Ridout, M., and Newcombe, G. (2016b). Fungal endophytes: modifiers of plant disease. *Plant Mol. Biol.* 90, 645–655. doi: 10.1007/s11103-015-0412-0

Camia, A., and Amatulli, G. (2009). "Weather factors and fire danger in the mediterranean," in *Earth Observation of Wildland Fires in Mediterranean Ecosystems*, ed. E. Chuvieco (Berlin: Springer).

Caporaso, J. G., Kuczynski, J., Stombaugh, J., Bittinger, K., Bushman, F. D., Costello, E. K., et al. (2010). QIIME allows analysis of high-throughput community sequencing data. *Nat. Methods* 7, 335–336. doi: 10.1038/nmeth.f.303

Corcobado, T., Vivas, M., Moreno, G., and Solla, A. (2014). Ectomycorrhizal symbiosis in declining and non-declining *Quercus ilex* trees infected with or free of *Phytophthora cinnamomi*. *For. Ecol. Manag.* 324, 72–80. doi: 10.1016/j.foreco.2014.03.040

Dutta, P., Deb, L., and Pandey, A. K. (2022). Trichoderma-From lab bench to field application: looking back over 50 years. *Front. Agron.* 91:932839. doi: 10.3389/fagro.2022.932839

Edgar, R. C., Haas, B. J., Clemente, J. C., Quince, C., and Knight, R. (2011). UCHIME improves sensitivity and speed of chimera detection. *Bioinformatics* 27, 2194–2200. doi: 10.1093/bioinformatics/btr381

Eichhorn, J., Roskams, P., Potočić, N., Timmermann, V., Ferretti, M., Mues, V., et al. (2016). "Part IV: visual assessment of crown condition and damaging agents," in *Manual on Methods and Criteria for Harmonized Sampling, Assessment, Monitoring and Analysis of the Effects of Air Pollution on Forests*, ed. UNECE ICP Forests Programme Coordinating Centre (Eberswalde: Thünen Institute of Forest Ecosystems).

Fernandes, D. A., Macklaim, J. M., Linn, T. G., Reid, G., and Gloor, G. B. (2013). ANOVA-like differential expression (ALDEx) analysis for mixed population RNA-Seq. *PLoS One* 8:e67019. doi: 10.1371/journal.pone.0067019

Fernandes, D. A., Reid, J., Macklaim, M. J., McMurrough, T. A., Edgell, D. R., and Gloor, B. G. (2014). Unifying the analysis of high-throughput sequencing datasets: characterizing RNA-seq, 16S rRNA gene sequencing and selective growth experiments by compositional data analysis. *Microbiome* 2:15. doi: 10.1186/2049-2618-2-15

Ferus, P., Barta, M., and Konôpková, J. (2019). Endophytic fungus Beauveria bassiana can enhance drought tolerance in red oak seedlings. *Trees* 33, 1179–1186. doi: 10.1007/s00468-019-01854-1

Gao, C. H. (2021). *ggVennDiagram: A 'ggplot2' Implement of Venn Diagram. R package version 1.2.0*.

Ghazoul, J., Burivalova, Z., Garcia-Ulloa, J., and King, L. A. (2015). Conceptualizing forest degradation. *Trends Ecol. Evol.* 30, 622–632. doi: 10.1016/j.tree.2015.08.001

Giordano, L., Gonthier, P., Varese, G. C., Miserere, L., and Nicolotti, G. (2009). Mycobiota inhabiting sapwood of healthy and declining Scots pine (*Pinus sylvestris* L.) trees in the Alps. *Fungal Divers.* 38:e83.

Gloor, B. G., and Reid, G. (2016). Compositional analysis: a valid approach to analyze microbiome high-throughput sequencing data. *Can. J. Microbiol.* 26, 322–329. doi: 10.1139/cjm-2015-0821

Gloor, G. B., Macklaim, J. M., and Fernandes, A. D. (2016). Displaying variation in large datasets: a visual summary of effect sizes. *J. Comput. Graph. Stat.* 25, 971–979. doi: 10.1080/10618600.2015.1131161

Gloor, G. B., Macklaim, J. M., Pawlowsky-Glahn, V., and Egozcue, J. J. (2017). Microbiome datasets are compositional: and this is not optional. *Front. Microbiol.* 8:2224. doi: 10.3389/fmicb.2017.02224

Gómez-Aparicio, L., Domínguez-Begines, J., Villa-Sanabria, E., García, L. V., and Muñoz-Pajares, A. J. (2022). Tree decline and mortality following pathogen invasion alters the diversity, composition and network structure of the soil microbiome. *Soil Biol. Biochem.* 166:108560. doi: 10.1016/j.soilbio.2022.108560

Gong, B., Liu, G., Liao, R., Song, J., and Zhang, H. (2017). Endophytic fungus *Purpureocillium* sp. A5 protect mangrove plant *Kandelia candel* under copper stress. *Brazil. J. Microbiol.* 48, 530–536. doi: 10.1016/j.bjm.2016.10.027

Gonthier, P., Gennaro, M., and Nicolotti, G. (2006). Effects of water stress on the endophytic mycota of *Quercus robur*. *Fungal Divers.* 21:e80.

Gordon, J., Knowlton, N., Relman, D. A., Rohwer, F., and Youle, M. (2013). Superorganisms and holobionts. *Microbe.* 8, 152–153. doi: 10.1128/microbe.8.152.1

Guangchuang, Y. (2021). *ggplotify: Convert Plot to 'grob' or 'ggplot' Object. R package version 0.1.0*.

Hossain, Z., Hubbard, M., Gan, Y., and Bainard, L. D. (2021). Root rot alters the root-associated microbiome of field pea in commercial crop production systems. *Plant Soil* 460, 593–607. doi: 10.1007/s11104-020-04779-8

Houston, D. R. (1981). *Stress Triggered Tree Diseases: The Diebacks and Declines*. Washington, DC: US Department of Agriculture, Forest Service.

Huang, Y. L., Devan, M. M., U'Ren, J. M., Furr, S. H., and Arnold, A. E. (2016). Pervasive effects of wildfire on foliar endophyte communities in montane forest trees. *Microb. Ecol.* 71, 452–468. doi: 10.1007/s00248-015-0664-x

Jones, M. L., Rivett, D. W., Pascual-García, A., and Bell, T. (2021). Relationships between community composition, productivity and invasion resistance in semi-natural bacterial microcosms. *eLife* 10:e71811. doi: 10.7554/eLife.71811.sa2

Jost, L. (2006). Entropy and diversity. *Oikos* 113:2. doi: 10.1111/j.2006.0030-1299.14714.x

Kassambara, A. (2020). *ggpubr: 'ggplot2' Based Publication Ready Plots. R package version 0.4.0*.

Kehr, R. D., and Wulf, A. (1993). Fungi associated with above-ground portions of declining oaks (*Quercus robur*) in Germany. *Eur. J. For. Pathol.* 23, 18–27. doi: 10.1111/j.1439-0329.1993.tb00803.x

Khan, Z., Rho, H., Firrincieli, A., Hung, S. H., Luna, V., Masciarelli, O., et al. (2016). Growth enhancement and drought tolerance of hybrid poplar upon inoculation with endophyte consortia. *Curr. Plant Biol.* 6, 38–47. doi: 10.1016/j.cpb.2016.08.001

Lasa, A. V., Fernández-González, A. J., Villadas, P. J., Toro, N., and Fernández-López, M. (2019). Metabarcoding reveals that rhizospheric microbiota of *Quercus pyrenaica* is composed by a relatively small number of bacterial taxa highly abundant. *Sci. Rep.* 9, 1–13. doi: 10.1038/s41598-018-38123-z

Lebreton, L., Guillerm-Erckelboudt, A. Y., Gazengel, K., Linglin, J., Ourry, M., Glory, P., et al. (2019). Temporal dynamics of bacterial and fungal communities during the infection of *Brassica rapa* roots by the protist *Plasmodiophora brassicae*. *PLoS One* 14:e0204195. doi: 10.1371/journal.pone.0204195

Linaldeddu, B. T., Sirca, C., Spano, D., and Franceschini, A. (2011). Variation of endophytic cork oak-associated fungal communities in relation to plant health and water stress. *For. Pathol.* 41, 193–201. doi: 10.1111/j.1439-0329.2010.00652.x

Liu, T. Y., Chen, C. H., Yang, Y. L., Tsai, I. J., Ho, Y. N., and Chung, C. L. (2022). The brown root rot fungus *Phellinus noxius* affects microbial communities in different root-associated niches of Ficus trees. *Environ. Microbiol.* 24, 276–297. doi: 10.1111/1462-2920.15862

Lyu, D., Zajonc, J., Pagé, A., Tanney, C. A. S., Shah, A., Monjezi, N., et al. (2021). Plant holobiont theory: the phytomicrobiome plays a central role in evolution and success. *Microorganisms* 9:675. doi: 10.3390/microorganisms9040675

Maghnia, F. Z., Abbas, Y., Mahé, F., Prin, Y., El Ghachtouli, N., Duponnois, R., et al. (2019). The rhizosphere microbiome: a key component of sustainable cork oak forests in trouble. *For. Ecol. Manag.* 434, 29–39. doi: 10.1016/j.foreco.2018.12.002

Manion, P. D. (1991). *Tree Disease Concepts*. Englewood Cliffs, NJ: Prentice Hall.

Manion, P. D. (2003). Evolution of concepts in forest pathology. *Phytopathology* 93, 1052–1055. doi: 10.1094/PHYTO.2003.93.8.1052

McDowell, N., Pockman, W. T., Allen, C. D., Breshears, D. D., Cobb, N., Kolb, T., et al. (2008). Mechanisms of plant survival and mortality during drought: why do some plants survive while others succumb to drought? *New Phytol.* 178, 719–739. doi: 10.1111/j.1469-8137.2008.02436.x

Microsoft Corporation, and Weston, S. (2022). *doParallel: Foreach Parallel Adaptor for the 'parallel' Package. R package version 1.0.17*.

Millberg, H., Boberg, J., and Stenlid, J. (2015). Changes in fungal community of Scots pine (*Pinus sylvestris*) needles along a latitudinal gradient in Sweden. *Fung. Ecol.* 17, 126–139. doi: 10.1016/j.funeco.2015.05.012

Morán-Ordóñez, A., Duane, A., Gil-Tena, A., De Cáceres, M., Aquilué, N., Guerra, C. A., et al. (2020). Future impact of climate extremes in the Mediterranean: soil erosion projections when fire and extreme rainfall meet. *Land Degradat. Dev.* 31, 3040–3054. doi: 10.1002/ldr.3694

Moricca, S., Ginetti, B., and Ragazzi, A. (2012). Species-and organ-specificity in endophytes colonizing healthy and declining Mediterranean oaks. *Phytopathol. Mediterranea* 51, 587–598.

Moricca, S., and Ragazzi, A. (2008). Fungal endophytes in Mediterranean oak forests: a lesson from *Discula quercina*. *Phytopathology* 98, 380–386. doi: 10.1094/PHYTO-98-4-0380

Newbold, T., Oppenheimer, P., Etard, A., and Williams, J. J. (2020). Tropical and Mediterranean biodiversity is disproportionately sensitive to land-use and climate change. *Nat. Ecol. Evol.* 4, 1630–1638. doi: 10.1038/s41559-020-01303-0

Nilsson, R. H., Larsson, K. H., Taylor, A. F. S., Bengtsson-Palme, J., Jeppesen, T. S., Schigel, D., et al. (2019). The UNITE database for molecular identification of fungi: handling dark taxa and parallel taxonomic classifications. *Nucleic Acids Res.* 47, D259–D264. doi: 10.1093/nar/gky1022

Ochoa-Hueso, R., Munzi, S., Alonso, R., Arróniz-Crespo, M., Avila, A., Bermejo, V., et al. (2017). Ecological impacts of atmospheric pollution and interactions with climate change in terrestrial ecosystems of the Mediterranean Basin: current research and future directions. *Environ. Pollut.* 227, 194–206. doi: 10.1016/j.envpol.2017.04.062

Palarea-Albaladejo, J., and Martin-Fernandez, J. A. (2015). zCompositions-R package for multivariate imputation of left-censored data under a compositional approach. *Chemom. Intell. Lab. Syst.* 143, 85–96. doi: 10.1016/j.chemolab.2015.02.019

Panagos, P., Ballabio, C., Borrelli, P., Meusburger, K., Klik, A., Rousseva, S., et al. (2015). Rainfall erosivity in Europe. *Sci. Total Environ.* 511, 801–814. doi: 10.1016/j.scitotenv.2015.01.008

Petrini, O., and Fisher, P. J. (1990). Occurrence of fungal endophytes in twigs of *Salix fragilis* and *Quercus robur*. *Mycol. Res.* 94, 1077–1080. doi: 10.1016/S0953-7562(09)81336-1

Põlme, S., Abarenkov, K., Henrik Nilsson, R., Lindahl, B. D., Clemmensen, K. E., Kauserud, H., et al. (2020). FungalTraits: a user-friendly traits database of fungi and fungus-like stramenopiles. *Fung. Divers.* 105, 1–16. doi: 10.1007/s13225-020-00466-2

Porras-Alfaro, A., and Bayman, P. (2011). Hidden fungi, emergent properties: endophytes and microbiomes. *Annu. Rev. Phytopathol.* 49, 291–315. doi: 10.1146/annurev-phyto-080508-081831

R Core Team (2022). *R: A Language and Environment for Statistical Computing*. Vienna: R Foundation for Statistical Computing.

Ragazzi, A., Moricca, S., Capretti, P., Dellavalle, I., and Turco, E. (2003). Differences in composition of endophytic mycobiota in twigs and leaves of healthy and declining *Quercus* species in Italy. *For. Pathol.* 33, 31–38. doi: 10.1046/j.1439-0329.2003.3062003.x

Ragazzi, A., Vagniluca, S., Moricca, S., and Vigniluca, S. (1995). European expansion of oak decline: involved microrganisms and methodological approaches. *Phytopathol. Mediterranea* 34, 207–226.

Redman, R. S., Sheehan, K. B., Stout, R. G., Rodriguez, R. J., and Henson, J. M. (2002). Thermotolerance generated by plant/fungal symbiosis. *Science* 298, 1581–1581. doi: 10.1126/science.1078055

Rodriguez, R. J., Henson, J., Van Volkenburgh, E., Hoy, M., Wright, L., Beckwith, F., et al. (2008). Stress tolerance in plants via habitat-adapted symbiosis. *ISME J.* 2, 404–416. doi: 10.1038/ismej.2007.106

Romeralo, C., Martín-García, J., Martínez-Álvarez, P., Muñoz-Adalia, E. J., Gonçalves, D. R., Torres, E., et al. (2022). Pine species determine fungal microbiome composition in a common garden experiment. *Fung. Ecol.* 56:101137. doi: 10.1016/j.funeco.2021.101137

Roswell, M., and Dushoff, J. (2022). *MeanRarity: Hill Diversity Estimation and Visualisation R package version 0.0.1.0004*.

Roswell, M., Dushoff, J., and Winfree, R. (2021). A conceptual guide to measuring species diversity. *Oikos* 130, 321–338. doi: 10.1111/oik.07202

Ruiz Gómez, F. J., Navarro-Cerrillo, R. M., Pérez-de-Luque, A., Oβwald, W., Vannini, A., and Morales-Rodríguez, C. (2019). Assessment of functional and structural changes of soil fungal and oomycete communities in holm oak declined dehesas through metabarcoding analysis. *Sci. Rep.* 9, 1–16. doi: 10.1038/s41598-019-41804-y

Schauberger, P., and Walker, A. (2021). *Openxlsx: Read, Write and Edit xlsx Files. R package version 4.2.5*.

Shakesby, R. A. (2011). Post-wildfire soil erosion in the Mediterranean: review and future research directions. *Earth Sci. Rev.* 105, 71–100. doi: 10.1016/j.earscirev.2011.01.001

Solís-García, I. A., Ceballos-Luna, O., Cortazar-Murillo, E. M., Desgarennes, D., Garay-Serrano, E., Patiño-Conde, V., et al. (2021). Phytophthora root rot modifies the composition of the avocado rhizosphere microbiome and increases the abundance of opportunistic fungal pathogens. *Front. Microbiol.* 11:574110. doi: 10.3389/fmicb.2020.574110

Soneson, C., and Delorenzi, M. (2013). A comparison of methods for differential expression analysis of RNA-seq Data. *BMC Bioinform.* 14:91. doi: 10.1186/1471-2105-14-91

Terhonen, E., Blumenstein, K., Kovalchuk, A., and Asiegbu, F. O. (2019). Forest tree microbiomes and associated fungal endophytes: functional roles and impact on forest health. *Forests* 10:42. doi: 10.3390/f10010042

Tiberi, R., Branco, M., Bracalini, M., Croci, F., and Panzavolta, T. (2016). Cork oak pests: a review of insect damage and management. *Ann. For. Sci.* 73, 219–232. doi: 10.1007/s13595-015-0534-1

Timm, C. M., Carter, K. R., Carrell, A. A., Jun, S. R., Jawdy, S. S., Vélez, J. M., et al. (2018). Abiotic stresses shift belowground Populus-associated bacteria toward a core stress microbiome. *mSystems* 3:e00070-17. doi: 10.1128/mSystems.00070-17

Torres-Vila, L. M., Sánchez-González, Á, Merino-Martínez, J., Ponce-Escudero, F., Conejo-Rodríguez, Y., Martín-Vertedor, D., et al. (2013). Mark–recapture of *Cerambyx welensii* in dehesa woodlands: dispersal behaviour, population density, and mass trapping efficiency with low trap densities. *Entomol. Exp. Appl.* 149, 273–281. doi: 10.1111/eea.12133

Trumbore, S., Brando, P., and Hartmann, H. (2015). Forest health and global change. *Science* 349, 814–818. doi: 10.1126/science.aac6759

Turco, M., von Hardenberg, J., AghaKouchak, A., Llasat, M. C., Provenzale, A., and Trigo, R. M. (2017). On the key role of droughts in the dynamics of summer fires in Mediterranean Europe. *Sci. Rep.* 7, 1–10. doi: 10.1038/s41598-017-00116-9

Vásquez-Grandón, A., Donoso, P. J., and Gerding, V. (2018). Forest degradation: when is a forest degraded? *Forests* 9:726. doi: 10.3390/f9110726

Venice, F., Vizzini, A., Frascella, A., Emiliani, G., Danti, R., Della Rocca, G., et al. (2021). Localized reshaping of the fungal community in response to a forest fungal pathogen reveals resilience of Mediterranean mycobiota. *Sci. Total Environ.* 800:149582. doi: 10.1016/j.scitotenv.2021.149582

Wallen, Z. D. (2021). Comparison study of differential abundance testing methods using two large Parkinson disease gut microbiome datasets derived from 16S amplicon sequencing. *BMC Bioinform.* 22:265. doi: 10.1186/s12859-021-04193-6

Wang, W., Peng, C., Kneeshaw, D. D., Larocque, G. R., and Luo, Z. (2012). Drought-induced tree mortality: Ecological consequences, causes, and modeling. *Environ. Rev.* 20, 109–121. doi: 10.1139/a2012-004

Wei, Z., Hu, J., Yin, S., Xu, Y., Jousset, A., Shen, Q., et al. (2018). Ralstonia solanacearum pathogen disrupts bacterial rhizosphere microbiome during an invasion. *Soil Biol. Biochem.* 118, 8–17. doi: 10.1016/j.soilbio.2017.11.012

Wickham, H. (2016). *ggplot2: Elegant Graphics for Data Analysis*. New York, NY: Springer-Verlag.

Wickham, H., François, R., Henry, L., and Müller, K. (2022). *dplyr: A Grammar of Data Manipulation. R Package Version 1.0.9*.

Wickham, H., and Girlich, M. (2022). *tidyr: Tidy Messy Data. R Package Version 1.2.0*.

Yang, R. H., Su, J. H., Shang, J. J., Wu, Y. Y., Li, Y., Bao, D. P., et al. (2018). Evaluation of the ribosomal DNA internal transcribed spacer (ITS), specifically ITS1 and ITS2, for the analysis of fungal diversity by deep sequencing. *PLoS One* 13:e0206428. doi: 10.1371/journal.pone.0206428

Zhu, J. J., and Li, F. Q. (2007). Forest degradation/decline: research and practice. *J. Appl. Ecol.* 18, 1601–1609.

frontiers | Frontiers in Forests and Global Change

TYPE Original Research
PUBLISHED 28 March 2023
DOI 10.3389/ffgc.2023.1146742

OPEN ACCESS

EDITED BY
Philippe Tanguay,
Laurentian Forestry Centre, Natural Resources Canada, Canadian Forest Service, Canada

REVIEWED BY
Raiza Castillo,
University of Florida, United States
Carrie J. Fearer,
University of New Hampshire, United States

*CORRESPONDENCE
Cameron D. McIntire
✉ cameron.mcintire@usda.gov

SPECIALTY SECTION
This article was submitted to Pests, Pathogens and Invasions, a section of the journal Frontiers in Forests and Global Change

RECEIVED 17 January 2023
ACCEPTED 28 February 2023
PUBLISHED 28 March 2023

CITATION
McIntire CD (2023) Physiological impacts of beech leaf disease across a gradient of symptom severity among understory American beech.
Front. For. Glob. Change 6:1146742.
doi: 10.3389/ffgc.2023.1146742

Physiological impacts of beech leaf disease across a gradient of symptom severity among understory American beech

Cameron D. McIntire*

Forest Health Protection, USDA Forest Service, Durham, NH, United States

Beech leaf disease (BLD) damage is associated with the parasitic nematode *Litylenchus crenatae* ssp. *mccannii*. Foliar symptoms manifest as darkened or chlorotic galls in the interveinal portions in the leaf, which become leathery and crinkled under high severity of infection. Though nearly a decade has passed since the discovery of this disease, little is known regarding the impact of BLD on leaf function and physiology. This study assesses the variation in leaf gas exchange and physiological leaf traits among asymptomatic and BLD-infected leaves across a gradient of symptom severity within a natural forested stand in central Connecticut, USA. Leaves with BLD symptoms are found to have significantly reduced carbon assimilation and instantaneous water use efficiency, with increased levels of stomatal conductance as symptom severity progresses. Leaf response to light manipulation is also affected, with an increase in dark respiration and the light compensation point among banded and crinkled leaves. Additionally, BLD symptoms are found to have a significant influence on leaf water content, specific leaf area, and leaf nitrogen content. Relationships between gas exchange and these leaf traits yield linear correlations that are used to infer functional relationships impacted by the disease.

KEYWORDS

tree physiology, forest pathology, beech leaf disease, plant parasitic nematodes, leaf gas exchange, leaf traits, *Fagus grandifolia*, *Litylenchus crenatae mccannii*

Introduction

Beech leaf disease (BLD) is an emerging threat to native American beech (*Fagus grandifolia* L.) of North American forests. Since 2012, BLD has expanded from an initial discovery in Ohio to 12 states throughout the eastern United States and the Canadian province of Ontario. Disease progression has accelerated in recent years, with respect to both the widespread occurrence and the severity within chronically infected stands. A foliar parasitic nematode, *Litylenchus crenatae* subspecies *mccannii* (*Lcm*), is believed to be the primary causal agent of BLD. Readily observable symptoms of BLD infection vary based on the severity of foliar damage, which is thought to be a product of nematode populations at the time of leaf development within the bud. Generalized leaf deformities associated with other parasitic nematodes are known to induce the formation of neoplastic tissue and

galls, similar to those sometimes associated with mite damage (Palomares-Rius et al., 2017). The milder symptomology of BLD, commonly referred to as *banding*, consists of a gall formation within the interveinal portions of a leaf that appears as a discolored band, where the size and number of bands is somewhat random. The more severe symptom expression is referred to as *crinkling*, where a leaf appears shrunken and deformed, with a thickened leathery feel and often bearing chlorotic tissue. Unlike many fungal-borne foliar diseases, the symptoms of BLD do not progress throughout the duration of a growing season, such that the symptom presentation of individual leaves at the time of bud break is consistent through leaf senescence (Fearer et al., 2022b). Under a high severity of infection, thought to occur when nematode populations within the bud are exceptionally high, buds are aborted from the stem and leaves fail to flush out in the spring. In some instances, a secondary flush of leaves will occur later in the growing season. However, these second-flush leaves are often stunted and only account for a small fraction of foliage lost from the crown. At the tree level, BLD causes a marked increase in canopy transparency and branch dieback (Reed et al., 2022), which is hypothesized to have impacts on growth, vigor, and long-term survival.

Pests and diseases that result in a reduction of foliage are often associated with declines in woody diameter increment (Oliva et al., 2016; McIntire et al., 2018), and in the longer term, reductions in stored carbohydrates (Landhausser and Lieffers, 2012). Among residual symptomatic leaves, it is unknown how symptoms associated with BLD are altering leaf function. Given that BLD symptoms persist from year to year, measuring the direct impacts on leaf gas exchange is useful for understanding the compounding stress on carbon assimilation capacity. While nematode-induced tree diseases that affect roots [*Meloidogyne* spp., (Elling, 2013)] and stem wood [*Bursaphelenchus xylophilus*, (Kim et al., 2020)] have been well studied, little is known regarding how a novel foliar parasitic nematode impacts tree physiology. At the cellular level, *Lcm* can induce widespread damage to the mesophyll (Carta et al., 2020). This can lead to chlorosis-necrosis and is expected to negatively impact the photosynthetic function of these tissues. Furthermore, *Lcm* is known to cause deformation of stomata (Carta et al., 2020), the pores on the leaf surface responsible for regulating gas exchange. It is plausible that this mechanical damage alters carbon assimilation rates, stomatal conductance, and in turn, the water use efficiency of the leaf. The deterioration of mesophyll may also impact physical properties of the leaf that play a role in photosynthesis and the regulation of gas exchange. Identifying leaf traits that vary with BLD infection may serve as an indicator of relative disease severity, beyond a coarse grouping based on observations of leaf morphology.

The objectives of this study were to measure leaf gas exchange coupled with leaf trait data to quantify physiological impacts across a gradient of BLD severity. This was accomplished through a field experiment in three parts. First, leaf gas exchange was measured systematically across BLD symptom categories, assessing both responses to manipulated light intensity and *via* instantaneous measurements at a saturated light level. Second, leaves sampled in the field were collected for laboratory analysis of specific leaf area, leaf water content, and leaf nitrogen content. Finally, correlation between leaf traits and instantaneous gas exchanged was evaluated for functional relationships with respect to BLD severity.

Materials and methods

Study site and plant material

The experiment was conducted the Meshomasic State Forest, approximately 8 km west of Marlborough, Connecticut (41.6164 N, −72.5530 W, 164 m above sea level). The stand consists of mature American beech, white oak (*Quercus alba* L.), red oak (*Quercus rubra* L.), black birch (*Betula lenta* L.), and sugar maple (*Acer saccharum* Marshall). Stand basal area is 25 m^2 ha^{-1} with 502 trees per acre, estimated using a BAF 10 prism. American beech represents 26% of the total basal area and also dominates the understory of the stand. Symptoms of BLD were first observed in this stand in 2021 and are now present on all observed host trees. All trees exhibited a mild infestation of the scale insect *Cryptococcus fagisuga,* with a low occurrence of cankers associated with *Neonectria*, also known as beech bark disease (Houston, 1994). Cankers were observed primarily on mature trees in the overstory stratum but were not present on the understory trees sampled in this study.

Sampled trees (n = 12) in the understory stratum were selected at random inside a 0.4 ha area within the stand. All leaves were accessed from intact stem segments between 0.5 and 2.0 m above ground level. Tree diameter at breast height (DBH, 1.3 m above ground level) ranged from 2.2 to 21.1 cm with a mean of 9.1 cm (SD ± 5.4). Three BLD symptom categories were established based on the visual presentation of symptoms at the time of measurement: asymptomatic, banded, and crinkled (**Supplementary Figure 1**). Asymptomatic leaves are those which appear healthy with normal size, color, and without the presence of galls or necrotic tissue. Banded leaves are those with normal size but with the presence of galls that present as darkened bands that manifest in the interveinal portions of infected leaf surfaces. Crinkled leaves are diminutive with a darkened green color throughout and often exhibit areas if chlorotic and/or necrotic tissue. While BLD symptoms do occur on a natural continuous gradient, the banded and crinkled distinction is readily identifiable in the field and can be an indicator of disease severity that corresponds to nematode populations within the leaf (Fearer et al., 2022a).

Leaf gas exchange measurements

All field data was collected on 18 August 2022 between the hours of 830 and 1400 EST. Leaf gas exchange was measured on intact leaves while attached to the branch using an LI-6400 infrared gas analyzer equipped with a 6400-02B LED light source (LI-COR, Lincoln, NB, USA). Light response curves were derived from a subset of trees (n = 3) using a leaf from each symptom category per tree, where the photosynthetic photon flux density (PPFD) was manipulated at 10 setpoints: 2,000, 1,500, 1,000, 500, 250, 120, 60, 30, 15, and 0 μmmol m^{-2} s^{-1}. Instantaneous measurements of gas exchange were performed at a PPFD of 1000 μmmol m^{-2} s^{-1} and replicated on three leaves per symptom category on a subset of trees (n = 3) and averaged. To maximize the amount of tree replication in the campaign due to time limitation, instantaneous gas exchange was measured on a single leaf from each symptom category for all other trees (n = 9). Leaves were allowed to equilibrate in the

leaf chamber for 2–5 min before logging three measurements over a span of 10 s, the average of those instantaneous logs are reported throughout. The conditions within the leaf chamber were maintained at a CO_2 concentration of 415 μmmol mol^{-1}, a temperature of 22.1°C (SD ± 0.01), and relative humidity of 47.1% (SD ± 5.2). Individual leaf samples were harvested into plastic bags and transported on ice for laboratory analyses of leaf traits. A total of 81 leaves were collected (n = 27 per symptom type).

Leaf traits

Each sampled leaf was measured for specific leaf area (SLA, cm^2 g^{-1}), leaf water content (LWC,%), and nitrogen content (Leaf N,%). Fresh leaves were weighed on an electronic balance, then imaged on the adaxial surface using a flatbed scanner at 600 dpi resolution (Epson Expression 12000XL, Nagano, Japan). Leaves were then oven dried at 60°C for 72 h and measured for dry mass. Total leaf area was determined using a protocol developed for the ImageJ software. The SLA is calculated as the ratio of total leaf area to dry mass. The LWC is calculated as:

$$LWC = \left(\frac{fresh\ mass\ -\ dry\ mass}{fresh\ mass}\right)\ 100$$

For leaf N analysis, whole dried leaves were ground to a homogonous powder using a mini Wiley Mill and passed through a 0.85 mm sieve (#20 mesh), followed by mortar and pestle. Ground samples were dried for an additional 24 h at 60°C. Aliquots of 2.0–5.0 mg dry mass were sealed in tin capsules and measured using a Flash EA 1112 elemental analyzer (Thermo Fisher Scientific, Waltham, MA, USA).

Statistical analyses

All statistical analysis and data visualizations were performed in R studio (version 4.0.2, R Foundation for Statistical Computing, Vienna, Austria). Light response curves were fit with a non-rectangular hyperbola model (Marshall and Biscoe, 1980) using the package "photosynthesis" (Stinziano et al., 2020). From these curve fits, estimates of light-saturated CO_2 assimilation (A_{max}), dark respiration rate (R_d), light compensation point (Γi), and apparent quantum yield (α) were derived. For instantons gas exchange measurements, the net assimilation rate (A_{net}), stomatal conductance (g_s), and intrinsic water use efficiency (A_{net}/g_s or δ) were evaluated. A one-way analysis of variance (ANOVA) was used determine significant effects ($p \leq 0.05$) attributed to observed BLD symptoms for each variable. *Post-hoc* contrasts between symptom categories were analyzed *via* a Tukey test using the estimated marginal means with the package "emmeans" (Lenth et al., 2018). Similarly, foliar trait data for LWC, SLA, and leaf N were analyzed by symptom category with one-way ANOVA and a Tukey's *post-hoc* test, using the mean of all leaves measured for each tree (n = 12).

Linear regression models were developed to evaluate relationships between A_{net}, g_s, and δ with foliar functional traits as dependent variables (LWC, SLA, and leaf N) by symptom category. Analysis of covariance (ANCOVA) was used to determine significant differences for interactions between leaf traits and symptom categories. To assess the interaction between the covariate and factor variables, significant differences in slopes of the covariate trend for each symptom category were evaluated with the "emtrends" function.

Results

Light response curves

Photosynthetic response to light varied by BLD symptom category (Table 1 and Figure 1). Compared to asymptomatic leaves, values of A_{max} were 25.9 and 23.6% lower in banded and crinkled leaves, respectively. However, these differences were not found to be significant (Table 1), in part due to a high amount of variability in carbon assimilation rates among asymptomatic leaves at high levels of light (PPFD > 1000 μmol m^{-2} s^{-1}). Leaf symptoms had a significant effect on both R_d [$F(2,6) = 9.21$, $p = 0.015$] and Γ_i [$F(2,6) = 7.58$, $p = 0.023$]. Estimates of R_d for asymptomatic leaves was nearly zero, while banded and crinkled leaves respired at a rate of 0.46 and 0.80 μmol m^{-2} s^{-1}, respectively. Similarly, Γ_i was higher among diseased leaves, where the compensation point was estimated at 0.23, 5.50, and 20.69 μmol m^{-2} s^{-1} among asymptomatic, banded, and crinkled leaves, respectively. No differences in α were found between leaf symptom categories.

Instantaneous gas exchange

Leaf symptoms influenced all metrics of gas exchanged evaluated in this study (Table 1 and Figure 2). Estimates of A_{net} were significantly lower in both banded and crinkled leaves with respect to asymptomatic leaves [$F(2,33) = 40.16$, $p < 0.001$]. *Post-hoc* analysis found both disease symptoms to be significantly lower than asymptomatic leaves ($p < 0.001$), but no difference between the banded and crinkled symptoms ($p = 0.115$; Figure 2A). Compared to asymptomatic leaves, A_{net} of banded and crinkled leaves was 40.7 and 53.3% lower, respectively. The highest A_{net} measured among individual leaves was 4.7 μmol CO_2 m^{-2} s^{-1} (Tree 7, asymptomatic) and the lowest was 0.8 μmol CO_2 m^{-2} s^{-1} (Tree 6, crinkled). Estimates of g_s are significantly different by symptom category [$F(2,33) = 11.68$, $p < 0.001$]. *Post-hoc* analysis found that conductance of crinkled leaves was significantly higher than either symptom category ($p \leq 0.001$, Figure 2B), an increase of 60% with respect to asymptomatic leaves. Estimates of δ were significantly different by symptom category [$F(2,33) = 75.59$, $p < 0.001$]. *Post-hoc* analysis found that δ differed significantly between each leaf symptom ($p < 0.001$, Figure 2C), such that compared to asymptomatic leaves, δ was 34.7 and 67.6% lower among banded and crinkled leaves, respectively.

Leaf traits

Progression of leaf symptoms evoked differences in LWC, SLA, and leaf N (Table 1 and Figure 3). Measured LWC was significantly

TABLE 1 Means ± standard deviation for leaf traits of light-saturated photosynthetic rate (A_{max}; μmol m^{-2} s^{-1}), dark respiration rate (R_d; μmol m^{-2} s^{-1}), light compensation point (Γ_i; μmol m^{-2} s^{-1}), apparent quantum yield (α), instantaneous net carbon assibilation rate (A_{net}; μmol m^{-2} s^{-1}), stomatal conductance (g_s; mol m^{-2} s^{-1}), intrinsic water use efficiency (δ; μmol CO_2 mol^{-1} H_2O), leaf water content (LWC,%), specific leaf area (SLA, cm^2 g^{-1}), and leaf nitrogen content (Leaf N,%).

	Symptom category			ANOVA			
	Asymptomatic	Banded	Crinkled	*n*	df	*F*-value	*p*-Value
A_{max}	3.13 ± 0.49^a	2.32 ± 0.06^a	2.39 ± 0.45^a	3	2	3.99	0.079
R_d	0.01 ± 0.02^a	0.46 ± 0.28^{ab}	0.80 ± 0.27^b	3	2	9.21	0.015
Γ_i	0.23 ± 0.40^a	5.50 ± 2.58^a	20.69 ± 11.28^a	3	2	7.58	0.023
α	0.06 ± 0.02^a	0.10 ± 0.05^{ab}	0.07 ± 0.03^b	3	2	1.20	0.364
A_{net}	3.66 ± 0.64^a	2.17 ± 0.42^b	1.71 ± 0.59^b	12	2	40.16	<0.001
g_s	0.05 ± 0.01^a	0.05 ± 0.01^a	0.08 ± 0.03^b	12	2	11.68	<0.001
δ	74.74 ± 9.95^a	48.77 ± 9.88^b	24.21 ± 10.37^c	12	2	75.59	<0.001
LWC	58.91 ± 1.07^a	63.00 ± 1.63^b	66.76 ± 3.12^c	12	2	41.12	<0.001
SLA	394.77 ± 28.99^a	266.86 ± 37.33^b	152.96 ± 21.42^c	12	2	195.60	<0.001
Leaf N	1.90 ± 0.18^a	2.01 ± 0.23^{ab}	2.16 ± 0.22^b	12	2	5.39	0.009

ANOVA indicates number of replicates used in analysis (*n*), degrees of freedom (df), *F*-value and *p*-value results for comparisons between symptom categories. Statistical differences determined *via* Tukey *post-hoc* analysis are indicated by difference in letters (^{a}, ^{b}, ^{c}) between symptom groups for each response variable.

different by symptom category [$F(2,33) = 41.12$, $p < 0.001$]. *Post-hoc* analysis found significant differences of LWC between each leaf symptom ($p < 0.001$, Figure 3A), where with respect to asymptomatic leaves, water content increased by 6.9% among banded leaves and 13.3% among crinkled leaves. Measured SLA was also significantly different by symptom category [$F(2,33) = 195.60$, $p < 0.001$]. *Post-hoc* analysis found significant differences of SLA between each leaf symptom ($p < 0.001$, Figure 3B), where with respect to asymptomatic leaves, SLA was reduced by 32.4% among banded leaves and 61.2% among crinkled leaves. Total leaf N was also impacted by leaf symptomology [$F(2,33) = 5.39$, $p = 0.009$], where crinkled leaves exhibit significantly higher N on a dry mass basis compared to asymptomatic leaves ($p = 0.007$, Figure 3C). The total leaf N among asymptomatic leaves was 1.90%, with crinkled leaves at 2.16%, a relative increase of 13.7%. Measured N values of banded leaves were intermediate between the other symptom categories and not significantly different from either asymptomatic or crinkled leaves.

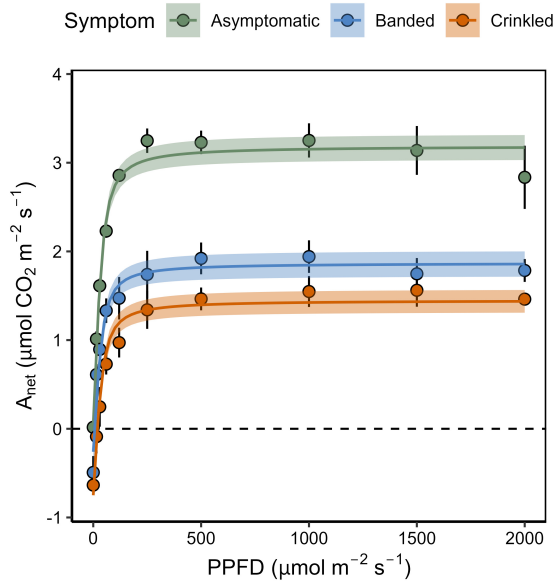

FIGURE 1
Net carbon assibilation rate (A_{net}) as a function of the photosynthetic photon flux density (PPFD) by BLD symptom category. Points show mean and standard error ($n = 3$), shaded region is the 95% confidence interval for the non-rectangular hyperbola model.

Functional relationships between leaf traits and gas exchange

Linear regression analysis revealed correlations between leaf trait data and instantaneous gas exchange. Photosynthesis had an overall negative linear relationship to LWC (Figure 4A) and Leaf N (Figure 4C), but a positive relationship to SLA (Figure 4B) across all symptom categories. Within symptom categories A_{net} was found to decline as function of SLA, in contrast to the across-group relationship, though ANCOVA found no significant difference in slopes between symptoms [$F(2,30) = 1.19$, $p = 0.319$]. Response of g_s as a function of LWC (Figure 4D) and leaf N (Figure 4F) did not yield significant correlations ($p > 0.05$). A significant negative correlation between g_s and SLA was found (Figure 4E), with a significant difference in slopes between leaf symptom categories [$F(2,30) = 5.297$, $p = 0.011$]. *Post-hoc* comparisons indicated that g_s of crinkled leaves decline more rapidly with increasing SLA (slope = -9.36×10^{-4}) with respect to both banded leaves (slope = 1.18×10^{-4}, $p = 0.009$) and asymptomatic leaves (slope = 1.82×10^{-4}, $p = 0.028$). This was the only trait relationship for which ANVOA revealed a significant difference between symptom categories. Measurements of δ exhibited a strong negative correlation with LWC (Figure 4G), a strong negative correlation with SLA (Figure 4H), and a weak but significant negative correlation with leaf N (Figure 4I). Coefficient of determination

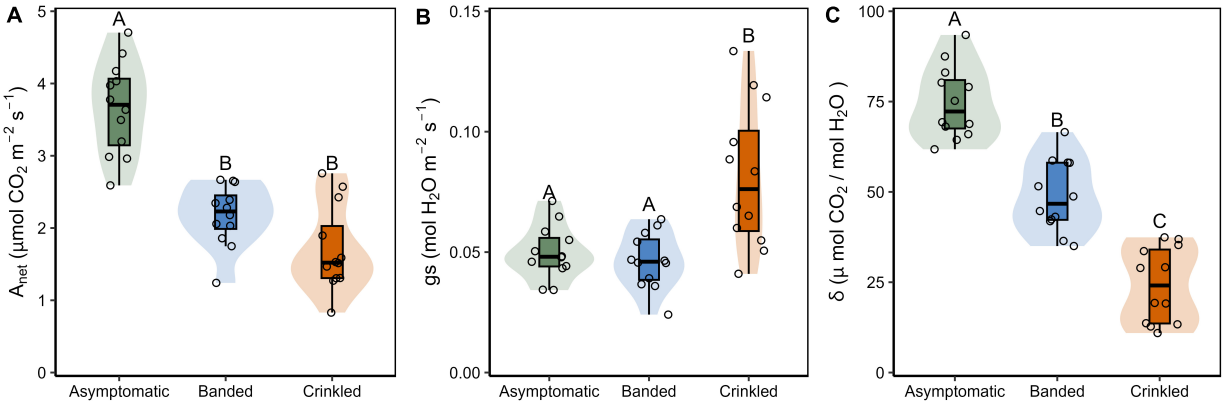

FIGURE 2
(A) Instantaneous net carbon assibilation rate (A_{net}); **(B)** stomatal conductance (g_s); and **(C)** intrinsic water use efficiency (δ) by BLD symptom category. Box plots show Q25–1.5 IQR, Q25, Q50, Q75, and Q75 + 1.5 IQR values, the shaded region is the continuous density distribution, and open circles are tree replicates (n = 12). Statistical differences are indicated by different letters between symptom categories (Tukey *post-hoc* analysis, $p < 0.05$).

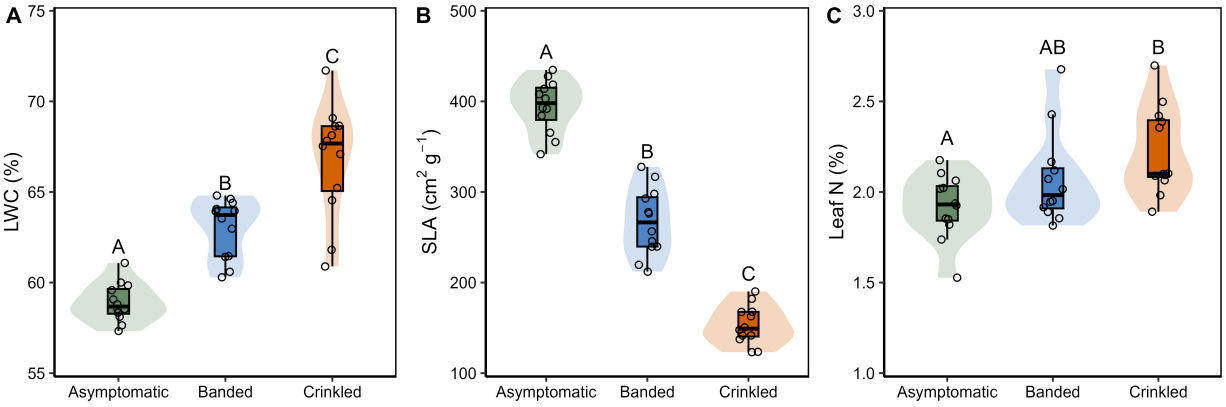

FIGURE 3
(A) Leaf water content (LWC); **(B)** specific leaf area (SLA); and **(C)** leaf N content by BLD symptom category. Box plots show Q25–1.5 IQR, Q25, Q50, Q75, and Q75 + 1.5 IQR values, the shaded region is the continuous density distribution, and open circles are tree replicates (n = 12). Statistical differences are indicated by different letters between symptom categories (Tukey *post-hoc* analysis, $p < 0.05$).

(R^2) and p-values across symptom linear regressions are shown within the panels of Figure 4.

Discussion

Light curve outputs that are significantly altered due to BLD symptoms are R_d and Γi, both of which are relevant under low and no-light conditions. The increased rates of R_d among diseased leaves suggests that stomates may not be able to close effectively, which is supported in part by the increased rates of g_s measured in leaves with the crinkled symptomology. Concerning Γ_i, the point where the rate of photosynthesis is equal to the rate of respiration, symptomatic leaves require a higher PPFD. A functional explanation for this finding may be attributed to changes in the cellular structure within infected leaves, specifically, a thickening and tighter arrangement of the palisade and spongey mesophyll cells. Under natural conditions, a thickening of the mesophyll can be correlated with Γ_i as leaf age progresses among non-deciduous hardwood species (Ashton and Turner, 1979). Canopy light exposure is also known to influence this compensation point, where a vertical gradient of diminishing photosynthetically active radiation causes trees to produce shade leaves in the lower crown that tend to be thinner (i.e., fewer mesophyll layers) with a lower Γi, whereas leaves near the top of the canopy are comparatively thicker with a higher Γi due to a greater intensity and availability of PPFD (Lewis et al., 2000; Norby et al., 2003). Leaves infected with BLD, especially those with crinkled symptomology, appear to be more anatomically similar to leaves that would be exposed to full sun, and thus require higher light intensity before carbon assimilation surpasses respiration. However, this comparison to sun exposed foliage does not hold true with regards to photosynthetic productivity, where such leaves would typically yield higher values of A_{net}. Instead, symptomatic leaves exhibit significantly lower rates of carbon assimilation compared to neighboring asymptomatic leaves. This loss of function is reflected in the instantaneous gas exchange measured under

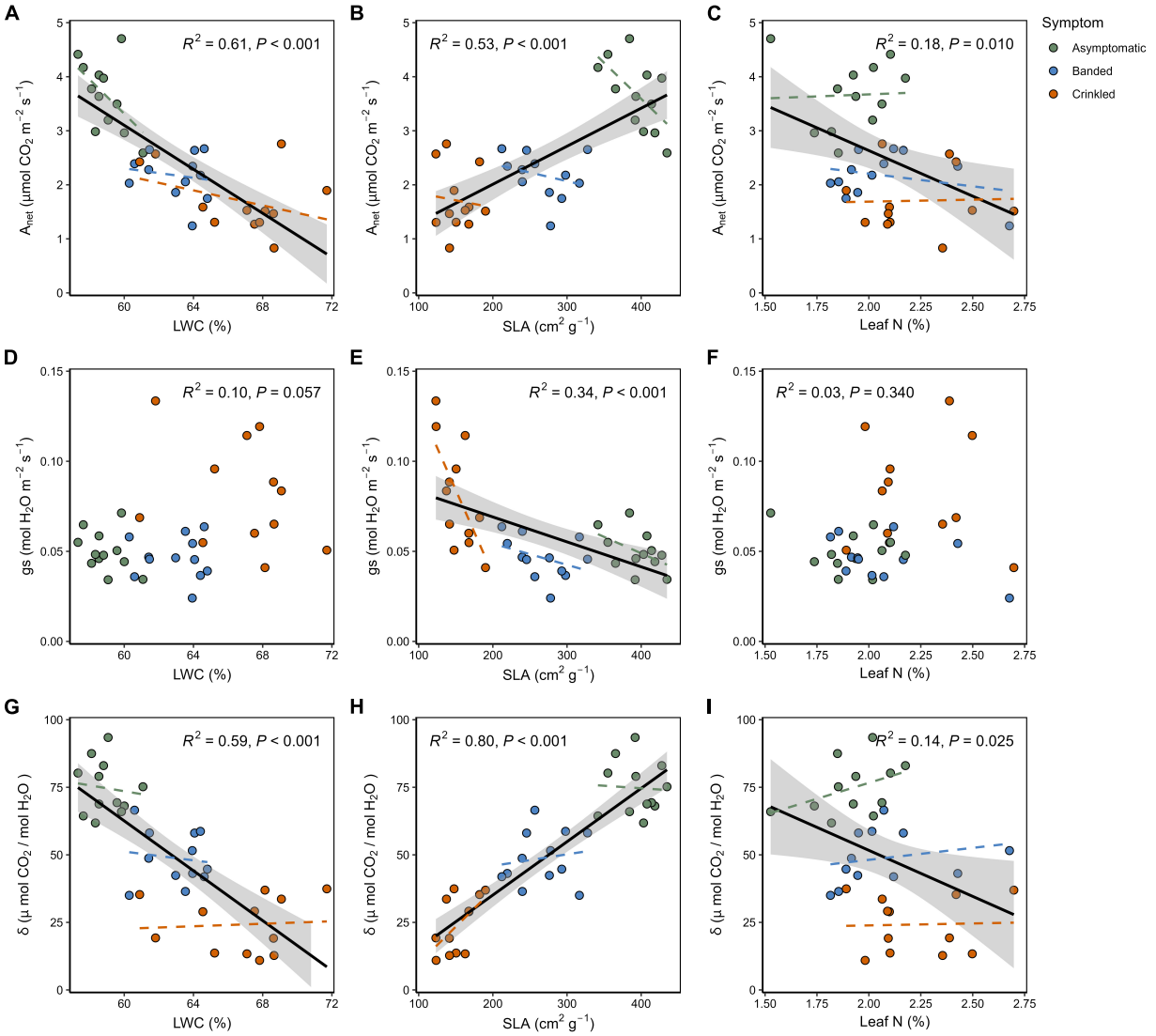

FIGURE 4
Continuous relationships between leaf treats and measured gas exchange: **(A)** A_{net} as a function of LWC; **(B)** A_{net} as a function of SLA, **(C)** A_{net} as a function of leaf N; **(D)** g_s as a function of LWC; **(E)** g_s as a function of SLA; **(F)** g_s as a function of leaf N; **(G)** δ as a function of LWC; **(H)** δ as a function of SLA; **(I)** δ as a function of leaf N. Black lines show the overall linear regressions across all symptom categories with the shaded region indicating the 95% confidence interval. Dashed colored lines show linear regressions within the respective symptom categories. Overall regression lines are omitted where not found significant ($p > 0.05$).

constant light conditions (1,000 µmmol m^{-2} s^{-1}) of this study.

Overall values of A_{net} are quite low, peaking at 4.7 µmol CO_2 m^{-2} s^{-1} for an asymptomatic leaf. This was anticipated given the understory canopy position of sampled trees, as well as the known shade tolerance of this species (Nyland et al., 2006). A comparable field study reports A_{max} of 2.9–3.1 µmol CO_2 m^{-2} s^{-1} among understory beech seedlings and roots sprouts, respectively (Farahat and Lechowicz, 2013), while A_{net} of light saturated codominant beech has been measured to range from 7.1 to 8.7 µmol CO_2 m^{-2} s^{-1} (Elvir et al., 2006). As a consequence of the shade regime, light manipulation of gas exchange revealed that A_{net} begins to taper at relatively low light levels (PPFD ≈ 500 µmol m^{-2} s^{-1}). A_{net} declines as a function of leaf N across all symptoms of BLD, contrary to the positive relationship that is generally found across tree species and functional types (Evans, 1989; Kattge et al., 2009). This finding is interesting given that crinkled leaves exhibit significantly higher leaf N (2.16%) compared to asymptotic leaves (1.90%), suggesting that mechanical damage to the photosystem outweighs any functional benefit of increased N content. Other studies have reported values for American beech leaf N on the order of 1.76% among root spouts (Farahat and Lechowicz, 2013), and from 2.14 to 2.47% among codominant trees (Elvir et al., 2006). Although leaf N can be influenced by site factors such as climate, elevation, and soil type (Gong et al., 2020), the variation measured in this study can clearly be attributed to disease symptoms given the close proximity of sampled trees.

Higher and more variable values of g_s measured among crinkled leaves resulted in a significantly diminished δ, where δ

among asymptomatic leaves is three-fold higher in comparison. This shift in water use efficiency at the leaf level has the potential to become problematic for maintaining stem xylem conductivity, in part due to the loss of foliage caused by BLD. Defoliation increases the leaf area to sapwood area ratio of trees (Kono et al., 2019), which can apply greater strain for maintaining hydraulic conductance (Mencuccini et al., 2019a,b). Controlled defoliation of balsam poplar (*Populus balsamifera* L.) is shown to reduce xylem-specific conductivity while increasing the vulnerability to cavitation among defoliated trees (Hillabrand et al., 2019). Furthermore, the risk of hydraulic failure is amplified as soil water becomes limiting (Brodribb and Cochard, 2009; Plaut et al., 2012; Sevanto et al., 2014), such is the case during seasonal droughts which are forecasted to become a more common phenomenon throughout the northeastern US (Hayhoe et al., 2007; Xue and Ullrich, 2022). Indeed, at the time of this study, 86% of the land area within the state of Connecticut was amid a severe drought, with an additional 13% classified as experiencing extreme drought (US Drought Monitor, 2022), inducing a wilting response among more sensitive tree species and those inhabiting shallow soils. As residual leaves infected with BLD exhibit greater water loss per unit carbon gained, the compounding stress of such drought events are likely to accelerate branch dieback and mortality. Further research to investigate the hydraulic traits of leaves symptomatic for BLD, and their associated branch segments, will be useful to elucidate the drought sensitivity among infected beech trees.

This work also demonstrates that SLA varies significantly within the BLD symptom categories, and therefore may serve as a proxy for quantifying disease severity on a continuous scale. The degree of separation in the SLA data is such that there is no overlap between the three symptom categories, while the variation within categories can likely be attributed to the degree of internal damage induced by parasitic nematode feeding. A study which evaluated the spectral properties of American beech leaves identified near-infrared bands that can be used to discriminate BLD symptom types and that symptom severity was associated with *Lcm* populations verified through both molecular techniques (qPCR) and counting *ex situ* nematodes (Fearer et al., 2022a). Measurements of SLA coupled with a direct estimate of *Lcm* populations within a leaf could be investigated to further explore this relationship.

The measured increase in LWC can be associated with cellular proliferation caused by damage induced while leaves are developing in the bud, leading to upregulated mesophyll cell production and presumably a higher abundance of vacuoles. Supporting evidence for this can be found among other plant parasitic nematodes in the Anguinidae family that are known stimulate cellular division and vacuolization (Stynes and Bird, 1982; Vovlas et al., 2016). Elevated LWC may also facilitate a more favorable environment for *Lcm*, as nematodes are generally reliant on hydric conditions throughout their lifecycle (Perry, 1999). Similarly, an increased leaf thickness caused by *Lcm* damage can also account for the reduced SLA as BLD symptom severity progresses. In other words, a thicker mesophyll coupled with a smaller total area, results in a denser and more hydrated leaf. It is notable that a higher water content was measured in crinkled leaves despite the presence of some necrotic and chlorotic tissue, which are generally presumed to be much drier areas of the leaf. The SLA is also linked to leaf function, as a positive linear relationship between SLA and A_{net} is well established for many hardwood tree species (Reich et al., 1998). This correlation is found to be significant across trees sampled in this study (**Figure 4B**), however, negative correlations were found within each BLD symptom category. The SLA is also found to be a strong predictor variable for g_s and δ across BLD symptom categories, emphasizing the role of this leaf trait in regulating gas exchange between leaf and atmosphere. The relationship of SLA to g_s shows that, within symptom categories, crinkled leaves exhibit a steeper negative slope that is significantly different from both banded and asymptomatic leaves. This may be partially explained by the stomatal deformations that have been reported in association with these advanced symptoms (Carta et al., 2023), resulting in poor stomatal closure and higher levels of g_s over the leaf surface. Naturally, differences in stomatal size and shape dictates mechanical function (Franks and Farquhar, 2007), while deformed stomates can alter the function of guard cells with respect to a healthy leaf (Ziv and Ariel, 1994).

This study did not assess the physiology of second-flush leaves that are associated within severely BLD-infected stands. Among trees that exhibit bud abortion, this second cohort of asymptomatic leaves was observed throughout the eastern US during the 2022 growing season. While these leaves may not harbor nematodes, they are markedly different from healthy leaves, appearing smaller and lighter in color. As a result, trees with a large quantity of aborted buds mimic trees that have undergone a defoliation event, though it should be noted that these thinned canopies were not foliated at the outset of the growing season and are colloquially referred to as "non-foliated." Furthermore, it would be meaningful to measure leaf traits in American beech trees that exhibit no symptoms of BLD to determine if there is a difference between asymptomatic leaves within an infected tree comparable within a tree that is void of disease. Many tree species demonstrate a compensatory response to defoliation *via* an upregulation of photosynthesis (Reich et al., 1993; Williams et al., 2016; McIntire et al., 2020), thus it's feasible that residual leaves within diseased American beech trees attempt to account for a net loss of carbohydrate. The compounding stress induced by multiple years of carbon limitation associated with BLD may become a consequential factor for inciting tree mortality, especially when coupled with other pests, diseases, and environmental elements.

Conclusion

Given the abundance and ecological value of American beech on the North American landscape, the impacts of BLD on tree health is a major concern for landowners and forest practitioners. The symptoms associated with BLD are shown to influence leaf gas exchange and physiological leaf traits that are linked to carbon assimilation capacity. Implications of these results point toward a compromised tree carbon budget, which can negatively affect growth, vigor, and long-term survival. Future work to build upon these findings should focus on assessing disease response among mature trees, second-flush leaves, and exploring the hydraulic sensitivity of BLD-infected American beech.

Data availability statement

Data pertaining to this study is available at Zenodo: https://zenodo.org/record/7612843#.Y-EzRnbMJZc.

Author contributions

The author confirms sole responsibility for the study conception and design, data collection, analysis and interpretation of results, and manuscript preparation.

Funding

This study was supported by the United States Department of Agriculture Forest Service, Region 9, State, Private and Tribal, Forestry, Forest Health and Forest Markets.

Acknowledgments

I thank Dr. Robert Marra for his assistance with selecting a suitable location to conduct this study and his continued efforts with the BLD long-term monitoring network. I also thank Emma Irvine and Jeff Merriam assisted with processing leaf samples for elemental analysis.

Conflict of interest

The author declares that the research was conducted in the absence of any commercial or financial relationships that could be construed as a potential conflict of interest.

Publisher's note

All claims expressed in this article are solely those of the authors and do not necessarily represent those of their affiliated organizations, or those of the publisher, the editors and the reviewers. Any product that may be evaluated in this article, or claim that may be made by its manufacturer, is not guaranteed or endorsed by the publisher.

Supplementary material

The Supplementary Material for this article can be found online at: https://www.frontiersin.org/articles/10.3389/ffgc.2023.1146742/full#supplementary-material

References

Ashton, D., and Turner, J. (1979). Studies on the light compensation point of *Eucalyptus regnans* F. Muell. *Aust. J. Bot.* 27, 589–607. doi: 10.1071/BT9790589

Brodribb, T. J., and Cochard, H. (2009). Hydraulic failure defines the recovery and point of death in water-stressed conifers. *Plant Physiol.* 149, 575–584. doi: 10.1104/pp.108.129783

Carta, L. K., Handoo, Z. A., Li, S., Kantor, M., Bauchan, G., Mccann, D., et al. (2020). Beech leaf disease symptoms caused by newly recognized nematode subspecies *Litylenchus crenatae mccannii* (*Anguinata*) described from *Fagus grandifolia* in North America. *For. Pathol.* 50, 1–15. doi: 10.1111/efp.12580

Carta, L. K., Li, S., and Mowery, J. (2023). Beech leaf disease (BLD), *Litylenchus crenatae* and its potential microbial virulence factors. *For. Microbiol.* 3, 183–192. doi: 10.1016/B978-0-443-18694-3.00018-3

Elling, A. A. (2013). Major emerging problems with minor *Meloidogyne* species. *Phytopathology* 103, 1092–1102. doi: 10.1094/PHYTO-01-13-0019-RVW

Elvir, J. A., Wiersma, G. B., Day, M. E., Greenwood, M. S., and Fernandez, I. J. (2006). Effects of enhanced nitrogen deposition on foliar chemistry and physiological processes of forest trees at the Bear Brook Watershed in Maine. *For. Ecol. Manag.* 221, 207–214. doi: 10.1016/j.foreco.2005.09.022

Evans, J. R. (1989). Photosynthesis and nitrogen relationships in leaves of C_3 plants. *Oecologia* 78, 9–19. doi: 10.1007/BF00377192

Farahat, E., and Lechowicz, M. J. (2013). Functional ecology of growth in seedlings versus root sprouts of *Fagus grandifolia* Ehrh. *Trees* 27, 337–340. doi: 10.1007/s00468-012-0781-9

Fearer, C. J., Volk, D., Hausman, C. E., and Bonello, P. (2022b). Monitoring foliar symptom expression in beech leaf disease through time. *For. Pathol.* 52:e12725. doi: 10.1111/efp.12725

Fearer, C. J., Conrad, A. O., Marra, R. E., Georskey, C., Villari, C., Slot, J., et al. (2022a). A combined approach for early in-field detection of beech leaf disease using near-infrared spectroscopy and machine learning. *Front. For. Glob. Chang.* 5:934545. doi: 10.3389/ffgc.2022.934545

Franks, P. J., and Farquhar, G. D. (2007). The mechanical diversity of stomata and its significance in gas-exchange control. *Plant Physiol.* 143, 78–87. doi: 10.1104/pp.106.089367

Gong, H., Li, Y., Yu, T., Zhang, S., Gao, J., Zhang, S., et al. (2020). Soil and climate effects on leaf nitrogen and phosphorus stoichiometry along elevational gradients. *Glob. Ecol. Conserv.* 23:e01138. doi: 10.1016/j.gecco.2020.e01138

Hayhoe, K., Wake, C. P., Huntington, T. G., Luo, L., Schwartz, M. D., Sheffield, J., et al. (2007). Past and future changes in climate and hydrological indicators in the US Northeast. *Clim. Dyn.* 28, 381–407. doi: 10.1007/s00382-006-0187-8

Hillabrand, R. M., Hacke, U. G., and Lieffers, V. J. (2019). Defoliation constrains xylem and phloem functionality. *Tree Physiol.* 39, 1099–1108. doi: 10.1093/treephys/tpz029

Houston, D. R. (1994). Major new tree disease epidemics: Beech bark disease. *Annu. Rev. Phytopathol.* 32, 75–87. doi: 10.1146/annurev.py.32.090194.000451

Kattge, J., Knorr, W., Raddatz, T., and Wirth, C. (2009). Quantifying photosynthetic capacity and its relationship to leaf nitrogen content for global-scale terrestrial biosphere models. *Glob. Change Biol.* 15, 976–991. doi: 10.1111/j.1365-2486.2008.01744.x

Kim, B.-N., Kim, J. H., Ahn, J.-Y., Kim, S., Cho, B.-K., Kim, Y.-H., et al. (2020). A short review of the pinewood nematode, *Bursaphelenchus xylophilus*. *Toxicol. Environ. Health Sci.* 12, 297–304. doi: 10.1007/s13530-020-00068-0

Kono, Y., Ishida, A., Saiki, S. T., Yoshimura, K., Dannoura, M., Yazaki, K., et al. (2019). Initial hydraulic failure followed by late-stage carbon starvation leads to drought-induced death in the tree Trema orientalis. *Commun. Biol.* 2, 1–9. doi: 10.1038/s42003-018-0256-7

Landhausser, S. M., and Lieffers, V. J. (2012). Defoliation increases risk of carbon starvation in root systems of mature aspen. *Trees* 26, 653–661. doi: 10.1007/s00468-011-0633-z

Lenth, R., Singmann, H., Love, J., Buerkner, P., and Herve, M. (2018). *Emmeans: Estimated marginal means, aka least-squares means. R package version, 1. 3.*

Lewis, J., Mckane, R., Tingey, D., and Beedlow, P. (2000). Vertical gradients in photosynthetic light response within an old-growth Douglas-fir and western hemlock canopy. *Tree Physiol.* 20, 447–456. doi: 10.1093/treephys/20.7.447

Marshall, B., and Biscoe, P. (1980). A model for C3 leaves describing the dependence of net photosynthesis on irradiance. *J. Exp. Bot.* 31, 29–39. doi: 10.1093/jxb/31.1.29

McIntire, C. D., Huggett, B. A., Dunn, E., Munck, I. A., Vadeboncoeur, M. A., and Asbjornsen, H. (2020). Pathogen-induced defoliation impacts on transpiration, leaf gas exchange, and non-structural carbohydrate allocation in eastern white pine (*Pinus strobus*). *Trees* 35, 357–373. doi: 10.1007/s00468-020-02037-z

McIntire, C. D., Munck, I. A., Vadeboncoeur, M. A., Livingston, W. H., and Asbjornsen, H. (2018). Impacts of white pine needle damage on seasonal litterfall dynamics and wood growth of eastern white pine (*Pinus strobus*) in northern New England. *For. Ecol. Manag.* 423, 27–36. doi: 10.1016/j.foreco.2018.02.034

Mencuccini, M., Rosas, T., Rowland, L., Choat, B., Cornelissen, H., Jansen, S., et al. (2019b). Leaf economics and plant hydraulics drive leaf : Wood area ratios. *New Phytol.* 224, 1544–1556. doi: 10.1111/nph.15998

Mencuccini, M., Manzoni, S., and Christoffersen, B. (2019a). Modelling water fluxes in plants: From tissues to biosphere. *New Phytol.* 222, 1207–1222.

Norby, R. J., Sholtis, J. D., Gunderson, C. A., and Jawdy, S. S. (2003). Leaf dynamics of a deciduous forest canopy: No response to elevated CO2. *Oecologia* 136, 574–584. doi: 10.1007/s00442-003-1296-2

Nyland, R. D., Bashant, A. L., Bohn, K. K., and Verostek, J. M. (2006). Interference to hardwood regeneration in northeastern North America: Ecological characteristics of American beech, striped maple, and hobblebush. *North. J. Appl. For.* 23, 53–61. doi: 10.1093/njaf/23.1.53

Oliva, J., Stenlid, J., Grönkvist-Wichmann, L., Wahlström, K., Jonsson, M., Drobyshev, I., et al. (2016). Pathogen-induced defoliation of Pinus sylvestris leads to tree decline and death from secondary biotic factors. *For. Ecol. Manag.* 379, 273–280. doi: 10.1016/j.foreco.2016.08.011

Palomares-Rius, J. E., Escobar, C., Cabrera, J., Vovlas, A., and Castillo, P. (2017). Anatomical alterations in plant tissues induced by plant-parasitic nematodes. *Front. Plant Sci.* 8:1987. doi: 10.3389/fpls.2017.01987

Perry, R. (1999). Desiccation survival of parasitic nematodes. *Parasitology* 119, S19–S30. doi: 10.1017/S0031182000084626

Plaut, J. A., Yepez, E. A., Hill, J., Pangle, R., Sperry, J. S., Pockman, W. T., et al. (2012). Hydraulic limits preceding mortality in a piñon–juniper woodland under experimental drought. *Plant Cell Environ.* 35, 1601–1617. doi: 10.1111/j.1365-3040.2012.02512.x

Reed, S. E., Volk, D., Martin, D. K. H., Hausman, C. E., Macy, T., Tomon, T., et al. (2022). The distribution of beech leaf disease and the causal agents of beech bark disease (*Cryptoccocus fagisuga*, *Neonectria faginata*, N. ditissima) in forests surrounding Lake Erie and future implications. *For. Ecol. Manag.* 503:119753.

Reich, P. B., Walters, M. B., Krause, S. C., Vanderklein, D. W., Raffs, K. F., and Tabone, T. (1993). Growth, nutrition and gas exchange of *Pinus resinosa* following artificial defoliation. *Trees* 7, 67–77. doi: 10.1007/BF00225472

Reich, P., Ellsworth, D., and Walters, M. (1998). Leaf structure (specific leaf area) modulates photosynthesis–nitrogen relations: Evidence from within and across species and functional groups. *Funct. Ecol.* 12, 948–958.

Sevanto, S., Mcdowell, N. G., Dickman, L. T., Pangle, R., and Pockman, W. T. (2014). How do trees die? A test of the hydraulic failure and carbon starvation hypotheses. *Plant Cell Environ.* 37, 153–161. doi: 10.1111/pce.12141

Stinziano, J., Roback, C., Gamble, D., Murphy, B., Hudson, P., and Muir, C. (2020). *Photosynthesis: tools for plant ecophysiology & modeling. R package version, 2.*

Stynes, B. A., and Bird, A. F. (1982). Development of galls induced in *Lolium rigidum* by *Anguina agrostis*. *Phytopathology* 72, 336–346.

US Drought Monitor (2022). *Connecticut Drought Monitor Map Archive*. Available online at: https://droughtmonitor.unl.edu/ (accessed December 12, 2022).

Vovlas, N., Troccoli, A., Palomares-Rius, J. E., De Luca, F., Cantalapiedra-Navarrete, C., Liébanas, G., et al. (2016). A new stem nematode, Ditylenchus oncogenus n. sp.(*Nematoda*: *Tylenchida*), parasitizing sowthistle from Adriatic coast dunes in southern Italy. *J. Helminthol.* 90, 152–165. doi: 10.1017/S0022149X14000947

Williams, J. P., Hanavan, R. P., Rock, B. N., Minocha, S. C., and Linder, E. (2016). Influence of hemlock woolly adelgid infestation on the physiological and reflectance characteristics of eastern hemlock. *Can. J. For. Res.* 46, 410–426. doi: 10.1139/cjfr-2015-0328

Xue, Z. Y., and Ullrich, P. A. (2022). Changing trends in drought patterns over the Northeastern United States using multiple large ensemble datasets. *J. Clim.* 35, 3813–3833. doi: 10.1175/JCLI-D-21-0810.1

Ziv, M., and Ariel, T. (1994). "Vitrification in relation to stomatal deformation and malfunction in carnation leaves in vitro," in *Physiology, growth and development of plants in culture*, eds P. J. Lumsden, J. R. Nicholas, and W. J. Davies (Dordrecht: Springer). doi: 10.1007/978-94-011-0790-7_15

frontiers | Frontiers in Forests and Global Change

TYPE Original Research
PUBLISHED 03 April 2023
DOI 10.3389/ffgc.2023.1149456

OPEN ACCESS

EDITED BY
Isabel Alvarez Munck,
Forest Health Protection, Forest Service (USDA), United States

REVIEWED BY
Cameron Ducayet McIntire,
Forest Service (USDA), United States
David Thoma,
United States Department of the Interior, United States

*CORRESPONDENCE
Kelly S. Burns
✉ kelly.burns@usda.gov
Jane E. Stewart
✉ jane.stewart@colostate.edu

SPECIALTY SECTION
This article was submitted to Pests, Pathogens and Invasions, a section of the journal Frontiers in Forests and Global Change

RECEIVED 22 January 2023
ACCEPTED 07 March 2023
PUBLISHED 03 April 2023

CITATION
Burns KS, Tinkham WT, Leddy KA, Schoettle AW, Jacobi WR and Stewart JE (2023) Interactions between white pine blister rust, bark beetles, and climate over time indicate vulnerabilities to limber pine health. *Front. For. Glob. Change* 6:1149456. doi: 10.3389/ffgc.2023.1149456

Interactions between white pine blister rust, bark beetles, and climate over time indicate vulnerabilities to limber pine health

Kelly S. Burns[1]*, Wade T. Tinkham[2], K. A. Leddy[3], Anna W. Schoettle[2], William R. Jacobi[3] and Jane E. Stewart[3]*

[1]Forest Health Protection, Rocky Mountain Region, U.S. Department of Agriculture, Forest Service, Golden, CO, United States, [2]Rocky Mountain Research Station, U.S. Department of Agriculture, Forest Service, Fort Collins, CO, United States, [3]Department of Agricultural Biology, Colorado State University, Fort Collins, CO, United States

Introduction: Limber pine is a keystone species in the Rocky Mountains that grows on harsh, high elevation sites where few other tree species can. Recent studies suggest the species is threatened by the combined impacts of the exotic, invasive disease, white pine blister rust (WPBR), native bark beetles, and climate change. Information on changes in the health of limber pine populations and long-term impacts posed by these threats is needed to inform management efforts.

Methods: We established 106 long-term monitoring plots in 10 study areas that were surveyed three times between 2004 and 2017. We assessed site and stand factors, tree health, and regeneration over time to detect changes in limber pine abundance and health, cumulative impacts of WPBR and bark beetles, and to evaluate the drivers of WPBR occurrence and severity.

Results: Limber pine health declined significantly over the study with more than 20% of initially live limber pine trees dead by the last measurement cycle, primarily due to WPBR and bark beetles. While some recruitment occurred, mortality rates greatly outpaced recruitment of ingrowth. Disease incidence and how it changed over time was variable, but disease severity increased substantially overall and in all study areas. Limber pine regeneration was low or absent in most sites and mortality caused by WPBR increased significantly. We found strong relationships between WPBR and aridity. Trees in habitats with high vapor pressure deficit were less likely to be infected with WPBR, but trees that were already infected were more likely to develop severe symptoms and die. Longer growing seasons increased the likelihood of WPBR presence and mortality. Growing season length and vapor pressure deficit tended to increase over the study, suggesting that climate change may exacerbate disease impacts.

Discussion: Declining health of limber pine coupled with high mortality rates, increasing disease severity, and low levels of natural regeneration indicate

successful recovery may not occur in some locations without management intervention. Proactive management strategies to reduce insect and disease impacts and promote stand recovery and resilience should be pursued in remaining, healthy limber pine ecosystems.

KEYWORDS

white pine blister rust, limber pine, mountain pine beetle, climate change, stand condition assessment, long-term monitoring, forest health management, vapor pressure deficit

1. Introduction

Limber pine (*Pinus flexilis*) is an ecologically and culturally important tree species that occurs throughout western North America spanning a vast latitudinal (34°–54° N) and elevational (870–3,810 m) range (Steele, 1990; **Figure 1**). Not only is limber pine an important component of the forested ecosystems it inhabits, as a keystone species it has a disproportionately large influence on ecosystem functions relative to its abundance (Steele, 1990; Schoettle et al., 2022a). Limber pines provide habitat and a food source for wildlife, regulate snow retention and runoff, facilitate the establishment of late successional tree species at treeline, and maintain cover on harsh, rugged sites where little else can grow (Schoettle, 2004). Limber pines are threatened by the combined impacts of climate change, bark beetles, and the exotic, invasive disease, white pine blister rust (WPBR) (Burns et al., 2011; Smith et al., 2013a; Kearns et al., 2014; Cleaver et al., 2015; Schoettle et al., 2022a).

Recent studies indicate limber pine health in the Rocky Mountains is declining (Jackson et al., 2010; Smith et al., 2013a; Cleaver et al., 2015, 2022; Shanahan et al., 2019) and mortality significantly exceeds growth (Goeking and Windmuller-Campione, 2021). Climate models predict that limber pine will be forced to higher elevations (Monahan et al., 2013) and the USDA Forest Service National Insect and Disease Risk Map predicts a 44% reduction in limber pine basal area by 2027 due to combined effects of WPBR, bark beetles, and dwarf mistletoe (Krist et al., 2014). Concerns over the status of the species have led limber pine to be listed as a "Species of Local Concern" on the Black Hills National Forest, a "Species of Management Concern" in Rocky Mountain National Park, and a "BLM Sensitive Species" in Wyoming. The listing of limber pine as Endangered under the Species at Risk Act in Canada is pending (COSEWIC, 2014). The Committee on the Status of Endangered Wildlife in Canada (COSEWIC) concluded "*this tree species is imminently and severely threatened throughout its Canadian range by white pine blister rust (an introduced pathogen), mountain pine beetle, and climate change.*"

The fungal pathogen that causes WPBR, *Cronartium ribicola*, was inadvertently introduced into western North America in the early 20th century (Geils et al., 2010). All nine North American white pine species are susceptible to the rust. WPBR was first reported in natural limber pine stands in southern Idaho in 1945 (Krebill, 1964) and has since slowly spread throughout a large portion of limber pine's range, now occurring in areas once thought to be too inhospitable for the pathogen to flourish (Blodgett and Sullivan, 2004; Burns, 2006; Vogler et al., 2017a,b; Jacobi et al., 2018a; Schoettle et al., 2018). The only states where WPBR has not been detected in limber pine to date include Utah, Oregon, and California (Kliejunas and Dunlap, 2007; Maloney, 2011; Dunlap, 2012; Vogler et al., 2017a). The relatively recent movement of the disease into limber pine forests of Colorado and portions of southern Wyoming coupled with the rising bark beetle epidemic, raise questions as to the future health of white pines in high-elevation forests of the U.S. Rocky Mountains.

Cronartium ribicola is a macrocyclic, heteroecious rust fungus and therefore requires an alternate host (*Ribes*, *Pedicularis*, or *Castilleja* species) to complete its life cycle. Sporulation, dispersal, and infection occur only when specific temperature and humidity requirements are met (McDonald and Hoff, 2001). "Wave years" with heavy pine infection occur during years when microclimatic conditions are suitable for *C. ribicola* infections. Unlike the Northern Rocky Mountains, wave years are likely infrequent in the warmer and drier ecosystems of the Southern Rocky Mountains leading to slower disease spread and intensification (Jacobi et al., 2018a). Spores produced on pines (aeciospores) in late spring/early summer infect alternate hosts; there is no pine-to-pine transmission. Aeciospores are thick-walled and hardy and can travel long distances (>100 km) in the wind. Basidiospores produced on alternate hosts in late summer/early fall infect pines. They are fragile and only travel short distances (1 km) in the wind. Following infection through needle stomata, fungal mycelium grows into the phloem eventually causing a canker. If an infection occurs close to the main stem, it will eventually grow into it and girdle the stem, killing the portion of the tree above the canker. Impacts on pines include branch death and topkill which reduce cone-production, and whole-tree mortality. The time it takes from infection to mortality depends on the location of the infection and tree size; small trees are killed rapidly (Geils et al., 2010).

Bark beetles may interact with WPBR to exacerbate declining health of limber pine. Mountain pine beetle (*Dendroctonus ponderosae*; MPB) is an aggressive, destructive bark beetle native to western North America. Nearly all western pine species are hosts, but lodgepole (*Pinus contorta*), ponderosa (*P. ponderosa*), whitebark (*P. albicaulis*), and limber pine are the most common hosts in the Rocky Mountains (Furniss, 1977; Alfaro et al., 2003; Gibson, 2003; Brown and Schoettle, 2008; Gibson et al., 2008). The most recent outbreak (roughly 1998–2013) particularly affected limber pine, a favored host (Langor, 1989; Cerezke, 1995), with concentrated mortality occurring on

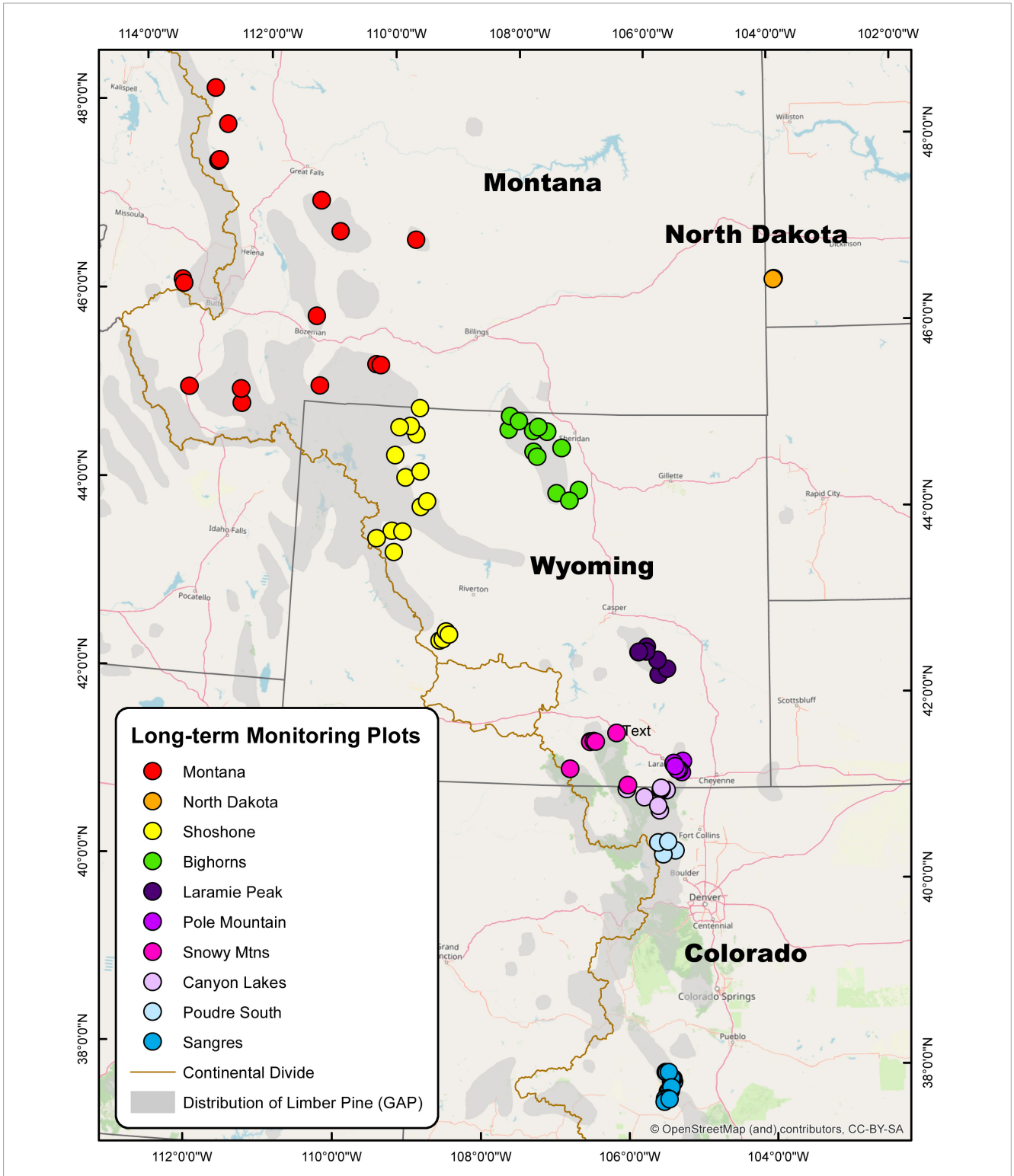

FIGURE 1
Map of 106 long-term limber pine health monitoring plots measured three times between 2004–2007 and 2016–2017 in the U.S. Rocky Mountains. The 10 study areas are denoted by color and include Montana (16), North Dakota (2), Shoshone (17), Bighorns (12), Laramie Peak (7), Pole Mountain (8), Snowy Mountains (7), Canyon Lakes (8), Poudre South (4), and Sangre de Cristos (25). Limber pine distribution (denoted in gray) was gathered from the USGS Gap Analysis Project (GAP).

over 500,000 ha in the Rocky Mountain Region and coinciding with severe drought, warm temperatures, and mild winters (Logan and Powell, 2001; Taylor et al., 2006; Vorster et al., 2017). As the MPB epidemic collapsed in northern Colorado and southern Wyoming, populations of *Ips woodi* increased, attacking, and killing limber pines in the absence of MPB (Witcosky, 2017). *Ips* activity continued for several years adding to the total losses of limber pine over the course of the epidemic.

The ability of limber pine to successfully regenerate is complicated by a variety of factors such as WPBR, its relatively slow ability to recover following natural disturbance (Schoettle, 2004; Coop and Schoettle, 2009), and climate change. WPBR quickly girdles young trees and cone-bearing branches on mature trees (Geils et al., 2010). Bark beetles can indiscriminately kill mature WPBR-resistant trees, reducing the favorable gene pool (Schwandt, 2006). Furthermore, evidence suggests that climates are becoming less hospitable for white pines (Rehfeldt et al., 2008; Larson, 2011; Malone et al., 2018; Millar et al., 2018), further exacerbating the ability for these species to recover. Knowledge of the current health status of limber pine and how stands are impacted by these damage agents over time will provide critical information to inform management and guide recovery efforts (Schoettle et al., 2022a).

Recent studies have surveyed limber pine health in a single time point (Burns, 2006; Kearns and Jacobi, 2007; Kliejunas and Dunlap, 2007; Burns et al., 2011; Klutsch et al., 2011; Maloney, 2011; Dunlap, 2012; Cleaver et al., 2015, 2017b, 2022; Shanahan et al., 2019) as well as in multiple time points (Smith et al., 2013a). In single time-point surveys, incidence and mortality rates show great variability between and even within mountain ranges (Burns, 2006; Kearns and Jacobi, 2007; Burns et al., 2011; Cleaver et al., 2015), demonstrating the complexity of forest health trends in the limber pine-WPBR pathosystem. Sites (not permanently monumented) in Wyoming and Colorado first measured by Kearns and Jacobi (2007) in 2002–2004 and remeasured by Cleaver et al. (2015) in 2011–2012 found WPBR incidence increased 6% (from 20 to 26%) and bark beetle mortality increased 17%. Smith et al. (2013a) surveyed limber pine throughout its range in the Canadian Rocky Mountains over 6 years from 2003 to 2009, with some sites surveyed over 13 years (1996–2009). They found incidence increased 10% and the disease continued to spread into new locations. Limber pines at the southernmost edge of their study, near the U.S.-Canada border, showed the highest WPBR infection and mortality rates. Results suggested long-term persistence of limber pine in some sites is in jeopardy.

Long-term surveys of permanent plots provide valuable insights into disease spread and development, which can be especially important in forested ecosystems, as changes to tree health may span many years (Cleaver et al., 2017a; Schoettle et al., 2019a,b). We assessed permanent plots throughout the U.S. Rocky Mountains and North Dakota over time to measure changes in health status and stand dynamics in limber pine populations. The objectives were to: (1) evaluate changes in limber pine abundance and health, (2) assess long-term, cumulative impacts of WPBR and bark beetles, and (3) evaluate site, stand, and environmental drivers of WPBR occurrence and severity at the tree and plot level. Results of this long-term study provide insight into temporal trends of the biotic agents threatening ecologically important limber pines to inform and guide management efforts.

2. Materials and methods

2.1. Study areas

The survey area extended through most of the distribution of limber pine in the U.S. Rocky Mountains and North Dakota. Permanent plots, ca. 106, were established within 10 study areas during the 2004 (Sangre de Cristo Mountains), 2006 (Poudre Canyon South, Canyon Lakes, Snowy Mountains, Pole Mountain, Laramie Peak, Bighorn NF, Shoshone NF), and 2007 (North Dakota, Montana) field seasons (**Figure 1**). Subsequent assessments took place from 2011 to 2014 and again in 2016 to 2017 (**Supplementary Table 1**). The northernmost plot was located on the Blackfeet Indian Reservation, Montana (48°15′7″ N, 112°48′2″ W) and the southernmost was on the Rio Grande National Forest, Colorado (37°36′41″ N, 105°31′48″ W). Two plots occurred on the west side of the Continental Divide, west of Butte, Montana, and the easternmost plots were in the badlands of western North Dakota. Plot locations were selected based on vegetation layers, limber pine composition >20% in previous surveys, and suggestions from local land managers. Plot locations were randomized across elevations, aspects, slope positions, WPBR incidence (where available), and stand species compositions.

2.2. Plot design

Plots were established as belt transects following methods adapted from the Whitebark Pine Ecosystem Foundation (Tomback et al., 2005). Each plot (60 × 15 m, 0.09 ha) was divided into three 20 × 15 m sections, except in the Sangre de Cristo Mountains where plot dimensions varied to include approximately 30 live white pines >1.37 m tall; but on average were 60 × 15 m (Burns et al., 2011). At the center point of each section, a fixed area circular subplot (0.004 ha, 3.6 m radius) was established to quantify ground cover, understory vegetation, and regeneration (stems <1.37 m tall). Plots were monumented with a labeled rebar stake (or PVC pipe) at the center point of each section and at the plot start and end points.

2.3. Survey methods

2.3.1. Site measurements

Site data collected included location (latitude/longitude), aspect (degrees), slope (percent), elevation (meters), slope position (summit, ridgetop, or plateau; shoulder; backslope; footslope; toeslope; valley bottom), stand structure (closed canopy single story, closed canopy multi-storied, open canopy scattered individuals, open canopy scattered clumps, mosaic), disturbance history (e.g., fire scars, tree cutting, mining activity, avalanche, and rock slides), and presence/absence of WPBR alternate hosts (*Ribes*, *Castilleja*, and *Pedicularis* spp.).

2.3.2. Trees >1.37 m in height

All trees (white pines only in the Sangre de Cristo Mountains) greater than 1.37 m tall were tagged and the following data were collected: species, diameter at breast height (dbh), health status (healthy: <15% damage to crown/stem; declining: 16–50% damage to crown/stem; dying: >50% damage to crown/stem; recent dead: no green needles, red needles/fine twigs present; old dead: no fine twigs, no needles), crown class (open grown, dominant, codominant, intermediate, overtopped, or krummholz), and damage agents and their severities. Trees growing in clumps

were considered individual stems if they were distinct at breast height (1.37 m). For white pines, additional information was collected including live crown ratio (the percent of total tree height that supports live foliage), canopy kill (visual estimate of the percentage of the canopy that was recently killed not including old dead branches lacking fine twigs or with <50% bark intact), presence or absence of live cones, and measurements to characterize WPBR presence and severity (see section "2.3.3. White pine blister rust assessments"). Trees that grew taller than 1.37 m during a measurement cycle were included as "ingrowth," tagged, and the above metrics were recorded. Cause of death was attributed to WPBR when an obvious extensive, lethal stem canker was present (regardless of beetle activity). Alternately, cause of death was attributed to bark beetles if the tree was mass attacked and did not have an extensive, lethal canker (otherwise, regardless of WPBR status). Year of attack for bark beetle-killed trees was estimated based on degradation classes of needles and fine branches as described by Klutsch et al. (2009). In the initial measurements, trees classified as "old dead" were not evaluated for damage or cause of death, as many were too degraded to accurately determine this information.

Species composition was assessed by categorizing stems as either limber pine or falling into one of the following categories: "Other Pines": lodgepole and ponderosa pine; "Other White Pines": whitebark and Rocky Mountain bristlecone (*Pinus aristata*) pine; "Spruce-Fir": Douglas-fir (*Pseudotsuga menziesii*), subalpine fir (*Abies lasiocarpa*), white fir (*Abies concolor*), and Engelmann spruce (*Picea engelmannii*); or "Other Spp.": Rocky Mountain juniper (*Juniperus scopulorum*) and quaking aspen (*Populus tremuloides*). In the Sangre de Cristo Mountains, a variable radius plot was established at the center point of the beginning, center, and end of each plot to collect data on stand composition including species, diameter class for trees taller than 1.37 m (0.1–12.6, 12.7–30.5, >30.5 cm dbh), and health status (see above) for all "in" trees.

Annualized mortality rates (M) were calculated as $M = 1 - (T_s / T_1)^{1/\Delta t}$ where T_s represents the number of live limber pine stems (>1.37 m tall) assessed during the first measurement cycle (2004/2006/2007) that were still alive in the final measurement cycle (2016/2017), T_1 represents the number of live limber pine stems (>1.37 m tall) assessed during the first measurement cycle, and Δt represents the number of growing seasons between each individual plot's first and final measurements (Dudney et al., 2020). Similarly, ingrowth recruitment rates (R) were calculated as $R = 1 - (T_s / T_3)^{1/\Delta t}$ where T_s represents the number of live limber pine stems (>1.37 m tall) assessed during the first measurement cycle (2004/2006/2007) that were still alive in the final measurement cycle (2016/2017), T_3 represents the number of live limber pine stems (>1.37 m tall) assessed during the final measurement cycle, and Δt represents the time interval (Dudney et al., 2020).

2.3.3. White pine blister rust assessments

Number of branch and stem cankers per crown and stem third were tallied for each infected white pine. This was done by visually dividing the entire length of the crown (using a planar method) and stem into thirds. In the absence of aecia or pycnia, at least three of the following five indicators needed to be present: roughbark, flagging, gnawing, sap production, and/or swelling. Stem cankers included all cankers on the main stem or within 15 cm of it. Branch canker lengths (horizontal extent of cankered bark, no measurements of radial canker extent were taken) were visually estimated for up to six branch cankers per crown third. These data were used as a surrogate for canker age allowing us to roughly estimate the year WPBR became established on a site and/or the frequency of infection events (Kearns et al., 2009). Cankers were put into 12-cm size classes that represented average annual canker growth (e.g., size 1 = >0–12 cm, size 2 = 12.1–24 cm, size 3 = 24.1–36 cm, etc.). Frequency of infection events was based on the number of canker size classes that occurred within a subregion. For example, if there were cankers in each of the 10 first size classes, we inferred infections occurred every year for the previous 10 years.

White pine blister rust disease severity was calculated for each tree based on cumulative crown and stem damage (Six and Newcomb, 2005). Crowns and stems were divided into thirds and evaluated based on the percentage of branches and bole circumference affected by cankers. For each crown and stem third, a score of 0 was assigned to 0% affected, 1 for <25% affected, 2 for 25–50% affected, and 3 for >50% affected. The 6 total scores per tree (3 crown and 3 stem) were summed to get the tree's severity rating. The maximum severity score possible for a tree was 18, however scores above 14 are unlikely as few trees survive with a score >12 (Six and Newcomb, 2005). Stand severity was characterized by calculating a mean severity score for all infected trees in the plot. Stand descriptors for rust infection included scores which ranged from 1 to 4.9 (light infection), 5 to 8.9 (moderate infection), and 9+ (heavily infected). Disease severity data were not collected in the Sangre de Cristo Mountains.

2.3.4. Regeneration

All regenerating tree species <1.37 m tall were evaluated within the three subplots (0.004 ha, 3.6 m radius). Data collected included species; height class (<25 cm or 25–137 cm); WPBR presence/absence; and cause of death (WPBR/not WPBR) for white pine species (see section "2.3.2. Trees >1.37 m in height"). Beginning in the 2011–2014 measurement cycle and onward, all white pine regeneration within the entire plot (60 m × 15 m, 0.09 ha) were tallied by species, with observations of WPBR presence/absence, and cause of death (WPBR/not WPBR). Regenerating species other than limber pine were only characterized from subplot data.

Additional data to assess the presence or absence of microsite conditions available for successful regeneration were collected in subplots. This included estimating percent ground cover of lichen/moss, rock, bare soil, litter, vegetation (shrubs and forbs), and tree stems/downed logs. The three most common shrub species were also noted.

2.4. Meteorological data

Meteorological data were summarized for the 4- and 15-year periods prior to the survey year for each plot per measurement cycle to assess their influence on *C. ribicola* occurrence, incidence, and severity. Information is lacking on the incubation period of *C. ribicola* on limber pine in the Rocky Mountains. The 4-year

cycles were used because early research in western white pine (*Pinus monticola*) indicates that while the timing varies by factors such as tree size and environmental conditions, 4-years is roughly the maximum length of time that it takes from infection to the appearance of obvious signs and symptoms of disease in the field (Lachmund, 1933).

Mean and total snow water equivalent were summarized for each 4- and 15-year period and maximum temperature, minimum temperature, average temperature, precipitation, and growing degree days (>5°C) were summarized for August and September (AS), the time when pine infection typically occurs; May to September (MS), the biological window when most *C. ribicola* sporulation occurs on pines and alternate hosts; and an annual average for the 4- and 15-year period using Daymet's 1-km daily surface weather grids (Thornton et al., 2016). Relative humidity (AS, MS, average annual) was derived from the Daymet dataset following the methods of Allen et al. (2006). Maximum and minimum vapor pressure deficit (daily values averaged for AS, MS, and the 4-year period) were obtained from PRISM Climate Group's 4-km recent year's climate data grids (PRISM Climate Group, Oregon State University).[1]

2.5. Data analyses

Statistical calculations were completed in SAS 9.4, JMP v14, or R (version 4.0.3; R Core Team, 2015). WPBR incidence values were estimated for each plot by calculating the number of live, infected trees out of total live limber pine surveyed. WPBR mortality was calculated as the number of limber pines killed by *C. ribicola* out of the total number (live and dead) limber pine. Mean incidence and mortality were determined by study area and overall using a generalized linear mixed model, PROC GLIMMIX, procedure in GLMM mode with plot location as random effect and year as fixed effect. Stand means were assessed for significant change ($P < 0.05$) by comparing the first measurement to the last measurement using *t*-tests in JMP or PROC TTEST option "paired" on count data (not percentages) in SAS. Standard error was calculated for the change between two means, pooling variance across measurements within a study area.

To evaluate the influence of site and stand factors and meteorological variables on the occurrence and severity of WPBR, generalized linear and logistic mixed-effects models were fit. Prior to model fitting, all climate variables were centered and scaled to enable comparison of model coefficients for variables measured on different scales (relative humidity, precipitation). Evaluation of meteorological data revealed summarization for the 4-years prior to each plot's measurement year provided the strongest correlation with WPBR parameters and thus only the 4-years data were used for modeling. All of the tree, plot, and climatic variables were evaluated for collinearity prior to model fitting, with variables exceeding 0.7 correlation removed. The model of WPBR occurrence was structured as a logistic regression from a binomial distribution with logit-link, where the presence of WPBR on a plot was denoted as a 1 and absence as a 0. The occurrence model treated plot and measurement period as random-effects, while evaluating the temporally dynamic fixed-effects. For the multiple linear models of WPBR severity change, it was necessary to use a Gamma distribution with log-link to account for the non-negative distribution of the response variable. In the severity model, plot was treated as a random-effect and years since the first measurement cycle at each plot (0–13 years) was added as a fixed-effect. The R statistical program was used for all modeling and significance testing using the lme4, lmerTest, and sjstats packages (Bates et al., 2014; Kuznetsova et al., 2017; Lüdecke et al., 2020). Parameters were backward eliminated from the models until the Akaike information criterion (AIC) could not be reduced further.

3. Results

3.1. Site characteristics

Plots were distributed across a variety of aspects, slopes, and slope positions and were located between 884–3,119 m (2,900–10,243 ft) elevation (**Supplementary Table 2**). When the study began, 7,174 (6,884 live) standing trees were assessed including 3,863 (3,623 live) limber pines (**Supplementary Table 2**). During the final assessment, plots contained 8,129 (6,461 live) standing trees, of which 4,176 (3,141 live) were limber pine (**Supplementary Table 2**). Plots had 34 (range 1–169) and 30 (range 1–162) live, limber pines on average at the start (2004–2007) and end (2016–2017) of the study, respectively. The percentage of plots with *Ribes* spp. present increased from 54 to 66% over the study. Other alternate hosts (*Castilleja* spp. and/or *Pedicularis* spp.) were present in 37% of plots during the final measurement cycle (data not collected in earlier measurements) (**Supplementary Table 1**).

3.2. Stand structure, species composition, and demographic rates

Mean dbh was 12.7 and 13.0 cm for live limber pines and 15.2 and 14.5 cm for dead limber pines, at the start and end of the study, respectively. At the beginning of the study, most recent mortality was mature trees (>12.7 cm dbh) and was attributed to bark beetles (**Table 1** and **Supplementary Table 6**). By the end of the study, most recent mortality was small trees (0.1–12.7 cm dbh) and was attributed to WPBR. Despite high levels of mortality, surveyed limber pine populations displayed a reverse-J size-class distribution throughout the study. This is typical in stable uneven-age stands, because the density of small trees is much greater than the density of large trees (O'Hara, 2002). While the proportion of limber pine stems to other tree species decreased by 4% (from 53 to 49%, **Supplementary Table 2**), the proportion that other co-occurring tree species contributed to species composition did not change significantly from start to end. After limber pine, spruce-fir and other species (Rocky Mountain juniper and quaking aspen) contributed the most to species composition (both contributed 16 and 18% to live stems at the start and end respectively) followed by other pines (13 to 11% of live stems, respectively), and other white

1 https://prism.oregonstate.edu

10.3389/ffgc.2023.1149456

TABLE 1 Causes of mortality for recently killed trees (>1.37 m tall) in each of the three measurement cycles.

Study area[a]	2004–2007				2004–2007 to 2011–2014				2011–2014 to 2016–2017			
	Count[b]	Bark beetles (no rust)[c] (%)	Bark beetles (w/rust)[d] (%)	Rust-killed[e] (%)	Count[b]	Bark beetles (no rust)[c] (%)	Bark beetles (w/rust)[d] (%)	Rust-killed[e] (%)	Count[b]	Bark beetles (no rust)[c] (%)	Bark beetles (w/rust)[d] (%)	Rust-killed[e] (%)
Overall	70	49	9	4	457	45	20	11	118	8	1	53
Sangres	*na*	*na*	*na*	*na*	34	3	0	6	29	0	0	45
Poudre South	0	0	0	0	9	100	0	0	6	33	0	0
Canyon Lakes	10	80	0	0	32	66	3	13	9	11	0	11
Pole Mountain	0	0	0	0	73	5	56	29	36	6	0	75
Snowy Mountains	6	100	0	0	28	96	4	0	2	0	0	0
Laramie Peak	16	31	0	0	45	27	9	11	10	0	10	80
Shoshone	14	71	0	0	118	58	17	12	13	23	0	38
Bighorns	2	100	0	0	52	54	29	8	2	0	0	50
Montana	22	14	27	14	66	56	14	3	11	9	0	73

[a]Dead trees were not evaluated during the first measurement cycle in the Sangre de Cristo Mountains. No dead trees were found in North Dakota. [b]Number of recent dead limber pines assessed. [c]Percentage of recent limber pine mortality caused by bark beetles (MPB and *Ips*) with no evidence of WPBR infection. [d]Percentage of recent limber pine mortality caused by bark beetles (MPB and *Ips*) on trees infected with WPBR. [e]Percentage of recent mortality caused by WPBR.

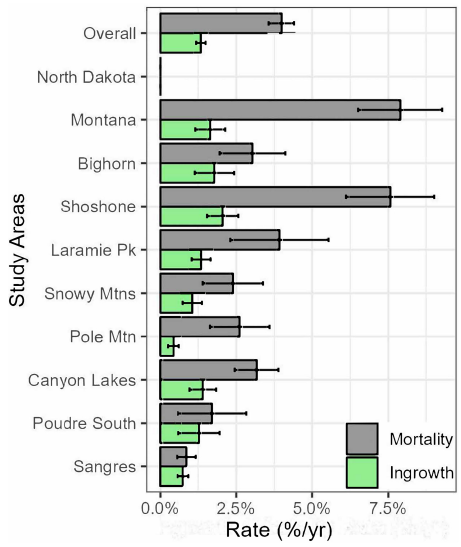

FIGURE 2
Annual mortality rate of trees >1.37 m tall from all causes (gray bars) and ingrowth recruitment rate (trees that grew taller than 1.37 m after the first measurement cycle; green bars) for limber pines overall and by study area from 2004–2007 to 2016–2017. Error bars indicate 95% confidence intervals.

pines (3 to 4% of live stems, respectively). The proportion of live limber stems declined slightly, though not significantly, in all study areas, except Laramie Peak and North Dakota (Supplementary Table 2).

Overall, average live tree density (stems ha^{-1}) declined significantly overall for all tree species over the study period (-55 ± 25 stems ha^{-1}, $P = 0.03$), and this was most pronounced in the Pole Mountain study area (-274 ± 84 stems ha^{-1}, $P = 0.01$; Supplementary Table 4a). However, while not significant, increases in aspen (Poudre South), spruce-fir (Snowy Mountain and Bighorns), and other pines (Bighorns) were observed (Supplementary Table 2). Live limber pine density also decreased significantly overall from 383 stems ha^{-1} in 2004–2007 to 333 stems ha^{-1} in 2016–2017 (-50 ± 10 stems ha^{-1}, $P < 0.001$). Decreases were greatest on Pole Mountain (-139 ± 47 stems ha^{-1}, $P = 0.02$), Shoshone NF (-99 ± 30 stems ha^{-1}, $P = 0.02$), and Montana (-66 ± 26 stems ha^{-1}, $P = 0.02$). Similarly, live limber pine basal area decreased significantly overall (-1.1 ± 0.2 m^2 ha^{-1}, $P = 0.01$; Supplementary Table 4b), with the most pronounced reduction at the Shoshone NF sites (-3.6 ± 1.6 m^2 ha^{-1}, $P = 0.03$). Density of live limber pine greater than 1.37 m tall in the small (<12.7 cm dbh) and medium (12.7–30.5 cm dbh) diameter classes decreased significantly while density in the large (>30.5 cm dbh) diameter class remained stable over the course of the study (Supplementary Table 5a).

The annualized mortality rate for limber pine was about 4%/year overall and ranged from <1%/year in the Sangre de Cristo Mountains to 8%/year in Montana (Figure 2). Ingrowth recruitment rates were lower than mortality rates overall (~1.25%) and in every study area. Ingrowth recruitment rates also had a narrower range than mortality rates from the lowest on Pole Mountain at <1% to the greatest on the Shoshone NF at ~2%.

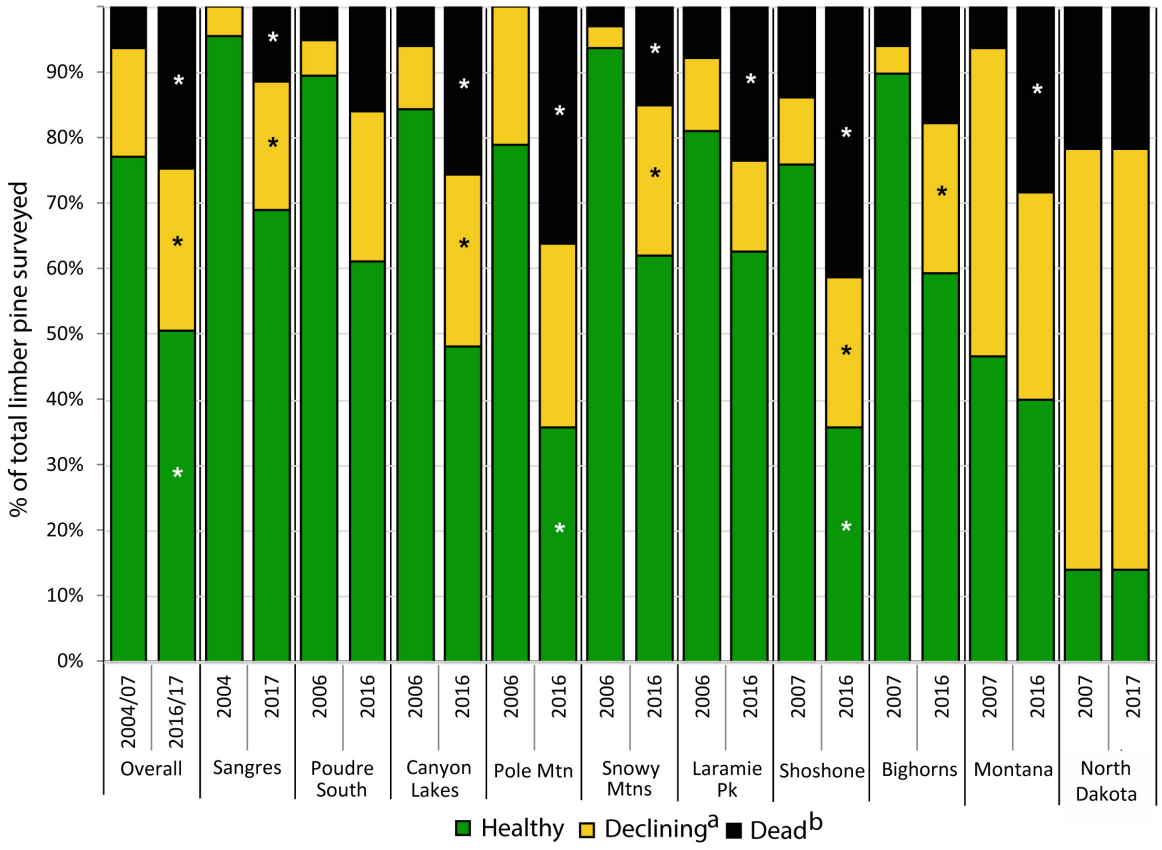

FIGURE 3
Changes in the health status of limber pine trees (>1.37 m tall) from 2004–2007 to 2016–2017 overall and within 10 study areas (a) includes all trees classified as declining or dying; (b) includes all trees classified as recent dead and old dead. Dead trees not measured in the Sangre de Cristos in 2004–2007. Asterisks represent significant change ($P < 0.05$) using paired *t*-test from 2004–2007 to 2016–2017 within study areas.

3.3. Limber pine health status

During the first measurement cycle, 81% of limber pines >1.37 m tall were classified as healthy, 14% were declining or dying, and 5% were dead. By the end of the study, only 50% were classified as healthy, while 25% were declining or dying and 25% were dead (Figure 3). WPBR was the most common damage agent observed and was detected on 52 and 50% of live, declining/dying trees at the start and end of the study respectively. Other damage agents noted on declining trees included bark beetles (3 and 15%), twig beetles (50 and 9%), animal damage (10 and 1%), and dwarf mistletoe (4 and 2%).

3.4. Limber pine mortality and causes

During the first measurement, 6% of all limber pines were standing dead (Figures 3, 4). Of the 70 recently killed trees assessed at the start of the study (cause of death not evaluated for old dead trees), 49% were killed by bark beetles with no evidence of WPBR, 9% were killed by bark beetles and were infected with WPBR, and 4% were killed by WPBR (Table 1). At that time, bark beetle mortality was detected in all study areas except Poudre South, Pole Mountain, and North Dakota. Mortality attributed to WPBR was only detected in Montana at the start of the study (Table 1). Mortality increased significantly overall and in most study areas from start to end (Figure 3) and the percentage of dead trees that were infected with WPBR increased significantly overall, and in most study areas (Figure 4; Pole Mountain, Laramie Peak, Shoshone, Bighorn, and Montana; data unavailable for Sangre de Cristos).

By the end of the study, 25% of limber pines were standing dead, this ranged from 12% in the Sangre de Cristo Mountains to 41% on the Shoshone NF (Figures 3, 4). Further, 5.1% of all initially living trees assessed were killed by WPBR over the study (Table 2). Of the recently killed trees assessed in the second measurement cycle (2011–2014, 457 trees), 45% were killed by bark beetles and had no evidence of WPBR, 20% were killed by bark beetles and had WPBR, and 11% were killed by WPBR (Table 1). Mortality attributed to bark beetles declined sharply between 2009 and 2013 and has remained at endemic levels since. Most (53%) of the recently killed trees assessed during the final measurement cycle (2016–2017, 118 trees) were killed by WPBR while only 9% were associated with bark beetles (Table 1). Cause of death could not be determined for most of the remaining recent dead trees. A small portion were killed by other factors including twig beetles (*Pityophthorus* and/or *Pityogenes* spp.), fire, limber pine dwarf mistletoe (*Arceuthobium cyanocarpum*), competition, and physical effects such as wind or lightning. Mortality caused by WPBR was observed in all study areas except Snowy Mountains,

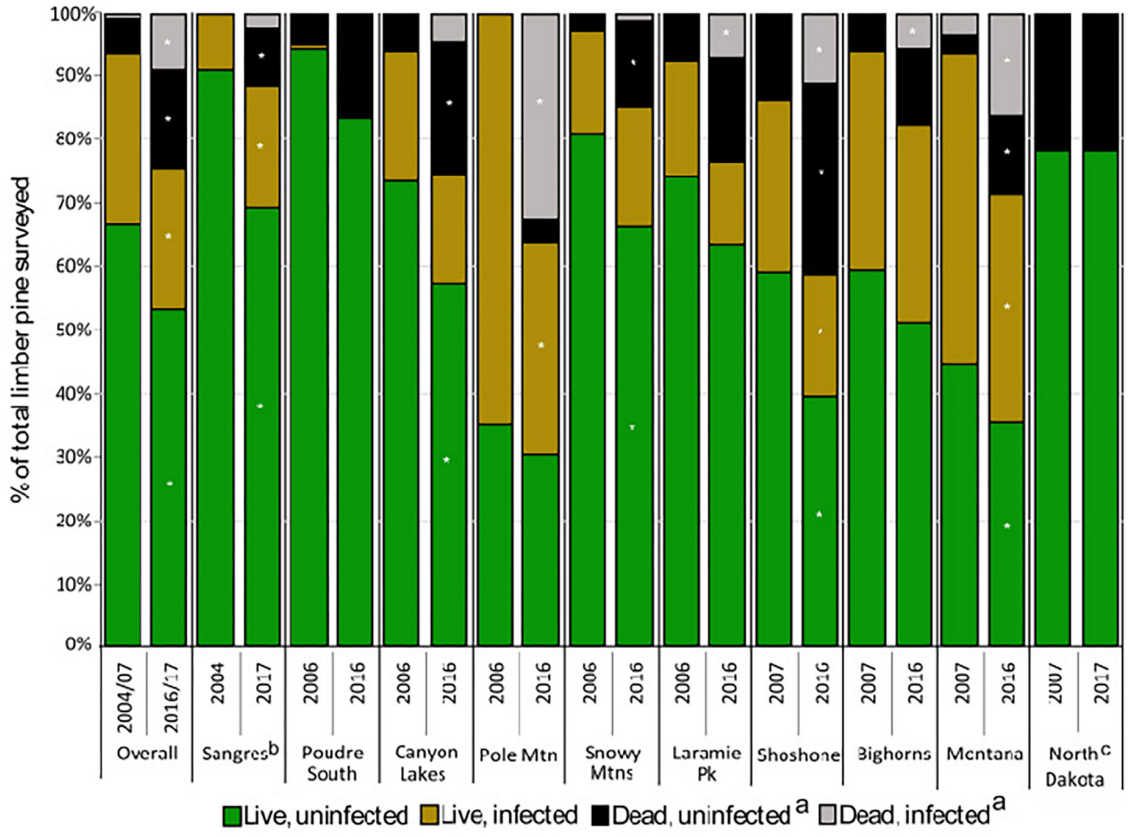

FIGURE 4
Status of limber pine (>1.37 m tall) and white pine blister rust infection (2004–2007 to 2016–2017) (a) dead from any cause; (b) dead trees were not recorded in the Sangres in 2004–2007; (c) rust was not detected in ND. Asterisks represent significant change ($P < 0.05$) using paired t-test from 2004–2007 to 2016–2017 within study areas.

Poudre Canyon South, and North Dakota. Bark beetle mortality was evident in all study areas except North Dakota but was very low in the Sangre de Cristo Mountains (<1% stems killed). Overall, more than 30% of trees killed by bark beetles were also infected with WPBR. On Pole Mountain, 84% of trees killed by bark beetles were also infected with WPBR.

Most bark beetle-killed trees (83%) were medium or large (≥12.7 cm dbh) while most WPBR-killed trees (84%) were small (<12.7 cm dbh) in size (Supplementary Table 6). The bark beetle mortality rate was greatest on the Shoshone NF (17%) and WPBR mortality rate was greatest on Pole Mountain (20%) (Supplementary Table 6).

3.5. Incidence and severity of white pine blister rust

White pine blister rust was found in all study areas except North Dakota and on 74 and 77% of all plots both at the start and end of the study, respectively (Supplementary Table 2). Over the study, six previously disease-free sites gained WPBR, 49% of plots gained more infected trees, and 5.9% of trees that were disease-free at the start became infected by the end (Table 3). The proportion of initially disease-free trees (>1.37 m tall) that became infected was highest in the Sangre de Cristo Mountains (13.6%) and lowest in the Canyon Lakes (3.1%) study areas. No new infected trees were detected in Poudre Canyon South. Further, of trees that grew taller than 1.37 m after the first measurement cycle ("ingrowth"), 7.1% were infected by the final measurement cycle; this ranged from 2.6% on the Bighorn NF to 14.1% in Montana. Overall, 65.2% of limber pines that were alive and disease-free at the start of the study (i.e., not including ingrowth) remained disease-free at the end. The lowest proportion of limber pines that remained disease-free occurred on Pole Mountain, where only 30.8% never showed any signs or symptoms of disease (Table 3). Nearly 15% of trees that were infected during the first measurement cycle were killed by rust impacts by the last measurement cycle (range 4–29%).

Disease incidence (# live infected trees/# live trees) increased slightly overall from start to end (29.0 to 30.5%, respectively) but not significantly (Table 4). Incidence increased significantly in the Sangre de Cristo Mountains over the study, going from 7.0 to 16.0% ($P = 0.006$), and declined significantly on Pole Mountain, going from 63.7 to 53.2% ($P = 0.0007$) (Table 4). Incidence was lowest in Poudre Canyon South (2.3%) and highest on Pole Mountain (53.2%) at the time of the final measurement cycle (no rust detected in North Dakota) (Table 4).

Stand density of limber pine (>1.37 m tall) declined by 33% over the study in the Pole Mountain area, where WPBR is well established, and by only 5% in the Sangre de Cristo Mountains,

10.3389/ffgc.2023.1149456

TABLE 2 Density of limber pine regeneration (<1.37 m tall) and WPBR incidence and mortality (2011–2013 to 2016–2017, whole plot counts of limber pine regeneration not collected in 2004–2007).

Study area	n[a]	Average density of live limber pine (stems ha^{-1})			Mean WPBR incidence[b] in live limber pine <1.37 m tall (%)			Mean mortality[c] in limber pine <1.37 m tall (%)		
		2011–2014	2016–2017	Change ± SE	2011–2014	2016–2017	Change ± SE	2011–2014	2016–2017	Change ± SE
Overall	106	161	181	20 ± 15	4.8	4.3	−0.4 ± 0.01	**1.0**	**2.6**	**1.6 ± 0.01**
Sangres	25	82	94	12 ± 16	3.8	5.7	1.9 ± 0.04	1.0	2.3	1.3 ± 0.02
Canyon Lakes	8	159	113	−46 ± 42	9.7	8.1	−1.6 ± 0.01	2.9	2.4	−0.5 ± 0.01
Laramie Peak	7	615	516	−99 ± 46	3.6	0.5	−3.1 ± 0.03	0.3	0	−0.3 ± 0.003
Pole Mountain	8	182	266	84 ± 64	12.7	12.5	−0.2 ± 0.05	3.4	7.5	4.0 ± 0.04
Snowy Mountains	7	101	85	−16 ± 12	0.6	0.0	−0.6 ± 0.01	0.0	1.4	1.4 ± 0.01
Poudre South	4	137	175	38 ± 14	0.0	0.0	0.0	0.0	0.0	0.0
Shoshone	17	142	173	31 ± 68	2.4	4.7	2.3 ± 0.04	0.2	0.4	0.2 ± 0.003
Bighorns	12	40	68	28 ± 17	4.2	1.1	−3.1 ± 0.03	0.0	6.7	6.7 ± 0.05
Montana	16	247	318	71 ± 45	5.3	2.6	−2.7 ± 0.02	1.0	2.5	1.5 ± 0.01
North Dakota[d]	2	–	16	–	–	0.0	–	–	0.0	–

[a]Number of plots. [b]Incidence is the number of infected, live limber pine (<1.37 m tall) divided by the total number of live limber pine (<1.37 m tall) in the plot. Due to our relatively long remeasurement cycles (~5 years), WPBR incidence in seedlings was likely greater than what we observed because of the short period in which seedlings may become infected with WPBR, die, and degrade. [c]Mortality includes the number of limber pines (<1.37 m tall) killed by WPBR divided by the total (live and dead) limber pines (<1.37 m tall) in the plot. Due to our relatively long remeasurement cycles (~5 years), seedling mortality was likely greater than what we observed because of the short period in which seedlings may become infected with WPBR, die, and degrade. [d]Plots in North Dakota were not measured during the second measurement cycle (2011–2014). SE represents standard error. Bolded values indicate significant change ($P < 0.05$) using paired t-test within the study area.

where WPBR has only recently invaded (Figures 5A, B). The decline at Pole Mountain was dominated by mortality of previously diseased trees (51%) while mortality of disease-free trees was largely offset by ingrowth (Table 3 and Figure 5A). The small decline in stand density in the Sangre de Cristo Mountains resulted from a proportionally similar mortality of trees that were diseased and disease-free (Figure 5B). The proportion of the stands composed of diseased trees decreased over time at Pole Mountain (65 to 52% from first to last measurement) and increased in the Sangres (9 to 22%) (Figures 5A, B). When all plots were combined, stand density of limber pine decreased by 14.4% overall with the decrease being experienced by both diseased and disease-free trees (Figure 5C).

While mean dbh of live limber pine overall was 13.0 cm, uninfected trees were 11.7 cm and infected trees 17.8 cm on average during the final measurement cycle, respectively. Most infected trees were less than 30.5 cm dbh and fairly equally distributed in the small and medium diameter classes (Supplementary Table 5b), but most rust-killed trees (85%) were small (<12.7 cm dbh).

Using the rating system established by Six and Newcomb (2005; see section "2.3.3. White pine blister rust assessments"), in 2004–2007, 14 sites (18%) had no rust detected, 62 sites (79%) were lightly infected, 3 sites (4%) were moderately infected, and 0 sites were heavily infected (Supplementary Table 7). However, by 2016–2017, 12 sites (15%) had no infection, 33 sites (42%) had light infection, 30 sites (38%) had moderate infection, and 4 sites (5%) were heavily infected. Overall, WPBR severity increased significantly from 2.5 to 5.0 (+2.5 ± 0.3, $P < 0.0001$; Table 4) from 2004–2007 to 2016–2017, as did severity in every study area except Poudre South and Laramie Peak (data not collected in Sangre de Cristo Mountains, no WPBR in North Dakota). The range of severity ratings over all plots in 2004–2007 was 1.0–5.3 which significantly increased to 1.0–11.4 in 2016–2017 ($P < 0.001$), with the highest severity sites (11+ rating) occurring in the Bighorn Mountains. Disease severity was lowest in Poudre South (2.0) and Snowy Mountains (2.3) study areas in 2016–2017.

As others have shown, branch cankers were well distributed throughout tree crowns (Burns et al., 2011; Crump et al., 2011; Jacobi et al., 2016). The average number of branch cankers per infected tree was 3.6 in 2004–2007 and decreased to 2.7 in 2016–2017 (−0.9 ± 0.1, $P < 0.0001$; Supplementary Table 7). However, the average number of stem cankers per tree increased significantly overall, from 0.7 to 1.0 (+0.3 ± 0.03, $P < 0.0001$), and in most study areas (Supplementary Table 7). During the first measurement cycle, 13% of infected limber pine (>1.37 m tall) had at least one stem canker in the lower stem third, but this increased to 16% in 2016–2017 (+3.6 ± 0.02%, $P = 0.04$). Similarly, 38% of infected trees had at least one stem canker at the beginning of the study but this increased to 50% (+11.8 ± 0.03%, $P = 0.0004$) by the end of the study.

At the time of the first measurement cycle, all subregions except Poudre South had cankers in 60% or more of the first 10 (12-cm) canker size classes. In the final measurement cycle, all subregions except Poudre South (20%) and Canyon Lakes (60%) had cankers in 80% or more of the first 10 (12-cm) canker size classes. Two of the more recently invaded study areas, the Sangre de Cristo and Snowy Mountains, had cankers in 90% or more of the (12-cm) canker size classes as did several study areas where the disease has been present for decades (Pole Mountain, Bighorns, and Shoshone).

10.3389/ffgc.2023.1149456

TABLE 3 Changes in the health and white pine blister status for all live limber pines assessed in the first measurement cycle to the last measurement cycle (2004/2006/2007 to 2016/2017) and white pine blister rust status for trees that grew taller than 1.37 m after the first measurement cycle and therefore were included in the plot as "ingrowth".

Study area	Plots (#)	Limber pines (>1.37 m tall) that were live in 2004–2007						Ingrowth trees	
		Live limber pines[a] (#)	Infected throughout[b] (%)	Became infected[c] (%)	Remained disease-free[d] (%)	Killed by WPBR[e] (%)	Mortality of infected trees[f] (%)	Ingrowth[g] (#)	Infected[h] (%)
Overall	106	3,624	29.0	5.9	65.2	5.1	32.6	298	7.1
Sangres	25	656	9.0	13.6	77.4	2.4	27.1	41	7.3
Poudre South	7	225	0.4	0.0	99.6	0.0	0.0	17	0.0
Canyon Lakes	4	223	22.0	3.1	74.9	4.0	22.5	25	4.0
Pole Mountain	8	312	65.1	4.2	30.8	20.2	50.7	16	6.3
Snowy Mountains	7	231	16.5	5.6	77.9	0.0	0.0	23	4.4
Laramie Peak	8	335	19.7	3.9	76.4	6.0	39.4	39	5.1
Shoshone	17	546	31.5	5.0	63.6	5.1	39.5	34	8.6
Bighorn	12	395	36.7	5.8	57.5	2.0	17.9	38	2.6
Montana	16	607	52.2	4.5	43.3	6.1	28.1	64	14.1
North Dakota	2	94	0.0	0.0	100.0	0.0	*na*	0	*na*

[a]Includes all live limber pines (> 1.37 m tall) that were assessed during the first measurement cycle (2004–2007). [b]Percentage of all limber pines that had WPBR throughout the entire study. [c]Percentage of all limber pines that were disease-free during the first measurement cycle but became infected by the end of the study. [d]Percentage of all limber pines that remained disease-free throughout the study. [e]Percentage of all limber pines that were live in 2004–2007 but were killed by WPBR during subsequent measurement cycles. [f]Percentage of all limber pines that were infected during the first measurement cycle but died from all causes by the end of the study. [g]Number of limber pines that grew taller than 1.37 m after the first measurement cycle and were therefore added as "ingrowth" trees. [h]Percentage of ingrowth trees that became infected by 2016–2017.

3.6. Limber pine regeneration (<1.37 m tall)

The average density of limber pine regeneration in 2011–2013 was 161 stems ha^{-1} and increased to 181 stems ha^{-1} in 2016–2017, though this change (20 ± 15 stems ha^{-1}) was not significant (Table 2). In 2011–2013, 4.8% of live stems <1.37 m tall were infected with WPBR which decreased to 4.3% in 2016–2017 though this change was also not significant (−0.4 ± 0.01%, $P > 0.5$). Of sites monitored for regeneration in 2011–2013 and 2016–2017 (Sangre de Cristo Mountains and North Dakota excluded), 24% had WPBR-infected regeneration in 2011–2013 which decreased to 18% in 2016–2017 though this change was not significant ($P = 0.26$; data not shown). However, mean WPBR-caused mortality increased significantly over all study areas from the start of the second measurement cycle to the end, going from 1.0% in 2011–2013 to 2.6% in 2016–2017 (+1.6 ± 0.9%, $P = 0.03$; Table 2). WPBR was the leading cause of death for regeneration (less than 1.37 m tall) during the final measurement cycle; roughly 47% of mortality was directly attributed to WPBR. Significant differences in regeneration density, WPBR incidence, and mortality were not observed in any study area (Table 2). Most sites had ≥20% limber pine species composition, however 6% of sites had no regeneration of any tree species and 24% had no limber pine regeneration observed during the study period. Most sites in the Bighorn Mountains (58%) had no limber pine regeneration throughout the study. Further, the Bighorn Mountains had the highest percentage of sites (25%) with no regeneration of any species followed by the Shoshone NF (18%) and Canyon Lakes (13%).

3.7. Modeling the drivers of white pine blister rust incidence and severity

Over the study period, the broader trends of increasing growing season length and aridity that have been seen in the central and southern Rocky Mountains (McGuire et al., 2012; Dee and Stambaugh, 2019) were also seen here at the plot and study area levels. Within all study areas, the average annual number of days above 5°C (growing degree days) increased by 13 to 53% (10 to 24 days) when comparing the 4-year window preceding the first and last measurement cycles. Similarly, August–September maximum vapor pressure deficit (VPD) increased 5.5 to 13% in six of the nine study areas, (North Dakota not included in this analysis; Supplementary Figure 1).

Variables selected in the final generalized logistic model of WPBR presence at the plot-level include both climatic and site variables. The probability of WPBR being present at a site increased with longer growing season length, if *Ribes* species were present, and at higher latitude (Table 5 and Figure 6A). The best model to predict tree-level WPBR infection probability included topographic and climatic variables. Probability of infection was greater for trees growing on northern slopes, at higher latitude, and on sites with lower maximum VPD in August and September (Table 5 and Figure 6B).

The final generalized linear model explaining changes in plot-level WPBR severity was only significantly linked with a single variable. Plot-level increases in disease severity were greatest on

10.3389/ffgc.2023.1149456

TABLE 4 Change in white pine blister rust incidence and severity in all live limber pine (>1.37 m tall) assessed for plots at the start (2004–2007) and end (2016–2017) of the study.

Study areas	*N*[c] plots	*N* trees		WPBR incidence (%)[a]			WPBR severity[b]		
		2004–2007	2016–2017	2004–2007	2016–2017	Change ± SE	2004–2007	2016–2017	Change ± SE
Overall	104	3,623	3,141	29.0 (0–100)	30.5 (0–100)	1.5 ± 0.01	**2.5 (1.0–5.3)**	**5.0 (1.0–11.4)**	**2.5 ± 0.3**
Sangres[d]	25	655	622	**7.0 (0–60)**	**16.0 (0–71)**	**9.0 ± 0.03**	*na*	*na*	*na*
Poudre South	4	225	214	2.3 (0–9)	2.3 (0–9)	0.0	1.0 (1.0–1.0)	2.0 (2.0–2.0)	1.0
Canyon Lakes	8	223	196	29.6 (0–83)	30.7 (0–83)	1.1 ± 0.01	**2.1 (1.0–4.4)**	**4.2 (1.5–8.1)**	**2.1 ± 0.6**
Pole Mountain	8	312	209	**63.7 (58–74)**	**53.2 (44–67)**	**−10.5 ± 0.02**	**3.5 (2.6–4.9)**	**7.1 (5.3–9.7)**	**3.7 ± 0.6**
Snowy Mountains	7	231	222	15.7 (0–47)	20.6 (0–38)	4.8 ± 0.03	**1.3 (1.0–1.7)**	**2.3 (1.5–4.2)**	**1.0 ± 0.4**
Laramie Peak	7	335	308	16.4 (0–45)	13.4 (0–40)	−2.9 ± 0.02	2.7 (1.0–5.0)	5.0 (1.7–8.7)	2.3 ± 1.1
Shoshone	17	546	391	29.7 (0–87)	31.3 (0–86)	1.6 ± 0.03	**2.0 (1.0–4.2)**	**4.5 (1.0–9.5)**	**2.4 ± 0.7**
Bighorns	12	395	377	48.6 (4–100)	48.5 (4–100)	−0.1 ± 0.03	**2.3 (1.0–3.9)**	**5.8 (1.3–11.4)**	**3.6 ± 0.8**
Montana	16	607	508	48.5 (0–94)	46.7 (0–94)	−1.8 ± 0.03	**3.6 (1.8–5.3)**	**5.4 (1.0–8.0)**	**1.8 ± 0.6**

Calculations are based on dynamic observations of the live trees at each monitoring period, such that the number of live trees varies between periods based on mortality and ingrowth. The two study areas with significant changes in disease incidence reflect both extremes along the disease progression spectrum. Incidence increased significantly in the newly invaded Sangre de Cristo Mountains and decreased significantly due to mortality of previously infected trees in the Pole Mountain area where WPBR is well established. [a]Number of infected live limber pine/total live limber pine per plot, per measurement cycle, averaged over all plots for the study area. [b]Within each plot, in each measurement cycle, disease severity was calculated for each infected tree based on cumulative crown and stem damage (Six and Newcomb, 2005). Crowns and stems were divided into thirds and evaluated based on percent of branches and bole circumference affected by WPBR. For each crown and stem third, a score of 0 was assigned to 0% affected, 1 for <25% affected, 2 for 25–50% affected, and 3 for >50% affected. The 6 total scores per tree (3 crown and 3 stem) were summed to get the tree's severity rating (i.e., maximum severity score possible for a tree was 18). Stand severity was characterized by calculating a mean severity score for all live infected trees (>1.37 m tall) in the plot. Stand severity scores ranged from 1 to 4.9 (light infection), 5 to 8.9 (moderate infection), and 9+ (heavily infected). [c]Number of plots in the study area. [d]Severity data not collected in the Sangre de Cristo Mountains. No rust detected in North Dakota. Bolded values indicate significant change ($P < 0.05$) using paired *t*-test within the study area.

sites with higher minimum VPD (Table 5). At the tree-level, changes in WPBR severity were explained by tree structure and climatic conditions. Infected trees with greater crown ratios had lower rates of annual change in WPBR severity. Additionally, trees on sites with more precipitation had lower annual change rates in WPBR severity, whereas trees at sites with greater maximum VPD had higher rate of change in WPBR severity over time (Table 5 and Figure 6C).

Variables selected in the final general logistic mixed-effects model predicting the probability of rust-caused mortality include tree structure and climatic attributes. The probability of mortality in infected trees was reduced as a tree's diameter increased. However, infected trees had a higher likelihood of being killed by WPBR on sites with higher maximum VPD in August and September, higher average temperatures in August and September, and as the number of growing degree days increased (Table 5).

4. Discussion

The cumulative impacts associated with WPBR and bark beetle-caused mortality resulted in notable declines of limber pine. Significant increases in the proportion of declining, dying, and dead trees were observed overall and in most study areas. These effects varied at the plot and study area levels depending on whether the disease was at an invading or established phase. By the end of the study, 25% of limber pines were declining or dying, another 25% were standing dead, and live limber pine density and basal area declined significantly. Live limber pine maintained a reverse J-shaped diameter distribution throughout the study indicating that some recruitment is occurring, but mortality (4%/year) greatly outpaced recruitment of ingrowth (~1%/year). Similar demographic trends have been observed in sugar pine (*Pinus lambertiana*) in the southern Sierra Nevada (Dudney et al., 2020) and in limber and whitebark pine in southern Alberta (Smith et al., 2013a,b). We also found strong relationships between meteorological factors and WPBR incidence and severity over time indicating long-term vulnerabilities to limber pine health.

While bark beetles and WPBR alone or in combination were significant mortality factors, the timing of these events varied. Most of the observed bark beetle mortality occurred between the first and second measurement cycles (i.e., after 2006/2007 but before 2014) whereas mortality caused by WPBR was chronic, becoming more common after the first measurement cycle and increasing steadily over time. We found similar cumulative mortality caused by bark beetles as Cleaver et al. (2015) in their 2011–2012 survey in a similar geographic area, but in contrast, by the end of our study WPBR was the leading cause of mortality in both trees and regeneration. Further, the proportion of all trees surveyed that were killed by blister rust in our study (5%) was double what Jacobi et al. (2018a) reported from their surveys of limber pine in Wyoming and Colorado between 2004 and 2012 (2.5%).

The incidence of WPBR increased slightly over the course of the study and across all study areas, though not significantly. The lack of significant change is likely due to high mortality of WPBR-infected trees caused by bark beetles and WPBR. However, this trend has shifted over time because new WPBR infections continue to occur consistently while bark beetle mortality has

10.3389/ffgc.2023.1149456

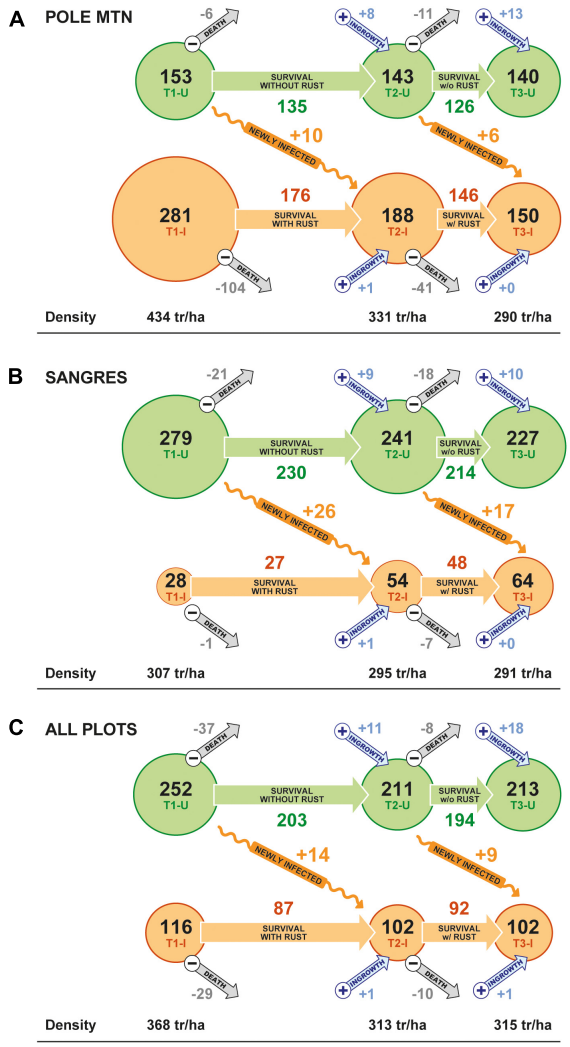

FIGURE 5
Changes in stand density (trees ha^{-1}) across the three measurement periods (T1, T2, and T3) of disease-free (green circles) and diseased (orange circles) limber pine trees greater than 1.37 m tall in the **(A)** Pole Mountain area, **(B)** Sangres area, and **(C)** for all plots combined. Pole Mountain is an example of where WPBR is well established, and the Sangre de Cristo area is one that has only recently been invaded by *C. ribicola*. Within each panel, gray arrows depict density loss to mortality (all causes) and blue arrows indicate ingrowth of new trees into the >1.37 m height class. The horizontal distance between T1, T2, and T3 circles generally reflects time between measurement periods. The orange squiggly arrows show the density of trees that transitioned from disease-free to diseased between the two time periods. Average tree density has been rounded to the nearest individual per hectare to simplify the presentation.

subsided. Like Jacobi et al. (2018a), our analysis demonstrated that infection events occur regularly throughout the relatively dry climates of our study area, both at the disease front and in areas where the pathogen is well established (Kearns et al., 2009). Disease incidence remained the same or increased in study areas where the pathogen is considered "invading" (Sangre de Cristo Mountains, Snowy Mountains, and Poudre South) and remained the same or decreased in study areas where it is considered "established" (e.g., Pole Mountain, Bighorns, and Montana; Jacobi et al., 2018a). Over the study, nearly half of all plots gained more infected trees and 6% of trees that were disease-free during the first measurement cycle and 7% of ingrowth became infected. Still, the current distribution of WPBR is likely underestimated since detection is especially difficult during the early stages of invasion. In the more recently identified outbreak areas, such as the Sangre de Cristo Mountains and Poudre South, blister rust was likely present for at least 10–15 years before it was detected and reported (Burns, 2006; Schoettle et al., 2018). More frequent surveys that coincide with the timing of sporulation on pines are needed to get a more accurate estimate of disease distribution.

Surges in disease severity were evident not only through increased rust-caused mortality but also by substantial increases in stem canker incidence and stand level disease severity ratings. Disease severity increased overall and in every study area where blister rust was detected. The number of stem cankers per infected limber pine also increased significantly from 0.7 to 1.0 stem canker per infected limber pine. This is much higher than the ~0.2 stem cankers per infected tree that Kearns and Jacobi (2007) found during their 2004 survey in southeast Wyoming and northern Colorado. Our results are in line with a 10-year study examining WPBR on limber pine in Canada that found a similar trend of increasing stem canker incidence over time (Smith et al., 2013a). Stem cankers in the upper and lower stem are both detrimental to limber pine health and survival. Stem cankers in the upper crown reduce cone production since cones occur more frequently on upper crown branches (Steele, 1990), leading to reduced regeneration. Lower stem cankers are much more likely to girdle and kill the entire tree, thus these observed increases suggest higher likelihoods of mortality. In both cases, increased incidence of stem cankers drives decline and mortality, especially in small trees and regeneration. Our data highlights that both sites where rust is well established and those closer to the disease front are facing increasing disease severity which will likely lead to increased mortality.

Variation in WPBR disease incidence across the landscape is likely to continue even as the pathogen becomes well established. Disease incidence is the outcome of complex interactions among environmentally controlled infection probabilities and severity (e.g., this article), geographically variable genetic disease resistance frequencies in pine populations (e.g., Schoettle et al., 2014), pine population size and dynamics (e.g., Field et al., 2012), biotic and abiotic stresses that affect pine health and mortality (e.g., this article; Fettig et al., 2022), and other factors. The ability of recruitment to offset tree mortality and support adaptation to WPBR will determine the sustainability of limber pine populations (Schoettle et al., 2019b, 2022a). Consequently, as WPBR becomes naturalized in North America, the surviving populations will likely exhibit diverse spatial and temporal patterns of disease prevalence, as is observed for native forest diseases (Burdon and Thrall, 1999).

We developed models to identify meteorological variables, tree and stand characteristics, and site factors associated with the probability of WPBR infection, rust-caused mortality, and changes in disease severity at the tree and stand level. The probability of tree infection was greater on sites with northern exposure (cooler), higher latitude (longer pathogen presence), and lower maximum August and September VPD (less arid). Unlike what others

10.3389/ffgc.2023.1149456

TABLE 5 Summary of best model subsets from final logistic and linear mixed-effects regressions predicting white pine blister rust presence, infection probability, change in disease severity, and probability of mortality at the tree and stand level.

Model and parameters	Coefficients	SE	*P*-value
Rust presence (stand)[a]	**$R^2_{cond} = 0.920$**	**$R^2_{Marg} = 0.107$**	**AIC = 181.2**
Intercept	−23.920	10.905	0.028
Growing degree days (4 years; >5°C)	0.053	0.033	0.104
Latitude	0.544	0.261	0.037
Ribes on the plot	0.000	0.000	
Ribes not on the plot	−1.248	1.023	0.223
Probability of infection (tree)[a]	**$R^2_{cond} = 0.817$**	**$R^2_{Marg} = 0.386$**	**AIC = 5147.7**
Intercept	−10.283	4.112	0.012
Cosine aspect[b] (1 = north, −1 = south)	1.778	0.416	<0.001
Latitude	0.653	0.099	<0.001
Maximum VPD[d] August–September (4 years; hPa)	−1.054	0.048	<0.001
Change in WPBR severity (stand)[c]	**$R^2_{cond} = 0.442$**	**$R^2_{Marg} = 0.027$**	**AIC = 147.9**
Intercept	−0.0338	0.3213	0.925
Minimum VPD[d] (4 years; hPa)	0.2643	0.1129	0.021
Change in WPBR severity (tree)[c]	**$R^2_{cond} = 0.246$**	**$R^2_{Marg} = 0.130$**	**AIC = 3726.9**
Intercept	1.386	0.618	0.056
Crown ratio (%)	−0.011	0.001	<0.001
Precipitation (4 years; mm)	−0.0015	0.0004	<0.001
Maximum VPD[d] (4 years; hPa)	0.053	0.043	0.025
Probability of mortality (tree)[a]	**$R^2_{cond} = 0.735$**	**$R^2_{Marg} = 0.488$**	**AIC = 1169.1**
Intercept	−20.952	2.156	<0.001
dbh (cm)	−0.344	0.042	<0.001
Growing degree days (>5°C)	0.041	0.011	<0.001
Maximum VPD[d] August–September (4 years; hPa)	0.275	0.081	<0.001
Average temperature August–September (4 years; °C)	0.752	0.143	<0.001

[a]Logistic mixed-effects regression. [b]A cosine transformation of aspect was used to obtain a continuous variable that characterized the north-south gradient (northness). Cosine aspect will be close to 1 if a site is more north-facing, close to −1 if it is more south-facing, and close to 0 if it is either east or west. [c]Linear mixed-effects regression. [d]Vapor pressure deficit (VPD) is the difference (deficit) between the amount of moisture in the air and how much moisture the air can hold at the ambient temperature when it is saturated. It is calculated as the difference between actual vapor pressure and saturation vapor pressure. In limber pine habitats, high VPD levels in general reflect hotter, drier conditions while lower VPD reflect cooler, more humid conditions.

have reported, tree and stand characteristics were not important predictors of rust presence or incidence in our study (Smith and Hoffman, 2001; Kearns and Jacobi, 2007; Kearns et al., 2014; Cleaver et al., 2015). However, our results align with other studies that found increasing probability of infection where environmental conditions are cooler and more humid, and on sites located in more northern geographic positions (Kearns and Jacobi, 2007; Cleaver et al., 2015). A recent study of limber pine condition along Montana's Rocky Mountain Front suggests the positive association between infection probability and latitude may not persist over time because new WPBR infections appear to have plateaued (Cleaver et al., 2022). While they reported a small proportion of new infections, they also found no evidence of recent wave years, which may be due to hotter, drier conditions associated with climate change. If western forests experience drought and warmer temperatures in the future as anticipated (McGuire et al., 2012; Dee and Stambaugh, 2019), wave year events may occur less frequently. However, our analysis of canker sizes indicated that infections occurred nearly every year in most areas throughout the study even though the U.S. Rocky Mountains were experiencing persistent drought.

Our study found strong relationships between aridity and WPBR infection probability, disease severity progression, and tree mortality. The probability of WPBR-induced mortality was greater for trees, particularly with smaller diameters, growing on sites with a longer growing season, and higher average temperature and maximum VPD in August and September (more arid), consistent with Dudney et al. (2021). Similarly, we observed greater annual change in WPBR severity for infected trees growing on sites with lower annual precipitation and higher maximum VPD (more arid), suggesting that disease severity and subsequent mortality may increase in the future as climates become warmer and drier. Limber pine stomata are particularly responsive to changes in VPD (Pataki et al., 2000) so at high maximum VPD, stomatal closure would likely restrict infection. Higher minimum VPD levels would suggest sustained conditions of high evaporative demand that could lead to water stress in trees if available soil water was limited (as is likely in August and September in most of the Rockies). Our modeling suggests that sustained late season water stress contributes to accelerated disease progression, resulting in mortality. Other studies have shown that canker diseases induce loss of sapwood hydraulic function thereby reducing a tree's capacity to survive increased exposure to severe drought conditions (Hossain et al., 2018). Drought can also reduce tree defenses to bark beetles

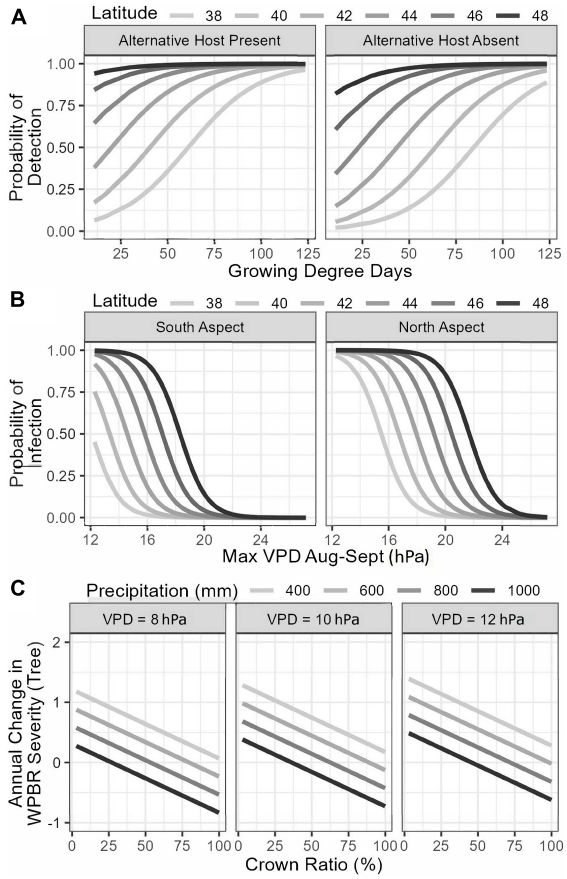

FIGURE 6
Best subset logistic regression **(A,B)** and final general linear mixed effects **(C)** models predicting white pine blister rust presence in a stand **(A)**, tree infection probability **(B)**, and annual change in disease severity **(C)** based on stand, site, and meteorological variables.

resulting in more successful beetle attacks leading to mortality (e.g., Bentz et al., 2022).

Natural selection against WPBR-susceptible individuals is evident, especially in study areas with high WPBR incidence such as Pole Mountain. Declining density of diseased trees within populations due to WPBR-caused mortality is reducing population size and thus disease incidence. This pattern was also reported for heavily impacted limber pine populations in southern Alberta (Smith et al., 2013a). The relative stability of the density of disease-free trees at Pole Mountain is, in part, a consequence of ingrowth offsetting new tree infections. Genetic resistance to WPBR is likely also a contributing factor as qualitative resistance, associated with a single resistance gene, is present in limber pine in this area (Schoettle et al., 2014). Qualitative resistance causes an immunity response which is conferred by a single dominant resistance gene (an R gene) which curtails disease progression, and therefore visible disease symptoms, in infected trees (Kinloch and Dupper, 2002). Qualitative resistance can also be referred to as complete resistance or major gene resistance (MGR). The resistance gene Cr4 conveys this immunity response in limber pine (Schoettle et al., 2014). An average of 5% of the pre-WPBR invaded limber pine population in the southern Rockies is estimated to have the Cr4 R gene and that frequency can be 13.9% or higher in some stands (Schoettle et al., 2014, 2019a). Therefore, it is likely that many of the remaining disease-free trees at Pole Mountain have the Cr4 resistance allele. If enough resistant trees persist and reproduce, stand density may recover over time (barring other disturbances). This may take many decades since it can take more than 50 years for limber pine to mature and many more to produce a full cone crop (Johnson, 2001). However, if a virulent strain of *C. ribicola* develops in the area that can overcome Cr4-resistance, there will likely be another surge in disease incidence and a further reduction in stand density.

Quantitative resistance to WPBR also exists in limber pine but the limited available research suggests that its frequency may be very low in limber pine populations (Jacobi et al., 2018b; Schoettle et al., 2022b). In contrast to qualitative resistance, quantitative resistance is conferred by the small contribution of many genes which makes it less likely to be overcome by a simple mutation in the rust and therefore is more durable over time. Quantitative resistance to WPBR suppresses but generally does not prevent disease (King et al., 2010). Individuals show a range of susceptibility, presumably dependent on which and how many genes are inherited that contribute to resistant phenotypes (King et al., 2010). The effectiveness of some of the traits can be reduced by high *C. ribicola* infection (King et al., 2010; Jacobi et al., 2018b). This in combination with other mortality factors (e.g., fire and bark beetles) can reduce the available quantitative and qualitative resistance traits to WPBR in the population, further increasing the probability of WPBR-caused mortality (Schoettle and Sniezko, 2007; Schoettle et al., 2022a). Furthermore, the frequency of quantitative resistance traits alone may be too low in limber pine to sustain viable populations, especially under high WPBR pressure, without active management (Schoettle et al., 2022a).

Tree mortality by WPBR, i.e., natural selection, has only just begun in the newly invaded study areas, such as the Sangre de Cristo Mountains. Increasing WPBR incidence over time demonstrates that the population contains abundant susceptible individuals on which selection can act. When combining results from all study plots, one could incorrectly infer that WPBR incidence is stable across the U.S. Rockies over the sampling time of this study. However, closer inspection reveals that the forest health condition is not uniform, highlighting the importance of scale over which forest health information is coalesced. The invasion and adaptation process to WPBR is at different stages and proceeding at different rates across the greater U.S. Rockies landscape (Schoettle et al., 2022a).

Regeneration was assessed over time and provides insight into trends regarding changes in limber pine composition and abundance over time. Though most sites surveyed had at least 20% composition of limber pine in the overstory, 24% of sites had no limber pine regeneration and 6% of sites had no regeneration of any species throughout the entire study period. Our study found limber pine regeneration on fewer sites than Cleaver et al. (2017b) in Colorado and Wyoming and Smith et al. (2013a) in Alberta, Canada. While we found increasing limber pine regeneration abundance over the course of the study, it was only present on 50, 55, and 59% of plots at the start, middle, and end, respectively. In contrast, Cleaver et al. (2017b) found limber pine regeneration present on 92% of plots in 2011–2012, but average density was slightly lower overall than what we report here (141 vs. our 181 stems ha^{-1}). Smith et al. (2013a) reported an increase in

limber pine regeneration in plots in Alberta, Canada over a 10-year period from 76% in 2003–2004 to 85% in 2009 having at least one limber pine seedling, and density increased from 100 seedling ha^{-1} to 150 seedling ha^{-1} in the same time frame. While limited in our study plots, it is possible that limber pine regeneration is present in other forest types of the U.S. Rocky Mountains (Windmuller-Campione and Long, 2016). Goeking and Windmuller-Campione (2021) analyzed a large USDA Forest Service, Forest Inventory and Analysis 10-year dataset and found that limber pine regeneration occurred more abundantly in non-limber pine forest types.

While WPBR incidence remained stable in limber pine regeneration (∼4.5%) over the study, we observed a significant increase (1.0–2.6%, +1.6%) in WPBR-caused morality in regeneration. When considered with our low regeneration rates, increasing mortality of regeneration is concerning because as overstory mortality occurs fewer limber pine seedlings may survive long enough to replace them. While rust incidence levels were similar to Cleaver et al. (2017b; 5.3%), our mortality levels were higher, which one would expect given more time. As observed in Smith et al. (2013a), the short period in which small seedlings may become infected with WPBR, die, and degrade from a site makes determining trends in WPBR infection and mortality difficult and likely underreported. Due to our relatively long remeasurement cycles (∼5 years) seedling infection and mortality was likely greater than what we observed.

It is likely that WPBR and episodic bark beetle outbreaks, the length and severity of which are dependent on many factors including favorable climatic and stand conditions, and proximity to bark beetle populations, will continue to be prominent damage agents in these regions (Jacobi et al., 2018a; Fettig et al., 2022). Therefore, long-term monitoring will be critical to inform and guide conservation and management efforts to retain and restore this ecologically important species as climates change in the U.S. Rocky Mountains. Though there are inherent difficulties in maintaining long-term study plots in remote areas, the data provided by measuring monumented trees over time enables characterizing changes in extent and progression of slow spreading damage agents. Such studies also allow the identification of healthy populations to focus proactive management strategies (Schoettle et al., 2019b, 2022a). Likewise, populations with high WPBR-caused mortality may provide putatively resistant seed sources for additional rust-resistance screening and outplanting. Additionally, management efforts to preserve multiple diameter classes can promote stand resilience when faced with future bark beetle episodes and continued WPBR impacts (Schoettle and Sniezko, 2007).

5. Conclusion

Assessing species composition over time, particularly after a significant portion of the limber pine population was killed by the recent bark beetle epidemic and ongoing WPBR infections, allowed for insight on how forest landscapes are being affected by these biotic factors. Live limber pine density and basal area significantly decreased over all plots. Limber pine is considered an early seral species outcompeted in moderate environmental conditions by species such as subalpine fir, Engelmann spruce, and Douglas-fir, but on harsh, rocky, and xeric sites it is considered a climax species (Veblen, 1986; Rebertus et al., 1991; Donnegan and Rebertus, 1999). However, 7% of study sites had no regenerating species of any kind recorded. Coupled with the significant health decline and mortality of limber pine, these numbers are unsettling regarding recruitment and resiliency in these sites in the future.

As WPBR is now a permanent biotic factor of North American ecosystems, evaluating disease spread through the remaining range of white pines and continued monitoring of disease intensification and impacts will be critical for developing effective management strategies that are appropriate for specific forest health conditions to preserve this ecologically important species. Though bark beetle populations have returned to endemic levels, a large proportion of live limber pines that survived are now declining or dying, primarily due to WPBR. These results confirm that WPBR is negatively affecting the health of limber pine populations in the U.S. Rocky Mountains and will continue to do so over time, as suggested by our modeling results. The dramatic increase in severity of WPBR impacts, both at the tree and plot levels, is further evidence of this. With climate models predicting continued warming, there is potential for more frequent and severe bark beetle epidemics in the future, making the identification and preservation of WPBR-resistant limber pines increasingly critical (Schoettle and Sniezko, 2007; Schoettle et al., 2022a).

Data availability statement

The raw data supporting the conclusions of this article will be made available by the authors, without undue reservation.

Author contributions

KB, WJ, AS, and JS conceived of the study. KB and KL collected the field data. All authors contributed to the data analysis and writing, editing, and approving the final manuscript.

Funding

This study was funded by the U.S. Department of Agriculture, Forest Service, Forest Health Protection, Evaluation Monitoring Program to KB and JS (INT-EM-B-16-01).

Acknowledgments

We thank Great Sand Dunes National Park and Preserve (F. Bunch and P. Pineda-Bovin), Rocky Mountain National Park (B. Verhulst and J. Connor), Blackfeet Indian Reservation, Montana DNRC (A. Gannon), and U.S. Department of Agriculture, Forest Service personnel from the Shoshone, Bighorn, Medicine Bow, Roosevelt, San Isabel, and Rio Grande National Forest for logistical support. We especially thank all of those who helped

with field work, data entry, and analyses: A. Casper, J. Blodgett, J. Backsen, M. Jackson, G. DeNitto, J. Klutsch, B. Howell, M. Halford, M. Laskowski, R. Beam, J. Hof, E. Janasov, S. Doria, B. Lalande, S. Stratton, B. Stone, C. Holtz, S. Stephens, and D. Shorrock. The contributions of U.S. Government employees to this work were supported in part by their respective agencies.

Conflict of interest

The authors declare that the research was conducted in the absence of any commercial or financial relationships that could be construed as a potential conflict of interest.

Publisher's note

All claims expressed in this article are solely those of the authors and do not necessarily represent those of their affiliated organizations, or those of the publisher, the editors and the reviewers. Any product that may be evaluated in this article, or claim that may be made by its manufacturer, is not guaranteed or endorsed by the publisher.

Author disclaimer

The findings and conclusions in this publication are those of the authors and should not be construed to represent any official U.S. Department of Agriculture or U.S. Government determination or policy.

Supplementary material

The Supplementary Material for this article can be found online at: https://www.frontiersin.org/articles/10.3389/ffgc.2023.1149456/full#supplementary-material

References

Alfaro, R. I., Campbell, R., Vera, P., Hawkes, B., and Shore, T. (2003). "Dendroecological reconstruction of mountain pine beetle outbreaks in the Chilcotin Plateau of British Columbia," in *Mountain pine beetle symposium: Challenges and solutions, information report BC-X-399*, eds T. L. Shore, J. E. Brooks, and J. E. Stone (Kelowna: Natural Resources Canada), 245–256.

Allen, M., Pereira, R. G., Raes, L. S., and Smith, D. (2006). *FAO irrigation and drainage paper. Crop evapotranspiration (Guidelines for computing crop water requirements)*. Paper No. 56. Rome: Food and Agriculture Organization, 46.

Bates, D., Mächler, M., Bolker, B., and Walker, S. (2014). Fitting linear mixed-effects models using lme4. *arXiv [Preprint]* doi: 10.48550/arXiv.1406.5823

Bentz, B. J., Millar, C. I., Vandygriff, J. C., and Hansen, E. M. (2022). Great Basin bristlecone pine mortality: Causal factors and management implications. *For. Ecol. Manag.* 509:120099. doi: 10.1016/j.foreco.2022.120099

Blodgett, J. T., and Sullivan, K. F. (2004). First report of white pine blister rust on Rocky Mountain bristlecone pine. *Plant Dis.* 88, 311–311. doi: 10.1094/PDIS.2004.88.3.311A

Brown, P. M., and Schoettle, A. W. (2008). Fire and stand history in two limber pine (*Pinus flexilis*) and Rocky Mountain bristlecone pine (*Pinus aristata*) stands in Colorado. *Int. J. Wildland Fire* 17, 339–347. doi: 10.1071/WF06159

Burdon, J. J., and Thrall, P. H. (1999). Spatial and temporal patterns in coevolving plant and pathogen associations. *Am. Nat.* 153, S15–S33. doi: 10.1086/303209

Burns, K. (2006). *White pine blister rust in the Sangre de Cristo and wet mountains of southern Colorado, biological evaluation, R2-06-05*. Lakewood, CO: US Forest Service Rocky Mountain Regional Office.

Burns, K., Blodgett, J., Jackson, M., Howell, B., Jacobi, W., Schoettle, A., et al. (2011). "Monitoring limber pine health in the Rocky Mountains and North Dakota," in *Proceedings of the future of high-elevation, five-needle white pines in Western North America: High five symposium, proceedings RMRS-P-63*, eds R. E. Keane, D. F. Tomback, M. P. Murray, and C. M. Smith (Fort Collins, CO: U.S. Department of Agriculture Forest Service), 47–50.

Cerezke, H. (1995). Egg gallery, brood production, and adult characteristics of mountain pine beetle, *Dendroctonus ponderosae* Hopkins (Coleoptera: Scolytidae), in three pine hosts. *Can. Entomol.* 127, 955–965. doi: 10.4039/Ent127955-6

Cleaver, C., Gannon, A., Hanna, D., McKeever, K., Jackson, M., Kramer, A., et al. (2022). "Limber pine condition along Montana's Rocky Mountain front," in *Forest health monitoring: National status, trends, and analysis 2021. General technical report. SRS-266*, eds K. M. Potter and B. L. Conkling (Asheville, NC: U.S. Department of Agriculture Forest Service Southern Research Station), 177–181. doi: 10.2737/SRS-GTR-266-Chap12

Cleaver, C. M., Burns, K. S., and Schoettle, A. W. (2017a). *Limber pine and white pine blister rust monitoring and assessment guide for Rocky Mountain National Park. Inter-agency agreement 15-IA-11221633-157*. Fort Collins, CO: U.S. Department of Agriculture Forest Service Rocky Mountain Research Station, 28.

Cleaver, C. M., Jacobi, W. R., Burns, K. S., and Means, R. E. (2017b). Limber pine regeneration and white pine blister rust in the central and southern Rocky Mountains. *For. Sci.* 63, 151–164. doi: 10.5849/forsci.16-052

Cleaver, C. M., Jacobi, W. R., Burns, K. S., and Means, R. E. (2015). Limber pine in the central and southern Rocky Mountains: Stand conditions and interactions with blister rust, mistletoe, and bark beetles. *For. Ecol. Manag.* 358, 139–153. doi: 10.1016/j.foreco.2015.09.010

Coop, J. D., and Schoettle, A. W. (2009). Regeneration of Rocky Mountain bristlecone pine (*Pinus aristata*) and limber pine (*Pinus flexilis*) three decades after stand-replacing fires. *For. Ecol. Manag.* 257, 893–903. doi: 10.1016/j.foreco.2008.10.034

COSEWIC (2014). *COSEWIC assessment and status report on the limber pine Pinus flexilis in Canada*. Ottawa: COSEWIC, 49.

Crump, A., Jacobi, W. R., Burns, K. S., and Howell, B. E. (2011). *Pruning to manage white pine blister rust in the Southern Rocky Mountains. Research note RMRS-RN-44*. Fort Collins, CO: U.S. Department of Agriculture Forest Service Rocky Mountain Research Station, 10. doi: 10.2737/RMRS-RN-44

Dee, J. R., and Stambaugh, M. C. (2019). A new approach towards climate monitoring in Rocky Mountain alpine plant communities: A case study using herb-chronology and *Penstemon whippleanus*. *Arct. Antarct. Alp. Res.* 51, 84–95. doi: 10.1080/15230430-2019.1585173

Donnegan, J. A., and Rebertus, A. J. (1999). Rates and mechanisms of subalpine forest succession along an environmental gradient. *Ecology* 80, 1370–1384. doi: 10.1890/0012-9658(1999)080[1370:RAMOSF]2.0.CO;2

Dudney, J., Willing, C. E., Das, A. J., Latimer, A. M., Nesmith, J. C., and Battles, J. J. (2021). Nonlinear shifts in infectious rust disease due to climate change. *Nat. Commun.* 12:5326. doi: 10.1038/s41467-021-25182-6

Dudney, J. C., Nesmith, J. C., Cahill, M. C., Cribbs, J. E., Duriscoe, D. M., Das, A. J., et al. (2020). Compounding effects of white pine blister rust, mountain pine beetle, and fire threaten four white pine species. *Ecosphere* 11:e03263. doi: 10.1002/ecs2.3263

Dunlap, J. (2012). Variability in and environmental correlates to white pine blister rust incidence in five California white pine species. *Northwest Sci.* 86, 248–263. doi: 10.3955/046.086.0402

Fettig, C. J., Asaro, C., Nowak, J. T., Dodds, K. J., Gandhi, K. J., Moan, J. E., et al. (2022). Trends in bark beetle impacts in North America during a period (2000–2020) of rapid environmental change. *J. For.* 120, 693–713. doi: 10.1093/jofore/fvac021

Field, S. G., Schoettle, A. W., Klutsch, J. G., Tavener, S. J., and Antolin, M. F. (2012). Demographic projection of high-elevation white pines infected with white pine blister rust: A nonlinear disease model. *Ecol. Appl.* 22, 166–183. doi: 10.1890/11-0470.1

Furniss, R. L. (1977). *Western forest insects*. Washington, DC: U.S. Department of Agriculture Forest Service. doi: 10.5962/bhl.title.131875

Geils, B. W., Hummer, K. E., and Hunt, R. S. (2010). White pines, *Ribes*, and blister rust: A review and synthesis. *For. Pathol.* 40, 147–185. doi: 10.1111/j.1439-0329.2010.00654.x

Gibson, K. (2003). *Mountain pine beetle: Conditions and issues in the western United States, 2003*, information report BC-X-399. Victoria: Pacific Forestry Centre, 57–61.

Gibson, K., Skov, K., Kegley, S., Jorgensen, C., Smith, S., and Witcosky, J. (2008). *Mountain pine beetle impacts in high-elevation five-needle pines: Current trends and challenges*, *R1-08-020*. Missoula, MT: U.S. Department of Agriculture Forest Service, 1–32.

Goeking, S. A., and Windmuller-Campione, M. A. (2021). Comparative species assessments of five-needle pines throughout the western United States. *For. Ecol. Manag.* 496:119438.

Hossain, M., Veneklass, E. J., Hardy, G. E. S. J., and Poot, P. (2018). Tree host-pathogen interactions as influenced by drought timing: Linking physiological performance, biochemical defense and disease severity. *Tree Physiol.* 39, 6–18. doi: 10.1093/treephys/tpy113

Jackson, M., Gannon, A., Kearns, H., and Kendall, K. (2010). *Current status of limber pine in Montana*. Report R1-10-06. Washington, DC: U.S. Department of Agriculture Forest Service, 14.

Jacobi, W. R., Bovin, P. P., Burns, K. S., Crump, A., and Goodrich, B. A. (2016). Pruning limber pine to reduce impacts from white pine blister rust in the Southern Rocky Mountains. *For. Sci.* 63, 218–224. doi: 10.5849/forsci.16-011

Jacobi, W. R., Kearns, H. S., Cleaver, C. M., Goodrich, B. A., and Burns, K. S. (2018a). Epidemiology of white pine blister rust on limber pine in Colorado and Wyoming. *For. Pathol.* 48:e12465. doi: 10.1111/efp.12465

Jacobi, W. R., Kearns, H. S., Kegley, A., Savin, D. P., Danchok, R., and Sniezko, R. A. (2018b). "Comparative look at rust infection and resistance in limber pine (*Pinus flexilis*) and Rocky Mountain bristlecone pine (*P. aristata*) following artificial inoculation at three inoculum densities," in *Proceedings of the IUFRO joint conference: Genetics of five-needle pines, rusts of forest trees, and Strobusphere*, *RMRS-P-76*, eds A. W. Schoettle, R. A. Sniezko, and J. T. Kliejunas (Fort Collins, CO: U.S. Department of Agriculture Forest Service), 151–157.

Johnson, K. A. (2001). *Pinus flexilis. Fire effects information system*. Fort Collins, CO: U.S. Department of Agriculture Forest Service Rocky Mountain Research Station.

Kearns, H., Jacobi, W., Reich, R., Flynn, R., Burns, K., and Geils, B. (2014). Risk of white pine blister rust to limber pine in Colorado and Wyoming, USA. *For. Pathol.* 44, 21–38. doi: 10.1111/efp.12065

Kearns, H. S., and Jacobi, W. R. (2007). The distribution and incidence of white pine blister rust in central and southeastern Wyoming and northern Colorado. *Can. J. For. Res.* 37, 462–472. doi: 10.1139/x06-231

Kearns, H. S., Jacobi, W. R., and Geils, B. W. (2009). A method for estimating white pine blister rust canker age on limber pine in the central Rocky Mountains. *For. Pathol.* 39, 177–191.

King, J., David, A., Noshad, D., and Smith, J. (2010). A review of genetic approaches to the management of blister rust in white pines. *For. Pathol.* 40, 292–313. doi: 10.1111/j.1439-0329.2010.00659.x

Kinloch, B. B. Jr., and Dupper, D. E. (2002). Genetic specificity in the white pine-blister rust pathosystem. *Phytopathology* 92, 278–280. doi: 10.1094/PHYTO.2002.92.3.278

Kliejunas, J., and Dunlap, J. (2007). "Status of whitebark pine and other high-elevation five-needle pines with emphasis on Pacific coast ecosystems; what are the issues and concerns? Perspective from California," in *Proceedings of the conference: Whitebark pine: A Pacific coast perspective*, eds E. M. Goheen and R. A. Sniezko (Princeton, NJ: Citeseer).

Klutsch, J. G., Goodrich, B. A., and Schoettle, A. W. (2011). "Limber pine forests on the leading edge of white pine blister rust distribution in northern Colorado," in *Proceedings of the future of high-elevation, five-needle white pines in Western North America: High five symposium, proceedings RMRS-P-63*, eds R. E. Keane, D. F. Tomback, M. P. Murray, and C. M. Smith (Fort Collins, CO: U.S. Department of Agriculture Forest Service), 222–225.

Klutsch, J. G., Negron, J. F., Costello, S. L., Rhoades, C. C., West, D. R., Popp, J., et al. (2009). Stand characteristics and downed woody debris accumulations associated with a mountain pine beetle (*Dendroctonus ponderosae* Hopkins) outbreak in Colorado. *For. Ecol. Manag.* 258, 641–649. doi: 10.1016/j.foreco.2009.04.034

Krebill, R. (1964). Blister rust found on limber pine in northern Wasatch Mountains. *Plant Dis. Rep.* 50:532.

Krist, F. Jr., Ellenwood, J., Woods, M., McMahan, A., Cowardin, J., Ryerson, D., et al. (2014). *National insect and disease forest risk assessment: 2013-2027*, *FHTET-14-01*. Washington, DC: U.S. Department of Agriculture.

Kuznetsova, A., Brockhoff, P. B., and Christensen, R. H. (2017). lmerTest package: Tests in linear mixed effects models. *J. Stat. Softw.* 82, 1–26. doi: 10.18637/jss.v082.i13

Lachmund, H. G. (1933). Mode of entrance and periods in the life cycle of *Cronartium ribicola* on *Pinus monticola*. *J. Agric. Res.* 47, 791–805.

Langor, D. W. (1989). Host effects on the phenology, development, and mortality of field populations of the mountain pine beetle, *Dendroctonus ponderosae* Hopkins (Coleoptera: Scolytidae). *Can. Entomol.* 121, 149–157. doi: 10.4039/Ent121149-2

Larson, E. R. (2011). Influences of the biophysical environment on blister rust and mountain pine beetle, and their interactions, in whitebark pine forests. *J. Biogeogr.* 38, 453–470. doi: 10.1111/j.1365-2699.2010.02430.x

Logan, J. A., and Powell, J. A. (2001). Ghost forests, global warming, and the mountain pine beetle (Coleoptera: Scolytidae). *Am. Entomol.* 47, 160–173. doi: 10.1093/ae/47.3.160

Lüdecke, D., Ben-Shachar, M. S., Patil, I., and Makowski, D. (2020). Extracting, computing and exploring the parameters of statistical models using R. *J. Open Source Softw.* 5:2445. doi: 10.21105/joss.02445

Malone, S. L., Schoettle, A. W., and Coop, J. D. (2018). The future of subalpine forests in the Southern Rocky Mountains: Trajectories for *Pinus aristata* genetic lineages. *PLoS One* 13:e0193481. doi: 10.1371/journal.pone.0193481

Maloney, P. E. (2011). Incidence and distribution of white pine blister rust in the high-elevation forests of California. *For. Pathol.* 41, 308–316.

McDonald, G. I., and Hoff, R. J. (2001). "Blister rust: An introduced plague," in *Whitebark pine communities: Ecology and restoration*, eds D. F. Tomback, S. F. Arno, and R. E. Keane (Washington, DC: Island Press), 193–220.

McGuire, C. R., Nufio, C. R., Bowers, M. D., and Guralnick, R. P. (2012). Elevation-dependent temperature trends in the Rocky Mountain Front Range: Changes over a 56- and 20-year record. *PLoS One* 7:e44370. doi: 10.1371/journal.pone.0044370

Millar, C. I., Charlet, D. A., Westfall, R. D., King, J. C., Delany, D. L., Flint, A. L., et al. (2018). Do low-elevation ravines provide climate refugia for subalpine limber pine (*Pinus flexilis*) in the Great Basin, USA? *Can. J. For. Res.* 48, 663–671. doi: 10.1139/cjfr-2017-0374

Monahan, W. B., Cook, T., Melton, F., Connor, J., and Bobowski, B. (2013). Forecasting distributional responses of limber pine to climate change at management-relevant scales in Rocky Mountain National Park. *PLoS One* 8:e83163. doi: 10.1371/journal.pone.0083163

O'Hara, K. L. (2002). The historical development of uneven-aged silviculture in North America. *Forestry* 75, 339–346. doi: 10.1093/forestry/75.4.339

Pataki, D. E., Oren, R., Smith, W. K. (2000). Sap flux of co-occurring species in a western subalpine forest during seasonal soil drought. *Ecology* 81, 2557–2566. doi: 10.1890/0012-9658(2000)081[2557:SFOCOS]2.0.CO;2

Rebertus, A., Burns, B., and Veblen, T. (1991). Stand dynamics of *Pinus flexilis*-dominated subalpine forests in the Colorado front range. *J. Veg. Sci.* 2, 445–458. doi: 10.2307/3236026

Rehfeldt, G. E., Ferguson, D. E., and Crookston, N. L. (2008). Quantifying the abundance of co-occurring conifers along Inland Northwest (USA) climate gradients. *Ecology* 89, 2127–2139. doi: 10.1890/06-2013.1

Schoettle, A. W. (2004). "Ecological roles of five-needle pine in Colorado: Potential consequences of their loss," in *Breeding and genetic resources of five-needle pines: Growth, adaptability and pest resistance*, *proceedings RMRS-P-32*, eds R. A. Sniezko, S. Samman, S. Schlarbaum, and H. Kriebel (Fort Collins, CO: US Department of Agriculture Forest Service), 124–135.

Schoettle, A. W., Burns, K. S., Cleaver, C. M., and Connor, J. J. (2019a). *Proactive limber pine conservation strategy for the Greater Rocky Mountain National Park Area. General Technical Report RMRS-GTR-379*. Fort Collins, CO: U.S. Department of Agriculture Forest Service Rocky Mountain Research Station, 81. doi: 10.2737/RMRS-GTR-379

Schoettle, A. W., Jacobi, W. R., Waring, K. M., and Burns, K. S. (2019b). Regeneration for resilience framework to support regeneration decisions for species with populations at risk of extirpation by white pine blister rust. *New For.* 50, 89–114. doi: 10.1007/s11056-018-9679-8

Schoettle, A. W., Burns, K. S., McKinney, S. T., Krakowski, J., Waring, K. M., Tomback, D. F., et al. (2022a). Integrating forest health conditions and species adaptive capacities to infer future trajectories of the high elevation five-needle white pines. *For. Ecol. Manag.* 521:120389. doi: 10.1016/j.foreco.2022.120389

Schoettle, A. W., Kegley, A., Sniezko, R. A., Burns, K. S., Vogler, D., Bovin, P. P., et al. (2022b). "Preparing for invasion: Rust resistance in limber, Great Basin bristlecone, and Rocky Mountain bristlecone pines," in *Proceedings of the research and management of high-elevation five-needle pines in Western North America: Second high-five conference*, eds M. P. Murray, C. M. Smith, S. T. McKinney, and P. L. Achuff (Arcata, CA: The Press at Cal Poly Humboldt), 77–80.

Schoettle, A. W., Goodrich, B., Klutsch, J., and Burns, K. S. (2018). "White pine blister rust confirmed on limber pine *(Pinus flexilis)* in Rocky Mountain National Park," in *Proceedings of the IUFRO joint conference: Genetics of five-needle pines, rusts of forest trees, and strobusphere*, *Proc. RMRS-P-76*, eds A. W. Schoettle, R. A. Sniezko, and J. T. Kliejunas (Fort Collins, CO: U.S. Department of Agriculture Forest Service Rocky Mountain Research Station), 201–204.

Schoettle, A. W., and Sniezko, R. A. (2007). Proactive intervention to sustain high-elevation pine ecosystems threatened by white pine blister rust. *J. For. Res.* 12, 327–336. doi: 10.1007/s10310-007-0024-x

Schoettle, A. W., Sniezko, R. A., Kegley, A., and Burns, K. S. (2014). White pine blister rust resistance in limber pine: Evidence for a major gene. *Phytopathology* 104, 163–173. doi: 10.1094/PHYTO-04-13-0092-R

Schwandt, J. W. (2006). *Whitebark pine in peril: A case for restoration. Report R1-06-28*. Missoula, MT: U.S. Department of Agriculture Forest Service.

Shanahan, E., Legg, K., Daley, R., Irvine, K., Wilmoth, S., and Jackson, J. (2019). *Monitoring five-needle pine on bureau of land management lands in Wyoming summary report for 2013, 2014, 2016, 2017. Natural resource report NPS/GRYN/NRR—2019/1931, 102*. Bozeman, MT: Northern Rocky Mountain Science Center.

Six, D. L., and Newcomb, M. (2005). A rapid system for rating white pine blister rust incidence, severity, and within-tree distribution in whitebark pine. *Northwest Sci.* 79, 189–195.

Smith, C. M., Langor, D. W., Myrholm, C., Weber, J., Gillies, C., and Stuart-Smith, J. (2013a). Changes in white pine blister rust infection and mortality in limber pine over time. *Can. J. For. Res.* 43, 919–928. doi: 10.1139/cjfr-2013-0072

Smith, C. M., Shepherd, B., Gillies, C., and Stuart-Smith, J. (2013b). Changes in blister rust infection and mortality in whitebark pine over time. *Can. J. For. Res.* 43, 90–96. doi: 10.1139/cjfr-2012-0127

Smith, J. P., and Hoffman, J. T. (2001). Site and stand characteristics related to white pine blister rust in high-elevation forests of southern Idaho and western Wyoming. *West. N. Am. Nat.* 61, 409–416.

Steele, R. (1990). *Pinus flexilis James limber pine, Agriculture Handbook 654*. Silvics N. Am. 1, 348–354.

Taylor, S. W., Carroll, A. L., Alfaro, R. I., and Safranyik, L. (2006). "Forest, climate and mountain pine beetle outbreak dynamics in western Canada," in *The mountain pine beetle. A synthesis of biology, management and impacts on lodgepole pine*, eds L. Safranyik and B. Wilson (Victoria: Natural Resources Canada - Canadian Forest Service-Pacific Forestry Centre), 67–94.

R Core Team (2015). *R: A language and environment for statistical computing*. Vienna: R Foundation for Statistical Computing.

Thornton, P., Thornton, M., Mayer, B., Wei, Y., Devarakonda, R., Vose, R., et al. (2016). *Daymet: Daily surface weather data on a 1-km grid for North America, version 3*. Oak Ridge, TN: ORNL DAAC.

Tomback, D. F., Keane, R. E., McCaughey, W. W., and Smith, C. (2005). *Methods for surveying and monitoring whitebark pine for blister rust infection and damage*. Missoula, MT: Whitebark Pine Ecosystem Foundation.

Veblen, T. T. (1986) *Age and size structure of subalpine forests in the Colorado Front Range*. Bulletin of the Torrey Botanical Club, pp. 225–240.

Vogler, D. R., Geils, B. W., and Coats, K. (2017a). First report of the white pine blister rust fungus, *Cronartium ribicola*, infecting *Ribes inerme* in north-central Utah. *Plant Dis.* 101, 386–386. doi: 10.1094/PDIS-09-16-1253-PDN

Vogler, D. R., Maloney, P. E., Burt, T., and Snelling, J. (2017b). First report of the white pine blister rust fungus, *Cronartium ribicola*, infecting *Pinus flexilis* on Pine Mountain, Humboldt National Forest, Elko County, Northeastern Nevada. *Plant Dis.* 101, 839–839. doi: 10.1094/PDIS-10-16-1502-PDN

Vorster, A. G., Evangelista, P. H., Stohlgren, T. J., Kumar, S., Rhoades, C. C., Hubbard, R. M., et al. (2017). Severity of a mountain pine beetle outbreak across a range of stand conditions in Fraser Experimental Forest, Colorado, United States. *For. Ecol. Manag.* 389, 116–126. doi: 10.1002/eap.2059

Windmuller-Campione, M. A., and Long, J. N. (2016). Limber pine (*Pinus flexilis* James), a flexible generalist of forest communities in the intermountain west. *PLoS One* 11:e0160324. doi: 10.1371/journal.pone.0160324

Witcosky, J. (2017). *Notes on the biology of Ips woodi in limber and Rocky Mountain bristlecone pines in Colorado and Wyoming and its response to the Ips pheromone components ipsdienol and ipsenol in the field, Biol. Eval. R2-17-01*. Lakewood, CO: US Forest Service Rocky Mountain Regional Office.

frontiers | Frontiers in Forests and Global Change

TYPE Original Research
PUBLISHED 06 June 2023
DOI 10.3389/ffgc.2023.1172889

OPEN ACCESS

EDITED BY
Julio Javier Diez Casero,
University of Valladolid, Spain

REVIEWED BY
Trudy Paap,
University of Pretoria, South Africa
Jane E. Stewart,
Colorado State University, United States

*CORRESPONDENCE
Tod D. Ramsfield
✉ tod.ramsfield@NRCan-RNCan.gc.ca

RECEIVED 23 February 2023
ACCEPTED 09 May 2023
PUBLISHED 06 June 2023

CITATION
Ramsfield TD, Feau N, Tanguay P, Hamelin RC, Herath P and Bozic T (2023) First report of *Melampsora epitea* causing stem cankers on *Salix pentandra* in Alberta, Canada. *Front. For. Glob. Change* 6:1172889. doi: 10.3389/ffgc.2023.1172889

First report of *Melampsora epitea* causing stem cankers on *Salix pentandra* in Alberta, Canada

Tod D. Ramsfield[1]*, Nicolas Feau[2], Philippe Tanguay[3], Richard C. Hamelin[4], Padmini Herath[4] and Toso Bozic[5]

[1]Northern Forestry Centre, Natural Resources Canada, Canadian Forest Service, Edmonton, AB, Canada, [2]Pacific Forestry Centre, Natural Resources Canada, Canadian Forest Service, Victoria, BC, Canada, [3]Laurentian Forestry Centre, Natural Resources Canada, Canadian Forest Service, Quebec, QC, Canada, [4]Forest Sciences Centre, Faculty of Forestry, University of British Columbia, Vancouver, BC, Canada, [5]ATTS Group, Edmonton, AB, Canada

In June, 2021, laurel willow (*Salix pentandra*) near Slave Lake, Alberta, was found to be infected by a *Melampsora* sp. that produced bright yellow urediniospores in uredia that were present on catkins, leaves, and stems. All *Melampsora* species previously reported in Canada are recorded as infecting leaves; therefore, further investigation was undertaken to ascertain the identity of this pathogen. To assess the relationship between this specimen and other *Melampsora* spp. previously collected from Canada, samples of willow leaves infected by *Melampsora* spp. were sourced from mycological herbariums located at the Laurentian Forestry Centre (QFB) and the Northern Forestry Centre (CFB, WINF(M)). DNA sequence data from the internal transcribed spacer (ITS) ribosomal RNA region of the fresh specimen, herbarium specimens, and DNA sequence data deposited within GenBank, were used to conduct a phylogenetic analysis. Sequencing and BLAST analysis of the material from the sample resulted in a 99.3% sequence identity match to *Melampsora epitea* "Mel J" collected from *Larix laricina* in New York State. The ITS sequence from the herbarium sample WINF(M)7356 (described as M. abieti-caprearum from Manitoba) had 100.0% identity with the Alberta sample. Additionally, specimens WINF(M)11892 (*Melampsora* sp. from Manitoba) and CFB8931 (*Melampsora* sp. from the Yukon) had 99.0% sequence identity with the Alberta sample. From these results we applied the identity of *M. epitea* to the rust discovered in Slave Lake, AB. With the current emphasis on willows for bioenergy production in Canada, growers must remain vigilant for this pathogen and the damages it could cause to willow plantations.

KEYWORDS

***Melampsora*, *Salix*, rust disease, willow health, canker**

Introduction

This study was initiated as a result of a public inquiry regarding *Salix pentandra* L. (laurel willow) infected by a rust pathogen in Alberta, Canada, in 2021. Laurel willow is native to Europe and Asia, although it has been introduced to Canada where its cold hardiness has facilitated its establishment (Farrar, 1995). The specimens that were received were subjected to further examination because uredinia were present in cankers found on stems, a symptom that is not listed in any of the descriptions of *Melampsora* spp., which infect willows in Western Canada, as outlined by Ziller (1974), leading to concerns that a new pathogen may have been introduced to Canada.

The taxonomy of rust pathogens infecting willows is complicated due to the morphological similarity of the uredinial states of *Melampsora* spp. on willows, resulting in

Melampsora epitea Thümen becoming a catch-all for *Melampsora* sp. infecting willow (Ziller, 1974). Recent studies based on morphology and ribosomal DNA sequences have revealed that *M. epitea* is a species complex (Smith et al., 2004; Bennett et al., 2011; Kenaley et al., 2014; Zhao et al., 2017). In total, 12–14 phylotypes were recognized in North America (Smith et al., 2004), and more recently, Zhao et al. (2017) have described 13 species based on specimens collected from East Asia. These groups are differentiated based on aecial hosts, subtle morphological differences in the urediniospores, uredinia and telia, and ribosomal DNA sequences (Smith et al., 2004; Bennett et al., 2011; Kenaley et al., 2014; Zhao et al., 2017). Morphology and host associations are important characters in making an identification, but within this group, this information must be supplemented with DNA sequence data to arrive at the best possible identification.

The objective of this study was to determine the identity of the *Melampsora* sp. causing disease on *S. pentandra* in Alberta to investigate its potential as a new introduction in Canada. This was achieved by comparing the ribosomal DNA sequence data from this specimen with the ribosomal DNA extracted from herbarium specimens collected from *Salix* spp. in Canada and ribosomal DNA sequence data present in GenBank.

Materials and methods

Collection information

The sample, which included infected catkins, leaves, and stems, was collected fresh from *Salix pentandra* growing on private property in the Slave Lake region of Alberta and received at the Northern Forestry Centre on 16 June 2021.

Herbarium samples

Specimens were retrieved from the QFB herbarium at the Laurentian Forestry Centre (Quebec City, Canada) and the CFB and WIN(F) herbaria at the Northern Forestry Centre (Edmonton, Canada) based on the host and proximity to the collection site (Table 1).

Morphology

Fresh urediniospores were mounted in water and the length (μm) and width (μm) of 10 urediniospores were measured under 400× and 1,000× magnification ($n = 20$) using a Zeiss Axiophot compound microscope using differential interference contrast (Carl Zeiss AG, Jena, Germany). One-way analysis of variance ($\alpha = 0.05$) was performed using Microsoft Excel to compare the size of urediniospores measured under 400× and 1,000× magnification. As there was no significant difference in the length or width of urediniospores observed under 400× and 1,000× magnification (length $F_{1,18} = 0.04$, $p = 0.839$; width $F_{1,18} = 2.48$, $p = 0.133$), urediniospore size was calculated based on the pooled sample ($n = 20$).

To compare urediniospore size between uredia present on catkins, stems, and leaves, a total of 30 urediniospores from each tissue type ($n = 90$) from specimen CFB 22329 were mounted in water, and the urediniospore length (μm) and width (μm) were measured under 400× magnification using a Zeiss Axiophot compound microscope (Carl Zeiss AG, Jena, Germany). One-way analysis of variance ($\alpha = 0.05$) was performed using Microsoft Excel to compare the size of urediniospores from uredia present in these different tissues. As there was no significant difference in the length or width of urediniospores collected from catkins, stems, or leaves (length $F_{2,87} = 1.24$, $p = 0.294$; width $F_{2,87} = 2.19$, $p = 0.119$), the size of urediniospore was calculated based on the pooled sample ($n = 90$).

DNA extraction: willow stems and seed catkins, herbarium samples

Urediniospores were collected from both fresh samples of willow stem and seed catkins and also herbarium samples of willow leaves. Plant materials were examined under a dissecting microscope, and urediniospores were aseptically harvested into 2 ml tubes with two 3.2 mm diameter stainless steel beads per tube. Due to the difficulty in harvesting from herbarium leaf samples, urediniospores were collected along with minute amounts of leaf, taking every care to minimize leaf material (Table 1). Afterward, the urediniospore samples were ground to a fine powder using the MM 300 TissueLyser (Retsch®, PA, USA) at 30 Hz for 2 min. The total genomic DNA of all urediniospore samples was extracted using the Qiagen DNeasy Plant mini kit (Qiagen, CA, USA) according to the manufacturer's instructions. DNA concentration of samples was measured using the Nanodrop ND-1000 spectrophotometer (ver. 3.8; Thermo Fisher Scientific Inc., Ottawa, ON, Canada).

Polymerase chain reaction (PCR) assay

For species identification, the ITS region of the ribosomal DNA was amplified by PCR using the universal fungal primers ITS1F (5′-CTTGGTCATTTAGAGGAAGTAA-3′; Gardes and Bruns, 1993)/ITS4 (5′-TCCTCCGCTTATTGATATGC-3′; White et al., 1990) following published protocols (White et al., 1990). Each PCR reaction (25 μl total volume) contained 1X buffer (Invitrogen, Carlsbad, CA, USA), 1.5 mM $MgCl_2$ (Invitrogen, Carlsbad, CA, USA), 0.2 mM each dNTP (Invitrogen, Carlsbad, CA, USA), 0.5 U Platinum Taq polymerase (Invitrogen, Carlsbad, CA, USA), each primer (forward and reverse) at 1 μM, and 2 μl of template DNA. The PCR protocol was performed in a Bio-Rad T100™ Thermal Cycler (Hercules, CA, USA) and included an initial denaturation step at 94°C for 3 min. This was followed by 35 cycles of denaturation (30 s at 94°C), annealing (30 s at 55°C), extension (1 min at 72°C), and final extension at 72°C for 10 min.

The PCR products were mixed with safe green dye (Applied Biological Materials, Canada) at a 1:5 ratio and were analyzed by gel electrophoresis using 1% agarose in 1X TBE (10X: Tris base 108 g, Boric acid 55 g, and EDTA 7.5 g in 1 L of distilled water). The PCR products were visualized using the Prepone Sapphire Blue LED Illuminator system (Embi Tec, CA, USA). Subsequently, the PCR products were sent for purification and Sanger sequencing to

TABLE 1 Herbarium specimens examined in this study.

Herbarium number	Alternative herbarium	Species as identified	Host	Location	Collected by	Determined by	Date	GenBank accession
WINF(M) 10956	DAOM 91232	*Melampsora epitea*	*Salix arctica*	Ellesmere Island	D.B.O. Savil	D.B.O Savil	24 July 1962	OQ076903
WINF(M) 3521		*Melampsora epitea*	*Salix lasiandra*	Honeymoon Bay, Vancouver Island, British Columbia	W.G. Ziller	W.G. Ziller	17 June 1957	OQ076902
WINF(M) 3522		*Melampsora epitea*	*Salix* sp.	Dawson, Yukon	J. Holms	W.G. Ziller	17 August 1961	OQ076909
WINF(M) 11892		*Melampsora* sp.	*Salix* sp.	Braintree, Manitoba	B. Sutherland		25 June 1969	OQ076905
CFB 4785		*Melampsora epitea*	*Salix* sp.	5 Mi. N. of Grouard, Alberta	G.J. Smith	R.J. Bourchier	7 September 1963	OQ076908
CFB 8931		*Melampsora* sp.	*Salix* sp.	Ross River, Yukon	J. Susut	Y. Hiratsuka	2 July 1969	OQ076907
WINF(M) 4979		*Melampsora bigelowi*	*Salix* sp.	Mile 10.5, Dore Lake Road, Saskatchewan	C. Rentz		9 August 1966	OQ076910
WINF(M) 7356		*Melampsora abieti-capraearum*	*Salix* sp.	Devils Lake, Manitoba	D. Shepherd		12 July 1967	OQ076904
QFB 11072		*Melampsora paradoxa*	*Salix* sp.	Mont Otish, Ungava, Quebec	R. Pomerleau	R. Pomerleau	August 1949	OQ076912
QFB 18297		*Melampsora paradoxa*	*Salix bebbiana*	Chapeau de paille, Quebec	G.B. Oullette	G.B. Oullette	27 July 1960	OQ076911, OQ076913

the CHUL Research Center Sequencing and Genotyping Platform (Québec City, Québec, Canada).

Sequences and phylogenetic analysis

ITS sequence data from the fresh specimen and herbarium specimens were aligned with ITS sequences from *M. epitea* and closely related *Melampsora* spp. retrieved from GenBank. Sequence chromatograms were trimmed, manually assessed for quality, and aligned for consensus using BioEdit ver 7.2 (Hall, 1999). Sequence identity was assigned using the BLASTn (Altschul et al., 1990) on the GenBank-NCBI nucleotide collection (nt) with homolog sequences. Maximum likelihood (ML) phylogenetic trees were constructed with RaxML (Stamatakis, 2014) using the GTR + GAMMA nucleotide evolution model. ModelTest-NG (Darriba et al., 2020) was used to identify the best-fitting nucleotide evolution model for this dataset. The maximum parsimony (MP) tree was identified by conducting a heuristic search and 100 random additions of sequences (RAS) with PAUP ver. 4.0b10 (Swofford, 2003). Statistical support for nodes on the ML and MP phylogenetic trees were obtained with 100 bootstrap replicates, saved in a Newick format, and then edited using TreeGraph 2 (Stöver and Müller, 2010), collapsing nodes for the minimum 70% consensus rule.

Results

Examination of the specimens revealed bright yellow uredinia present on leaves, catkins, and stems (Figure 1). Fresh urediniospores were yellow, echinulate, and globoid to broadly ellipsoid and measured [(length × width) (min-) $\bar{x} \pm$ SD (-max)]: (20-) 25.4 ± 3.17 (−35) × (17.5-) 20.6 ± 1.62 (−23) µm. Further examination of dried material revealed no significant difference in urediniospore size produced in uredia on catkins, stems, or leaves (length $F_{2,87} = 1.24$, $p = 0.294$; width $F_{2,87} = 2.19$, $p = 0.119$), suggesting that all tissues were infected by the same pathogen. Urediniospores from the dried material were no longer yellow and measured (20-) 23.8 ± 1.89 (−30) × (12.5-) 15.9 ± 1.41 (−20) µm.

When the ITS sequence data were aligned with sequence data from close relatives that were deposited in GenBank, it was found that the rust collected in this study was part of the *Melampsora epitea* complex. Comparison of the ITS sequence data from the fresh material with ITS sequence data generated from herbarium material resulted in a 100% identity with the specimen WINF(M)7356, identified as *Melampsora abietis-caprearum*, which was collected in 1967 from Devils Lake, Manitoba. The sequence was also 100% identical with the GenBank sequence GQ479229, *M. epitea*, collected from Edmonton, Alberta, in 2006 (Figure 2), and had a 99% identity match with the herbarium specimens CFB8931, *Melampsora* sp. collected from the Ross River in the Yukon in 1969

10.3389/ffgc.2023.1172889

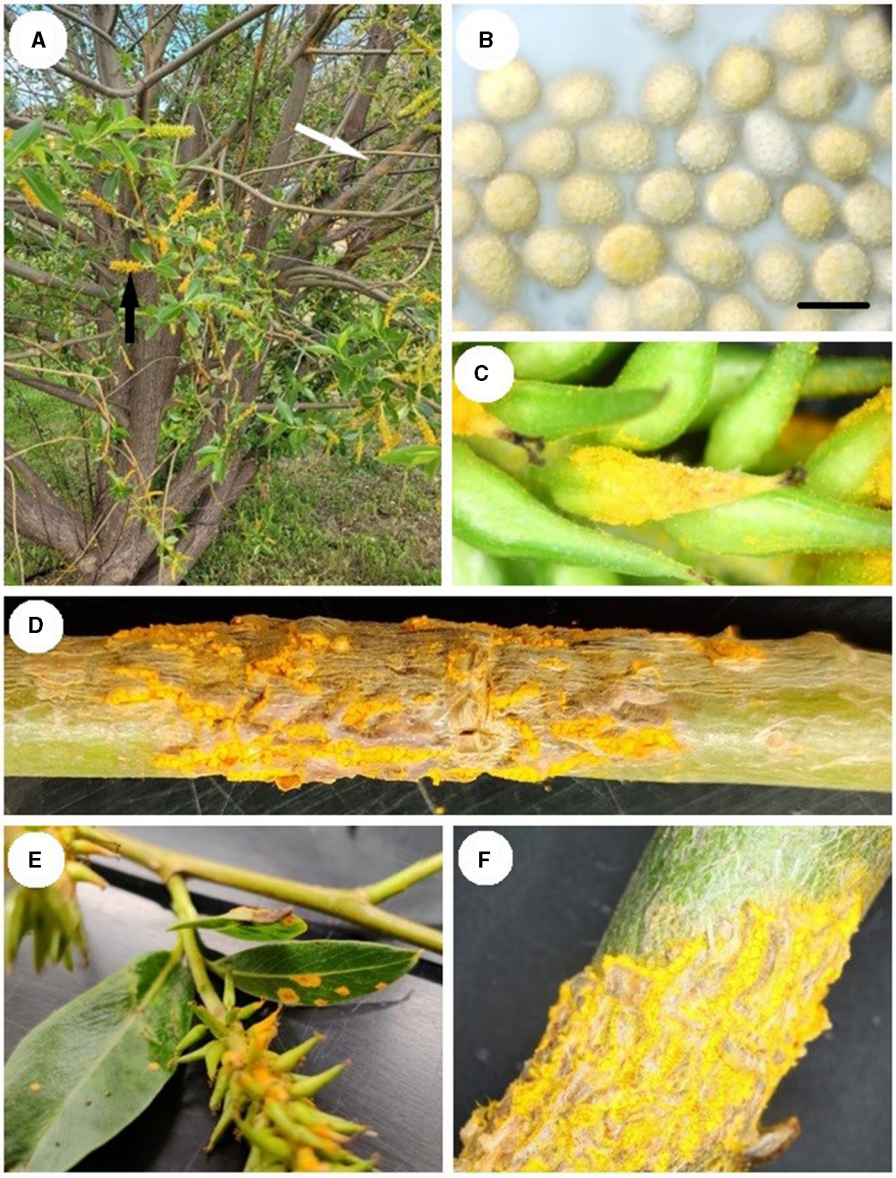

FIGURE 1
Melampsora epitae-infected *Salix pentranda*: **(A)** Uredinia on the stem (white arrow) and seed catkins (black arrow). **(B)** Urediniospores under 1,000× magnification in water, scale bar 20 μm. **(C)** Uredinia on seed catkin. **(D)** Uredinia on a stem. **(E)** Uredinia on leaves and catkins. **(F)** Uredinia on branch.

and WINF(M)11892, *Melampsora* sp. collected from Braintree, Manitoba, in 1969.

A representative sample from the specimen has been entered into the CFB herbarium under the accession number CFB22329. The ITS sequence data from this specimen has been accessioned in GenBank under the numbers OQ076914 for urediniospores from the stem and OQ076915 for urediniospores from catkins.

Discussion

Diseased *S. pentandra* with uredinia on stems, catkins, and leaves were collected from northern Alberta, Canada. As Ziller (1974) states that *M. epitea* is responsible for yellow leaf spots or blight, further examination of this material was undertaken. Urediniospores were larger than that reported by Ziller (1959) but otherwise matched the description. Further examination using DNA sequence data to determine the identity of this pathogen was performed. When the ITS sequence data from this specimen was compared with sequence data in GenBank, it was revealed that the specimen was part of the *Melampsora epitea* species complex. Phylogenetic analysis of the ITS data from this specimen and sequence data from herbarium specimens and GenBank accessions resulted in a 100% match with the specimen WINF(M)7356, which is morphologically identified as *M. abieti-capraearum* [which Ziller (1974) states as indistinguishable from *M. epitea* in the aecial,

FIGURE 2
Maximum likelihood phylogenetic tree constructed from a nucleotide alignment of 613 bp of the internal transcribed spacer regions (ITS) of the nuclear rDNA including sequence data collected from the willow rust specimen identified in Alberta (in red), various herbaria specimens (in blue), and sequence data from GenBank (in black). The numbers above the nodes are statistical support values obtained from 100 bootstrap samples in maximum likelihood/maximum parsimony; statistical support under 70% is not represented. Scale bars indicate the number of nucleotide substitutions per site.

uredinial, and telial stages] collected in 1967 from Manitoba, and GenBank accession GQ479229, which is identified as *M. epitea* collected from Edmonton, Alberta, in 2006. Stem cankers have also been observed on *Salix* sp. in Minnesota (Ostry and Anderson, 2001) and on *Salix arctica* Pall. from Ellesmere Island (Smith et al., 2004). Stem cankers have been hypothesized to provide an overwintering mechanism in the closely related species *M. paradoxa* (Crowell et al., 2022). Altogether, these results suggest that the diseased material collected in northern Alberta in 2021 is not the product of a recent introduction. Instead, the pathogen responsible for this stem canker symptom on willows seems to be relatively widespread in Western Canada. Two additional public inquiries during the summer of 2022 from ornamental willows in the Edmonton region determined it to be the same pathogen, further supporting the conclusion that the pathogen is established in Canada.

This study has demonstrated the importance of preserving specimens in biological collections. The CFB, DACFP, S, and WINF(M) collections maintained at the Northern Forestry Centre in Alberta contain a combined 237 accessions of *Salix* spp. infected by *Melampsora* spp. that are identified as, *M. epitea*, *M. paradoxa*, *M. abieti-capaearum*, and *M. bigelowii*. The QFB collection maintained in the Pomerleau herbarium at the Laurentian Forestry Centre in Quebec contains 87 specimens of willow infected by *Melampsora* rusts. Analysis of the ITS sequence data generated from a subset of these herbaria specimens was key to determining

that the pathogen collected in this study was already present in Canada. The specimens housed in these herbaria were all identified based on morphology and host associations. Identifying the causal agent of rust disease on willows based on morphology is difficult due to the similarity of key characteristics (Ziller, 1974), and recent DNA-based studies have suggested that *M. epitea* is far more complex than revealed by morphological examination (Smith et al., 2004; Bennett et al., 2011; Kenaley et al., 2014; Zhao et al., 2017). Having these specimens available for research will be an important resource for any future studies related to understanding the composition of the *M. epitea* complex in Canada.

Within Canada, short-rotation willow plantations are becoming increasingly common for phytoremediation (Jerbi et al., 2023) and bioenergy production (Buss et al., 2022). These plantations rely on genotypes that have been selected for growth and yield, and some of these genotypes have been demonstrated to become infected by *M. epitea* (McCracken and Dawson, 2003). Losses caused by a stem-infecting form of *Melampsora* that caused stem cankers on *Salix viminalis* L. in the United Kingdom (Pei et al., 1995) also demonstrated the risk posed to Canadian willows. Surveys of phytoremediation willow plantations in the Edmonton area that were conducted as part of a project to assess willow health have not revealed the presence of any *Melampsora* spp. on leaves or stems to date. As these plantations become more prominent in Canada, health surveys should include *M. epitea* as a pathogen of concern.

Further research is necessary to understand the exact identity of the pathogen observed in this study and to determine the aecial host as all materials that were examined were from the uredinial host. The finding that the ITS sequence data from the specimen examined in this study was a 100% match with herbarium material, collected between 1967 and 2006 in Canada, suggests that it is not a recent introduction, but rather that the pathogen has been long-established in central and northwestern parts of Canada. The formation of stem cankers, however, appears to have been rarely observed due to the lack of herbarium specimens that include stem material and the descriptions included within Ziller (1974). It is unknown why stem cankers have not been observed more frequently in the past, but the sample examined in this study was collected from an exotic ornamental by a homeowner who was closely monitoring the health of the trees on their property.

Data availability statement

The datasets presented in this study can be found in online repositories. The names of the repository/repositories and accession number(s) can be found at: https://www.ncbi.nlm.nih.gov/genbank/, OQ076902–OQ076913.

Author contributions

This work was conceived by TDR who led writing of the manuscript, performed microscopic analysis, and provided herbarium material from the Northern Forestry Centre. NF conducted the phylogenetic analysis and contributed to writing. PT provided herbarium material from the Laurentian Forestry Centre and contributed to writing. RCH provided funding for DNA sequence analysis and contributed to writing. PH performed DNA extractions and sequencing and contributed to writing. TB provided sample material and observations from Alberta. All authors contributed to the article and approved the submitted version.

Funding

Funding provided by the Canadian Forest Service. RCH was funded by Genome Canada's Large Scale Applied Research Program Project 10106.

Acknowledgments

Pascal Frey (INRAE, France) and Salvatore Moricca (UniFI, Italy) provided important information early in this study that helped to focus our research direction. The technical assistance of Malithi Sella Kapu and Bradley Tomm is greatly appreciated.

Conflict of interest

TB was employed by ATTS Group Inc.

The remaining authors declare that the research was conducted in the absence of any commercial or financial relationships that could be construed as a potential conflict of interest.

Publisher's note

All claims expressed in this article are solely those of the authors and do not necessarily represent those of their affiliated organizations, or those of the publisher, the editors and the reviewers. Any product that may be evaluated in this article, or claim that may be made by its manufacturer, is not guaranteed or endorsed by the publisher.

References

Altschul, S. F., Gish, W., Miller, W., Myers, E. W., and Lipman, D. J. (1990). Basic local alignment search tool. *J. Mol. Biol.* 215, 403–410. doi: 10.1016/S0022-2836(05)80360-2

Bennett, C., Aime, M. C., and Newcombe, G. (2011). Molecular and pathogenic variation within *Melampsora* on *Salix* in western North America reveals numerous cryptic species. *Mycologia* 103, 1004–1018. doi: 10.3852/10-289

Buss, J., Mansuy, N., Laganière, J., and Persson, D. (2022). Greenhouse gas mitigation potential of replacing diesel fuel with wood-based bioenergy in an arctic Indigenous community: A pilot study in Fort McPherson, Canada. *Biomass Bioenergy* 159, 106367. doi: 10.1016/j.biombioe.2022.106367

Crowell, C. R., Wilkerson, D. G., Smart, L. B., and Smart, C. D. (2022). Evidence of asexual overwintering of *Melampsora paradoxa* and mapping of stem rust host resistance in *Salix*. *Plants* 11, 2385. doi: 10.3390/plants11182385

Darriba, D., Posada, D., Kozlov, A. M., Stamatakis, A., Morel, B., and Flouri, T. (2020). ModelTest-NG: A new and scalable tool for ethe selection of DNA and protein evolutionary models. *Mol. Biol. Evol.* 37, 291–294. doi: 10.1093/molbev/msz189

Farrar, J. L. (1995). *Trees in Canada*. Ottawa: Fitzhenry & Whiteshade Limited and the Canadian Forest Service, Natural Resources Canada. Canada Communication Group – Publishing Supply and Services Canada.

Gardes, M., and Bruns, T. D. (1993). ITS primers with enhanced specificity for basidiomycetes—application to the identification of mycorrhizae and rusts. *Mol. Ecol.* 2, 113–118. doi: 10.1111/j.1365-294X.1993.tb00005.x

Hall, T. A. (1999). BioEdit: A user-friendly biological sequence alignment editor and analysis program for Windows 95/98/NT. *Nucl. Acids Symp. Ser.* 41, 95–98.

Jerbi, A., Kalwahali-Muissa, M., Krygier, R., Johnston, C., Blank, M., Sarrazin, M., et al. (2023). Comparative wood anatomy, composition and saccharification yields of wastewater irrigated willow cultivars at three plantation in Canada and Northern Ireland. *Biomass Bioenergy* 170, 106683. doi: 10.1016/j.biombioe.2022.106683

Kenaley, S. C., Smart, L. B., and Hudler, G. W. (2014). Genetic evidence for three discrete taxa of *Melampsora* (*Pucciniales*) affecting willows (*Salix* spp.) in New York State. *Fungal Biol.* 118, 704–720. doi: 10.1016/j.funbio.2014.05.001

McCracken, A. R., and Dawson, W. M. (2003). Rust disease (*Melampsora epitea*) of willow (*Salix* spp.) grown as short rotation coppice (SRC) in inter- and intra-species mixtures. *Ann. App. Biol.* 143, 381–393. doi: 10.1111/j.1744-7348.2003.tb00308.x

Ostry, M. E., and Anderson, N. A. (2001). Melampsora leaf rust of willow causing a stem canker in Minnesota. *Plant Dis.* 85, 229. doi: 10.1094/PDIS.2001.85.2.229C

Pei, M. H., Royle, D. J., and Hunter, T. (1995). A comparative study of stem- and leaf-infecting forms of *Melampsora* rust on *Salix viminalis* in the U.K. *Mycol. Res.* 99, 357–363. doi: 10.1016/S0953-7562(09)80913-1

Smith, J. A., Blanchette, R. A., and Newcombe, G. (2004). Molecular and morphological characterization of the willow rust fungus, *Melampsora epitea*, from arctic and temperate hosts in North America. *Mycologia* 96, 1330–1338. doi: 10.1080/15572536.2005.11832882

Stamatakis, A. (2014). RAxML version 8: A tool for phylogenetic analysis and post—analysis of large phylogenies. *J. Bioinform.* 30, 1312–1313. doi: 10.1093/bioinformatics/btu033

Stöver, B. C., and Müller, K. F. (2010). TreeGraph 2: Combinin and visualizing evidence from different phylogenetic analyses. *BMC Bioinform.* 11, 7. doi: 10.1186/1471-2105-11-7

Swofford, D. L. (2003). *PAUP*: Phylogenetic Analysis Using Parsimony (*and Other Methods). Version 4.0b10*. Sunderland, MA: Sinauer Associates Inc.

White, T. J., Bruns, T. D., Lee, S. B., and Taylor, J. W. (1990). "Amplification and direct sequencing of fungal ribosomal RNA genes for phylogenetics," in *PCR Protocols: A Guide to Methods and Applications*, eds M. Innis, D. Gelfand, J. Shinsky, and T. White (San Diego, CA: Academic Press), 315–322. doi: 10.1016/B978-0-12-372180-8.50042-1

Zhao, P., Kakishima, M., Wang, Q., and Cai, L. (2017). Resolving the *Melampsora epitea* complex. *Mycologia* 109, 391–407. doi: 10.1080/00275514.2017.1326791

Ziller, W. G. (1959). Studies of western tree rusts V. The rusts of hemlock and fir caused by *Melampsora epitea*. *Can. J. Bot.* 37, 109–119. doi: 10.1139/b59-010

Ziller, W. G. (1974). *The Tree Rusts of Western Canada*. Ottawa, ON: Canadian Forestry Service Publication No. 1329.

frontiers | Frontiers in Forests and Global Change

TYPE Original Research
PUBLISHED 24 August 2023
DOI 10.3389/ffgc.2023.1229456

OPEN ACCESS

EDITED BY
Isabel Alvarez Munck,
Forest Service (USDA), United States

REVIEWED BY
Claudia S. L. Vicente,
University of Évora, Portugal
Minggang Wang,
Beijing Forestry University, China

*CORRESPONDENCE
Tamara Sánchez-Gómez
✉ tamara.sanchez@uva.es

RECEIVED 26 May 2023
ACCEPTED 11 August 2023
PUBLISHED 24 August 2023

CITATION
Sánchez-Gómez T, Harte SJ, Zamora P, Bareyre M, Díez JJ, Herrero B, Niño-Sánchez J and Martín-García J (2023) Nematicidal effect of *Beauveria* species and the mycotoxin beauvericin against pinewood nematode *Bursaphelenchus xylophilus*. *Front. For. Glob. Change* 6:1229456. doi: 10.3389/ffgc.2023.1229456

Nematicidal effect of *Beauveria* species and the mycotoxin beauvericin against pinewood nematode *Bursaphelenchus xylophilus*

Tamara Sánchez-Gómez[1,2]*, Steven J. Harte[3], Paula Zamora[1,2,4], Matéo Bareyre[1,5], Julio Javier Díez[1,2], Baudilio Herrero[6], Jonathan Niño-Sánchez[1,2] and Jorge Martín-García[1,2]

[1]Recognised Research Group AGROBIOTECH, UIC-370 (JCyL), Department of Plant Production and Forest Resources, University of Valladolid, Palencia, Spain, [2]Sustainable Forest Management Research Institute (iuFOR), University of Valladolid, Palencia, Spain, [3]Natural Resources Institute, University of Greenwich, Kent, United Kingdom, [4]Sección Sanidad Forestal, Centro de Sanidad Forestal de Calabazanos, Consejería de Fomento y Medio Ambiente, Dirección General de Patrimonio Natural y Política Forestal, Palencia, Spain, [5]National School of Agricultural Engineering of Bordeaux (Bordeaux Sciences Agro), Gradignan, France, [6]Departamento de Ciencias Agroforestales, Universidad de Valladolid, Palencia, Spain

Introduction and main objective: *Bursaphelenchus xylophilus*, commonly known as pine wood nematode (PWN), is considered one of the greatest threats to European and Asian pines. Regarding its management, most efforts have been directed toward control measures for the major vector (*Monochamus* spp.) and screening for genetic resistance in its hosts. However, an integrated pest management strategy which also implements pinewood nematode control is currently lacking. The aim of this study was to evaluate the nematicidal effect of two *Beauveria* species, a genus well known for its entomopathogenic activity.

Summary methodology: For this purpose, *in vitro* antagonism tests of fungi (*Beauveria bassiana* and *B. pseudobassiana*) and the mycotoxin beauvericin ($C_{45}H_{57}N_3O_9$) on *B. xylophilus* populations were conducted. Finally, the production of beauvericin in *B. bassiana* and *B. pseudobassiana* strains was quantified by high-performance liquid chromatography - mass spectrometry (HPLC-MS).

Results and discussion: Both the *B. bassiana* and *B. pseudobassiana* fungal species and the mycotoxin beauvericin showed a clear nematicidal effect on *B. xylophilus* populations, substantially reducing their survival rate and even attaining 100% mortality in one case. HPLC-MS analysis confirmed and quantified the production of beauvericin by *B. bassiana* and demonstrated for the first-time beauvericin production in *B. pseudobassiana*.

Final conclusion: These findings highlight the potential of *Beauveria* species and the mycotoxin beauvericin to be implemented in an integrated pest management strategy to control both nematode and vector.

KEYWORDS

pine wilt disease, integrated management, biological control, nematophagous fungi, fungal toxins

1. Introduction

Bursaphelenchus xylophilus (Nematoda: Aphelenchoididae) poses a serious threat, endangering coniferous forests worldwide. This pathogen, commonly known as pine wood nematode (PWN) and belonging to the group of plant-parasitic nematodes (PPNs), causes decay of afflicted trees, leading to the so-called pine wilt disease (PWD) and eventually, tree mortality. Although PWN is thought to originate in North America, PWD was firstly detected in the early twentieth century in Japan and quickly spread to other Asian countries (Kim et al., 2020). In the late 1990s it was introduced into Europe via Portugal (Mota et al., 1999) where it has subsequently caused significant forest damage. PWD is now found in more than 30% of the Portuguese forest area (De la Fuente et al., 2018) and in several Spanish regions bordering Portugal: Extremadura, Galicia and Castilla y León (Zamora et al., 2015). Although the pathogen currently appears fairly contained, it is listed as a quarantine pest in Europe (List A2) (EPPO, 2016) due to its high pathogenicity and dispersive capacity. Moreover, the impact is predicted to worsen under future climate change scenarios (Hirata et al., 2017; De la Fuente et al., 2018).

The spread of PWN within Europe is linked to insect vectors belonging to genus *Monochamus*, and more specifically *M. galloprovincialis* (Coleoptera: Cerambycidae). The pathogen is transmitted via these beetles from dead or dying trees to healthy ones through feeding (Mamiya and Enda, 1972) or oviposition (Edwards and Linit, 1992). Once the nematodes have entered the tree, they lodge in the resiniferous canals and feed on epithelial and parenchymal cells, triggering a host response which leads to disruption of water transport and rapid death by cavitation (Fukuda and Suzuki, 1988; Hara et al., 2006). Thus far, disease control mitigation techniques have been mainly focused on the search for genetic resistance in the host organisms and controlling disease spread by reducing populations of the insect vector. The first reported program for breeding genetic resistance to PWD started in western Japan in 1978, on Japanese black and red pine (*Pinus thunbergii* and *P. densiflora*, respectively) and obtained high post-inoculation survival rates in both (Fujimoto and Ohba, 1981; Toda and Kurinobu, 2002). Since then, many resistance programs have been operational, such as on *P. massoniana* (Liu et al., 2017; Zhu et al., 2021), *P. pinaster* (Gaspar et al., 2017; Carrasquinho et al., 2018) and *P. radiata* (Zas et al., 2015; Menéndez-Gutiérrez et al., 2018, 2021) in China, Portugal and Spain, respectively.

In terms of insect vector control, several strategies have been developed to reduce *M. galloprovincialis* populations such as a trapping method combining pheromone and kairomones (Álvarez-Baz et al., 2016; Galloprotect 2D®), the use of entomopathogenic fungi (Naves et al., 2008; Álvarez-Baz et al., 2015; Petersen-Silva et al., 2015) and the development of an auto-infection device based on the combined use of the attractant and the entomopathogenic fungi (Sacristán-Velasco et al., 2018). To date, only the use of traps with attractants has been implemented more widely, but successful field trials have been performed combining this system with the auto-infection device and powdered formulations of an entomopathogenic fungus (Martín-García, Unpublished data).

Despite progress in other areas, an effective integrated pest management technique for this disease will require nematode control. Progress toward achieving this goal has been made with the effect of fungi and bacteria on different PPNs being studied (Mankau, 1980; Askary, 2015; Abd-Elgawad and Askary, 2018; Migunova and Sasanelli, 2021). For PWN specifically, the most studied antagonistic fungal species is *Esteya vermicola*, which was first found infecting PWN in Taiwan in 1999 (Liou et al., 1999) and reported as a natural enemy of the nematode. Subsequent laboratory and field tests have corroborated this efficacy as a biological agent against the pathogen (Kubátová et al., 2000; Wang et al., 2008, 2009, 2018; Lin et al., 2013; Pires et al., 2022). Other fungal genera such as *Verticillium* spp. or *Trichoderma* spp. have also exhibited nematicidal effect on PWN populations (Maehara and Futai, 2000). More recently, some fungal species within the genera *Leptographium* and *Graphilbum* have also been shown to have a nemastatic effect on this pathogen (Vicente et al., 2022). However, little attention has been paid to potential nematicidal effects of the genus *Beauveria* spp. on PWN, despite significant mortality effect on other nematodes species being thoroughly documented (Youssef et al., 2020; Ye et al., 2021; Karabörklü et al., 2022) and its entomopathogenic effect on *M. galloprovincialis* is well known (Naves et al., 2008; Álvarez-Baz et al., 2015; Petersen-Silva et al., 2015). Maehara et al. (2007) proved the reduction of PWN transmission from vectors due to *Beauveria bassiana* was possible; however, this potential control method has not been examined in depth.

Most fungi's nematicidal properties appear at least in part due to excreting secondary metabolites (mycotoxins) (Anke and Sterner, 1997, 2002; Li et al., 2007; Anke, 2011; Baazeem et al., 2021; Seong et al., 2021). However, some fungi (e.g., *E. vermicola*) appear to have alternate control mechanisms against the nematode, such as the emission of attractant volatiles similar to the host pine and subsequently the production of specific types of spores (lunate conidia) to trap the attracted nematodes (Kubátová et al., 2000; Lin et al., 2013). It is likely that the antagonistic effect of these fungi on the pathogen is the result of the combination of these two modes of action: nematode-trapping capacity and production of mycotoxins.

The nematicidal mycotoxin mechanism is probably the prime mode of action for the *Beauveria* genus and the most studied mycotoxin from this genus is beauvericin (BEA). Chemically, BEA is defined as a cyclic hexadepsipeptide consisting of alternating D-α-hydroxy-isovaleryl-(2-hydroxy-3-methylbutanoic acid) and amino acid units (Hamill et al., 1969; **Figure 1**) and is considered an emerging mycotoxin since it is still neither routinely determined, nor legislatively regulated (Jestoi, 2008; Vaclavikova et al., 2013; EFSA, 2014).

The compound is not only produced by *Beauveria* species such as *B. bassiana* (Hamill et al., 1969), but also by others, for example *Fusarium* spp (Gupta et al., 1991; Logrieco et al., 2002; Moretti et al., 2002, 2008). In comparison to *B. bassiana*, *B. pseudobassiana* has to date few studies identifying and assessing the toxins produced by this species. Berestetskiy et al. (2018) proved that *B. pseudobassiana* strain BCu22 produces different metabolites depending on the culture medium and demonstrated its insecticidal effect on grain aphid larvae. A subsequent study confirmed the existence of a gene cluster coding for BEA in the strain RGM 2184 of *B. pseudobassiana* (Altimira et al., 2022). However, none of them were able to corroborate the actual production of BEA by this fungal species. The toxicity of BEA was first tested on the crustacean *Artemia salina* (Hamill et al., 1969) but soon found to have insecticidal (Grove and Pople, 1980; Gupta et al., 1991; Ganassi et al., 2002; Fornelli et al., 2004; Leland et al., 2005) and nematicidal effects, tested first on *Meloidogyne incognita*

(Mayer, 1995) and later on *Caenorhabditis elegans* and PWN (Shimada et al., 2010). Additionally, according to the Technical Commission on Contaminants in the Food Chain, acute exposure to BEA does not indicate concern for human health (EFSA, 2014). This fact, together with the nematicidal activity, makes BEA one of the most promising mycotoxins that could be implemented in integrated pest management of PWN.

This evidence suggests that *Beauveria* species and the mycotoxin BEA could be a potential control option against not only the PWN insect vector (*M. galloprovincialis*), but also against the nematode itself. The goals of the work presented here were firstly to demonstrate the nematicidal effect of different strains of *B. bassiana* and *B. pseudobassiana* on PWN populations, secondly to prove whether BEA has nematicidal effect on PWN and lastly to test whether not only *B. bassiana* is able to produce BEA, but also potentially *B. pseudobassiana*.

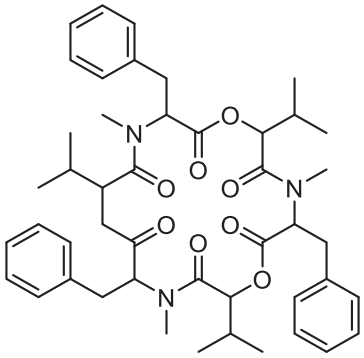

FIGURE 1
Chemical structure of BEA. Diagram created using the software ChemDraw®.

2. Materials and methods

2.1. Fungal and nematode strains for the *in vitro* assays

Two different strains of *B. bassiana* (EABps 11/01-Mg* and 95b) and one of *B. pseudobassiana* (MG-BU-17-001) were used for the assays.

*Note: EF1α and ITS classification of several strains of *Beauveria* species (*B. bassiana* and *B. pseudobassiana*) were modified in GenBank a few years ago (see accession numbers AY531938.1 and AY531931). So, the isolate EABps 11/01-Mg was wrongly identified by Álvarez-Baz et al. (2015) as *B. pseudobassiana* based on the homology of the isolates AY531938.1 and AY531931 (previously identified as *B. pseudobassiana* and currently *B. bassiana*). However, we have again analyzed the isolate EABps 11/01-Mg (EF1α and ITS) and checked in GenBank and it should be classified as *B. bassiana*.

Esteya vermicola CBS 115803 (supplied by the Czech Collection of Microorganisms), which has already demonstrated nematicidal effect on PWN (Wang et al., 2016; Pires et al., 2022) was used as negative-growth control. A non-sporulating *Botrytis cinerea* isolate, which is used to grow the PWN colonies for fostering its reproduction, was used as positive-growth control. All the isolates were cultivated using potato dextrose agar medium (PDA Scharlau, Spain).

The nematode strain was *B. xylophilus* CSF-N-1 and was grown using glass vials [28 mm (Ø), 43 mm (h), 25 mL (V)] with medium composed of hulled barley and non-sporulating *B. cinerea* (**Supplementary Figure 1A**). The vials were kept at room temperature with the cover ajar, always with oxygen flow inward, and under continuous darkness.

2.2. *In vitro* antagonism tests of *Beauveria* spp. on *B. xylophilus* populations

Thirty glass vials with 3 g hulled barley and 3 mL distilled water inside were autoclave sterilized and separated into 6 treatments (*B. bassiana* 95b, *B. bassiana* EABps 11/01-Mg, *B. pseudobassiana* MG-BU-17-001, *B. cinerea*, *E. vermicola* CCM 8247 and mock inoculated). A mycelium plug of each fungus was introduced into each vial (except for mock inoculated treatment, in which a plug of PDA was added) and left to grow for 13 days. After this growth period, a 100 μL aliquot with 270 nematodes (*B. xylophilus* CSF-N-1) was added to each vial and they were kept for a further 13 days at 25°C in continuous darkness.

The extraction of the nematodes from the vials was conducted according to a slightly modified version of the Baermann (1917) funnel technique. A tea filter (M-size, Finum®) was placed with the content of each vial on an autoclaved beaker (100 mL). The content was covered with autoclaved distilled water, so that the nematodes pass through the filter and remain in a clean aqueous suspension. After 24 h, they were washed with distilled water using a nylon sieve of 20 μm mesh size (NY-0073-Labopolis, Spain). The nematodes were retained by the sieve, washed with a washing bottle and finally resuspended into 55 mm (Ø) petri dishes. Three aliquots (100 μL) of each replicate were counted using a counting grid and binocular loupe to determine nematode concentration (**Supplementary Figures 1B, C, D**).

2.3. Effect of commercial BEA on *B. xylophilus* populations

Considering the nematicidal effect of the metabolite beauvericin naturally extracted from strains of *Fusarium bulbicola* on PWN is already published (Shimada et al., 2010), we decided to test the effect of BEA commercial (Merck Life Science S.L.U, USA) on populations of *B. xylophilus*. Solutions of 0.1 mM, 1 mM and 2 mM of BEA with 5% dimethyl sulfoxide (DMSO) were prepared with eight replicates for each concentration by dividing each stock solution into eight 1.5 mL Eppendorf tubes. For the negative controls, another eight replicates were prepared with 5% DMSO only. A 75 μL nematode suspension (400 nm/mL) was added to each tube and live nematodes were then counted. A small hole was made in the top of each tube (with a heated entomological pin) to ensure oxygen flow, and the rack was covered with aluminum foil for continuous dark conditions. The assay was incubated at 25°C for 48 h, each tube was vortex mixed once per day to resuspend the

nematodes. After 2 days, the contents of each tube were poured on a grid and the live nematodes counted.

2.4. Extraction and quantification of BEA produced by the strains of *Beauveria* spp.

Four replicates of each strain were grown on PDA plates and kept in an incubator at 28°C for 21 days. The PDA plates were subsequently cut into 2 cm cube pieces and all cubes from each PDA plate was placed in individual 150 mL conical flasks. MeOH (100 mL) was then added to each flask and the flasks sonicated for 15 min at 40°C. The organic extract was removed, and the solid media washed with MeOH (50 mL). The organic extracts were combined, filtered, and dried under vacuum. The subsequent oily extract was dissolved in 80% MeOH (7 mL), filtered again, and transferred to a sample vial. The organic solvent was removed under N_2 and the aqueous mixture was frozen at −75°C before being dried using a freeze drier. All extract samples were weighed and dissolved in 90% MeOH in a 20 mg/mL concentration.

2.4.1. HPLC protocol

Samples were analyzed using an Agilent 1260 series HPLC system with attached 1200 series diode array detector and MSD-XT single quad mass spectrometer with attached atmospheric pressure chemical ionisation (APCI) source. The LC-MS used a Phenomenex Kinetex, 2.6 μm, C18, 75 mm × 2.1 mm column with a three solvent system A: H_2O, B: acetonitrile and C: 2% formic acid in acetonitrile. The solvent method had a constant flow rate of 0.4 ml/min and started with 90/5/5 initial mix which increases to 45/50/5 over 1 min, then rises again to 5/90/5 over 7 min (8 min total) and held for a further 1 min. The system was allowed re-equilibrate to starting conditions before the next sample was run. BEA was identified in samples using retention time, UV spectra and mass spectrometry. BEA was quantified using UV absorbance (190–210 nm), with a calibration curve obtained using a beauvericin standard purchased from Cayman Chemical Company (concentrations 0.2, 0.1, 0.05 and 0.025 mg/mL).

2.5. Statistical analysis

One-way analysis of variance (ANOVA) and multiple comparison procedures were performed to test the effects of fungi and commercial BEA on nematode populations and to test the concentrations of BEA extracted from each *Beauveria* strain by HPLC. The ANOVA assumptions (normality and homogeneity of variances) were tested in each analysis by the Shapiro and Bartlett tests. When neither assumption was violated (concentrations of BEA extracted from each *Beauveria* strain), classical one-way ANOVA and Tukey's honestly significant difference (HSD) tests was applied. When at least one of these assumptions was violated (effects of fungi and commercial BEA on nematode populations) robust statistical methods were applied (García-Pérez, 2010). In particular, heteroscedastic one-way ANOVAs were performed using the generalized Welch procedure and a 0.1 trimmed mean transformation. These analyses were carried out using the Wilcox' robust statistics (WRS2) package implemented in the R software environment (R Core Team, 2021).

3. Results and discussion

3.1. *In vitro* antagonism tests of *Beauveria* spp. on *B. xylophilus* populations

Growth of *B. xylophilus* populations were strongly inhibited by the presence of *Beauveria* species ($F = 28.29$, $p < 0.001$). All three *Beauveria* strains showed a clear nematicidal effect on *B. xylophilus* populations, with no significant differences between the treatments (**Figure 2**). The nemastatic or nematicidal effect of *B. bassiana* has already demonstrated on other nematode species such as *M. incognita* (Kepenekci et al., 2017; Youssef et al., 2020; Karabörklü et al., 2022) and *C. elegans* (Ye et al., 2021). Thus, our results are congruent with previous evidence and confirm the potential biocontrol agent role of this fungus on *B. xylophilus*. To our knowledge, this is the first study that demonstrates the nematicidal activity of *B. pseudobassiana*. However, considering the phenotypic proximity of both *Beauveria* species (Rehner et al., 2011; Berestetskiy et al., 2018), this is not an unexpected result.

Growing methods for *B. xylophilus* are not standardized, but cultivation with *B. cinerea* (a non-sporulating isolate) grown on barley is the most widely used (Aikawa and Kikuchi, 2007; Espada et al., 2016; Pimentel et al., 2020) and the one recommended by EPPO (2013). Thus, as predicted, the nematode population in the presence of *B. cinerea* exponentially increased during the 13-day assay, obtaining a final population of approximately 165,000 individuals (**Figure 2**), corroborating its role as a positive-growth control. In contrast, the results obtained from the negative-growth control *E. vermicola* were unexpected. The final population (≈ 96,000 nematodes) from *E. vermicola* is much larger than obtained in the barley base-growth control (around 2,700 individuals) (**Figure 2**). The nematophagous effect of this fungus had been previously demonstrated, although this result could be due to the lack of lunate adhesive conidia detected in this study. Previous studies had linked the nematophagous effect to the production of this specific type of conidia (Liou et al., 1999; Kubátová et al., 2000; Wang et al., 2008, 2009, 2018; Lin et al., 2013; Pires et al., 2022).

3.2. Effect of commercial BEA on *B. xylophilus* populations

The results obtained show a clear nematicidal effect of beauvericin on populations of *B. xylophilus.* While the control treatment had a survival rate (after 48 h) of almost 60%, the BEA treatments survival rates were significantly lower ($F = 18.26$, $p < 0.001$). The 0.1 mM BEA treatment attained a survival rate of 35.1%, and 1 mM and 2 mM BEA treatments resulted in 23.5 and 20.8% survival rates, respectively, with no significant differences between them (**Figure 3**). Compared to control treatment (i.e., deducting the natural mortality), the mortality rates of each BEA treatment were 39.2, 59.2 and 63.9% (0.1, 1, and 2 mM, respectively), demonstrating the nematicidal activity of BEA.

The anthelmintic capacity of numerous compounds chemically close to BEA (cyclic-depsipeptides) have been quantified on many occasions (Scherkenbeck et al., 2002; Jeschke et al., 2005; Firakova et al., 2007; Prosperini et al., 2017). More specifically, the disruptive effect of BEA on the model nematode *C. elegans*

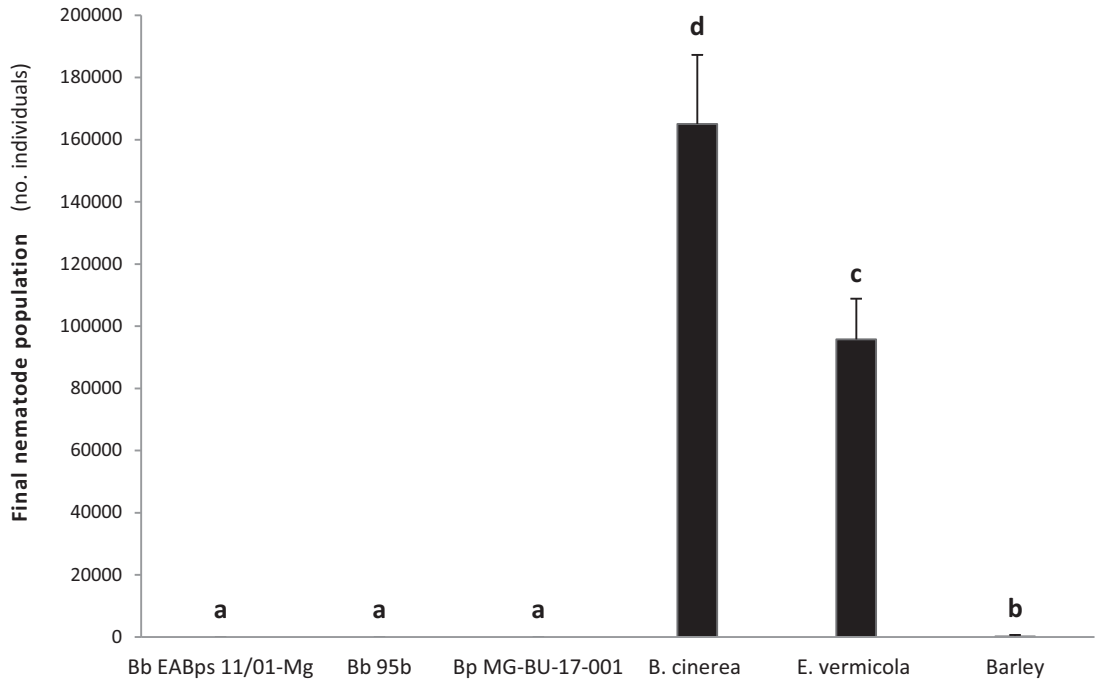

FIGURE 2
Effect on *B. xylophilus* populations from *B. bassiana* and *B. pseudobassiana* strains after 13 days. Bars with different letters indicate significantly different means (α = 0.05).

(Büchter et al., 2020) and on *B. xylophilus* (Shimada et al., 2010) has been confirmed. Comparing the results of beauvericin obtained from *F. bulbicola* (Shimada et al., 2010) with the commercial one used in this study, both exhibited similar linear trends: with higher concentrations of BEA resulting in higher mortality, although this effect seems to stabilize when the concentration approaches 2 mM. In the present study even the lowest BEA treatment (0.1 mM) showed a high nematode mortality (≈ 23% higher than mock treatment), however, Shimada et al. (2010) found only weak nematicidal activity using the same concentration. Of the concentrations of BEA tested, it appears the most suitable one for field application is 1 mM BEA, since it retained a similar nematicidal effect when compared with the 2 mM solution, but with lower product expenditure.

The mechanism of action of BEA on animal cells is still not completely understood, but seems linked to its ionophoric activity, which increases ion permeability in biological membranes and the consequent oxidative stress at molecular level (Mallebrera et al., 2018). In our trials, a brownish "encapsulation" was observed during the final visual assessment of BEA treatments individuals (**Figure 4**) which could be related to the combination of BEA molecules to the lipids of the nematode epicuticle.

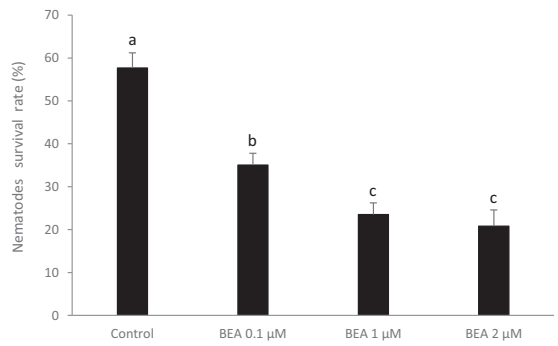

FIGURE 3
Survival rate of *B. xylophilus* in control (DMSO 5%) and treatments (BEA + DMSO 5%). Bars with different letters indicate significantly different means (α = 0.05).

3.3. Extraction, identification and quantification of BEA produced by our indigenous strains of *Beauveria* spp.

Beauvericin (BEA) was positively identified in all three strains using a mixture of UV, MS and HPLC column retention. Shown in **Figure 5**, is chromatograms of the BEA standard and *B. pseudobassiana* MG-BU-17-001, in both UV (200 nm) and single ion mode (SIM) MS (m/z = 784.3). BEA was assigned as a single peak [retention time (RT) = 6.85 min (UV) and 6.86 min (MS)] which was found in all experiments. This assignment was further confirmed by comparing the MS spectra (m/z = 100–1,050) of the BEA standard with all three strains showing we believe, for the first time the presence of BEA in *B. pseudobassiana* (**Figure 6**).

All three strains tested produced BEA, but significant differences were found between them (F = 10.06, p = 0.02). *B. bassiana* EABps 11/01-Mg exhibits the highest levels of BEA (151.4 µg/mL), followed by *B. bassiana* 95b (119.3 µg/mL) and lastly *B. pseudobassiana* MG-BU-17-001 (56.7 µg/mL) (**Figure 7**).

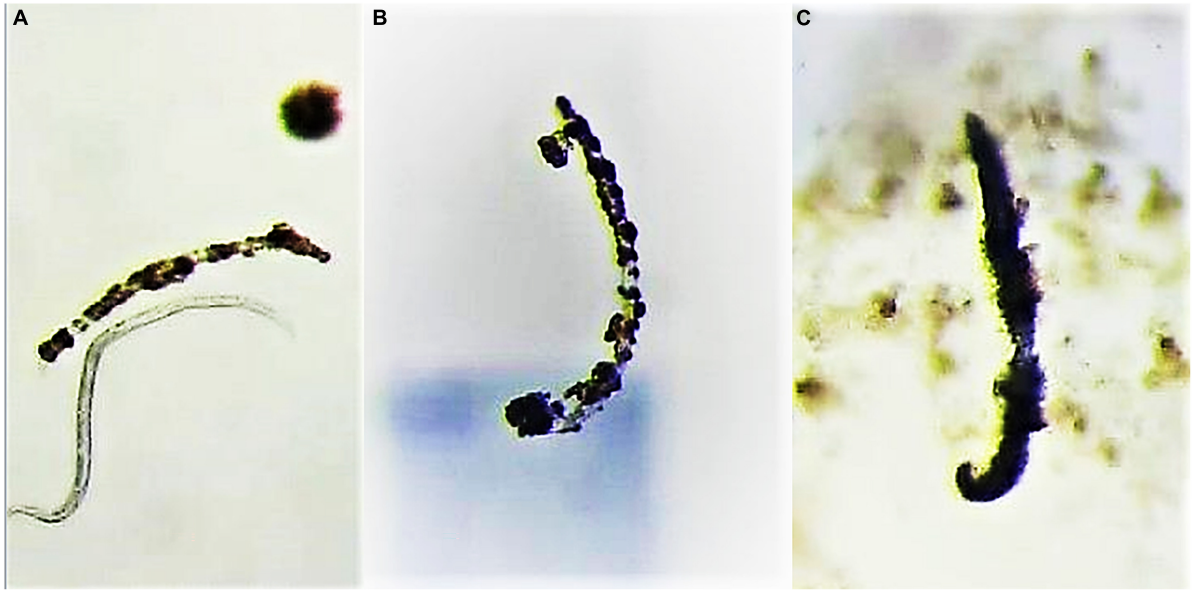

FIGURE 4
A nematode with a normal appearance together with a "encapsulated" one in 0.1 mM BEA **(A)** and other "encapsulated" nematodes found in 1 and 2 mM BEA treatments [**(B,C)**, respectively].

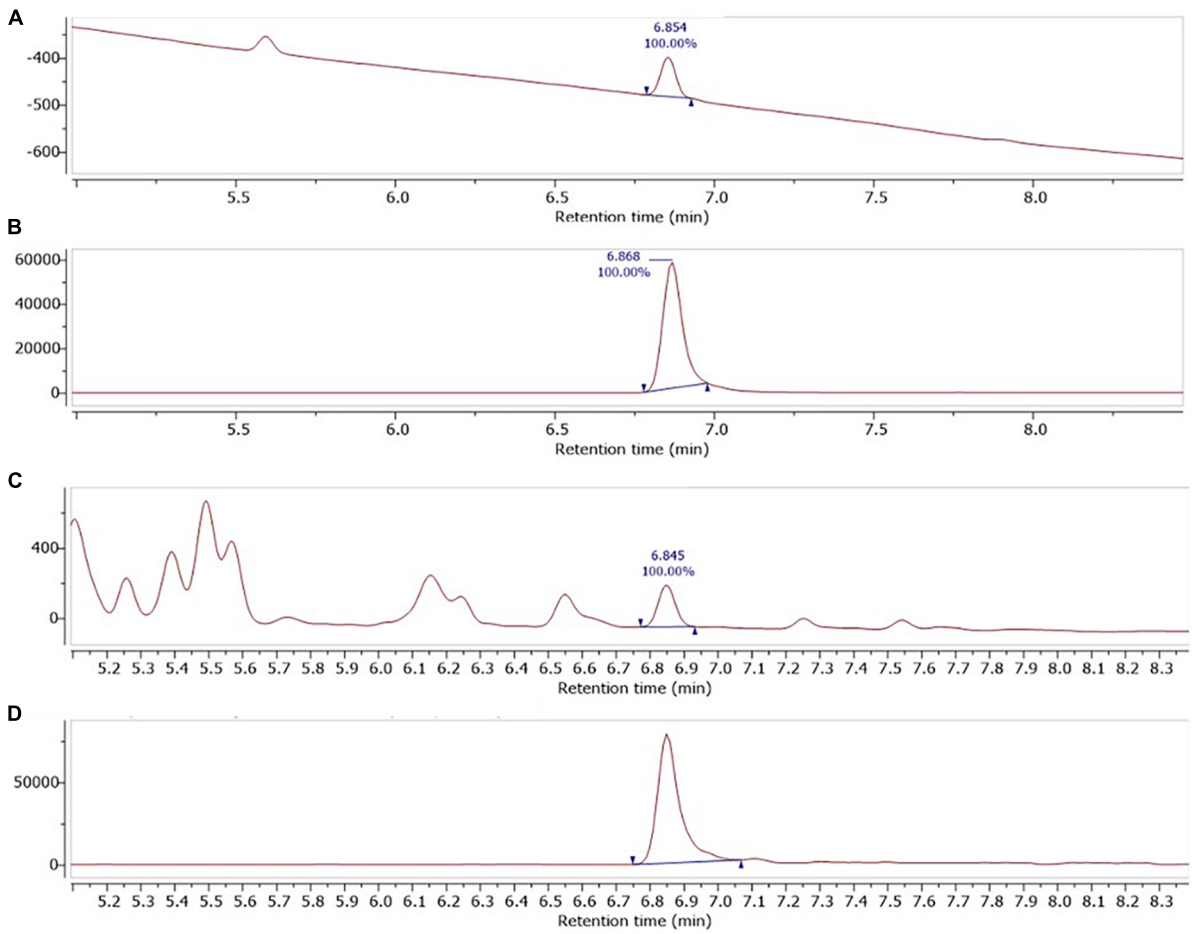

FIGURE 5
UV diode array detector (DAD) (200 ± 10 nm) and single ion mode (SIM) (784.3) atmospheric pressure chemical ionisation (APCI) chromatograms of, **(A,B)** BEA standard (10 μg/mL), and **(C,D)** *B. pseudobassiana* MG-BU-17-001.

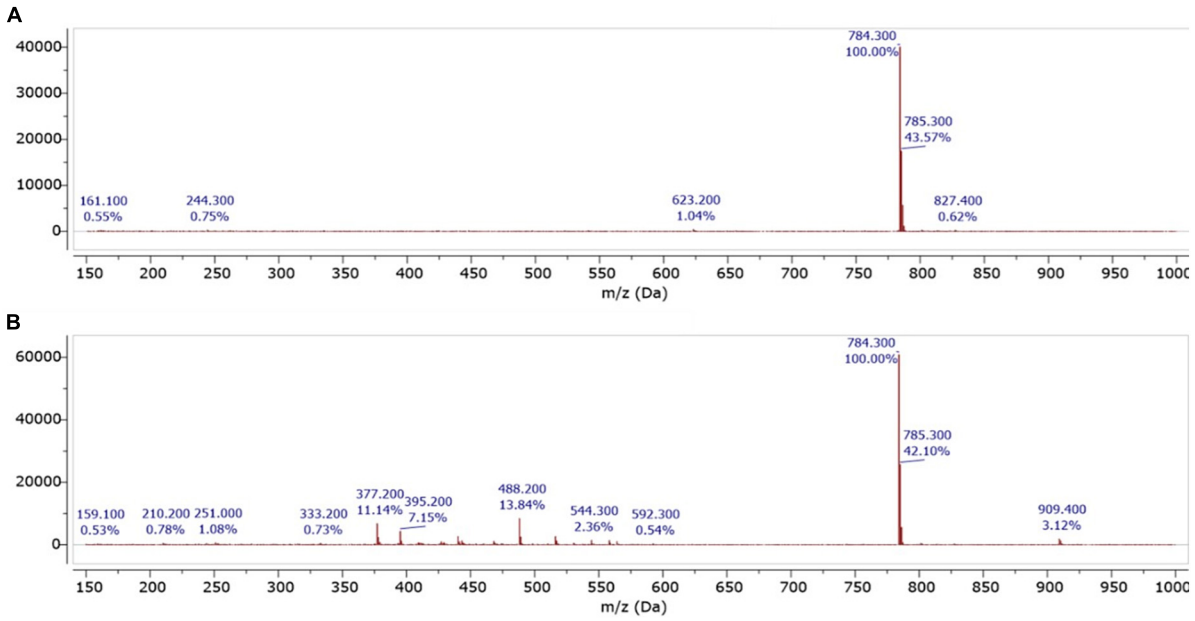

FIGURE 6
APCI MS spectra for **(A)** BEA standard (10 μg/mL), and **(B)** *B. pseudobassiana* "MG-BU-17-001."

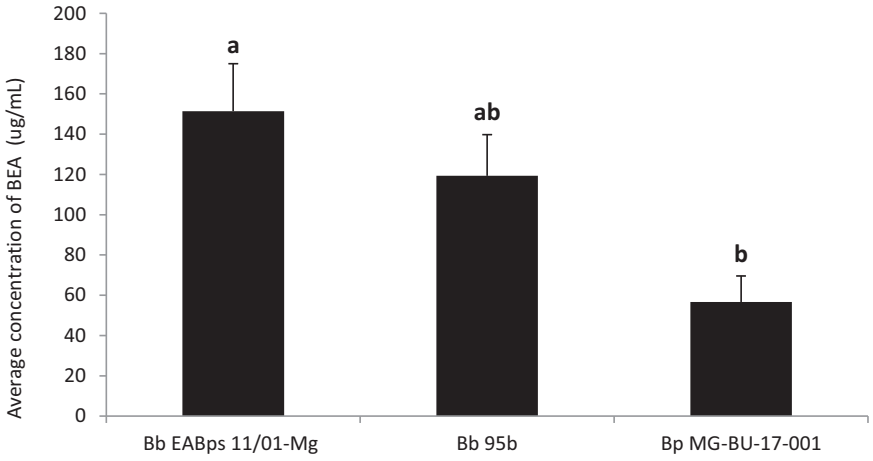

FIGURE 7
Average concentration of BEA (μg /mL) in extracts obtained from the three strains of *Beauveria* spp. Bars with different letters indicate significantly different means (α = 0.05).

While previous studies have confirmed the production of BEA by *B. bassiana* (Hamill et al., 1969; Valencia et al., 2011; Berestetskiy et al., 2018), this assay showed that the *B. bassiana* strains tested here produced a higher amount of beauvericin than other strains tested by Valencia et al. (2011), which should lead to stronger nematicidal and insecticidal effects. Moreover, to our knowledge, this is the first study that identified and quantified this mycotoxin in extracts of *B. pseudobassiana*. This finding opens the possibility of using both *Beauveria* species as potential antagonistic organisms against *B. xylophilus*. Further studies testing more strains of both species are needed to elucidate whether the differences found in this study are related to intraspecific or interspecific variability. Beyond the field of biopesticides, this outcome has parallel relevance for nutrition and human health, since BEA is classified as an emerging mycotoxin (Jestoi, 2008; Vaclavikova et al., 2013; EFSA, 2014) with high occurrence in food commodities (Al Khoury et al., 2021). It is therefore vital for food monitoring chains to have as much information as possible on all fungal species able to produce BEA.

4. Conclusion

Taking into account the high risk of spread of *B. xylophilus* and the serious threat that this species of nematode poses to European pines, the development of an effective tool for controlling the pine wilt disease is essential. Different antagonistic

fungi could exert biological control against the nematode or the beetle vector, although ideally a single fungus would be used to control both. This study found that *Beauveria* species, which had already demonstrated its entomopathogenic activity against *M. galloprovincialis* (Álvarez-Baz et al., 2015) also exhibited nematicidal activity against *B. xylophilus*. This finding paves the way for new research into the potential of these fungal strains to be tested in a self-infection device for PWN population control (Sacristán-Velasco et al., 2018) and their subsequent implementation in field conditions.

Data availability statement

The raw data supporting the conclusions of this article will be made available by the authors, without undue reservation.

Ethics statement

The manuscript presents research on animals that do not require ethical approval for their study.

Author contributions

JM-G, TS-G, and PZ conceived and designed the experiment. TS-G, PZ, MB, and SH performed the experiments. JM-G analyzed the data. TS-G and JM-G wrote the manuscript. All authors contributed to the article and approved the submitted version.

Funding

This publication was supported and financed by the BBVA Foundation (Becas Leonardo a Investigadores y Creadores Culturales 2020, Grant No. ING_0140). The Foundation takes no responsibility for the opinions, statements and contents of this project, which are entirely the responsibility of its authors. JN-S was also supported by the European Union's Horizon Europe research and innovation programme under the Marie Sklodowska-Curie Actions (MSCA) agreement No. 101068728. This study was also part of the research project "Estrategias para la contención de la enfermedad del marchitamiento del pino, causada por *Bursaphelenchus xylophilus*: resistencia del hospedante y manejo del insecto vector (NEMOPLAN)" (RTA2017-00012-C02-02) supported by Ministerio de Ciencia, Innovación y Universidades.

Acknowledgments

We thank to Masaryk University (Brno, Czech Republic) for kindly providing the strain *Esteya vermicola* CCM 8247. We would also like to thank CIF Lourizán, especially to Dra. Raquel Díaz Vázquez for her collaboration and support in the trials related to the nematode.

Conflict of interest

The authors declare that the research was conducted in the absence of any commercial or financial relationships that could be construed as a potential conflict of interest.

The handling editor IM is currently organizing a research topic with the author JD.

Publisher's note

Supplementary material

The Supplementary Material for this article can be found online at: https://www.frontiersin.org/articles/10.3389/ffgc.2023.1229456/full#supplementary-material

References

Abd-Elgawad, M. M., and Askary, T. H. (2018). Fungal and bacterial nematicides in integrated nematode management strategies. *Egypt. J. Biol. Pest Control* 28, 1–24. doi: 10.1186/s41938-018-0080-x

Aikawa, T., and Kikuchi, T. (2007). Estimation of virulence of *Bursaphelenchus xylophilus* (*Nematoda*: *Aphelenchoididae*) based on its reproductive ability. *Nematology* 9, 371–377. doi: 10.1163/156854107781352007

Al Khoury, C. A., Nemer, N., Tokajian, S., and Nemer, G. (2021). Beauvericin: The journey of a pesticide into a humanized drug. *Preprints* [Preprint]. doi: 10.20944/preprints202107.0506.v1

Altimira, F., Arias-Aravena, M., Jian, L., Real, N., Correa, P., González, C., et al. (2022). Genomic and experimental analysis of the insecticidal factors secreted by the entomopathogenic fungus *Beauveria pseudobassiana* RGM 2184. *J. Fungi* 8:253. doi: 10.3390/jof8030253

Álvarez-Baz, G., Fernández-Bravo, M., Pajares, J., and Quesada-Moraga, E. (2015). Potential of native *Beauveria pseudobassiana* strain for biological control of pine wood nematode vector *Monochamus galloprovincialis*. *J. Invertebr. Pathol.* 132, 48–56.

Álvarez-Baz, G., Gallego, D., Hall, D. R., Jactel, H., and Pajares, J. A. (2016). Combining pheromone and kairomones for effective trapping of the pine sawyer beetle *Monochamus galloprovincialis*. *J. Appl. Entomol.* 140, 58–71. doi: 10.1111/jen.12297

Anke, H. (2011). "Insecticidal and nematicidal metabolites from fungi," in *Industrial applications the mycota, Vol 10*, ed. M. Hofrichter (Berlin: Springer), 151–163. doi: 10.1007/978-3-642-11458-8_7

Anke, H., and Sterner, O. (1997). Nematicidal metabolites from higher fungi. *Curr. Organ. Chem.* 1, 361–374.

Anke, H., and Sterner, O. (2002). "Insecticidal and nematicidal metabolites from fungi," in *Industrial applications the mycota*, ed. H. D. Osiewacz (Berlin: Springer), 109–127. doi: 10.1007/978-3-662-10378-4_6

Askary, T. H. (2015). "Nematophagous fungi as biocontrol agents of phytonematodes," in *Biocontrol agents of phytonematodes*, eds T. Askary and P. Martinelli (Wallingford: CAB International), 81–125. doi: 10.1079/9781780643755.0081

Baazeem, A., Almanea, A., Manikandan, P., Alorabi, M., Vijayaraghavan, P., and Abdel-Hadi, A. (2021). In vitro antibacterial, antifungal, nematicidal and growth promoting activities of *Trichoderma hamatum* FB10 and its secondary metabolites. *J. Fungi* 7:331. doi: 10.3390/jof7050331

Baermann, G. (1917). "A simple method for the detection of Ankylostomum (nematode) larvae in soil tests," in *Mededelingen uit het geneeskundig laboratorium te weltevreden*, ed. G. Baermann (Batavia: Javasche Boekhandel & Drukkerij), 41–47.

Berestetskiy, A. O., Ivanova, A. N., Petrova, M. O., Prokof'eva, D. S., Stepanycheva, E. A., Uspanov, A. M., et al. (2018). Comparative analysis of the biological activity and chromatographic profiles of the extracts of *Beauveria bassiana* and *B. pseudobassiana* cultures grown on different nutrient substrates. *Microbiology* 87, 200–214. doi: 10.1134/S0026261718020030

Büchter, C., Koch, K., Freyer, M., Baier, S., Saier, C., Honnen, S., et al. (2020). The mycotoxin beauvericin impairs development, fertility and life span in the nematode *Caenorhabditis elegans* accompanied by increased germ cell apoptosis and lipofuscin accumulation. *Toxicol. Lett.* 334, 102–109. doi: 10.1016/j.toxlet.2020.09.016

Carrasquinho, I., Lisboa, A., Inácio, M. L., and Gonçalves, E. (2018). Genetic variation in susceptibility to pine wilt disease of maritime pine (*Pinus pinaster* Aiton) half-sib families. *Ann. For. Sci.* 75:85. doi: 10.1007/s13595-018-0759-x

De la Fuente, B., Saura, S., and Beck, P. S. (2018). Predicting the spread of an invasive tree pest: The pine wood nematode in Southern Europe. *J. Appl. Ecol.* 55, 2374–2385. doi: 10.1111/1365-2664.13177

Edwards, O. R., and Linit, M. J. (1992). Transmission of *Bursaphelenchus xylophilus* through oviposition wounds of *Monochamus carolinensis* (*Coleoptera*: *Cerambycidae*). *J. Nematol.* 24:133.

EFSA (2014). Scientific opinion on the risks to human and animal health related to the presence of beauvericin and enniatins in food and feed. *EFSA J.* 12:3802. doi: 10.2903/j.efsa.2014.3802

EPPO (2013). Diagnostics. PM 7/4 (3) *Bursaphelenchus xylophilus*. *EPPO Bull.* 43, 105–118. doi: 10.1111/epp.12024

EPPO (2016). *EPPO A1 and A2 Lists of pest recommended for regulation as quarantine pests*. Paris: European and Mediterranean Plant Protection Organization.

Espada, M., Silva, A. C., Eves van den Akker, S., Cock, P. J., Mota, M., and Jones, J. T. (2016). Identification and characterization of parasitism genes from the pinewood nematode *Bursaphelenchus xylophilus* reveals a multilayered detoxification strategy. *Mol. Plant Pathol.* 17, 286–295. doi: 10.1111/mpp.12280

Firakova, S., Proksa, B., and Šturdíková, M. (2007). Biosynthesis and biological activity of enniatins. *Die Pharm. Int. J. Pharmaceut. Sci.* 62, 563–568. doi: 10.1691/ph.2007.8.7600

Fornelli, F., Minervini, F., and Logrieco, A. (2004). Cytotoxicity of fungal metabolites to lepidopteran (*Spodoptera frugiperda*) cell line (SF-9). *J. Invertebr. Pathol.* 85, 74–79. doi: 10.1016/j.jip.2004.01.002

Fujimoto, Y., and Ohba, K. (1981). "The first year results of the breeding of Japanese pines for resistance to the wood nematode," in *Proceeding of the XVII IUFRO World Congress*, (Kyoto), 287–291.

Fukuda, K., and Suzuki, K. (1988). Changes of water relation parameters in pinewood nematode-infested Japanese red pine. *J. Jap. For. Soc.* 70, 390–394. doi: 10.11519/jjfs1953.70.9_390

Ganassi, S., Moretti, A., Pagliai, A. M. B., Logrieco, A., and Sabatini, M. A. (2002). Effects of beauvericin on *Schizaphis graminum* (*Aphididae*). *J. Invertebr. Pathol.* 80, 90–96. doi: 10.1016/S0022-2011(02)00125-8

García-Pérez, A. (2010). *Métodos avanzados de estadística aplicada. métodos robustos y de remuestreo*. Madrid: UNED Universidad Nacional a Distancia.

Gaspar, D., Trindade, C., Usié, A., Meireles, B., Barbosa, P., Fortes, A. M., et al. (2017). Expression profiling in *Pinus pinaster* in response to infection with the pine wood nematode *Bursaphelenchus xylophilus*. *Forests* 8:279. doi: 10.3390/f8080279

Grove, J. F., and Pople, M. (1980). The insecticidal activity of beauvericin and the enniatin complex. *Mycopathologia* 70, 103–105. doi: 10.1007/BF00443075

Gupta, S., Krasnoff, S. B., Underwood, N. L., Renwick, J. A. A., and Roberts, D. W. (1991). Isolation of beauvericin as an insect toxin from *Fusarium semitectum* and *Fusarium moniliforme* var. *subglutinans*. *Mycopathologia* 115, 185–189. doi: 10.1007/BF00462223

Hamill, R. L., Higgens, C. E., Boaz, H. E., and Gorman, M. (1969). The structure of beauvericin, a new depsipeptide antibiotic toxic to *Artemia salina*. *Tetrahedron Lett.* 10, 4255–4258. doi: 10.1016/S0040-4039(01)88668-8

Hara, N., Takeuchi, Y., and Futai, K. (2006). Cytological changes in ray parenchyma cells of seedlings of three pine species infected with the pine wilt disease. *Jap. J. Nematol.* 36, 23–32. doi: 10.3725/jjn.36.23

Hirata, A., Nakamura, K., Nakao, K., Kominami, Y., Tanaka, N., Ohashi, H., et al. (2017). Potential distribution of pine wilt disease under future climate change scenarios. *PLoS One* 12:e0182837. doi: 10.1371/journal.pone.0182837

Jeschke, P., Harder, A., Schindler, M., and Etzel, W. (2005). Cyclohexadepsipeptides (CHDPs) with improved anthelmintical efficacy against the gastrointestinal nematode (*Haemonchus contortus*) in sheep. *Parasitol. Res.* 97, S17–S21. doi: 10.1007/s00436-005-1440-5

Jestoi, M. (2008). Emerging *Fusarium*-mycotoxins fusaproliferin, beauvericin, enniatins, and moniliformin—A review. *Crit. Rev. Food Sci. Nutr.* 48, 21–49. doi: 10.1080/10408390601062021

Karabörklü, S., Aydinli, V., and Dura, O. (2022). The potential of *Beauveria bassiana* and *Metarhizium anisopliae* in controlling the root-knot nematode *Meloidogyne incognita* in tomato and cucumber. *J. Asia Pac. Entomol.* 25:101846. doi: 10.1016/j.aspen.2021.101846

Kepenekci, I., Saglam, H. D., Oksal, E., Yanar, D., and Yanar, Y. (2017). Nematicidal activity of *Beauveria bassiana* (Bals.-Criv.) Vuill. against root-knot nematodes on tomato grown under natural conditions. *Egypt. J. Biol. Pest Control* 27:117.

Kim, B. N., Kim, J. H., Ahn, J. Y., Kim, S., Cho, B. K., Kim, Y. H., et al. (2020). A short review of the pinewood nematode, *Bursaphelenchus xylophilus*. *Toxicol. Environ. Health Sci.* 12, 297–304. doi: 10.1007/s13530-020-00068-0

Kubátová, A., Novotný, D., Prášil, K., and Mráček, Z. (2000). The nematophagous hyphomycete *Esteya vermicola* found in the Czech Republic. *Czech Mycol.* 52, 227–235. doi: 10.33585/cmy.52305

Leland, J. E., McGuire, M. R., Grace, J. A., Jaronski, S. T., Ulloa, M., Park, Y. H., et al. (2005). Strain selection of a fungal entomopathogen, *Beauveria bassiana*, for control of plant bugs (*Lygus* spp.) (*Heteroptera*: *Miridae*). *Biol. Control* 35, 104–114. doi: 10.1016/j.biocontrol.2005.06.005

Li, G., Zhang, K., Xu, J., Dong, J., and Liu, Y. (2007). Nematicidal substances from fungi. *Recent Patents Biotechnol.* 1, 212–233. doi: 10.2174/187220807782330165

Lin, F., Ye, J., Wang, H., Zhang, A., and Zhao, B. (2013). Host deception: Predaceous fungus, *Esteya vermicola*, entices pine wood nematode by mimicking the scent of pine tree for nutrient. *PLoS One* 8:e71676. doi: 10.1371/journal.pone.0071676

Liou, J. Y., Shih, J. Y., and Tzean, S. S. (1999). Esteya, a new nematophagous genus from Taiwan, attacking the pinewood nematode (*Bursaphelenchus xylophilus*). *Mycol. Res.* 103, 242–248. doi: 10.1017/S0953756298006984

Liu, Q., Wei, Y., Xu, L., Hao, Y., Chen, X., and Zhou, Z. (2017). Transcriptomic profiling reveals differentially expressed genes associated with pine wood nematode resistance in masson pine (*Pinus massoniana* Lamb.). *Sci. Rep.* 7:4693. doi: 10.1038/s41598-017-04944-7

Logrieco, A., Rizzo, A., Ferracane, R., and Ritieni, A. (2002). Occurrence of beauvericin and enniatins in wheat affected by *Fusarium avenaceum* head blight. *Appl. Environ. Microbiol.* 68, 82–85. doi: 10.1128/AEM.68.1.82-85.2002

Maehara, N., and Futai, K. (2000). Population changes of the pinewood nematode, *Bursaphelenchus xylophilus* (*Nematoda*: *Aphelenchoididae*), on fungi growing in pine-branch segments. *Appl. Entomol. Zool.* 35, 413–417. doi: 10.1303/aez.2000.413

Maehara, N., He, X., and Shimazu, M. (2007). Maturation feeding and transmission of *Bursaphelenchus xylophilus* (*Nematoda*: *Parasitaphelenchidae*) by *Monochamus alternatus* (*Coleoptera*: *Cerambycidae*) inoculated with *Beauveria bassiana* (*Deuteromycotina*: *Hyphomycetes*). *J. Econ. Entomol.* 100, 49–53. doi: 10.1093/jee/100.1.49

Mallebrera, B., Prosperini, A., Font, G., and Ruiz, M. J. (2018). In vitro mechanisms of Beauvericin toxicity: A review. *Food Chem. Toxicol.* 111, 537–545. doi: 10.1016/j.fct.2017.11.019

Mamiya, Y., and Enda, N. (1972). Transmission of *Bursaphelenchus lignicolus* (*Nematoda*: *Aphelenchoididae*) by *Monochamus alternatus* (*Coleoptera*: *Cerambycidae*). *Nematologica* 18, 159–162. doi: 10.1163/187529272X00395

Mankau, R. (1980). Biocontrol: Fungi as nematode control agents. *J. Nematol.* 12:244.

Mayer, A. (1995). *Bekämpfung von pflanzenparasitären Nematoden der Gattung Meloidogyne mit Pilzen und deren Toxinen*. Ph.D thesis. Kaiserslautern: University of Kaiserslautern.

Menéndez-Gutiérrez, M., Alonso, M., and Díaz, R. (2021). Assessing genetic variation in resistance to Pinewood Nematode (*Bursaphelenchus xylophilus*) in *Pinus radiata* D. Don Half-Sib Families. *Forests* 12:1474. doi: 10.3390/f12111474

Menéndez-Gutiérrez, M., Alonso, M., Toval, G., and Díaz, R. (2018). Testing of selected *Pinus pinaster* half-sib families for tolerance to pinewood nematode (*Bursaphelenchus xylophilus*). *Forestry* 91, 38–48. doi: 10.1093/forestry/cpx030

Migunova, V. D., and Sasanelli, N. (2021). Bacteria as biocontrol tool against phytoparasitic nematodes. *Plants* 10:389. doi: 10.3390/plants10020389

Moretti, A., Belisario, A., Tafuri, A., Ritieni, A., Corazza, L., and Logrieco, A. (2002). "Production of beauvericin by different races of *Fusarium oxysporum* f. sp. *melonis*, the *Fusarium* wilt agent of muskmelon," in *Mycotoxins in plant disease*, eds A. Logrieco, J. A. Bailey, L. Corazza, and B. M. Cooke (Dordrecht: Springer), 661–666. doi: 10.1007/978-94-010-0001-7_8

Moretti, A., Mulé, G., Ritieni, A., Láday, M., Stubnya, V., Hornok, L., et al. (2008). Cryptic subspecies and beauvericin production by *Fusarium subglutinans* from Europe. *Int. J. Food Microbiol.* 127, 312–315. doi: 10.1016/j.ijfoodmicro.2008.08.003

Mota, M., Burgermeister, W., Braasch, H., Sousa, E., Penas, A. C., Metge, K., et al. (1999). First report of *Bursaphelenchus xylophilus* in portugal and in Europe. *Nematology* 1, 727–734. doi: 10.1163/156854199508757

Naves, P. M., Sousa, E., and Rodrigues, J. M. (2008). Biology of *Monochamus galloprovincialis* (*Coleoptera*, *Cerambycidae*) in the pine wilt disease affected zone, Southern Portugal. *Silva Lusitana* 16, 133–148.

Petersen-Silva, R., Inácio, L., Henriques, J., Naves, P., Sousa, E., and Pujade-Villar, J. (2015). Susceptibility of larvae and adults of *Monochamus galloprovincialis* to entomopathogenic fungi under controlled conditions. *Int. J. Pest Manag.* 61, 106–112. doi: 10.1080/09670874.2015.1016472

Pimentel, C. S., Firmino, P. N., and Ayres, M. P. (2020). Comparison of methods to obtain and maintain cultures of the pinewood nematode, *Bursaphelenchus xylophilus*. *J. For. Res.* 25, 101–107. doi: 10.1080/13416979.2020.1745989

Pires, D., Vicente, C. S., Inácio, M. L., and Mota, M. (2022). The potential of *Esteya* spp. for the biocontrol of the Pinewood Nematode, *Bursaphelenchus xylophilus*. *Microorganisms* 10:168. doi: 10.3390/microorganisms10010168

Prosperini, A., Berrada, H., Ruiz, M. J., Caloni, F., Coccini, T., Spicer, L. J., et al. (2017). A review of the mycotoxin enniatin B. *Front. Public Health* 5:304. doi: 10.3389/fpubh.2017.00304

R Core Team (2021). *R: A language and environment for statistical computing*. Vienna: R Foundation for Statistical Computing.

Rehner, S. A., Minnis, A. M., Sung, G. H., Luangsa-ard, J. J., Devotto, L., and Humber, R. A. (2011). Phylogeny and systematics of the anamorphic, entomopathogenic genus *Beauveria*. *Mycologia* 103, 1055–1073. doi: 10.3852/10-302

Sacristán-Velasco, A., Bravo, M. D. C. F., Moraga, E. Q., and Alonso, J. A. P. (2018). Control biológico del vector del nematodo de la madera del pino *Monochamus galloprovincialis* Olivier mediante autoinfección con el hongo entomopatógeno *Beauveria pseudobassiana* SA Rehner & Humber. *Cuadernos Soc. Española Ciencias For.* 44, 147–168.

Scherkenbeck, J., Jeschke, P., and Harder, A. (2002). PF1022A and related cyclodepsipeptides-a novel class of anthelmintics. *Curr. Top. Med. Chem.* 2, 759–777. doi: 10.2174/1568026023393624

Seong, J., Shin, J., Kim, K., and Cho, B. K. (2021). Microbial production of nematicidal agents for controlling plant-parasitic nematodes. *Process Biochem.* 108, 69–79. doi: 10.1016/j.procbio.2021.06.006

Shimada, A., Fujioka, S., Koshino, H., and Kimura, Y. (2010). Nematicidal activity of beauvericin produced by the fungus *Fusarium bulbicola*. *Zeitschrift Für Naturforschung C* 65, 207–210. doi: 10.1515/znc-2010-3-407

Toda, T., and Kurinobu, S. (2002). Realized genetic gains observed in progeny tolerance of selected red pine (*Pinus densiflora*) and black pine (*P. thunbergii*) to pine wilt disease. *Silvae Genet.* 51, 42–44.

Vaclavikova, M., Malachova, A., Veprikova, Z., Dzuman, Z., Zachariasova, M., and Hajslova, J. (2013). 'Emerging'mycotoxins in cereals processing chains: Changes of enniatins during beer and bread making. *Food Chem.* 136, 750–757. doi: 10.1016/j.foodchem.2012.08.031

Valencia, J. W. A., Gaitán Bustamante, A. L., Jiménez, A. V., and Grossi-de-Sá, M. F. (2011). Cytotoxic activity of fungal metabolites from the pathogenic fungus *Beauveria bassiana*: An intraspecific evaluation of Beauvericin production. *Curr. Microbiol.* 63, 306–312. doi: 10.1007/s00284-011-9977-2

Vicente, C. S., Soares, M., Faria, J., Espada, M., Mota, M., Nóbrega, F., et al. (2022). Fungal communities of the pine wilt disease complex: Studying the interaction of ophiostomatales with *Bursaphelenchus xylophilus*. *Front. Plant Sci.* 13:908308. doi: 10.3389/fpls.2022.908308

Wang, C. Y., Fang, Z. M., Sun, B. S., Gu, L. J., Zhang, K. Q., and Sung, C. K. (2008). High infectivity of an endoparasitic fungus strain, *Esteya vermicola*, against nematodes. *J. Microbiol.* 46:380. doi: 10.1007/s12275-007-0122-7

Wang, C. Y., Fang, Z. M., Wang, Z., Gu, L. J., Sun, B. S., Zhang, D. L., et al. (2009). High infection activities of two *Esteya vermicola* isolates against pinewood nematode. *Afr. J. Microbiol. Res.* 3, 581–584.

Wang, C. Y., Yin, C., Fang, Z. M., Wang, Z., Wang, Y. B., Xue, J. J., et al. (2018). Using the nematophagous fungus *Esteya vermicola* to control the disastrous pine wilt disease. *Biocontrol. Sci. Technol.* 28, 268–277. doi: 10.1080/09583157.2018.1441369

Wang, H., Chu, H., Xie, Q., Dou, Q., Feng, H., Yang, C., et al. (2016). Variation in sporulation of four Esteya vermicola isolates and their infectivity against pinewood nematode. *Sci. Silvae Sin.* 52, 139–146. doi: 10.11707/j.1001-7488.20160917

Ye, S., Shang, L., Xie, X., Cao, Y., and Chen, C. (2021). Optimization of in vitro culture conditions for production of *Cordyceps bassiana* spores (*Ascomycetes*) and the effect of spore extracts on the health of *Caenorhabditis elegans*. *Int. J. Med. Mushrooms* 23, 44–55. doi: 10.1615/IntJMedMushrooms.2021038683

Youssef, M., El-Nagdi, W., and Lotfy, D. E. (2020). Evaluation of the fungal activity of *Beauveria bassiana*, *Metarhizium anisopliae* and *Paecilomyces lilacinus* as biocontrol agents against root-knot nematode, *Meloidogyne incognita* on cowpea. *Bull. Natl. Res. Centre* 44, 1–11. doi: 10.1186/s42269-020-00367-z

Zamora, P., Rodríguez, V., Renedo, F., Sanz, A. V., Domínguez, J. C., Pérez-Escolar, G., et al. (2015). First report of *Bursaphelenchus xylophilus* causing pine wilt disease on *Pinus radiata* in Spain. *Plant Dis.* 99:1449. doi: 10.1094/PDIS-03-15-0252-PDN

Zas, R., Moreira, X., Ramos, M., Lima, R. M. R., Da Silva, M. N., Solla, A., et al. (2015). Intraspecific variation of anatomical and chemical defensive traits in Maritime pine (*Pinus pinaster*) as factors in susceptibility to the pinewood nematode (*Bursaphelenchus xylophilus*). *Trees* 29, 663–673. doi: 10.1007/s00468-014-1143-6

Zhu, P., Chen, Y., Zhang, J., Wu, F., Wang, X., Pan, T., et al. (2021). Identification, classification, and characterization of AP2/ERF superfamily genes in masson pine (*Pinus massoniana* Lamb.). *Sci. Rep.* 11:5441. doi: 10.1038/s41598-021-84855-w

frontiers | Frontiers in Forests and Global Change

TYPE Original Research
PUBLISHED 25 August 2023
DOI 10.3389/ffgc.2023.1253022

OPEN ACCESS

EDITED BY
Nicolas Feau,
Natural Resources Canada, Canada

REVIEWED BY
Ippolito Camele,
University of Basilicata, Italy
Loukas I. Kanetis,
Cyprus University of Technology, Cyprus

*CORRESPONDENCE
Alessandra Benigno
✉ alessandra.benigno@unifi.it
Salvatore Moricca
✉ salvatore.moricca@unifi.it

RECEIVED 04 July 2023
ACCEPTED 09 August 2023
PUBLISHED 25 August 2023

CITATION
Benigno A, Bregant C, Aglietti C, Rossetto G, Tolio B, Moricca S and Linaldeddu BT (2023) Pathogenic fungi and oomycetes causing dieback on *Fraxinus* species in the Mediterranean climate change hotspot region.
Front. For. Glob. Change 6:1253022.
doi: 10.3389/ffgc.2023.1253022

Pathogenic fungi and oomycetes causing dieback on *Fraxinus* species in the Mediterranean climate change hotspot region

Alessandra Benigno[1]*, Carlo Bregant[2], Chiara Aglietti[1], Giovanni Rossetto[2], Beatrice Tolio[2,3,4], Salvatore Moricca[1]* and Benedetto T. Linaldeddu[2]

[1]Department of Agricultural, Food, Environmental and Forestry Science and Technology (DAGRI), Plant Pathology and Entomology Section, University of Florence, Florence, Italy, [2]Dipartimento Territorio e Sistemi Agro-Forestali, Università degli Studi di Padova, Viale dell'Università, Legnaro, Italy, [3]Skogforsk, The Forestry Research Institute of Sweden, Svalöv, Sweden, [4]Southern Swedish Forest Research Centre, Swedish University of Agricultural Sciences, Alnarp, Sweden

Environmental changes are occurring on a global scale, but their effects are most pronounced in climate change hotspot zones, such as the Mediterranean basin. Within this area Italy, extending from its southern coasts in the core of the Mediterranean Sea to its northernmost pre-Alpine and Alpine regions, is characterized by a variety of climatic conditions and vegetation types. Surveys conducted in 2018–2022 in forest formations of Central-Northern Italy revealed that the enhanced warming trend and irregular distribution of precipitations are strongly impacting the health of *Fraxinus* species, with some pathogenic fungi and oomycetes being important contributing factors to the decline of the three main ash species growing there: common ash (*Fraxinus excelsior*), flowering ash (*Fraxinus ornus*), and narrow-leaved ash (*Fraxinus angustifolia*). Isolation from symptomatic plant material collected countrywide under different site conditions and pathogenicity tests revealed a complex phytopathological framework, with several pathogenic species in addition to *Hymenoscyphus fraxineus* involved with a prominent role in the ash dieback etiology. Key microbial taxa included the fungal and oomycete pathogens *Botryosphaeria dothidea*, *Diplodia fraxini*, *Diplodia subglobosa*, *Phytophthora acerina*, and *Phytophthora plurivora*. The disease impact was higher on sites where ash trees grew under environmental stress (i.e., areas characterized by mild dry winters, hot summers with intense and prolonged drought) and exhibited reduced vigor, also as a consequence of anthropogenic interference (i.e., silvicultural management and fires). The identified causative agents are emerging pathogens that thrive under warmer conditions, their impact in the investigated areas being prevalent compared to *H. fraxineus*, which appears to be restricted on the Italian peninsula to the cooler and wetter valleys of the Alps and Central-Northern Apennines.

KEYWORDS

ash-tree dieback, stem cankers, leaf and shoot blight, collar necrosis, root diseases, invasive pathogens, climate change

1. Introduction

The Mediterranean basin lies in a transition zone between the semi-arid climate of North Africa and the temperate and rainy conditions of central Europe, affected by interactions between temperate and tropical processes (Giorgi and Lionello, 2008). Due to their particularly favorable geographical and climatic features, Mediterranean regions are characterized by an enormous floral and faunistic diversity, recognized as the second most important biodiversity hotspot on the planet (Myers et al., 2000). The vastness and heterogeneity of this large geographical area allows the survival of over 25000 species, distributed in countless habitats, ranging from the coastal areas, islands and typical low-altitude formations to the closely subalpine and alpine regions; this high biodiversity is mostly linked to intense processes of speciation and extinction during the Quaternary age (Cowling et al., 1996; Myers et al., 2000).

Despite their relative integrity, Mediterranean forests show a high fragility and vulnerability to several natural and human-induced threats such as fires, pests and pathogens, habitat destruction and deforestation (Linaldeddu et al., 2014; Nunes et al., 2022). Climate change has also threatened the survival of these habitats in recent decades; due to its features and geographic position, the Mediterranean basin is considered one of the most prominent climatic hotspots on the planet, representing one of the areas more vulnerable to the impact of climate change in the future (Giorgi, 2006; Giorgi and Lionello, 2008).

Some authors have investigated the profound changes taking place in these regions, correlating them directly to the global climate change; the main factor is a much higher increase in temperatures than the rest of the planet (Ulbrich et al., 2012; Lionello and Scarascia, 2018). In addition, an irregular distribution of the rainfall regime characterizes the Mediterranean area, with increasing and anomalous episodes of drought alternating with extreme events and brief very rainy periods (Valdes-Abellan et al., 2017).

In this scenario of radical change for natural environments, trees are often under conditions of accentuated stress, exposing them more to diseases and pests and posing the potential for forest decline phenomena. These involve a complex group of abiotic and biotic elements and contributors to the losses in tree health and increasing mortality (Manion, 1981; Brasier et al., 1993). During the last three decades, extensive dieback and mortality phenomena have been affecting many European forests, with a greater incidence in the Mediterranean basin (Scanu et al., 2015; Bregant et al., 2020, 2023). One of the most significant examples characterizing the Mediterranean areas with particular incidence is certainly oak decline; recently, many studies have investigated the causes of these widespread phenomena, confirming the direct correlation between climate change as a predisposing factor and pathogens as primary cause of death (Moricca and Ragazzi, 2008; Moricca et al., 2016).

Unlike vast forests involved in decline phenomena, like oak-dominated forests, less widespread but ecologically important *Fraxinus* formations have received relatively little attention. However, in various regions of the Mediterranean in recent years there has been a progressive decline and dieback of the three species of the genus *Fraxinus* that are the main representatives of the genus, namely common ash (*Fraxinus excelsior* L.), flowering ash (*Fraxinus ornus* L.), and narrow-leaved ash (*Fraxinus angustifolia* Vahl.). The damage was particularly serious in some areas, where high mortality, especially in young seedlings, caused a strong limitation to natural regeneration. The attacked trees exhibited a variety of symptoms, the most typical being: sunken cankers on the stem and branches, with a characteristic wedge-shaped necrotic sector in cross section; leaf and shoot blight, resulting in a progressive dieback of the canopy; production of tarry exudates on the lower stem; root and collar rot; in response to the bark and root damages, the canopy evidenced non-specific symptoms of progressive or sudden decline (Orlikowski et al., 2011; Linaldeddu et al., 2020a; Peters et al., 2023).

All these variable symptoms represent a complex syndrome that substantially differ in its etiology and pattern from the simple pathosystem model ash dieback–*Hymenoscyphus fraxineus*. Regarding this latter fungus, it has being expanding since 2009 in various Italian regions starting from the North-Eastern Alps to some areas in the center of the country along the Apennines (Ogris et al., 2010; Luchi et al., 2016; Migliorini et al., 2022). The disease involves all the three above-named ash species, with particular incidence on common ash (*Fraxinus excelsior*) (Panconesi et al., 2014; Rigling et al., 2018). This helotiaceous fungus prefers the cold and humid valleys of the mountain areas of North Italy and North-Central Apennines, its current southern range being some scattered sites in mountain areas with Mediterranean climatic conditions, characterized by cold and snowy winters and cool summers with absence of drought (Migliorini et al., 2022). However, it is unlikely that it will succeed in expanding southward, being limited by the unfavorable conditions of the Mediterranean climate, characterized by mild-dry winters and hot summers with prolonged droughts even in mountainous areas.

This different and more complex phytopathological framework of ash decline in the Mediterranean region emerged in some recent studies and observations in Italy (Benigno et al., 2019; Linaldeddu et al., 2020a) and, paralleled by similar findings in Slovenia, (Linaldeddu et al., 2022), prompted the present investigation, aimed at clarifying the possible role of the new causal agents involved. There is compelling evidence that the rapid changing of climatic conditions occurring in the Mediterranean region is altering the ecology, biogeography and above all infection biology of plant pathogens, creating conditions conducive to new disease emergence and spread (Dukes et al., 2009; Sturrock et al., 2011). These changes markedly alter the relationship between pathogens and their hosts (Sturrock et al., 2011). Some groups of pathogens in particular, like some members of the *Botryosphaeriaceae* family, seem to gain advantage from and thrive under warmer conditions, spreading pervasively over new hosts and areas (Hansen, 2008; Rehfeldt et al., 2009; Venette, 2009). Furthermore, the increasing temperature and altered precipitation regimes also affect the physiology of trees while, at the same time, drought conditions may compromise the fine roots, making trees more susceptible to water stress and attack by root oomycete pathogens (Ginetti et al., 2014; Haavik et al., 2015; Moricca et al., 2016; Colangelo et al., 2018).

In this study, we present new insight into the infection and aggressive colonization of *Fraxinus* species by several emerging pathogens in Central-Northern Italy, with identification of the fungal (endophytic and canker-associated *Botryosphaeriaceae*) and oomycete (*Phytophthora*) species involved, proof of pathogenicity, and elucidation of the key role of some of these pathogens in the dieback of ash species in the investigated areas.

2. Materials and methods

2.1. Sampling and isolation procedures

Investigations were conducted in 40 ash formations distributed from the plains to the mountainous areas in four regions of Central and North-eastern Italy: Toscana, Emilia Romagna, Veneto, and Friuli Venezia Giulia. Survey areas involved the natural ecological range of all three Italian spontaneous ash species: *Fraxinus angustifolia*, *F. excelsior*, and *F. ornus* (**Supplementary Table 1**). Study sites ranged from 0 to 1424 m. a.s.l, covering the entire altitude range for *Fraxinus* spp. in these regions and including the natural reserve of the lowland forest Boscone della Mesola (site 40). Forest sites were characterized by very different meteorological and climate conditions (**Supplementary Table 1**).

From spring 2018 to summer 2022 trees in each site were visually checked for the presence of disease symptoms on canopy (shoot blight, branch canker, bleeding canker), collar and roots (bark necrosis, exudates and root rot). A roughly 50 m long transect was established to evaluate disease incidence and mortality rate, estimated as the number of symptomatic individuals out of the total number of trees (DI = n/N × 100) and the number of dead trees out of the total number of trees (M = d/N × 100), respectively (Moricca et al., 2012a; Linaldeddu et al., 2020a). An amount of 362 samples representative of all symptoms observed on roots including rhizosphere (R = 75 samples), at the collar (TC = 21) and on main stem and branches (C = 262) (**Supplementary Table 1**). The highest number of samples was collected from flowering ash (211), followed by common ash (116 samples) and narrow-leaved ash (35).

All branch, stem and collar samples were taken to the laboratory to be visually examined and the outer bark surface was initially disinfected with 90% ethanol and then removed with a sterile scalpel. Isolations were performed from about 5 mm^2 fragments of inner bark and xylem cut aseptically from the margin of necrotic lesions (Panzavolta et al., 2018; Linaldeddu et al., 2020a). All fragments were placed on 90 mm Petri dishes containing potato dextrose agar (PDA, Oxoid Ltd., UK). After incubation at 25°C for 5–7 days in the dark, hyphal tips from the margin of emerging fungal colonies were sub-cultured onto half-strength PDA and incubated at room temperature under natural daylight to enhance sporulation.

Isolation of root rot agents was performed as reported by Bregant et al. (2020). In the laboratory root and rhizosphere samples were placed in a plastic box and flooded with 2 L of distilled water. After 24 h, young cork oak and elder leaves were placed on the water surface and used as baits. Boxes were kept at 20°C under natural daylight and after 5 days, leaves showing necrotic lesions were cut in small pieces (2–3 mm^2) and placed on 90 mm Petri dishes containing PDA supplemented with 100 ml/L of carrot juice, 0.015 g/L of pimaricin and 0.05 g L^{-1} of hymexazol (PDA +) (Linaldeddu et al., 2020b). Isolation of root rot agents was also directly attempted from roots. Necrotic root tissues were cut in 2 cm long samples, externally disinfected with 90% ethanol, rinsed in distilled water, blotted dry on filter paper and then placed onto PDA + . Petri dishes were incubated in the dark at 20°C and examined every 12 h. Hyphal tips from the emerging colonies were sub-cultured on carrot agar (CA) (Erwin and Ribeiro, 1996) and PDA and incubated at 20°C in the dark. To enhance sporangia production, CA plugs (5 mm diameter) of each isolate were placed in Petri dishes containing unsterile pond water. Sporangial production was assessed every 12 h for 7 days by microscopic observation.

2.2. Isolate identification

Molecular analysis was used to confirm the identification of all isolates at species level. Instagene Matrix (BioRad Laboratories, Hercules, CA, USA) was used to extract genomic DNA from mycelium of 5-day-old colonies grown on PDA and incubated at 20°C in the dark. The universal primers ITS1 and ITS4 were used to amplify the internal transcribed spacer regions (ITS), including the complete 5.8S gene (White et al., 1990). Polymerase chain reaction (PCR) mixtures and amplification conditions were as described by Linaldeddu et al. (2020a). The PCR products were purified using a EUROGOLD gel extraction kit (EuroClone S.p.A., Pero, Italy) following the manufacturer's instructions. ITS regions were sequenced in both directions with the primers used for amplification by the BMR Genomics DNA sequencing service (BMR Genomics, Padua, Italy) and by the CIBIACI University service (Florence, Italy). The nucleotide sequences were read and edited with FinchTV 1.4.0 (Geospiza, Inc., Seattle, WA, USA) and then compared with reference sequences (ex-type culture or representative strains) available in GenBank (NCBI/EMBL) using the BLAST search function (Altschul et al., 2010). Isolates were assigned to a species when their sequences were at least 99.9% homologous to the sequence of type material or representative isolates. ITS sequences from representative isolates obtained in this study were deposited in GenBank (**Table 1**).

For *Botryosphaeriaceae* species ITS sequences of eight representative isolates obtained in this study were compiled in a dataset together with sequences of other 15 isolates belonging to the genera *Botryosphaeria*, *Diplodia*, *Dothiorella*, and *Neofusicoccum*. For *Phytophthora* species ITS sequences of 11 representative isolates obtained in this study were compiled in a dataset together with sequences of other 19 isolates belonging to the phylogenetic clades 2, 3, 6, 7, 8, and 9.

Sequences were aligned with ClustalX v. 1.83 (Thompson et al., 1997), using the parameters reported by Bregant et al. (2020). Maximum likelihood (ML) analyses were performed with MEGA-X 10.1.8, including all gaps in the analyses. The best model of DNA sequence evolution was determined automatically by the software (Kumar et al., 2018).

2.3. Pathogenicity tests

The pathogenicity of four *Phytophthora* species, *P. acerina* Ginetti, Jung, Cooke and Moricca, *P. cinnamomi* Rands, *P. plurivora* Jung and Burgess and *P. pseudosyringae* Jung and Delatour, was tested on 3-year-old common ash seedlings grown in plastic pots (10 cm diameter, 1 L volume). The four species of *Phytophthora* were chosen taking into account: (a) their

TABLE 1 Number of isolates obtained from each ash species from rhizosphere (R), collar tissue (TC), and canker (C) samples in the investigated sites.

Species	ITS GenBank code	*Fraxinus angustifolia*			*Fraxinus excelsior*			*Fraxinus ornus*			Sites	Average temperature range(s) (°C)*	Average annual precipitation range(s) (mm)*
		R	TC	C	R	TC	C	R	TC	C			
Armillaria mellea	OR141502	–	–	–	–	3	–	–	–	–	1	13.7	986
Botryosphaeria dothidea	OR141137	–	–	–	–	–	4	–	–	20	1–20, 23, 35	4.0–15.1	887–1387
	OR119871												
Diplodia fraxini	OR140928	–	–	9	–	3	23	–	–	14	1, 5–8, 12, 13, 19, 20, 22–24, 28, 29, 31, 33–35, 37, 40	4.0–15.1	650–2050
	OR177960												
D. mutila	OR140929				–	–	5	–	–	–	21, 24	6.1–6.5	1250–2050
D. seriata	OR140930	–	–	1	–	–	7	–	–	7	2, 7–9, 13, 19, 20, 23, 34, 40	4.0–15.1	650–1387
	OR177959												
D. subglobosa	OR140931	–	–	–	–	–	18	–	–	5	3, 4, 6, 9, 20, 21, 24, 28, 29, 34	6.1–15.0	887–2050
	OR177962												
Dothiorella iberica	OR140932	–	–	–	–	–	–	–	–	1	34	14	1300
Do. symphoricarposicola	OR140933	–	–	–	–	–	1	–	–	–	20	6.5	1250
Hymenoscyphus fraxineus	OR140935	–	–	–	–	–	12	–	–	–	20, 23, 24, 31	4.0–7.6	1250–2050
Neofusicoccum parvum	OR140934	–	–	1	–	–	2	–	-	13	1–6, 8, 28, 37	13–15	887–1585
	OR177966												
Phytophthora acerina	OR140916	–	–	–	12	4	–	1	–	–	20, 22, 24, 28, 31, 33	6.1–13.0	1250–2050

(Continued)

10.3389/ffgc.2023.1253022

TABLE 1 (Continued)

Species	ITS GenBank code	*Fraxinus angustifolia*			*Fraxinus excelsior*			*Fraxinus ornus*			Sites	Average temperature range(s) (°C)*	Average annual precipitation range(s) (mm)*
		R	TC	C	R	TC	C	R	TC	C			
P. bilorbang	OR140917	1	–	–	–	–	–	–	–	–	40	13	650
P. cinnamomi	OR140918	–	–	–	6	2	–	4	1	–	25, 29, 36, 40	10.5–13.8	650–1460
P. hydropathica	OR140919	3	–	–	–	–	–	–	–	–	40	13	650
P. lacustris	OR140920	12	–	–	–	–	–	–	–	–	40	13	650
P. multivora	OR140921	4	–	–	–	–	–	–	–	–	38,40	13.0–13.6	650–1190
P. plurivora	OR140922	10	1	-	21	5	–	5	–	–	20, 21, 25–30, 32, 34, 36, 38–40	6.5–13.8	650–2390
P. polonica	OR140923	2	–	–	–	–	–	–	–	–	40	13	650
P. pseudocryptogea	OR140924	3	–	–	–	–	–	–	–	–	37, 40	13.0–13.4	650–1132
P. pseudosyringae	OR140925	–	–	–	3	1	–	–	–	–	20, 23	4.0–6.5	1250–1387
P. syringae	OR140926	1	–	–	–	–	–	–	–	–	40	13	650

*Where only one value is reported it is because the microorganism was found at only one site; two values report average extreme values (recorded in sites with extreme values).

10.3389/ffgc.2023.1253022

high isolation frequency; (b) the severity of symptoms observed in nature; and (c) the absence of information as common ash pathogens. Eight common ash seedlings were inoculated with a representative isolate of each species, and six were used as control. Inoculation point at the collar was surface-disinfected with 70% ethanol and a small piece of outer and inner bark (5 mm diameter) was removed with a flamed cork borer and replaced with an agar-mycelium plug, of the same size, taken from the margin of an actively growing pure culture colony. The inoculation point was covered with cotton wool soaked in sterile water and wrapped in a piece of aluminum foil. Controls were inoculated with a sterile PDA plug applied as described above. All inoculated seedlings were kept in field conditions at 10 to 34°C and watered regularly for 30 days. At the end of the experimental period, seedlings were checked for the presence of disease symptoms, the outer bark was carefully removed with a scalpel and the length of necrotic lesion surrounding each inoculation point was measured. Re-isolation of fungal isolates was attempted by transferring 5 pieces of inner bark taken around the margin of the necrotic lesions onto PDA + . Growing colonies were sub-cultured onto CA and PDA, incubated in the dark at 20°C and identified by morphological and molecular analysis (ITS region).

2.4. Statistical analyses

Pathogenicity assay data were checked for normality, then subjected to analysis of variance (ANOVA). Significant differences among mean values were determined using Fisher's least significant differences (LSD) multiple range test (P = 0.05) using XLSTAT software (Addinsoft SARL, New York, NY, USA).

3. Results

3.1. Field survey

Symptoms of ash decline with high mortality were common in some hilly areas of Central Italy on flowering ash and everywhere in North-East Italy on common ash.

In Central Italy, disease severity was high on flowering ash, with typical *Botryosphaeria* cankers and dieback on natural regeneration. Cankers initials appeared as small, sunken, brown-purplish necroses; lesions then extended longitudinally, giving rise to narrow, elongated cankers. Cankers were often multiple along the axis, causing wilting and dieback of young trees. Leaf and shoot blight with crown dieback were also frequently observed (**Figure 1**).

In North-East Italy, *Fraxinus excelsior* was severely affected, exhibiting a range of aerial symptoms including partial or complete dieback of the crown, abnormal production of epicormic shoots, bark discolorations and sunken cankers. The same symptoms but with a lower incidence were observed on the other two species of ash, in particular on *F. angustifolia*.

Disease incidence was very high, ranging between 70 and 100% among the sites, with a mortality range of 30–70%; the disease symptoms were observed on trees of all ages, with particular virulence and mortality on young seedlings, often reaching 100% of sudden death.

In addition to these common canopy symptoms, the same plants often exhibited root and collar rot, necrosis of inner bark and wood tissues in the basal part of the stem and in some cases bleeding cankers with production of blackish exudates. Root symptoms were often associated with forms of sudden death on young and mature trees. The complex symptomatology was also accentuated by the presence of some secondary pathogens and wood decay fungi, such as *Armillaria* spp. (**Figure 1**).

3.2. Etiology

Isolation performed on 362 ash samples yielded a total of 251 isolates belonging to 21 different species of oomycetes (102 isolates), ascomycetes (146) and basidiomycetes (3). Of these, 132 isolates were obtained from *Fraxinus excelsior*, 71 from *F. ornus* and 48 from *F. angustifolia* (**Table 1**). With respect to the type of sample, 143 isolates were obtained from cankers, 83 from roots and rhizosphere and 20 from necrotic inner bark tissues collected at the collar level. Based on morphology, colony appearance and ITS sequence data the 102 isolates of oomycetes were identified as *Phytophthora plurivora* Jung and Burgess (42 isolates), *Phytophthora acerina* Ginetti, Jung, Cooke and Moricca (17), *Phytophthora cinnamomi* Rands (13), *Phytophthora lacustris* Brasier, Cacciola, Nechw., Jung and Bakonyi (13), *Phytophthora multivora* Scott and Jung (4), *Phytophthora pseudosyringae* Jung and Delatour (4), *Phytophthora hydropathica* Hong and Gallegly (3), *Phytophthora pseudocryptogea* Safaief., Mostowf., Hardy and Burgess (3), *Phytophthora polonica* Belbahri, Moralejo and Lefort (2), *Phytophthora bilorbang* Aghighi, Hardy, Scott and Burgess (1) and *Phytophthora syringae* Kleb. (1) (**Table 1**). The 146 fungal isolates belonged to 9 species of ascomycetes in the families *Botryosphaeriaceae* (134) and *Helotiaceae* (12). In particular, colonies were identified as *Diplodia fraxini* (Fr.) Fr. (49), *Botryosphaeria dothidea* (Moug.) Ces. and De Not. (24), *Diplodia subglobosa* A.J.L. Phillips, Deidda and Linald. (23), *Neofusicoccum parvum* (Pennycook and Samuels) Crous, Slippers and A.J.L. Phillips (16), *Diplodia seriata* De Not. (15), *Hymenoscyphus fraxineus* (T. Kowalski) Baral, Queloz and Hosoya (12), *Diplodia mutila* (Fr.) Mont. (5), *Dothiorella iberica* A.J.L. Phillips, J. Luque and A. Alves (1) and *Dothiorella symphoricarposicola* W.J. Li, Jian K. Liu and K.D. Hyde(1). Finally, 3 isolates from *F. excelsior* were identified as *Armillaria mellea* (Vahl) P. Kumm. (*Physalacriaceae*, *Basidiomycota*).

In the phylogenetic analysis of *Botryosphaeriaceae* species 15 terminal clades were resolved. The isolates obtained in this study clustered in eight well-supported clades (ML bootstrap >90%) together with sequences of ex-type cultures (**Supplementary Figure 1**). Phylogenetic relationships among the *Phytophthora* isolates were elucidated using ITS sequences. In particular, the 11 isolates included in the phylogenetic analysis were distributed in 11 terminal clades, which belong to formally described species (**Supplementary Figure 2**).

Phytophthora plurivora and *Diplodia fraxini* were the most commonly detected species. The isolates of these two species were obtained from all three investigated ash species (**Figure 2**). *Phytophthora plurivora* was isolated from root and collar tissues while *D. fraxini* from branch cankers and necrotic lesions at the

FIGURE 1
Overview of symptoms detected on the ash species monitored in the study: extensive canopy dieback of *Fraxinus excelsior* **(A)**, *F. angustifolia* **(B,C)** and *F. ornus* **(D)**; bleeding canker **(E)**, *Phytophthora* flame necrotic lesions at the collar of *F. angustifolia* **(F)**, *F. excelsior* **(G,H)** and *F. ornus* **(I)**; shoot blight **(J)**, sunken canker **(K)** and inner bark discoloration **(L)** of *F. excelsior* and *F. angustifolia* **(M)**; cross-section of branches showing wedge-shaped necrotic sector **(N)**. Red arrow indicates the white mycelium of *Armillaria mellea* on a necrotic lesion caused by *Phytophthora plurivora*.

collar. Also, *D. seriata* was detected on all host species, albeit less frequently than the other two species.

3.3. Pathogenicity tests

At the end of the experimental trial, all common ash seedlings inoculated with *Phytophthora* spp. displayed dark brown inner bark lesions that spread up and down from the inoculation point (Figure 3). *Phytophthora plurivora* and *P. acerina* were the most aggressive species, causing the longest necrotic lesions (Table 2). Control plants did not show any disease symptoms and exhibited faster growth; only a small light brown discoloration restricted to the inoculation point was observed. All *Phytophthora* isolates were successfully re-isolated from the margin on the necrotic inner bark lesions of all seedlings, thus fulfilling Koch's postulates. No *Phytophthora* isolates or other pathogens were recovered from control seedlings.

4. Discussion

A complex of pathogenic fungi and oomycetes resulted associated with stem and branch cankers, leaf and shoot blights, collar necroses and root rot symptoms on common ash, flowering ash and narrow-leaved ash trees. From a phytopathological perspective, it emerged that ash trees in the investigated forest ecosystems live under significant pathogenic constraints, to which at least two distinct groups of major pathogens concur: prominent members of the *Botryosphaeriaceae* family and aggressive and emerging species of the *Phytophthora* genus.

TABLE 2 Mean lesion length ± standard deviation caused by each *Phytophthora* species inoculated on common ash seedlings.

Species	Isolate	Mean lesion length (cm)*	Re-isolation (%)
P. acerina	CB3	3.9 ± 1.1a	100
P. cinnamomi	CB121	2.8 ± 1b	100
P. plurivora	CB122	4.4 ± 1.7a	100
P. pseudosyringae	CB183	2.4 ± 0.4b	100
Control	–	0.5 ± 0.2c	–
LSD critical value		2.03	

*Values with the same letter do not differ significantly at $p = 0.05$, according to LSD multiple range test.

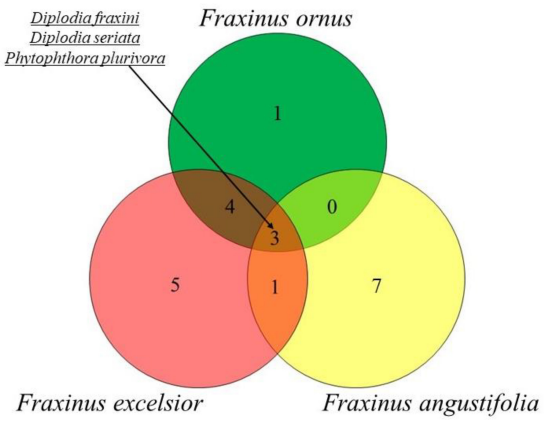

FIGURE 2
Venn diagrams illustrating the number of unique and shared species among ash species.

Other opportunistic pathogens such as *Armillaria* spp., were often found coinfecting declining/dying ash trees. *Hymenoscyphus fraxineus* was found on *F. excelsior* at a few sites but its impact on infected trees appeared less than that caused by the other pathogens. Some species prevailed at one site or another, depending on the particular context and microclimatic conditions. *H. fraxineus* was isolated in the coldest sites (mean annual temperature ranging from 4 to 7.6°C) and with an average annual precipitation ranging from 1250 to 2050 mm.

The *Botryosphaeriaceae* (*Botryosphaeriales*, Ascomycetes) are an emerging family of plant pathogenic fungi affecting various tree and shrub species typical of the Mediterranean area (Ragazzi et al., 1997; Moricca et al., 2008, 2010; Linaldeddu et al., 2016; Moricca and Linaldeddu, 2017). This family encompasses 22 genera, of which *Botryosphaeria*, *Diplodia*, *Dothiorella*, and *Neofusicoccum* are the most common in forest ecosystems (Moricca et al., 2012b; Phillips et al., 2013; Batista et al., 2021). Affected plants can show a wide range of symptoms, the most typical of which are cankers on the stem and branches with a characteristic wedge-shaped necrotic sector in cross section resulting in a progressive dieback of the canopy (Ragazzi et al., 1999a; Linaldeddu et al., 2016; Manca et al., 2020).

The relevance of *Botryosphaeriaceae* as pathogens stands out by taking into consideration the number of disease reports caused by members of this family, that has undergone an exponential increase worldwide, rising from around 100 in the period 1960–2000 to over 1500 in the last 20 years (Scopus, June 2023); this is mainly due to a greater scientific interest in these diseases, the development of new molecular and bioinformatic diagnostic techniques, enabling more accurate identification of fungal taxa, and the ongoing climate change (Batista et al., 2021). The stressful conditions for host species triggered by global warming have provoked the manifestation of epidemic diseases by endophytic and latent species of *Botryosphaeriaceae* (Ragazzi et al., 1999b,c); therefore, the introduction and establishment of invasive *Botryosphaeriaceae* in new areas of the planet driven by the rising temperatures, caused the occurrence of new emerging diseases incited by these fungi in regions previously considered unsuitable to many of them (Batista et al., 2020, 2021).

Diseases caused by *Botryosphaeriaceae* are drawing the attention of researchers especially in the Mediterranean region, consider one of the most striking examples regarding the emerging diseases (Ragazzi et al., 1996; Linaldeddu et al., 2017; Panzavolta et al., 2017; Smahi et al., 2017). Italy is certainly one of the most affected countries within the Mediterranean region. Indeed, countless studies have reported about 60 species of *Botryosphaeriaceae* in this country, resulting in over 250 host-pathogen interactions threatening diverse sectors of primary production (Moral et al., 2010; Urbez-Torres, 2011; Batista et al., 2021; Fiorenza et al., 2023). Although the economic impact is higher in crop production, the diseases caused by *Botryosphaeriaceae* species can also be devastating in forestry, causing losses of biodiversity and impairing ecosystem integrity (Slippers and Wingfield, 2007; Marsberg et al., 2017).

Prominent examples are the decline of Mediterranean vegetation caused by several *Diplodia* and *Neofusicoccum* species (Moricca et al., 2012b), pine shoot blight due to the invasive species *Diplodia sapinea*, oak canker disease due to *D. corticola* and ash dieback caused by *D. fraxini* (Luchi et al., 2014; Cimmino et al., 2016; Manca et al., 2020).

The dieback of ash formations has been associated for a long time, especially in Eastern Europe, to the ascomycete fungus *H. fraxineus* (Kowalski, 2006). Recent investigations in Germany, Italy and Slovenia, as well as this study, better clarify the key role of *Botryosphaeriaceae* species in the etiology of ash dieback (Linaldeddu et al., 2020a, 2022; Peters et al., 2023). In this study, *B. dothidea* was isolated at very high frequency from cankered tree tissues of *F. ornus* individuals in hilly areas of Central Italy. This cosmopolitan pathogen has been isolated worldwide from sites characterized by very different climatic conditions (mean annual temperature between 4 and 15.1°C) and mean annual rainfall between 887 and 1387 mm (Marsberg et al., 2017; Xue et al., 2021). In central Italy, the impact of the disease was greater on poor soils rich in gravel, on slopes facing south or south-west, at sites exposed to high daily temperatures and heat waves during the growing season and generally in stands suffering from drought stress. Mortality was high on young seedlings, especially following long dry periods. *Diplodia fraxini* was the most constantly isolated species from symptomatic ash trees and its virulence was confirmed by independent pathogenicity assays (Elena et al., 2018; Linaldeddu et al., 2020a). This fungus seems to manifest a

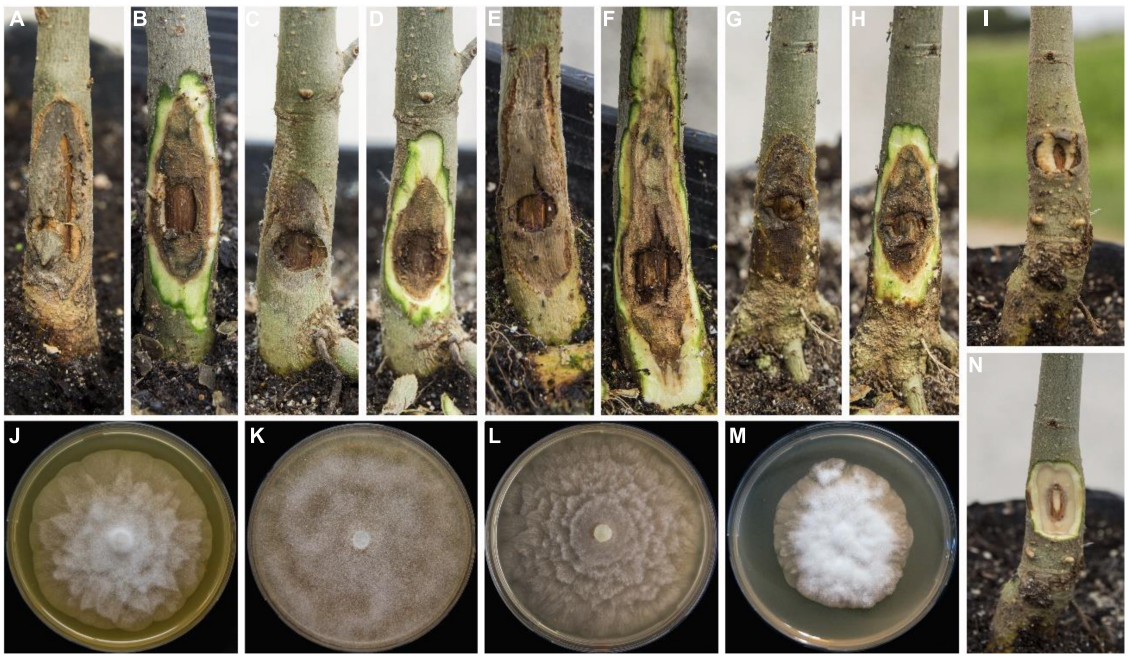

FIGURE 3
Symptoms caused by *Phytophthora acerina* **(A,B)**, *P. cinnamomi* **(C,D)**, *P. plurivora* **(E,F)** and *P. pseudosyringae* **(G,H)** on common ash seedlings. Control seedling **(I,N)**. Colony morphology of *P. acerina* **(J)**, *P. cinnamomi* **(K)**, *P. plurivora* **(L)**, and *P. pseudosyringae* **(M)** on carrot agar after 7 days at 20°C in the dark.

particular host-specificity for the genus *Fraxinus*, including the capacity to produce selective phytotoxic secondary metabolites (Cimmino et al., 2017).

Diplodia fraxini, included for a long time in the *Diplodia mutila* complex, was recently re-instated; therefore, many isolates from *Fraxinus* that were assigned in GenBank to *Diplodia mutila* belong in reality to *D. fraxini*, a fact that demonstrates a wider distribution of this species in Europe (Alves et al., 2014; Linaldeddu et al., 2020a). The current distribution of *D. fraxini* is still unknown; however, the impact of ash dieback, that appear to be growing in central Europe and new areas of the Mediterranean region such as Central Italy, the Balkans and Iberian Peninsula, underline the strong adaptation of this fungus to changing environmental conditions (Alves et al., 2014; Elena et al., 2018; Peters et al., 2023). The plasticity of this pathogen is confirmed by its discovery in numerous sites with very different climatic conditions: average temperature ranging from 4 to 15.1°C and average annual precipitation ranging from 650 to 2050 mm.

Phytophthora spp. are another important group of lethal pathogens that are overbearingly emerging in many forest areas globally (Jung et al., 2016). Most *Phytophthora* species have a soilborne lifestyle, causing primarily root and collar rot on thousands of plant species, but some of them are endowed with an aerial dispersal lifestyle. These oomycetes cause a broad range of symptoms on affected hosts; in response to the bark and root damages, the canopy evidences non-specific symptoms of progressive or sudden decline (Bregant et al., 2020).

Over the past two decades, countless studies have demonstrated the involvement of a large number of soilborne *Phytophthora* species in the widespread declines of forest ecosystems dominated by the *Fagaceae* and the *Betulaceae* in Europe, especially in the Mediterranean basin (Brasier et al., 1993; Jung et al., 2000; Vettraino et al., 2005; Linaldeddu et al., 2014; Scanu et al., 2015; Corcobado et al., 2020; Riolo et al., 2020; Bregant et al., 2023).

In some cases, attacks were a matter of re-emergence of old-known *Phytophthora* species which, after decades of infrequent, sporadic outbreaks, in the past 20 years have come back to cause major epidemic outbreaks. A key to understanding the resurgence of diseases caused by old-known *Phytophthora* related diseases (e.g., the "ink disease" on chestnut) is the current climate trend. It must be considered that the Mediterranean-type climate ecosystems present today conditions particularly conducive to the lifestyle and development of this group of pathogens: the relatively warm and wet winter period can induce an easy zoospore production for host infection in combination with the subsequent long and dry summers that cause severe stress in tree populations (Serrano et al., 2022). In this scenario, an increasing number of *Phytophthora* species are emerging or re-emerging from the Mediterranean areas of the planet, such as SW Australia, California, South Africa and the classic Mediterranean Basin (Burgess et al., 2017).

Crown and root diseases related to *Fraxinus* spp. dieback are to date still little studied. Current knowledge about the association between *Phytophthora* spp. and ash is limited. Until a few years ago, the *Fraxinus* genus was considered resistant to *Phytophthora* attacks, as also ascertained by some pathogenicity tests (Jung and Nechwatal, 2008; Mràzkovà et al., 2013). The first study to report attacks of *Phytophthora* spp. on natural *Fraxinus* formations took place in 2011 in Poland and Denmark, highlighting root and collar root symptoms, although the *Phytophthora* presence had been ascertained a few years earlier in areas of Central and Eastern Europe such as Germany and the Czech Republic (Mràzkovà et al., 2010, 2013; Orlikowski et al., 2011; Langer, 2017).

A study conducted by Tkaczyk et al. (2016) found five *Phytophthora* species from common ash in a nature reserve in Poland. In this study, *P. cactorum* and *P. plurivora* appeared to be the most frequent and virulent species associated with common ash (Orlikowski et al., 2011; Tkaczyk et al., 2016). Recent studies have also demonstrated a high susceptibility to *Phytophthora* species of natural riparian formations of *Fraxinus angustifolia* in Sicily and Türkiye (Akilli et al., 2013; Jung et al., 2019). Some studies conducted in Northern and Eastern Europe highlighted a possible synergistic action between canopy and root pathogens (Orlikowski et al., 2011; Tkaczyk et al., 2016; Milenković et al., 2017, 2018; Peters et al., 2023). Other studies have shown a frequent association of declining ash trees with secondary root pathogens such as *Armillaria* spp. (Lygis et al., 2005; Skovsgaard et al., 2010; Langer, 2017; Kranjec Orlović et al., 2020; Peters et al., 2023).

Given the above, this study stands as the most complete census of *Phytophthora* species attacking members of the genus *Fraxinus*, with 11 different species, namely *P. acerina*, *P. bilorbang*, *P. cinnamomi*, *P. hydropathica*, *P. lacustris*, *P. multivora*, *P. plurivora*, *P. polonica*, *P. pseudocryptogea*, *P. pseudosyringae*, and *P. syringae* that are reported for the first time on these hosts in Italy.

The 4 *Phytophthora* species used in the pathogenicity tests, *P. acerina*, *P. cinnamomi*, *P. plurivora*, and *P. pseudosyringae*, selected on the basis of their high isolation frequencies and the severity of symptoms caused on ash trees, confirmed to be aggressive pathogens on ash and provided important information about their impact and pervasiveness in forest ecosystems. In particular, *Phytophthora plurivora* and *P. acerina* proved to be the most virulent species in the artificial inoculation tests, producing the longest lesions on inoculated seedlings. It is noteworthy that both species are members of the former *P. citricola* complex (Ginetti et al., 2014).

Phytophthora plurivora is a root and stem pathogen very widespread in Europe, known to occur in different settings and environments (plantations, nurseries, ornamental green, streams, primary forests) and to cause widespread declines on alder (*Alnus* spp.), beech (*Fagus sylvatica*), and oak (*Quercus* spp.) ecosystems (Jung, 2009; Jung and Burgess, 2009; Lilja et al., 2011; Prospero et al., 2013; Schoebel et al., 2014; Bregant et al., 2023). Having been found at very high frequencies even in ash formations confirms its widespread presence in forest ecosystems and suggests it might have a major role also in the decline of ash formations.

Phytophthora acerina was first reported and described about 10 years ago from a wooded area in a peri-urban park on the Lombardy plain (Northern Italy). Here, it infected and killed thousands of individuals of *Acer pseudoplatanus*, making this tree species literally disappear from the area (Ginetti et al., 2014). The pathogen was able to spread pervasively among water sources, the whole area being rich in water (some plots were in the past cultivated with rice). *Phytophthora acerina* was in fact recovered from streams, ponds, canals, reservoirs, runoffs, irrigation waters, as well as—of course—from bleeding cankers on the stem, root tissues and soil samples taken under the crown of dead/dying trees. The pathogen was reported a few years later, in 2018, causing sudden death to olive trees in the nearby Veneto region, a few hundred kms from the site of its first report. On olive trees *P. acerina* exhibited high virulence as well, causing a range of symptoms such as partial or complete crown dieback, reddening of drying foliage, loss of rootlets and collar rot (Linaldeddu et al., 2020c). These literature data and the high virulence displayed by *P. acerina* on inoculated seedlings as well as on ash trees in the woods prove it to be an extremely dangerous and highly pervasive pathogen, whose host and geographic range is still largely unexplored, but which certainly includes the *Fraxinus* species.

Phytophthora cinnamomi was isolated from ash trees at many sites and this confirms this generalist pathogen to be rather ubiquitous and to become invasive in some areas, often causing enormous damage to natural ecosystems (Hardham and Blackman, 2018). This oomycete shows a rather accentuated seasonality and is favored, in particular, by frequent rains in the spring and by mild winters, a condition typical of the Mediterranean climate; current climate anomalies could significantly modify these conditions, further favoring the epidemiological spread of this pathogen (Serrano et al., 2022). The recent description in the Mediterranean of two species close to *P. cinnamomi* with a further adaptation to even higher temperatures is proof of the vulnerability of natural ecosystems to this group of pathogens in the era of climate change (Scanu et al., 2014; Yang et al., 2017; Bregant et al., 2021).

5. Conclusion

Global climate change is altering site factors, biochemical processes and biotic interactions in natural plant communities (Sturrock et al., 2011). The impact of climate change is exacerbated in climate change hotspots. Italy, a peninsula jutting out into the center of the Mediterranean climate change hotspot region, is experiencing unprecedented mild dry winters, hot summers and prolonged droughts that are seriously impacting forest vegetation and changing the landscape. As the scientific community debates if species migration will be able to keep pace with climate change, with projections about climate-driven range shifts in tree species, forest pathologists tirelessly record extended forest diebacks, invasions by new pathogens and altered densities and distribution of forest tree species within natural plant communities (Singh et al., 2023). That's what seems to be going on with ash formations: common ash, flowering ash and narrow-leaved ash stands are under unprecedented attack by new pathogens and the almost total loss of natural regeneration observed at some locations indicates these species might be retreating from the less favorable sites.

Another reason for concern arises from knowledge on the contrasting infection biologies and lifestyles of the two groups of causative agents involved. The fungal and oomycete pathogens reported here, being endowed with different thermo-hygrometric requirements, could be vicariant throughout the year in their pathogenetic action, with *Phytophthora* spp. being more active in mild and moist seasons and *Botryosphaeriaceae* that become more aggressive during hot and dry periods. If this pattern of vicariance, already observed in oak forests (Moricca et al., 2012c), would also be reproduced in ash stands, it could catch infected ash trees in a deadly spiral, as the two groups of pathogens would act synergistically in weakening ash trees and lead to their death.

The large number of pathogenic species found in this study agrees with the results of a recent research conducted in Germany (Peters et al., 2023), and underlines that while the litter species *H. fraxineus* has been getting the most attention in the last decades,

the most common species associated with *Fraxinus* spp. with ash dieback symptoms are *Diplodia fraxini* and *P. plurivora*. The overall framework indicates that multi-trophic interactions are common in ash stands, representing an important and matter-of-fact aspect of tree-pathogen relationships, and this provides a more realistic picture of what's going on in forests (Pillay et al., 2013; Smahi et al., 2017). Clarifying this complex etiology is critical to assess if, and to what extent, ash disease management and prevention measures can be effectively applied.

Data availability statement

The datasets presented in this study can be found in online repositories. The names of the repository/repositories and accession number(s) can be found in the article/ **Supplementary material**.

Author contributions

AB, CB, SM, and BL contributed to conception and design of the study. AB and CB conducted the field and laboratory trials, analyzed the data, and wrote the original manuscript. CA, GR, and BT helped with laboratory investigations, data curation and preparation of the first draft of the manuscript. SM and BL supervised and funding acquisition. All authors contributed to manuscript revision, read, and approved the submitted version.

Funding

This research was partially funded by the Regione Toscana—Servizio Fitosanitario, within the project "Accordo di collaborazione scientifica tra Regione Toscana—Servizio Fitosanitario e Università di Firenze—Dipartimento di Scienze e Tecnologie Agrarie, Alimentari, Ambientali e Forestali (DAGRI), per la realizzazione di attività congiunte in materia di organismi nocivi da quarantena e di interesse fitosanitario per le principali colture agrarie regionali (cereali, olivo, vite, vivaismo ornamentale e frutticolo) e in campo forestale" and by grant number DOR2305524/2023 "Monitoraggio dei marciumi radicali da *Phytophthora* negli ecosistemi forestali Italiani."

Acknowledgments

Part of this study was conducted by AB within her Ph.D. doctoral project at the University of Florence, Italy, Ph.D. doctoral program in Agricultural and Environmental Sciences and by C.B. within by the Land Environment Resources and Health (L.E.R.H.) doctoral course (University of Padova). We are grateful to the Unione dei Comuni della Val di Merse (SI), Ten. Col. Giovanni Nobili and to Carabinieri of the Bosco della Mesola (FE), for their technical and logistic support.

Conflict of interest

The authors declare that the research was conducted in the absence of any commercial or financial relationships that could be construed as a potential conflict of interest.

Publisher's note

All claims expressed in this article are solely those of the authors and do not necessarily represent those of their affiliated organizations, or those of the publisher, the editors and the reviewers. Any product that may be evaluated in this article, or claim that may be made by its manufacturer, is not guaranteed or endorsed by the publisher.

Supplementary material

The Supplementary Material for this article can be found online at: https://www.frontiersin.org/articles/10.3389/ffgc.2023.1253022/full#supplementary-material

References

Akilli, S., Ulubaş Serçe, Ç, Katırcıoğlu, Y. Z., and Maden, S. (2013). *Phytophthora* dieback on narrow leaved ash in the black sea region of Turkey. *For. Pathol.* 43, 252–256. doi: 10.1111/efp.12024

Altschul, S. F., Wootton, J. C., Zaslavsky, E., and Yu, Y. K. (2010). The construction and use of log-odds substitution scores for multiple sequence alignment. *PLoS Comput. Biol.* 6, e1000852. doi: 10.1371/journal.pcbi.1000852

Alves, A., Linaldeddu, B. T., Deidda, A., Scanu, B., and Phillips, A. J. L. (2014). The complex of *Diplodia* species associated with *Fraxinus* and some other woody hosts in Italy and Portugal. *Fungal Diver.* 67, 143–156. doi: 10.1007/s13225-014-0282-9

Batista, E., Lopes, A., and Alves, A. (2020). *Botryosphaeriaceae* species on forest trees in Portugal: Diversity, distribution and pathogenicity. *Eur. J. Plant Pathol.* 158, 693–720. doi: 10.1007/s10658-020-02112-8

Batista, E., Lopes, A., and Alves, A. (2021). What do we know about *Botryosphaeriaceae*? An overview of a worldwide cured dataset. *Forests* 12:313. doi: 10.3390/f12030313

Benigno, A., Cerboneschi, M., and Moricca, S. (2019). "Dieback of natural regeneration of Flowering ash (*Fraxinus ornus*) in a hilly area of central Tuscany," in *Paper Presented at the Joint Meeting IUFRO WP 7.02. 02 and 7.02. 03, Figline Valdarno, Florence, Italy*, (Florence), 28.

Brasier, C. M., Robredo, F., and Ferraz, J. F. P. (1993). Evidence for *Phytophthora cinnamomi* involvement in Iberian oak decline. *Plant Pathol.* 42, 140–145.

Bregant, C., Batista, E., Hilário, S., Linaldeddu, B. T., and Alves, A. (2023). *Phytophthora* species involved in *Alnus glutinosa* decline in Portugal. *Pathogens* 12:276. doi: 10.3390/pathogens12020276

Bregant, C., Mulas, A. A., Rossetto, G., Deidda, A., Maddau, L., Piras, G., et al. (2021). *Phytophthora mediterranea* sp. nov., a new species closely related to *Phytophthora cinnamomi* from nursery plants of *Myrtus* communis in Italy. *Forests* 12:682. doi: 10.3390/f12060682

Bregant, C., Sanna, G. P., Bottos, A., Maddau, L., Montecchio, L., and Linaldeddu, B. T. (2020). Diversity and pathogenicity of *Phytophthora* species associated with

declining alder trees in Italy and description of *Phytophthora alpina* sp. nov. *Forests* 11:848. doi: 10.3390/f11080848

Burgess, T. I., Scott, J. K., Mcdougall, K. L., Stukely, M. J., Crane, C., Dunstan, W. A., et al. (2017). Current and projected global distribution of *Phytophthora cinnamomi*, one of the world's worst plant pathogens. *Glob. Change Biol.* 23, 1661–1674. doi: 10.1111/gcb.13492

Cimmino, A., Maddau, L., Masi, M., Evidente, M., Linaldeddu, B. T., and Evidente, A. (2016). Further secondary metabolites produced by *Diplodia corticola*, a fungal pathogen involved in cork oak decline. *Tetrahedron* 72, 6788–6793. doi: 10.1016/j.tet.2016.09.008

Cimmino, A., Maddau, L., Masi, M., Linaldeddu, B. T., Pescitelli, G., and Evidente, A. (2017). Fraxitoxin, a new isochromanone isolated from *Diplodia fraxini*. *Chem. Biodivers.* 14:e1700325. doi: 10.1002/cbdv.201700325

Colangelo, M., Camarero, J. J., Borghetti, M., Gentilesca, T., Oliva, J., Redondo, M. A., et al. (2018). Drought and *Phytophthora* are associated with the decline of oak species in southern Italy. *Front Plant Sci.* 9:1595. doi: 10.3389/fpls.2018.01595

Corcobado, T., Cech, T. L., Brandstetter, M., Daxer, A., Hüttler, C., Kudláček, T., et al. (2020). Decline of European beech in Austria: Involvement of *Phytophthora* spp. and contributing biotic and abiotic factors. *Forests* 11:895. doi: 10.3390/f11080895

Cowling, R. M., Rundel, P. W., Lamont, B. B., Arroyo, M. K., and Arianoutsou, M. (1996). Plant diversity in Mediterranean-climate regions. *Trends Ecol. Evol.* 11, 362–366. doi: 10.1016/0169-5347(96)10044-6

Dukes, J. S., Pontius, J., Orwig, D., Garnas, J. R., Rodgers, V. L., Brazee, N., et al. (2009). Responses of insect pests, pathogens, and invasive plant species to climate change in the forests of northeastern North America: What can we predict? *Can. J. For. Res.* 39, 231–248. doi: 10.1139/X08-171

Elena, G., León, M., Abad-Campos, P., Armengol, J., Mateu-Andrés, I., and Güemes-Heras, J. (2018). First report of *Diplodia fraxini* causing dieback of *Fraxinus angustifolia* in Spain. *Plant Dis.* 102:2645. doi: 10.1094/PDIS-05-18-0792-PDN

Fiorenza, A., Gusella, G., Vecchio, L., Aiello, D., and Polizzi, G. (2023). Diversity of *Botryosphaeriaceae* species associated with canker and dieback of avocado (*Persea americana*) in Italy. *Phytopathol. Mediterr.* 62, 47–63. doi: 10.36253/phyto-14057

Ginetti, B., Moricca, S., Squires, J. N., Cooke, D. E. L., Ragazzi, A., and Jung, T. (2014). *Phytophthora acerina* sp. nov., a new species causing bleeding cankers and dieback of acer pseudoplatanus trees in planted forests in Northern Italy. *Plant Pathol.* 63, 858–876. doi: 10.1111/ppa.12153

Giorgi, F. (2006). Climate change hot-spots. *Geophys. Res. Lett.* 33:8. doi: 10.1029/2006GL025734

Giorgi, F., and Lionello, P. (2008). Climate change projections for the Mediterranean region. *Glob. Planet Change* 63, 90–104. doi: 10.1016/j.gloplacha.2007.09.005

Haavik, L. J., Billings, S. A., Guldin, J. M., and Stephen, F. M. (2015). Emergent insects, pathogens and drought shape changing patterns in oak decline in North America and Europe. *For. Ecol. Manag.* 354, 190–205. doi: 10.1016/j.foreco.2015.06.019

Hansen, E. M. (2008). Alien forest pathogens: *Phytophthora* species are changing world forests. *Boreal Environ. Res.* 13, 33–41.

Hardham, A. R., and Blackman, L. M. (2018). Phytophthora cinnamomi. *Mol. Plant Pathol.* 19, 260–285. doi: 10.1111/mpp.12568

Jung, T. (2009). Beech decline in Central Europe driven by the interaction between *Phytophthora* infections and climatic extremes. *For. Pathol.* 39, 73–94. doi: 10.1111/j.1439-0329.2008.00566.x

Jung, T., and Burgess, T. I. (2009). Re-evaluation of *Phytophthora citricola* isolates from multiple woody hosts in Europe and North America reveals a new species, *Phytophthora plurivora* sp. nov. *Persoonia* 22, 95–110. doi: 10.3767/003158509X442612

Jung, T., and Nechwatal, J. (2008). *Phytophthora gallica* sp. nov., a new species from rhizosphere soil of declining oak and reed stands in France and Germany. *Mycol. Res.* 112, 1195–1205. doi: 10.1016/j.mycres.2008.04.007

Jung, T., Blaschke, H., and Osswald, W. (2000). Involvement of soilborne *Phytophthora* species in Central European oak decline and the effect of site factors on the disease. *Plant Pathol.* 49, 706–718. doi: 10.1046/j.1365-3059.2000.00521.x

Jung, T., La Spada, F., Pane, A., Aloi, F., Evoli, M., Horta Jung, M., et al. (2019). Diversity and distribution of *Phytophthora* species in protected natural areas in Sicily. *Forests* 10:259. doi: 10.3390/f10030259

Jung, T., Orlikowski, L., Henricot, B., Abad Campos, P., Aday, A. G., Aguín Casal, O., et al. (2016). Widespread *Phytophthora* infestations in European nurseries put forest, semi-natural and horticultural ecosystems at high risk of *Phytophthora* diseases. *For. Pathol.* 46, 134–163. doi: 10.1111/efp.12239

Kowalski, T. (2006). *Chalara fraxinea* sp. nov. associated with dieback of ash (*Fraxinus excelsior*) in Poland. *For. Pathol.* 36, 264–270. doi: 10.1111/j.1439-0329.2006.00453.x

Kranjec Orlović, J., Moro, M., and Diminić, D. (2020). Role of root and stem base fungi in *Fraxinus angustifolia* (Vahl) dieback in croatian floodplain forests. *Forests* 11:607. doi: 10.3390/f11060607

Kumar, S., Stecher, G., Li, M., Knyaz, C., and Tamura, K. (2018). MEGA X: Molecular evolutionary genetics analysis across computing platforms. *Mol. Biol. Evol.* 35, 1547–1549.

Langer, G. (2017). Collar rots in forests of Northwest Germany affected by ash dieback. *Bal. For.* 23, 4–19.

Lilja, A., Rytkönen, A., and Hantula, J. (2011). Introduced pathogens found on ornamentals, strawberry and trees in Finland over the past 20 years. *Agric. Food Sci.* 20, 74–85. doi: 10.2137/145960611795163051

Linaldeddu, B. T., Bottecchia, F., Bregant, C., Maddau, L., and Montecchio, L. (2020a). *Diplodia fraxini* and *Diplodia subglobosa*: The main species associated with cankers and dieback of Fraxinus excelsior in north-eastern Italy. *Forests* 11:883. doi: 10.3390/f11080883

Linaldeddu, B. T., Bregant, C., Montecchio, L., Brglez, A., Piškur, B., and Ogris, N. (2022). First report of *Diplodia fraxini* and *Diplodia subglobosa* causing canker and dieback of *Fraxinus excelsior* in Slovenia. *Plant Dis.* 106, 26–29. doi: 10.1094/PDIS-06-21-1204-SC

Linaldeddu, B. T., Bregant, C., Montecchio, L., Favaron, F., and Sella, L. (2020c). First report of *Phytophthora acerina*, *P. pini*, and *P. plurivora* causing root rot and sudden death of olive trees in Italy. *Plant Dis.* 104, 996–996. doi: 10.1094/PDIS-10-19-2080-PDN

Linaldeddu, B. T., Bregant, C., Ruzzon, B., and Montecchio, L. (2020b). *Coniella granati* and *Phytophthora palmivora*: The main pathogens involved in pomegranate dieback and mortality in north-eastern Italy. *Italian J. Mycol.* 49, 92–100. doi: 10.6092/issn.2531-7342/11170

Linaldeddu, B. T., Maddau, L., and Franceschini, A. (2017). First report of *Diplodia corticola* causing canker and dieback of *Quercus ilex*, *Q. petraea*, and *Q. suber* in Corsica (France). *Plant Dis.* 101:256. doi: 10.1094/PDIS-07-16-1076-PDN

Linaldeddu, B. T., Maddau, L., Franceschini, A., Alves, A., and Phillips, A. J. L. (2016). *Botryosphaeriaceae* species associated with lentisk dieback in Italy and description of *Diplodia insularis* sp. nov. *Mycosphere* 7, 962–977. doi: 10.5943/mycosphere/si/1b/8

Linaldeddu, B. T., Scanu, B., Maddau, L., and Franceschini, A. (2014). *Diplodia corticola* and *Phytophthora cinnamomi*: The main pathogens involved in holm oak decline on Caprera Island (Italy). *For. Pathol.* 44, 191–200. doi: 10.1111/efp.12081

Lionello, P., and Scarascia, L. (2018). The relation between climate change in the Mediterranean region and global warming. *Reg. Environ. Change* 18, 1481–1493. doi: 10.1007/s10113-018-1290-1

Luchi, N., Ghelardini, L., Santini, A., Migliorini, D., and Capretti, P. (2016). First record of ash dieback caused by *Hymenoscyphus fraxineus* on Fraxinus excelsior in the Apennines (Tuscany, Italy). *Plant Dis.* 100:535. doi: 10.1094/PDIS-09-15-0975-PDN

Luchi, N., Oliveira Longa, C. M., Danti, R., Capretti, P., and Maresi, G. (2014). *Diplodia sapinea*: The main fungal species involved in the colonization of pine shoots in Italy. *For. Pathol.* 44, 372–381. doi: 10.1111/efp.12109

Lygis, V., Vasiliauskas, R., Larsson, K. H., and Stenlid, J. (2005). Wood-inhabiting fungi in stems of *Fraxinus excelsior* in declining ash stands of northern Lithuania, with particular reference to *Armillaria cepistipes*. *Scand. J. For. Res.* 20, 337–346. doi: 10.1080/02827580510036238

Manca, D., Bregant, C., Maddau, L., Pinna, C., Montecchio, L., and Linaldeddu, B. T. (2020). First report of canker and dieback caused by *Neofusicoccum parvum* and *Diplodia olivarum* on oleaster in Italy. *Italian J. Mycol.* 49, 85–91. doi: 10.6092/issn.2531-7342/11048

Manion, P. D. (1981). *Tree disease concepts*. Englewood Cliffs, NJ: Prentice-Hall, Inc.

Marsberg, A., Kemler, M., Jami, F., Nagel, J. H., Postma-Smidt, A., Naidoo, S., et al. (2017). *Botryosphaeria dothidea*: A latent pathogen of global importance to woody plant health. *Mol. Plant Pathol.* 18, 477–488. doi: 10.1111/mpp.12495

Migliorini, D., Luchi, N., Nigrone, E., Pecori, F., Pepori, A. L., and Santini, A. (2022). Expansion of ash dieback towards the scattered *Fraxinus excelsior* range of the Italian Peninsula. *Biol. Invas.* 24, 1359–1373.

Milenković, I., Jung, T., Stanivuković, Z., and Karadžić, D. (2017). First report of *Hymenoscyphus fraxineus* on *Fraxinus excelsior* in Montenegro. *For Pathol.* 47:e12359. doi: 10.1111/efp.12359

Milenković, I., Keèa, N., Karadžić, D., Nowakowska, J. A., Oszako, T., Sikora, K., et al. (2018). Interaction between *Hymenoscyphus fraxineus* and *Phytophthora* species on young *Fraxinus excelsior* seedlings. *For. Chron.* 94, 135–139. doi: 10.5558/tfc2018-020

Moral, J., Muñoz-Díez, C., González, N., Trapero, A., and Michailides, T. J. (2010). Characterization and pathogenicity of *Botryosphaeriaceae* species collected from olive and other hosts in Spain and California. *Phytopathology* 100, 1340–1351. doi: 10.1094/PHYTO-12-09-0343

Moricca, S., and Linaldeddu, B. (2017). "Climate change triggers the pervasive spread of botryosphaeriaceous fungi in the Mediterranean region," in *Proceedings of the Invasive Forest Pathogens and Implications for Biology and Policy IUFRO Working Party 7.02. 02, May 7-11, 2017, Niagara Falls, Ontario*, Niagara Falls, ON, 34.

Moricca, S., and Ragazzi, A. (2008). Fungal endophytes in Mediterranean oak forests: A lesson from *Discula quercina*. *Phytopathology* 98, 380–386. doi: 10.1094/phyto-98-4-0380

Moricca, S., Ginetti, B., and Ragazzi, A. (2012a). Species- and organ-specificity in endophytes colonizing healthy and declining Mediterranean Oaks. *Phytopathol. Mediterr.* 51, 587–598.

Moricca, S., Linaldeddu, B. T., Ginetti, B., Scanu, B., Franceschini, A., and Ragazzi, A. (2016). Endemic and emerging pathogens threatening cork oak trees: Management options for conserving a unique forest ecosystem. *Plant Dis.* 100, 2184–2193. doi: 10.1094/PDIS-03-16-0408

Moricca, S., Uccello, A., Ginetti, B., and Ragazzi, A. (2012b). First report of *Neofusicoccum parvum* associated with bark canker and dieback of acer pseudoplatanus and Quercus robur in Italy. *Plant Dis.* 96:1699. doi: 10.1094/PDIS-06-12-0543-PDN

Moricca, S., Uccello, A., Ginetti, B., and Ragazzi, A. (2012c). Isolation and growth temperature requirements of oomycetes and *Botryosphaeriaceae* from the same oak hosts: Evidence for a vicariant pathogenic action? *IOBC/WPRS Bull.* 76, 79–84.

Moricca, S., Uccello, A., Turco, E., Ginetti, B., and Ragazzi, A. (2010). Multiple *Botryosphaeriaceae* infection in forest trees: Synergistic or antagonistic interaction? *J. Plant Pathol.* 92:91.

Moricca, S., Uccello, A., Zini, E., Campana, F., Gini, R., Selleri, B., et al. (2008). Spread and virulence of *Botryosphaeria dothidea* on broadleaved trees in urban parks of northern Italy. *J. Plant Pathol.* 90:452.

Mràzkovà, M., Černy, K., Tomšovský, M., Holub, V., Strnadova, V., Zlatohlavek, A., et al. (2010). First report of root rot of pedunculate oak and other forest tree species caused by *Phytophthora plurivora* in the Czech Republic. *Plant Dis.* 94, 272–272. doi: 10.1094/PDIS-94-2-0272B

Mràzkovà, M., Černý, K., Tomšovský, M., Strnadova, V., Gregorová, B., Holub, V., et al. (2013). Occurrence of *Phytophthora multivora* and *Phytophthora plurivora* in the Czech Republic. *Plant Prot. Sci.* 49, 155–164. doi: 10.17221/74/2012-PPS

Myers, N., Mittermeier, R. A., Mittermeier, C. G., da Fonseca, G. A. B., and Kent, J. (2000). Biodiversity hotspots for conservation priorities. *Nature* 403, 853–858.

Nunes, L. J., Meireles, C. I., Gomes, C. J. P., Ribeiro, N., and Almeida, M. C. (2022). The impact of climate change on forest development: A sustainable approach to management models applied to Mediterranean-type climate regions. *Plants* 11:69. doi: 10.3390/plants11010069

Ogris, N., Hauptman, T., Jurc, D., Floreancig, V., Marsich, F., and Montecchio, L. (2010). First report of *Chalara fraxinea* on common ash in Italy. *Plant Dis.* 94:133. doi: 10.1094/PDIS-94-1-0133A

Orlikowski, L. B., Ptaszek, M., Rodziewicz, A., Nechwatal, J., Thinggaard, K., and Jung, T. (2011). *Phytophthora* root and collar rot of mature *Fraxinus excelsior* in forest stands in Poland and Denmark. *For. Pathol.* 41, 510–519. doi: 10.1111/j.1439-0329.2011.00714.x

Panconesi, A., Moricca, S., Ragazzi, A., Dellavalle, I., and Tiberi, R. (2014). *Parassiti delle piante arboree forestali ed ornamentali: Specie introdotte e di temuta introduzione*. Bologna: Pàtron Editore.

Panzavolta, T., Panichi, A., Bracalini, M., Croci, F., Benigno, A., Ragazzi, A., et al. (2018). Tree pathogens and their insect-mediated transport: Implications for oak tree die-off in a natural park area. *Glob. Ecol. Conserv.* 15:e00437.

Panzavolta, T., Panichi, A., Bracalini, M., Croci, F., Ginetti, B., Ragazzi, A., et al. (2017). Dispersal and propagule pressure of *Botryosphaeriaceae* species in a declining oak stand is affected by insect vectors. *Forests* 8:228. doi: 10.3390/f8070228

Peters, S., Fuchs, S., Bien, S., Bußkamp, J., Langer, G. J., and Langer, E. J. (2023). Fungi associated with stem collar necroses of *Fraxinus excelsior* affected by ash dieback. *Mycol. Prog.* 22:52. doi: 10.1007/s11557-023-01897-2

Phillips, A. J., Alves, A., Abdollahzadeh, J., Slippers, B., Wingfield, M. J., Groenewald, J. Z., et al. (2013). The *Botryosphaeriaceae*: Genera and species known from culture. *Stud. Mycol.* 76, 51–167. doi: 10.3114/sim0021

Pillay, K., Slippers, B., Wingfield, M. J., and Gryzenhout, M. (2013). Diversity and distribution of co-infecting *Botryosphaeriaceae* from *Eucalyptus grandis* and *Syzygium cordatum* in South Africa. *S. Afr. J. Bot.* 84, 38–43. doi: 10.1016/j.sajb.2012.09.003

Prospero, S., Vercauteren, A., Heungens, K., Belbahri, L., and Rigling, D. (2013). *Phytophthora* diversity and population structure of *Phytopthora ramorum* in Swiss ornamental nurseries. *Plant Pathol.* 62, 1063–1071. doi: 10.1111/ppa.12027

Ragazzi, A., Moricca, S., and Dellavalle, I. (1997). Vegetative compatibility and pathogenicity of *Diplodia mutila* isolates on oak. *Eur. J. Plant Pathol.* 27, 391–396.

Ragazzi, A., Moricca, S., and Dellavalle, I. (1999a). Water stress and the development of cankers by *Diplodia mutila* on *Quercus robur*. *J. Phytopathol.* 147, 425–428.

Ragazzi, A., Moricca, S., and Dellavalle, I. (1999b). Interactions between *Quercus* spp. and *Diplodia mutila* under water stress conditions. *Z. Pflanzenkr. Pflanzenschutz* 106, 495–500.

Ragazzi, A., Moricca, S., Vagniluca, S., and Dellavalle, I. (1996). Antagonism of *Acremonium mucronatum* towards *Diplodia mutila* in tests *in vitro* and *in situ*. *Eur. J. Plant Pathol.* 26, 235–243.

Ragazzi, A., Moricca, S., Vagniluca, S., Comparini, C., and Dellavalle, I. (1999c). Leaf water potential and peroxidase activity in *Quercus cerris* and *Quercus pubescens* after inoculation with *Diplodia mutila*. *J. Phytopathol.* 147, 55–59.

Rehfeldt, G. E., Ferguson, D. E., and Crookston, N. L. (2009). Aspen, climate, and sudden decline in western USA. *For. Ecol. Manag.* 258, 2353–2364. doi: 10.1016/j.foreco.2009.06.005

Rigling, D., Hilfiker, S., Schöbel, C., Meier, F., Engesser, R., Scheidegger, C., et al. (2018). *Il deperimento del frassino. Biologia, sintomi e raccomandazioni per la gestione. Notizie per la pratica 57*. Birmensdorf: Istituto federale di ricerca WSL, 8.

Riolo, M., Aloi, F., La Spada, F., Sciandrello, S., Moricca, S., Santilli, E., et al. (2020). Diversity of *Phytophthora* communities across different types of Mediterranean vegetation in a nature reserve area. *Forests* 11, 853–873. doi: 10.3390/f11080853

Scanu, B., Hunter, G. C., Linaldeddu, B. T., Franceschini, A., Maddau, L., Jung, T., et al. (2014). A taxonomic re-evaluation reveals that *Phytophthora cinnamomi* and *P. cinnamomi* var. *parvispora* are separate species. *For. Pathol.* 44, 1–20. doi: 10.1111/efp.12064

Scanu, B., Linaldeddu, B. T., Deidda, A., and Jung, T. (2015). Diversity of *Phytophthora* species from declining Mediterranean maquis vegetation, including two new species, *Phytophthora crassamura* and *P. ornamentata* sp. nov. *PLoS One* 10:e0143234. doi: 10.1371/journal.pone.0143234

Schoebel, C. N., Stewart, J., Gruenwald, N. J., Rigling, D., and Prospero, S. (2014). Population history and pathways of spread of the plant pathogen *Phytophthora plurivora*. *PLoS One* 9:e85368. doi: 10.1371/journal.pone.0085368

Serrano, M. S., Romero, M. Á, Homet, P., and Gómez-Aparicio, L. (2022). Climate change impact on the population dynamics of exotic pathogens: The case of the worldwide pathogen *Phytophthora cinnamomi*. *Agric. For. Meteorol.* 322:109002. doi: 10.1016/j.agrformet.2022.109002

Singh, S., Dalbehera, M. M., Maiti, S., Bisht, R. S., Balam, N. B., and Panigrahi, S. K. (2023). Investigation of agro-forestry and construction demolition wastes in alkali-activated fly ash bricks as sustainable building materials. *J. Waste Manag.* 159, 114–124. doi: 10.1016/j.wasman.2023.01.031

Skovsgaard, J. P., Thomsen, I. M., Skovgaard, I. M., and Martinussen, T. (2010). Associations among symptoms of dieback in even-aged stands of ash (*Fraxinus excelsior* L.). *For. Pathol.* 40, 7–18. doi: 10.1111/j.1439-0329.2009.00599.x

Slippers, B., and Wingfield, M. J. (2007). *Botryosphaeriaceae* as endophytes and latent pathogens of woody plants: Diversity, ecology and impact. *Fungal Biol. Rev.* 21, 90–106. doi: 10.1016/j.fbr.2007.06.002

Smahi, H., Belhoucine-Guezouli, L., Berraf-Tebbal, A., Chouih, S., Arkam, M., Franceschini, A., et al. (2017). Molecular characterization and pathogenicity of *Diplodia corticola* and other *Botryosphaeriaceae* species associated with canker and dieback of *Quercus suber* in Algeria. *Mycosphere* 8, 1261–1272. doi: 10.5943/mycosphere/8/2/10

Sturrock, R. N., Frankel, S. J., Brown, A. V., Hennon, P. E., Kliejunas, J. T., Lewis, K. J., et al. (2011). Climate change and forest diseases. *Plant Pathol.* 60, 133–149. doi: 10.1111/j.1365-3059.2010.02406.x

Thompson, J. D., Gibson, T. J., Plewniak, F., Jeanmougin, F., and Higgins, D. G. (1997). The CLUSTAL_X windows interface: Flexible strategies for multiple sequence alignment aided by quality analysis tools. *Nucleic Acids Res.* 25, 4876–4882.

Tkaczyk, M., Nowakowska, J. A., and Oszako, T. (2016). *Phytophthora* species isolated from ash stands in Białowieża Forest nature reserve. *For. Pathol.* 46, 660–662. doi: 10.1111/efp.12295

Ulbrich, U., Lionello, P., Belušić, D., Jacobeit, J., Knippertz, P., Kuglitsch, F. G., et al. (2012). "Climate of the Mediterranean: Synoptic patterns, temperature, precipitation, winds, and their extremes," in *The Climate of the Mediterranean Region*, ed. P. Lionello (Amsterdam: Elsevier).

Urbez-Torres, J. R. (2011). The status of *Botryosphaeriaceae* species infecting grapevines. *Phytopathol. Mediterr.* 50, S5–S45. doi: 10.14601/Phytopathol_Mediterr-9316

Valdes-Abellan, J., Pardo, M. A., and Tenza-Abril, A. J. (2017). Observed precipitation trend changes in the western Mediterranean region. *Int. J. Climatol.* 37, 1285–1296. doi: 10.1002/joc.4984

Venette, R. C. (2009). "Implication of global climate change on the distribution and activity of *Phytophthora ramorum*," in *Proceedings of the 20th US Department of Agriculture Interagency Research Forum on Invasive Species*, (Newtown Square, PA), 58–59.

Vettraino, A. M., Morel, O., Perlerou, C., Robin, C., Diamandis, S., and Vannini, A. (2005). Occurrence and distribution of *Phytophthora* species in European chestnut stands, and their association with ink disease and crown decline. *Eur. J. Plant Pathol.* 111, 169–180. doi: 10.1007/s10658-004-1882-0

White, T. J., Bruns, T., Lee, S. J. W. T., and Taylor, J. (1990). "Amplification and direct sequencing of fungal ribosomal RNA genes for phylogenetics," in *PCR protocols: A guide to methods and applications*, Vol. 18, eds M. A. Innis, D. H. Gelfand, J. J. Sninsky, and T. J. White (New York, NY: Academic Press), 315–322.

Xue, D. S., Liu, J., Li, B. H., Xu, X. M., Liu, N., Lian, S., et al. (2021). Effect of rainfall and temperature on perithecium production of *Botryosphaeria dothidea* on cankered apple branches. *Phytopathology* 111, 982–989.

Yang, X., Tyler, B. M., and Hong, C. (2017). An expanded phylogeny for the genus *Phytophthora*. *IMA Fungus* 8, 355–384.

frontiers | Frontiers in Forests and Global Change

TYPE Original Research
PUBLISHED 21 September 2023
DOI 10.3389/ffgc.2023.1212192

OPEN ACCESS

EDITED BY
Isabel Alvarez Munck,
Forest Service (USDA), United States

REVIEWED BY
Angus J. Carnegie,
NSW Government, Australia
Oscar Santamaria,
University of Valladolid, Spain

*CORRESPONDENCE
Nicolas Anger
✉ nanger@ufl.edu

†PRESENT ADDRESS
Jason A. Smith,
Department of Biological and Environmental Sciences, College of Natural and Health Sciences, University of Mount Union, Alliance, OH, United States

RECEIVED 25 April 2023
ACCEPTED 28 August 2023
PUBLISHED 21 September 2023

CITATION
Anger N, Held BW, Blanchette RA, Ono Y, Aime CM and Smith JA (2023) Ironwood/hophornbeam leaf rust, an emergent disease across the southeastern United States affiliated to *Melampsoridium asiaticum*. *Front. For. Glob. Change* 6:1212192. doi: 10.3389/ffgc.2023.1212192

Ironwood/hophornbeam leaf rust, an emergent disease across the southeastern United States affiliated to *Melampsoridium asiaticum*

Nicolas Anger[1]*, Benjamin W. Held[2], Robert A. Blanchette[2], Yoshitaka Ono[3], Catherine M. Aime[4] and Jason A. Smith[1†]

[1]Forest Pathology Laboratory, School of Forest, Fisheries and Geomatics Sciences, University of Florida, Gainesville, FL, United States, [2]Department of Plant Pathology, University of Minnesota, St. Paul, MN, United States, [3]Faculty of Education, Ibaraki University, Mito, Ibaraki, Japan, [4]Department of Botany and Plant Pathology, Purdue University, West Lafayette, IN, United States

In the late fall of 2018, foliar rust (referred to as ironwood/hophornbeam leaf rust [IHLR]) was discovered in several counties in Florida, United States, on ironwood (*Carpinus caroliniana*) and hophornbeam (*Ostrya virginiana*), both members of the *Betulaceae*. Uredinia were observed on leaves and, in some cases, samaras of both species at numerous locations on trees of all age classes. Similar reports across the southeastern United States (Georgia, the Carolinas, Tennessee, and Texas) were detected the following year, with European hornbeam (*Carpinus betulus*) being reported as an additional host, while *Ostrya virginiana* var. *guatemalensis* in El Salvador was also discovered showing signs of uredinial infection. Field observations and analyses of morphological data obtained with light and scanning electron microscopy on IHLR and related *Melampsoridium* herbarium samples and combined molecular data from the ITS and LSU loci indicate that (i) IHLR across samples from the southeastern United States and El Salvador belong to the same taxon; (ii) IHLR is closely affiliated to *M. asiaticum*; and (iii) some taxonomic modifications might be necessary at the genus level. No alternative (gametophyte) host has been identified, and the rust is likely overwintering in the uredinial stage. This disease represents a novel leaf pathogen on these hosts in North America, and efforts are needed to monitor future disease epidemiology and impacts on these native and cultivated tree species.

KEYWORDS

***Melampsoridium*, *Carpinus*, *Ostrya*, urediniospore, emergence**

1. Introduction

Betulaceae species, American hornbeam or ironwood (*Carpinus caroliniana* Walt.) and Eastern hophornbeam (*Ostrya virginiana* Mill. K. Koch), are distributed in eastern North America, more precisely east of a Minnesota–Louisiana axis plus Texas and Oklahoma, as well as Ontario and Quebec in Canada (Nesom et al., 2003). *Ostrya virginiana* also has disjunct populations in Wyoming (USA), Manitoba (Canada), Mexico, Guatemala, Honduras, and El Salvador (https://www.fs.fed.us/database/feis/plants/tree/ostvir). However, populations south of the United States are considered either a different species, *O. guatemalensis*, or a variety, *O. virginiana* var. *guatemalensis* (https://powo.science.kew.org/taxon/urn:lsid:ipni.org:names:295249-1). Naturally occurring as forest understory

components, these two species are also planted for ornamental landscaping purposes. Both are important to wildlife, notably *O. virginiana*, whose buds and catkins constitute winter food for a variety of bird species and other wildlife (Burns and Honkala, 1990).

Yellow pustules developing on the lower (abaxial) surface of the leaves of *Carpinus caroliniana* and *Ostrya virginiana* were first observed in the fall of 2018 near Gainesville in Alachua County, Florida (Figures 1A–E). There was no record of rust occurring on these two *Betulaceae* species in Florida prior to these observations. Similar observations across the southeastern United States were reported by collaborators in the following year (J.A. Smith, personal communication). *Melampsoridium* species are obligate biotrophic fungi and have their telial (sporophytic) stage on *Betulaceae* hosts across the globe: *M. alni* on *Alnus* spp., *M. asiaticum* on *Carpinus* spp. and *Ostrya japonica*, *M. betulinum* on *Betula* spp. and *Alnus* spp., *M. carpini* on *Carpinus* spp. and *O. virginiana*, and *M. hiratsukanum* on *Alnus* spp. (https://nt.ars-grin.gov/fungaldatabases/fungushost/fungushost.cfm).

The genus *Melampsoridium* was erected by Klebahn in 1899 and was segregated from *Melampsora* based on the presence of a peridium on both aecia and uredinia and the absence of paraphyses (Engler and Prantl, 1899). In addition, Klebahn mentioned that *Melampsoridium* species are heteroecious, although sporophytic hosts have only been reported for *M. alni*, *M. hiratsukanum*, and *M. betulinum* (Hiratsuka et al., 1992). No alternative host has been recorded for *M. carpini* and *M. asiaticum* (the only known taxa to occur on *Carpinus* and *Ostrya*), although the distribution of some *Larix* species overlaps the distribution of these two fungal taxa (Mamet et al., 2019). A key for the genus was created by Kaneko and Hiratsuka (1981), and species delimitation relied on urediniospore morphological comparisons: length, width, echinulation pattern (echinulated opposed to smooth apex), and number and position of germ pores. These features facilitated the description of *M. asiaticum* in Kaneko and Hiratsuka (1983), which is present in Japan and China. This also separated rusts from both *Carpinus* and *Ostrya* species into two morphological species: *M. asiaticum* and *M. carpini*. Some records for the genus worldwide have been made based on these morphological characteristics but require re-examination and, in some cases, have been re-annotated. A record of *Melampsoridium carpini* from New York State (Accession number PUR006358, collected by Mains and Kauffman in 1914), the only record of rust on *Ostrya* from North America, was originally annotated as having been collected from "*Ostrya virginiana*". However, our examination determined it was *M. betulinum* based on the length of urediniospores and position of germ pores (Kaneko and Hiratsuka, 1983), and the host is more likely to be yellow birch (*Betula alleghaniensis*). Kurkela et al. (1999) used, for the first time in the study of this genus, genetic data (ITS rDNA sequence data) and morphology (urediniospore roundness) to determine that the rust species infecting alder in northeastern Europe (Estonia and Finland) was *M. hiratsukanum* and not *M. betulinum*. This study underlined the limitation in the use of this locus for broader phylogenetic studies among the Pucciniales order due to a lack of variation, notably within *Cronartium*, *Pucciniastrum*, and *Chrysomyxa* genera (Aime et al., 2017). However, it remains pertinent for species delimitation between species in the genus *Melampsoridium* in combination with morphological data. Hantula et al. (2009) also used a combination of ITS data and morphological observations to better distinguish the two rust species co-occurring on *Alnus* leaves in Europe: the native species *M. betulinum* and the introduced species *M. hiratsukanum*.

Therefore, using morphological and genetic data, we propose in this study to test the hypotheses (i) that the observed epidemic in the southeastern United States referred to as IHLR is caused by a *Melampsoridium* rust species, and (ii) that this taxon represents a novel taxon previously undescribed.

2. Methods

2.1. Fungal material studied

2.1.1. Emergent IHLR taxon

Uredinia from the lower leaf surface of *Carpinus caroliniana* (*Cc*—American hornbeam), *Ostrya virginiana* (*Ov*—Eastern hophornbeam), and *Carpinus betulus* (*Cb*—European hornbeam) (Figure 1F) were collected on 11 infected samples from across the southeastern United States: three from Texas, three from Tennessee, two from Florida, one from Georgia, one from South Carolina, and one from North Carolina. *Cc* and *Ov* samples are from natural areas and botanical gardens, while *Cb* samples are from nursery and landscape settings. The locations of IHLR samples are mapped in Figure 2 and listed in Table 1. *Ostrya virginiana* var. *guatemalensis*-infected leaves from El Salvador were requested as well from a collaborator on site and shipped to colleagues at the University of Minnesota (USDA-APHIS/PPQ Permit P526P-18-04404). All isolates were given a code that included the state where they were collected and letters referring to their host (e.g., FLCc1). Details about samples and their name codes are listed in Table 1.

One of the diagnostic tools in the genus *Melampsoridium* consists of plotting roundness against the length of the urediniospores (Kurkela et al., 1999; Hantula et al., 2009, 2012). We therefore used it to make the comparison between the sample from El Salvador and a selection of the ones obtained across the southeastern United States in 2019 from both *C. caroliniana* and *O. virginiana* hosts in Gainesville, FL (FLCc1 and FlOv1, respectively), *C. caroliniana* in Harris County, TX (TXCc2), and *C. betulus* in a nursery setting in 2019 in Tennessee (TNCb1). Two more samples from 2020 were added from another *C. betulus* host in Charleston, SC, and another *C. caroliniana* host in Atlanta, GA (SCCb1 and GACc1, respectively).

Given that these hosts are closely related within the *Betulaceae*, the synchronicity of the emergence of these samples, the nature of their host (*Ostrya virginiana* var. *guatemalensis*), and the conspecificity of the sample obtained from El Salvador with the taxon sampled across the Southeastern United States are discussed below.

2.1.2. Herbarium specimens

We requested 27 herbarium specimens belonging to all accepted taxa in the genus *Melampsoridium* for morphological and molecular investigations. Three specimens were obtained from

10.3389/ffgc.2023.1212192

FIGURE 1
Uredinial infection of IHLR on *Betulaceae* hosts in the southeastern United States. **(A)** *Carpinus caroliniana* leaf upper surface, **(B)** *Ostrya virginiana* leaf upper surface, **(C)** severe sporulation on *C. caroliniana* leaves, **(D, E)** *C. caroliniana* seedlings, **(F)** abaxial surface of *Carpinus betulus* leaves grown in a nursery, **(G)** *C. caroliniana samaras*, **(H, I)** *C. caroliniana* new leaves coexisting with leaves from previous growth year.

the United States Department of Agriculture National Fungus Collections (BPI), 14 from the Arthur Fungarium at Purdue University (PUR), six from the University of Michigan Herbarium (MICH), one from the Tottori Mycological Institute (TMI), and three from the Ibaraki University Herbarium (Table 1). Among them, several were likely incorrectly identified. As mentioned above, *M. asiaticum* was described in Kaneko and Hiratsuka (1983), and some specimens were erroneously treated as *M. carpini*. This is the case for specimens PUR 006369 from 1931, PUR 006371 from 1929, and PUR 006375 from 1939, which were labeled as *M.*

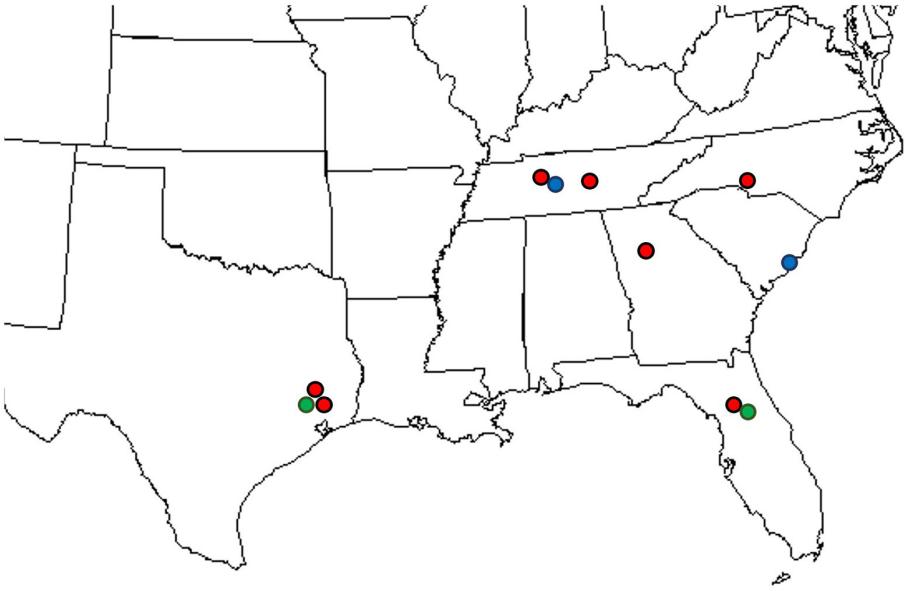

FIGURE 2
Locations where IHLR was sampled across the southeastern United States: red dots on *Carpinus caroliniana*, blue dots on *Carpinus betulus*, and green dots on *Ostrya virginiana* hosts.

carpini but likely represent *M. asiaticum*. These specimens were not included in the study.

2.2. Incidence and severity

Incidence and severity data were determined by processing digital pictures of the host tissue with Leaf Doctor software (Pethybridge and Nelson, 2015), optimized for Apple's iOS operating system. Twenty leaves from each of 10 *Carpinus caroliniana* and 10 *Ostrya virginiana* individuals were sampled in July 2020 at two sites: Loblolly Woods and John Mahon Nature Park in Gainesville, Florida. As uredinial infection was observed on the samaras of two additional *Carpinus caroliniana* individuals at Loblolly Woods later in the 2020 summer season, severity measurements were also recorded on 20 leaves from these two individuals, as well as on five samaras on both trees. Average severity values were determined for each host at each location. The severity value for each leaf corresponds to a disease percentage, i.e., the proportion of symptomatic tissue area infected by the rust pathogen divided by the total leaf tissue area. The incidence was recorded as positive when at least one yellow pustule was observed on the sampled leaves/samaras.

2.3. Morphological observations

2.3.1. Light microscopy

All IHLR isolates from the southeastern United States, one from El Salvador, and all the requested herbarium specimens were systematically used for urediniospore measurements, including length, width, perimeter, and area. These measurements were also used to investigate the conspecificity of the sample from El Salvador with the emergent taxon across the southeastern United States. Urediniospore morphological characters of each collected sample or herbarium specimen were visualized on slides in 5% KOH under 400×, 600×, or 1,000× magnification using a Nikon Eclipse 55i light microscope (Melville, NY). Cell measurements were performed using ImageJ2 software (http://imagej.net). Up to 20 urediniospores were measured per specimen. Urediniospore roundness was determined as described in Kurkela et al. (1999) using the following formula:

$$\text{Roundness} = \frac{\text{perimeter}^2}{4 \times \Pi \times \text{area} \times 1.064}$$

where 1 is the minimum value that indicates a perfect circle.

2.3.2. Scanning electron microscopy

In order to generate higher-resolution images of the urediniospores of the different taxa used in this study, specimens were examined using scanning electron microscopy (SEM) at the University of Minnesota Imaging Center. Leaf tissue infected with *Melampsoridium* was mounted on 1.5-mm aluminum stubs with carbon tape and sputter-coated with gold/palladium using a Cressington 108 Auto Sputter Coater (Cressington Scientific Instruments, Watford, United Kingdom). Samples were then examined using a Hitachi S3500N scanning electron microscope (Hitachi, Tokyo, Japan). This allowed for a consistent observation of the urediniospore echinulation pattern (homogeneous echinulation vs. smooth apex) and the measurement of interspine distance. We measured 10 interspine distances on 10 spores per sample/herbarium specimen. The echinulation pattern was observed and noted on these same 10 spores per sample/herbarium specimen.

TABLE 1 Herbarium specimens, isolates, and samples of the different taxa used in this study.

Taxon	Herbarium accession number/isolate name/ lab number	Host	Date	Location	GenBank		
					LSU accession number	ITS accession number	References
M. alni	MICH 255953[a]	*Alnus mirbelii*	1920	Cuenca, Azuay, Ecuador	-	-	-
	Strain J0525[b]	*Alnus stricta*	2005	Japan	-	EF564165.1	Hantula et al., 2009
	Voucher H 7019539[b]	*Alnus mandshurica*	1976	Russia	KF031534.1	KF031557.1	McKenzie et al., 2013
M. asiaticum	IBAR 6599[a]	*Carpinus tschonoskii*	1992	Mt. Nantaisan, Ibaraki, Japan	-	-	-
	IBAR 10328[ab]	*Carpinus tschonoskii*	2010	Mt. Goshayama, Fukushima, Japan	OQ371314	OQ366470	This study
	IBAR 10339[ab]	*Carpinus tschonoskii*	2010	Dangoishi, Kasama, Ibaraki, Japan	-	OQ366471	This study
	TMI 7277[a]	*Carpinus tschonoskii*	1941	Mount Senjyo-san, Tottori Prefecture, Japan	-	-	-
M. betulinum	MICH 255975[a]	*Betula alleghaniensis*	1914	US, NY, Hoel Pond, Upper Saranac	-	-	-
	MICH 255977[a]	*Betula alleghaniensis*	1914	US, NY, Hoel Pond, Upper Saranac	-	-	-
	PUR 006358[a]	*Betula alleghaniensis*	1914	US, NY, Hoel Pond, Upper Saranac	-	-	-
	PDD 77196[b]	*Betula nana*	2001	Austria	KF031549.1	KF031562.1	McKenzie et al., 2013
	PDD 64927[b]	*Betula pendula*	1995	New Zealand	KF031548.1	KF031563.1	McKenzie et al., 2013
M. carpini	BPI 910402 [ab]	*Carpinus betulus*	2014	Austria, district Waltendorf. Pointnergasse	OQ371315	OQ366472	This study
	BPI 910474[a]	*Carpinus betulus*	2014	Austria, district Waltendorf. Pointnergasse	-	-	-
	BPI 910746[ab]	*Carpinus betulus*	2018	Austria, district Mariatrost, ravine Rettenbachklamm	OQ371316	OQ366473	This study
	KR-M-0048587[b]	*Carpinus betulus*	-	-	-	MH908486	Bubner et al., 2019
M. hiratsukanum	PUR 006499[a]	*Alnus acuminata*	1915	Solola, Guatemala	-	-	-
	PUR 006500[ab]	*Alnus acuminata arcuta*	1977	El Salvador, Santa Ana Volcano	OQ371317	-	This study
	PUR 006506[a]	*Alnus jorullensis*	1917	Quezaltenango, Guatemala	-	-	-
	PUR 006509[a]	*Alnus* sp.	N/A	Tacubaya, Mexico	-	-	-
	PUR 006511[a]	*Alnus acuminata arcuta*	1920	Cuenca, Ecuador	-	-	-

(Continued)

10.3389/ffgc.2023.1212192

TABLE 1 (Continued)

Taxon	Herbarium accession number/isolate name/ lab number	Host	Date	Location	GenBank		
					LSU accession number	ITS accession number	References
IHLR	FLCc1[ab]	*Carpinus caroliniana*	2019	Loblolly Woods, Gainesville, FL, USA	OQ361385	OQ360722	This study
	FLOv1[ab]	*Ostrya virginiana*	2019	Loblolly Woods, Gainesville, FL, USA	OQ640215	OQ597694	This study
	TXCc1[ab]	*Carpinus caroliniana*	2019	Jasper County, TX, USA	OQ640216	OQ597695	This study
	TXOv1[ab]	*Ostrya virginiana*	2019	Jasper County, TX**, USA**	OQ640217	OQ597696	This study
	TXCc2[ab]	*Carpinus caroliniana*	2019	Mercer Botanical Gardens, Harris County, TX, USA	OQ640218	OQ597697	This study
	TNCc1 [ab]	*Carpinus caroliniana*	2019	Beaman Park, Nashville, TN, USA	OQ640219	OQ597698	This study
	TNCc2[ab]	*Carpinus caroliniana*	2019	TN Landscape, USA	OQ640220	OQ597699	This study
	TNCb1[ab]	*Carpinus betulus*	2019	Mc Minnville, Nursery, TN, USA	OQ640221	OQ597700	This study
	NCCc1[ab]	*Carpinus caroliniana*	2019	Bartlett Arboretum, Charlotte, NC, USA	OQ640222	OQ597701	This study
	GACc1[ab]	*Carpinus caroliniana*	2020	Atlanta, GA, USA	OQ640223	OQ597702	This study
	SCCb1[ab]	*Carpinus betulus*	2020	Charleston, SC, USA	OQ640224	OQ597703	This study
	SalOv1[ab]	*Ostrya virginiana* var. *guatemalensis*	2020	Chalatenango, San Ignacio, El Salvador	OQ640225	OQ597704	This study
Pucciniastrum coryli	IBAR 8641[b]	*Corylus sieboldiana*	1995	Fukushima, Japan	AB221381.1	AB221419.1	Liang et al., 2006

[a]Specimens used for morphology observations only. [b]Specimens used for molecular analysis only. [ab]Specimens used for morphology observations and molecular analysis. MICH, University of Michigan; IBAR, Ibaraki University; TMI, Tottori Mycological Institute; PUR, Purdue University; BPI, U.S. National Fungus Collection.

10.3389/ffgc.2023.1212192

2.4. Statistical analysis

Morphological characteristics average values were calculated for each specimen (IHLR and herbarium) to establish statistical comparisons. The principal component analysis (PCA), based on urediniospore morphological measurements (length, width, perimeter, area, and roundness), pairwise tests (Welsh two-sample *t*-test for normally distributed data), and Kruskal–Wallis tests (non-parametric test) were carried out using R software version 4.1.1 (R Core Team, 2023). When the original data were not normally distributed, logarithmic base 10 and square root transformations were attempted for pairwise comparisons. The PCA analysis is used to test affinities between the different taxa in the genus based on morphological characteristics.

2.5. DNA extraction, amplification, and sanger sequencing

DNA was extracted by crushing uredinia between a clean microscope slide and a clean cover slip in 50 μL of Extract-N-Amp DNA extraction buffer (Millipore Sigma, St. Louis, MO), placing the solution for 1 h at 37°C, 10 min at 90°C, and at 4°C. This protocol is based on the work of Liang et al. (2006). When recalcitrant herbarium samples were processed, the QIAGEN DNeasy Plant Mini Kit (Qiagen, Hilden, Germany) was used instead, and the extraction process was optimized by soaking samples in liquid nitrogen and disrupting them with glass beads in a shaker. The incubation time in the extraction buffer was also increased from 10 min to up to 4 h at 90°C. All amplification reactions were run in a MJ Mini thermocycler (Bio-Rad Inc., Hercules, CA) in 25 μL reaction volumes with 12 μL Immomix Red Master Mix (Bioline, London, UK), 9 μL of PCR-grade H2O, 1 μL Bovine Serum Albumine (BSA) (3% w/v), 1 μL of each primer, and 1 ng/μL of DNA template. For the nuclear large subunit (28S) locus of the ribosomal DNA, amplification was achieved using the primers Rust2Inv (forward) (Aime, 2006)/LR6 (reverse) (Vilgalys and Hester, 1990) with the following conditions: initial denaturation step of 2 min at 94°C, 40 cycles of 30 s at 94°C, 1 min at 57°C, and 1.5 min at 72°C, for a final extension of 7 min at 72°C. The internal transcribed spacer (ITS) region was amplified using ITS1F (White et al., 1990) and ITS4b (Gardes and Bruns, 1993) primer pairs. Amplicons were sequenced with the same primers. A nested PCR was performed on weaker LSU PCR amplicons with Rust28SF (Aime et al., 2018)/LR5 (Vilgalys and Hester, 1990). Primers were designed for specimens recalcitrant to the ITS locus amplification, notably *M. asiaticum* specimens from Japan and *M. carpini* specimens from Austria. These primers, based on the universal ITS2 and ITS3 primers (White et al., 1990), are named ITS2_Mel and ITS3_Mel (see Table 2 for primer sequences). These same primers were used for Sanger sequencing on amplicons obtained from nested PCRs. PCR amplicons were purified with the ExoSAP-IT purification kit (ThermoFisher, Waltham, MA) and sequenced by Genewiz (Genewiz LLC, NJ). Forward and reverse sequences were analyzed in GENEIOUS software v. 10.2.6 (Kearse et al., 2012) for manual editing and alignment.

2.6. Amplicon-based identification

First investigations on the identity of the rust sampled across the southeastern United States were undertaken by using manually curated ITS and LSU sequences for BLASTn searches against the GenBank database (https://blast.ncbi.nlm.nih.gov/Blast.cgi) and aligned for comparison to validate affiliation to the genus *Melampsoridium*.

2.7. Phylogenetic analysis

LSU and ITS sequences were used to reconstruct the phylogenetic position of the IHLR taxon observed across the southeastern United States, notably resolving its position within the genus *Melampsoridium*. Sequences obtained in this study and voucher sequences from previously published work (Liang et al., 2006; McKenzie et al., 2013; Bubner et al., 2019) were aligned using the MUSCLE (Edgar, 2004) plugin for GENEIOUS 10. Sequences were visually edited to treat ambiguities and sequencing errors. Independent phylogenetic analyses based on single locus data were undertaken using the RAxML plugin (Stamatakis, 2014) and the MrBayes plugin (Huelsenbeck and Ronquist, 2001) within GENEIOUS 10. Sixteen sequences were aligned for an ITS-based analysis (505 nucleotides) and 15 sequences for an LSU-based analysis (455 nucleotides). The general time reversal (GTR) evolutionary model was used with rapid bootstrapping and 1,000 bootstrapping replications. *Pucciniastrum coryli* isolate TSH-R4237 (IBA8641) was used as an outgroup to root the trees, given that it is a closely related taxon in the Pucciniastraceae (Aime et al., 2018). All the taxa used in this phylogenetic study and their GenBank accession numbers are reported in Table 1. A multilocus approach was also undertaken by using a concatenated dataset of 960 nucleotides to run Bayesian and maximum likelihood phylogenetic analysis.

3. Results

3.1. Incidence and severity

The disease survey and sample collection in this study include locations in the states of Florida, Georgia, the Carolinas, Tennessee, and Texas (Figure 2, Table 1). In this survey, the rust disease incidence and severity on *Carpinus caroliniana* and *Ostrya virginiana* were recorded at two locations in Gainesville, Alachua County, Florida, in July 2020. The sample tree selection was arbitrary. At the time of observation, all sampled trees from the two locations ($n = 42$; 100% incidence) showed uredinial sporulation on the leaves. The average severity recorded on *Carpinus caroliniana* leaves was 13.17% at John Mahon Nature Park and 7.25% at Loblolly Woods, while on *Ostrya virginiana*, it was 14.64% at the former and 11.34% at the latter. In addition to the foliar infection, uredinia were produced on samara wings on *Carpinus caroliniana* in late summer (Figure 1G). Rust severity data were recorded for the samara infection on two *Carpinus caroliniana* individuals at the Loblolly Woods location ($n = 5$ per tree), where the average value was 33.3%. No comprehensive survey

TABLE 2 Primers used in this study and their sequences.

Locus	Primer	Sequence	References
ITS	ITS 1F	CTT GGT CAT TTA GAG GAA GTA A	Gardes and Bruns, 1993
	ITS 4B	CAG GAG ACT TGT ACA CGG TCC AG	Gardes and Bruns, 1993
	ITS2	GCT GCG TTC TTC ATC GAT GC	White et al., 1990
	ITS3	GCA TTC ATG AAG AAC GCA GC	White et al., 1990
	ITS2_Mel	ACT GTG TTC TTC ATC GAT GT	This study
	ITS3_Mel	ACA TCG ATG AAG AAC ACA GT	This study
LSU	Rust2Inv	GAT GAA GAA CAC AGT GAA A	Aime, 2006
	LR6	CGC CAG TTC TGC TTA CC	Vilgalys and Hester, 1990
	Rust28SF	TTT TAA GAC CTC AAA TCA GGT G	Aime et al., 2018
	LR5	TCC TGA GGG AAA CTT CG	Vilgalys and Hester, 1990

for the incidence and severity of rust on the two tree species was undertaken at the locations in the other five states. However, the level of rust sporulation across the samples collected at all sites appears consistent.

3.2. Morphological observations

3.2.1. Light microscopy

3.2.1.1. Conspecificity of El Salvador sample with IHLR from the southeastern United States

While testing the conspecificity of the El Salvador sample with IHLR, only the width of urediniospores was statistically different (Welch *t*-test *p*-value = 0.0003) between the sample from El Salvador (average of 10.88 µm ± 1.12) and specimens collected in the southeastern US (12.03 µm ± 1.44). A principal component analysis including IHLR and *M. asiaticum* specimens on the same morphological traits allows further comparisons to investigate the affinities between the two taxa. The first two components represent more than 87% of the variance in the original five-dimensional dataset and allow a similarly reliable assessment using this technique. The ellipse centroids are close to each other, while the point projections appear to be slightly spread for *M. asiaticum* (Supplementary Figure 1). This reflects the pairwise statistical analysis where width, perimeter, and area traits are comparable at a 5% confidence level and roundness at a 1% confidence level. However, the length trait is significantly different between the two groups.

A similar pattern of variability is observed when plotting roundness against the length of the urediniospores from the El Salvador sample ($n = 20$) and a selection of samples from across the southeastern US ($n = 120$) (Supplementary Figure 2). This is confirmed by a comparison of roundness:length ratios that are comparable for all IHLR samples ($n = 215$ urediniospores) and the El Salvador sample ($n = 20$ urediniospores), with an average value of 0.056 for both.

3.2.1.2. Pairwise comparison of *Melampsoridium*

Pairwise comparisons of morphological traits between every recognized species in the genus *Melampsoridium* revealed diagnostic features and allowed for the observation of morphological affinities. Urediniospore length was statistically different for all taxa except between IHLR and *M. carpini* specimens (Welch *t*-test *p*-value on log10 transformed data = 0.6724) and between *M. alni* and *M. hiratsukanum* specimens (Welch *t*-test *p*-value on log10 transformed data = 0.3875). Urediniospore width is diagnostic for most taxa but could not discriminate between *M. alni*/*M. hiratsukanum* (Welch *t*-test *p*-value = 0.2966), *M. asiaticum*/*M. carpini* (Kruskal–Wallis *p*-value = 0.3875), and IHLR/*M. asiaticum* (Welch *t*-test *p*-value = 0.7023). Urediniospore perimeter and area in a similar way segregate all taxa combinations except *M. betulinum*/*M. hiratsukanum* (Kruskal–Wallis *p*-value = 0.1169 and Welch *t*-test *p*-value = 0.8450, respectively) and IHLR/*M. asiaticum* (Welch *t*-test *p*-values = 0.2517 and 0.9047, respectively). The urediniospore roundness trait significantly discriminates species in only 7 out of the 15 possible combinations in the genus and does not appear to be a reliable diagnostic tool by itself. Statistical differences and similarities among taxa in pairwise comparisons are presented in a heat map (Figure 3). A more detailed heat map including *p*-values is presented in Supplementary Figure 3. Its visual observation allows a preliminary interpretation of the morphological affinities of the different taxa within the genus, i.e., taxa with comparable traits. The overall size of the spores (area) is comparable for *M. hiratsukanum* (286.67 µm^2) and *M. betulinum* (288.19 µm^2) (Welch *t*-test *p*-value = 0.8450). However, the specimens from these two taxa differ in their length (Welch *t*-test *p*-value on square root transformed data = 1.35 E-05, 5.163664 and 5.436891 values, respectively) and width (Welch *t*-test *p*-value = 0.0002, 13.82 µm and 12.76 µm values, respectively). Specimens of *M. alni* (13.98 µm) and *M. hiratsukanum* (13.81 µm) are similar in terms of width (Welch *t*-test *p*-value = 0.6823). Their overall size (area) is also not statistically different at a 1% significance level (Welch *t*-test *p*-value = 0.0218, 319.71 µm^2 and 288.19 µm^2 values, respectively). Finally, *M. alni* and *M. betulinum* specimens have comparable lengths as explained above with log10 transformed average measurements of 1.46 and 1.47, but also area values that are not statistically different at a 1% significance level (Welch *t*-test *p*-value = 0.0156, 319.71 µm^2 and 286.67 µm^2 values, respectively).

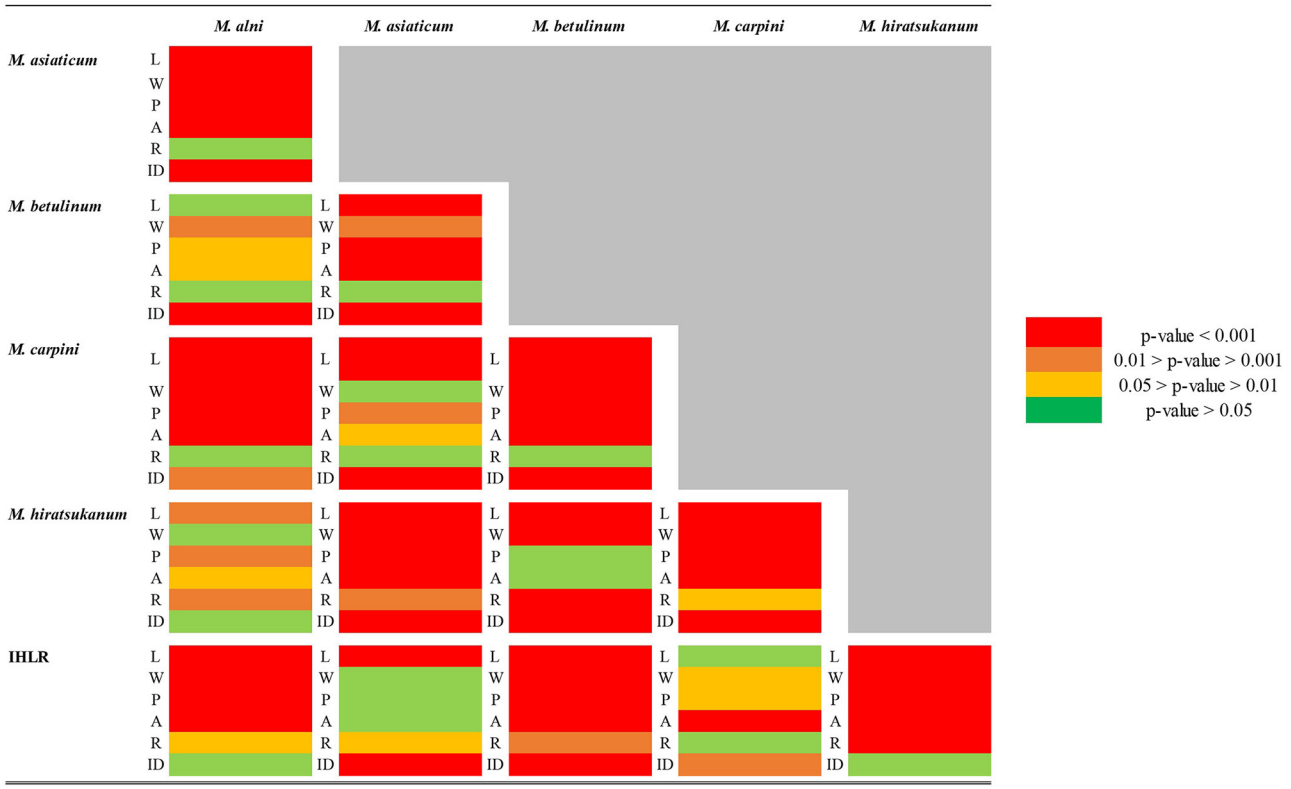

FIGURE 3
Heat map table of the *p*-values obtained from pairwise comparison of different urediniospore morphological traits (L = length; W = width; P = perimeter; A = area; and R = roundness) among the *Melampsoridium* genus. Welch *t*-test was used when data normality and variance homogeneity assumptions were satisfied. Kruskal–Wallis test was used when one or both of the data normality and/or variance homogeneity assumptions were not satisfied. When not satisfied with the original measurements, the normality of the distribution was tested on logarithm base 10 (log10) and square root (SQRT) transformed data.

The two taxa with the most comparable traits appear to be IHLR and *M. asiaticum*, with statistically comparable width (11.93 μm and 12.03 μm values, respectively, Welch *t*-test *p*-value = 0.7023), perimeter (56.91 μm and 57.91 μm values, respectively, Welch *t*-test *p*-value = 0.2517), and area values (203.42 and 204.16 values, respectively, Welch *t*-test *p*-value = 0.9047). Moreover, there is no statistical difference at a significance level of 1% regarding the roundness trait (1.20 and 1.26 values, respectively, Kruskal–Wallis *p*-value = 0.0174). IHLR specimen measurements are similar to those of *M. carpini* on urediniospore length log10 transformed values (Welch *t*-test *p*-value on log10 transformed data = 0.6724), where both values = 1.34. Finally, morphological affinities are also observed between *M. carpini* and *M. asiaticum*, whose average width is comparable (Kruskal–Wallis *p*-value = 0.2966, values of 11.39 μm and 12.03 μm, respectively). The average area is also comparable between the two taxa at a significance level of 1% (Kruskal–Wallis *p*-value = 0.0238, values of 188.30 μm and 204.16 μm, respectively). The pooled average values for each trait and per taxon are presented in Table 3.

The principal component analysis (PCA) based on five morphological traits (length, width, perimeter, area, and roundness) allows for a visual assessment of the relationships among the genus (Figure 4). The two first components represent more than 90% of the variance in the original five-dimensional dataset and provide a reliable assessment using this technique. The ellipse centroids appear to group in two clusters. The first includes *M. alni*, *M. betulinum*, and *M. hiratsukanum* species, while the second includes IHLR specimens of *M. asiaticum* and *M. carpini*. This is congruent with the results obtained from the pairwise comparisons above. This trend is also observable from the boxplot graph of the urediniospore area in the Supplementary Figure 4.

3.2.1.3. IHLR morphological description

The IHLR taxon across the southeastern United States and El Salvador presents the following morphological characteristics: spermogonia and aecia unknown, uredinia hypophyllous, scattered or aggregate, round (0.05–0.30 mm), yellow to orange, ostiolar cells extending in an acute apex (Figure 5A), urediniospores are obovate, (15–)17–27(−31) × (8–)9–15 μm wide, walls 1–3 μm thick, echinulate, colorless. Cytoplasm is orange (Figure 5B), germ pores are inconsistently observed (Figures 5C, D), mostly subequatorial. Telia was not observed.

3.2.2. Scanning electron microscopy

Micrographs were obtained from 13 specimens to assess urediniospore echinulation patterns (smooth apex vs. uniformly echinulate). First, specimens FLCc1 and SalOv1 collected from

10.3389/ffgc.2023.1212192

TABLE 3 Diagnostic features used in this study for each taxon in the *Melampsoridium* genus.

Diagnostic features	*Melampsoridium alni*	*Melampsoridium asiaticum*	*Melampsoridium betulinum*	*Melampsoridium carpini*	*Melampsoridium hiratsukanum*	IHLR
Echinulation pattern	Homogeneous	Homogeneous	Bald apex	Bald apex	Homogeneous	Homogeneous
Length (µm)	28.86	24.47	29.7	21.76	26.77	21.95
Width (µm)	13.98	12.03	12.76	11.39	13.82	11.93
Area (µm^2)	319.71	204.16	286.67	188.3	288.19	203.42
Perimeter (µm)	72.77	57.91	69.16	55.3	67.24	56.92
Larix spp. As a known aecial host?	Yes	No	Yes	No	Yes	No

Florida on *Carpinus caroliniana* and from El Salvador on *Ostrya virginiana* var. *guatemalensis* consistently had a homogeneous echinulation pattern, supporting their conspecificity (Figure 6). Similarly, *M. alni* (MICH 255953), *M. asiaticum* (IBAR 6599, IBAR 10328, and IBAR 10339), and *M. hiratsukanum* (PUR 006499, PUR 006500, PUR 006506, PUR 006509, and PUR 006511) specimens consistently show urediniospores with a homogeneous echinulation pattern. On the contrary, *M. betulinum* (MICH 255975, MICH 255977, and PUR 006358) and *M. carpini* (BPI 910402) specimens consistently have urediniospores with a bold apex. These observations (Figures 7, 8) agree with the previously published literature. Additionally, specimen PUR006358, labeled *M. carpini* and collected by Kauffman in 1914 in New York on *Ostrya virginiana*, was identified as *M. betulinum* by Kaneko and Hiratsuka (1981) based on the size of the urediniospores. Similarly, several specimens collected by Kauffman in 1914 at the MICH herbarium (e.g., MICH 255975 and MICH 255977) named *M. betulae* should be considered as *M. betulinum*. Close observations of the leaves included in these specimens indicate that the host is likely *Betula alleghaniensis* (yellow birch), which supports the species determination of *M. betulinum*. Interspine distance was also determined for every taxon and was diagnostic in most taxa combinations except *M. alni*/*M. hiratsukanum* (Welch *t*-test *p*-value on log10 transformed data = 0.0664), *M. alni*/IHLR (Welch *t*-test *p*-value = 0.6022), and *M. hiratsukanum*/IHLR (Welch *t*-test *p*-value on square root transformed data = 0.3557).

3.3. Sanger sequencing and phylogenetic analysis

In total, 35 sequences were generated in this study, including 24 sequences for the emergent IHLR taxon for each of the 11 locations in the southeastern United States, as well as for the sample obtained from El Salvador. In addition, sequences used in this study were downloaded from GenBank and obtained from published studies (Table 1). DNA extraction was attempted on all requested herbarium specimens, but only the relatively recently collected specimen PUR 006500 (1977, *M. hiratsukanum* from El Salvador) resulted in the amplification of a DNA sequence from the LSU locus (GenBank accession number OQ371317). However, a partial LSU sequence was obtained from the *M. asiaticum* specimen TMI 7277 collected in 1941 from Japan but was not included in the phylogenetic analysis due to its short length (223 bp). Only one locus was available for *M. hiratsukanum* specimen PUR 006500 (LSU) and for *M. alni* strain J0525, *M. asiaticum* IBAR 10339 (GenBank accession number OQ366471), and *M. carpini* KR-M-0048587 (ITS).

ITS and LSU sequences obtained from samples of the IHLR taxon across the southeastern United States and from the El Salvador sample are 100% similar, supporting the hypothesis of conspecificity. The sequences were deposited in GenBank (accession numbers are reported in Table 1) and searched against the NCBI GenBank database using the BLASTn function. The ITS analysis revealed a 93.9% homology with the *Melampsoridium hiratsukanum* specimen KF031553 (on *Alnus incana* from Finland), while the nuLSU analysis revealed 97.5% homology with

FIGURE 4
Principal component analysis of *Melampsoridium* species and IHLR specimens based on urediniospore morphology. Each point projection is based on urediniospore length, width, perimeter, area, and roundness measurement. Ellipses have 95% interval confidence; their respective centroid corresponds to the barycenter belonging to the intervals.

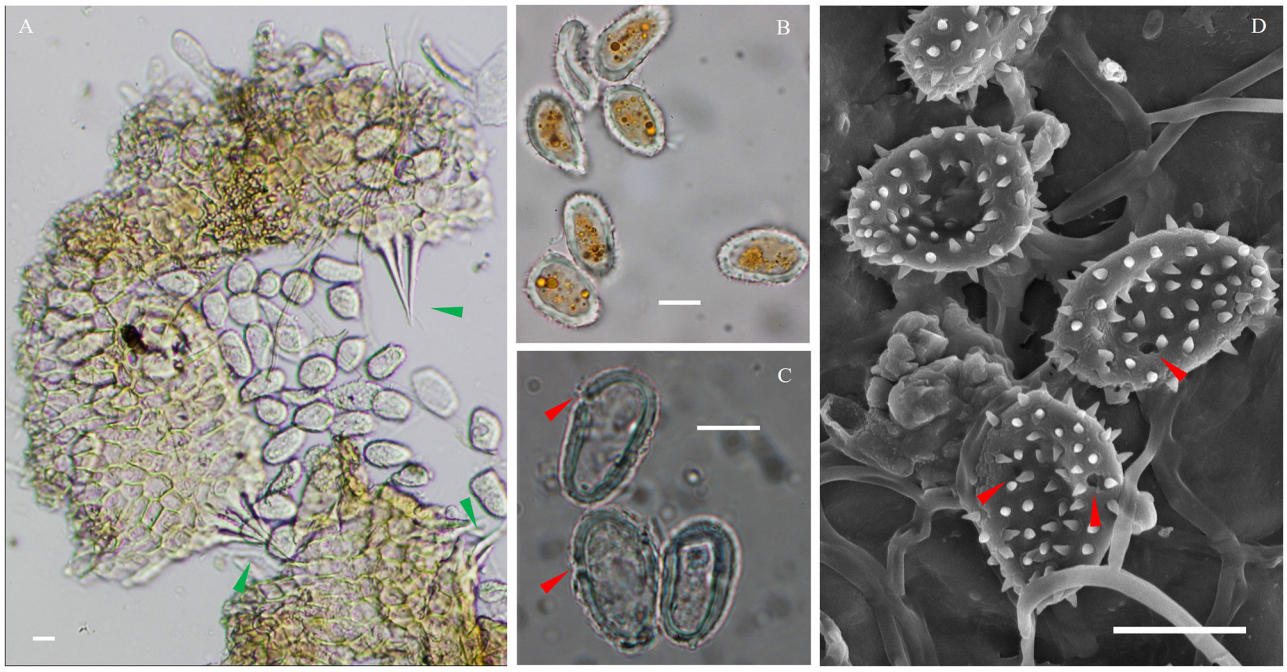

FIGURE 5
Microscopic observations of the IHLR FLCc1 specimen. **(A)** Urediniospores released from uredinia through ostioles. **(B)** Urediniospores general aspect and orange cytoplasm. **(C, D)** Germ pores in a subequatorial position. Green arrows indicate ostiolar cells, and red arrows indicate germ pores. Bars are 10 μm.

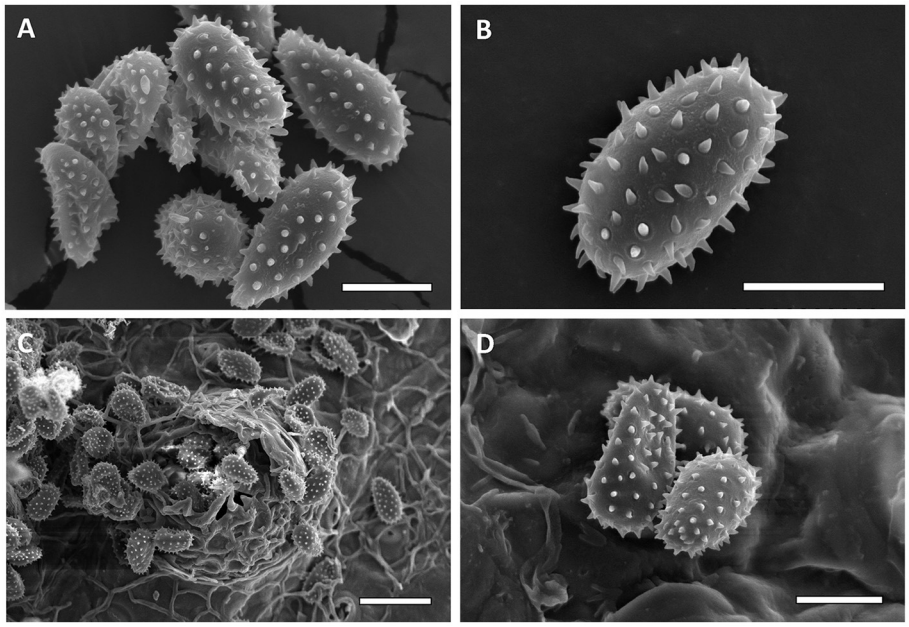

FIGURE 6
Scanning electron micrographs of urediniospores from FLCc1 IHLR sample [**(A, B)**—Bar = 10 μm] and SALOv1 IHLR sample [**(C)**—bar = 25 μm, **(D)**—bar = 10 μm].

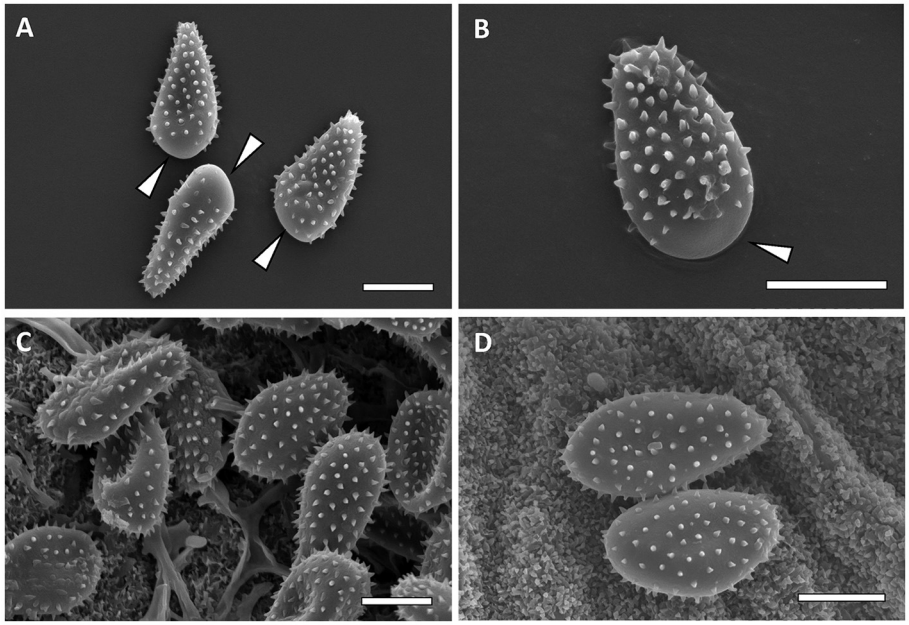

FIGURE 7
Scanning electron micrographs of urediniospores from *M. carpini* [**(A, B)**—Bar = 10 μm] and *M. hiratsukanum* [**(C, D)**—Bar = 10 μm]. Bald apex of the spores is indicated by white arrows.

Melampsoridium hiratsukanum (accession number KC 313888) sampled from white alder (*Alnus rhombifolia*) in California. Bayesian and maximum likelihood analysis yielded comparable topologies with six supported terminal clades corresponding to the five described species: *M. betulinum* (ML–BS = 100%, PP = 1), *M. alni* (ML–BS = 94%, PP = 0.83), *M. asiaticum* (ML–BS = 99%, PP = 0.99), *M. carpini* (ML–BS = 100%, PP = 0.99), and IHLR specimens. The clade including *M. hiratsukanum* specimens is weakly supported by the maximum likelihood analysis (BS value = 39%) and moderately supported using the Bayesian inference method (PP = 0.78). The only discrepancy between the two methods corresponds to *M. hiratsukanum* specimen PUR

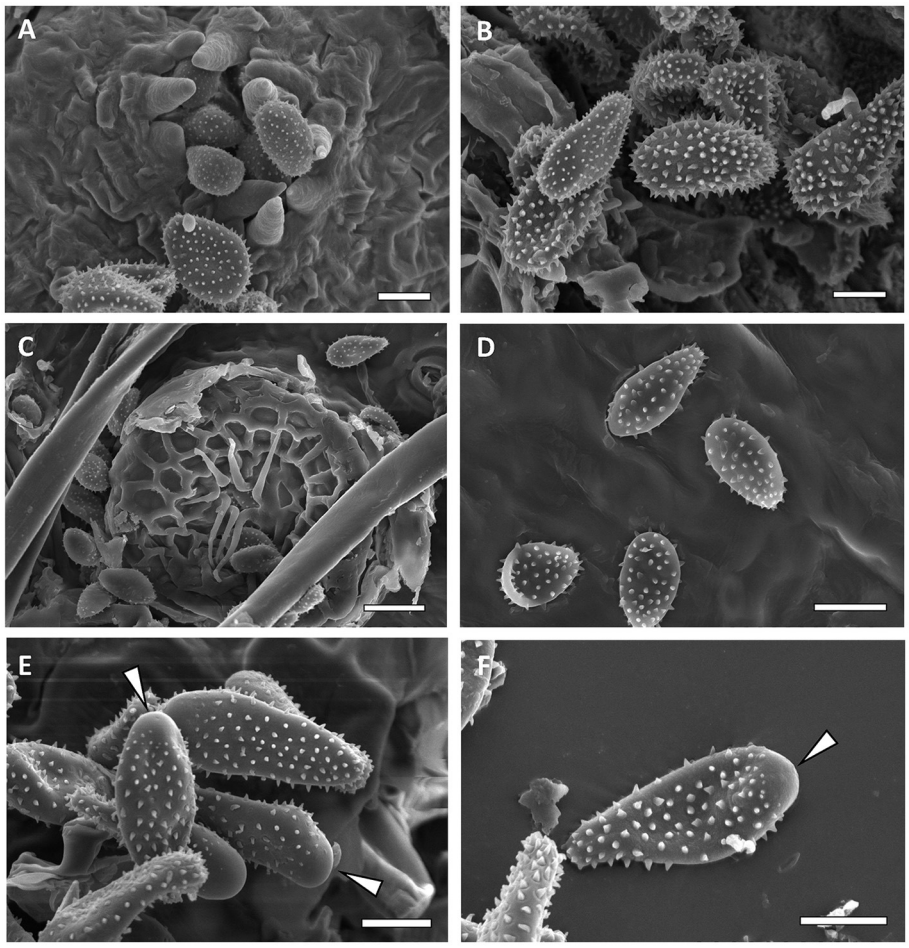

FIGURE 8
Scanning electron micrographs of urediniospores from *M. alni* [**(A, B)**—Bar = 10 μm], *M. asiaticum* [**(C)**—bar = 10 μm, **(D)**—bar 20 = μm], and *M. betulinum* [**(E, F)**—Bar = 10 μm]. Bald apex of the spores is indicated by white arrows.

006500 falling between *M. alni* and the two other *M. hiratsukanum* specimens with the Bayesian inference method. All *M. alni*, *M. betulinum*, and *M. hiratsukanum* specimens fall into a highly supported subclade (ML–BS = 98%, PP = 1), hereafter called Clade A. IHLR specimens are grouped with *M. asiaticum* specimens in a second subclade (ML–BS = 90%, PP = 1) called Clade B. Finally, *M. carpini* specimens are clustering into their own group (ML–BS = 100%, PP = 1) called Clade C. Both analyses display *M. betulinum*, *M. hiratsukanum*, *M. asiaticum*, and IHLR specimens grouped in one clade, while *M. carpini* specimens fall into another one (Clade C). However, that aspect is not statistically supported. The topology obtained from the maximum likelihood analysis is presented in Figure 9.

4. Discussion

Prior to the report in this study, there was no record of rust disease on *Carpinus* and *Ostrya* in the southeastern United States. Typically, rust epidemics in this tree host family are caused by *Melampsoridium* species. Simple morphological investigations, notably through observations of urediniospore echinulation patterns, allow for differentiation of IHLR from *M. betulinum* and *M. carpini* (homogeneously echinulated vs. bald apex, respectively). The ecology of *M. hiratsukanum*, *M. alni*, and *M. betulinum*, with known macrocyclic life cycles, i.e., alternating *Larix* spp. as gametophyte hosts and alder or birch as sporophyte host species, and other morphological differences, such as greater urediniospore size (length, perimeter, or area), support being non-conspecific with IHLR. The diagnostic features used in this study are summarized in Table 3. These discrepancies are also supported by the molecular analysis, where *M. hiratsukanum*, *M. alni*, and *M. betulinum* are clustered in Clade A. The reconstruction of the genus phylogeny also confirms the IHLR assignment to *Melampsoridium*. More precisely, IHLR specimens form a well-supported subclade with *M. asiaticum* specimens. In addition, the dichotomy within the genus between clades B and C (*M. carpini*, *M. asiaticum*, and IHLR) and clade A (*M. alni*, *M. betulinum*, and *M. hiratsukanum*) indicates that some taxonomic adjustments might be needed to better accommodate these discrepancies. Taxa from clades B and C do not have a known gametophyte host; their sporophyte hosts belong to both *Ostrya* and *Carpinus* and have overall smaller

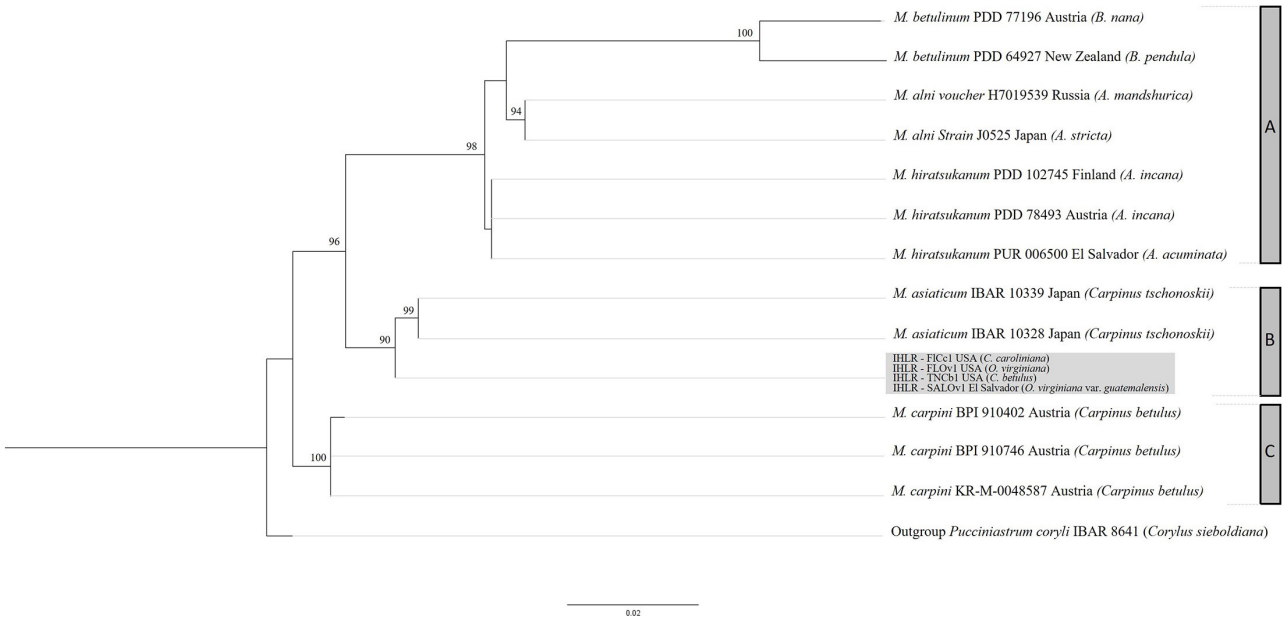

FIGURE 9
RAxML topology obtained from a 960 nucleotide multilocus alignment (LSU + ITS) under a GTR model with 1,000 bootstrap replicates. Bootstrap values below 75% are not shown. IHLR specimens are in the light gray box. *Melampsoridium* tree hosts are mentioned in parenthesis. Clade A includes *M. betulinum*, *M. alni*, and *M. hiratsukanum* specimens. Clade B includes *M. asiaticum* and IHLR specimens, and clade C includes *M. carpini* specimens. Specimen IBAR 8641 (*Pucciniastrum coryli*) is used as an outgroup.

urediniospores. On the contrary, the taxa belonging to Clade C have known gametophyte hosts (*Larix* spp.), alder and/or birch species as sporophyte hosts, and present bigger urediniospores.

In this context, we propose the designation *Melampsoridium* cf. *asiaticum* to refer to IHLR specimens. The two groups (IHLR and *M. asiaticum* specimens) have *Ostrya* and *Carpinus* species as hosts; quantitative morphological traits (urediniospore width, perimeter, and area) are statistically similar; and no gametophyte host has been observed for IHLR and *M. asiaticum* specimens. However, a few discrepancies are noted (e.g., urediniospore length feature), and nuclear ITS and LSU sequences differ as well (13 polymorphic sites total), resulting in IHLR and *M. asiaticum* specimens being sister subclades in the topology of the reconstructed phylogeny. Additional DNA information and sequences at the genus level would allow the better phylogenetic signal resolution needed to confirm IHLR identity. The denomination *Melampsoridium* cf. *asiaticum* is justified by these discrepancies, which may be due to local adaptation following introduction from Asia or correspond to the characteristics specific to an emergent, novel taxon in the genus.

IHLR specimens from El Salvador and the ones isolated across the southeastern United States share the exact same ITS and LSU sequences. The conspecificity of these isolates raises the question of whether an introduction was first made into Central America or there was a second introduction into the southeastern United States, and therefore the current geographical range of the epidemics needs further study. Overwintering is likely to occur in tropical or subtropical regions (Florida and/or Central America) through repetitive uredinial infections. The observed coexistence of new leaves and infected leaves from previous growth year (Figures 1G, H) support that statement. While a survey with several time points would be necessary and informative, the IHLR geographical distribution area and severity in the southeastern United States likely increase as temperature and humidity, especially in spring and summer, increase as well. Despite the isolated sites of this survey across the southeastern United States, our data suggests that the IHLR pathogen is successfully established in this area. The fitness of the host species *in situ* can be significantly impacted given the observed incidence and severity data, as well as the ability of the rust to infect seedlings and samaras (Figure 1I). Uredinial sporulation on *Carpinus caroliniana* samaras represents a novel aspect of the infection biology of a taxon in the *Melampsoridium* genus on its host.

Data availability statement

The datasets presented in this study can be found in online repositories. The names of the repository/repositories and accession number(s) can be found in the article/Supplementary material.

Author contributions

NA and JS designed the research. NA, JS, YO, and CA performed the sampling. NA, BH, and JS performed the molecular analyses. NA, BH, YO, and RB performed the microscopic analyses. NA analyzed the data and wrote the manuscript with inputs from JS, YO, CA, RB, and BH. All authors contributed to the article and approved the submitted version.

Conflict of interest

The authors declare that the research was conducted in the absence of any commercial or financial relationships that could be construed as a potential conflict of interest.

Publisher's note

All claims expressed in this article are solely those of the authors and do not necessarily represent those of their affiliated organizations, or those of the publisher, the editors and the reviewers. Any product that may be evaluated in this article, or claim that may be made by its manufacturer, is not guaranteed or endorsed by the publisher.

Supplementary material

The Supplementary Material for this article can be found online at: https://www.frontiersin.org/articles/10.3389/ffgc.2023.1212192/full#supplementary-material

References

Aime, M. C. (2006). Toward resolving family-level relationships in rust fungi (Uredinales). *Mycoscience* 47, 112–122. doi: 10.1007/S10267-006-0281-0

Aime, M. C., Bell, C. D., and Wilson, A. W. (2018). Deconstructing the evolutionary complexity between rust fungi (*Pucciniales*) and their plant hosts. *Stud. Mycol. Lead. Women Fungal Biol.* 89, 143–152. doi: 10.1016/j.simyco.2018.02.002

Aime, M. C., McTaggart, A. R., Mondo, S. J., and Duplessis, S. (2017). "Chapter seven - phylogenetics and phylogenomics of rust fungi," in *Advances in Genetics, Fungal Phylogenetics and Phylogenomics,* eds. J. P., Townsend, Z., Wang (New York, NY: Academic Press) 267–307. doi: 10.1016/bs.adgen.2017.09.011

Bubner, B., Buchheit, R., Friedrich, F., Kummer, V., and Scholler, M. (2019). Species identification of European forest pathogens of the genus *Milesina* (Pucciniales) using urediniospore morphology and molecular barcoding including *M. woodwardiana* sp. nov. *MycoKeys* 48, 1–40. doi: 10.3897/mycokeys.48.30350

Burns, R., and M., Honkala, B., H. (1990). *Silvics of North America. Volume 2. Harwoods., Agriculture Handbook 654.* Washington, DC: U.S. Department of Agriculture, Forest Service.

Edgar, R. C. (2004). MUSCLE: a multiple sequence alignment method with reduced time and space complexity. *BMC Bioinf.* 5, 113. doi: 10.1186/1471-2105-5-113

Engler, A., and Prantl, K. (1899). "Uredinales (Nachträge)," in *Die Natürlichen Pflanzenfamilien* 546–553.

Gardes, M., and Bruns, T. (1993). ITS primers with enhanced specificity for basidiomycetes-application to the identification of mycorrhizae and rusts. *Molec. Ecol.* 2, 113–118. doi: 10.1111/j.1365-294X.1993.tb00005.x

Hantula, J., Kurkela, T., Hendry, S., and Yamaguchi, T. (2009). Morphological measurements and ITS sequences show that the new alder rust in Europe is conspecific with *Melampsoridium hiratsukanum* in eastern Asia. *Mycologia* 101, 622–631. doi: 10.3852/07-164

Hantula, J., Stringer, R. N., Lilja, A., and Kurkela, T. (2012). Alder rust, *Melampsoridium hiratsukanum* Ito, identified from Wales, UK and British Columbia, Canada. *Forest Pathol.* 42, 348–350. doi: 10.1111/j.1439-0329.2012.00761.x

Hiratsuka, N., Sato, S., Katsuya, K., Kakishima, M., Hiratsuka, Y., Kaneko, S., et al. (1992). "*Melampsoridium* Klebahn 1899," in *The Rust Flora of Japan* (Ibaraki, Japan: Sukuba Shuppankai Takezono).

Huelsenbeck, J. P., and Ronquist, F. (2001). MRBAYES: Bayesian inference of phylogenetic trees. *Bioinformatics* 17, 754–755. doi: 10.1093/bioinformatics/17.8.754

Kaneko, S., and Hiratsuka, N. (1981). Classification of the *Melampsoridium* species based on the position of urediniospore germ pores. *Trans. Mycol. Soc. Japan* 22, 463–473.

Kaneko, S., and Hiratsuka, N. (1983). A new species of *Melampsoridium* on *Carpinus* and *Ostrya*. *Mycotaxon* 18, 1–4.

Kearse, M., Moir, R., Wilson, A., Stones-Havas, S., Cheung, M., Sturrock, S., et al. (2012). Geneious Basic: An integrated and extendable desktop software platform for the organization and analysis of sequence data. *Bioinformatics* 28, 1647–1649. doi: 10.1093/bioinformatics/bts199

Kurkela, T., Hanso, M., and Hantula, J. (1999). Differentiating characteristics between *melampsoridium* rusts infecting birch and alder leaves. *Mycologia* 91, 987–992. doi: 10.1080/00275514.1999.12061108

Liang, Y.-M., Tian, C.-M., and Kakishima, M. (2006). Phylogenetic relationships on 14 morphologically similar species of *Pucciniastrum* in Japan based on rDNA sequence data. *Mycoscience* 47, 137–144. doi: 10.1007/S10267-006-0284-X

Mamet, S. D., Brown, C. D., Trant, A. J., and Laroque, C. P. (2019). Shifting global *Larix* distributions: Northern expansion and southern retraction as species respond to changing climate. *J. Biogeogr.* 46, 30–44. doi: 10.1111/jbi.13465

McKenzie, E. H. C., Padamsee, M., and Dick, M. (2013). First report of rust on Alnus in New Zealand is *Melampsoridium betulinum*, not *M. hiratsukanum*. *Plant Pathol. Quarant.* 3, 59–65. doi: 10.5943/ppq/3/2/1

Nesom, G., Briggs, R., and Moore, L. (2003). "American hornbeam," in *Plant Fact Sheet/Guide Coordination* 2.

Pethybridge, S. J., and Nelson, S. C. (2015). Leaf doctor: a new portable application for quantifying plant disease severity. *Plant Dis.* 99, 1310–1316. doi: 10.1094/PDIS-03-15-0319-RE

R Core Team (2023). *R: A Language and Environment for Statistical Computing*. Vienna: R Foundation for Statistical Computing. Available online at: https://www.R-project.org

Stamatakis, A. (2014). RAxML version 8: a tool for phylogenetic analysis and post-analysis of large phylogenies. *Bioinformatics* 30, 1312–1313. doi: 10.1093/bioinformatics/btu033

Vilgalys, R., and Hester, M. (1990). Rapid genetic identification and mapping of enzymatically amplified ribosomal DNA from several *Cryptococcus* species. *J. Bacteriol.* 172, 4238–4246. doi: 10.1128/jb.172.8.4238-4246.1990

White, T. J., Bruns, T., Lee, S., and Taylor, J. (1990). "Amplification and direct sequencing of fungal ribosomal RNA genes for phylogenetics," in *PCR Protocols* (Elsevier) 315–322. doi: 10.1016/B978-0-12-372180-8.50042-1

frontiers | Frontiers in Forests and Global Change

TYPE Original Research
PUBLISHED 22 September 2023
DOI 10.3389/ffgc.2023.1239835

OPEN ACCESS

EDITED BY
Juan A. Martin,
Polytechnic University of Madrid, Spain

REVIEWED BY
Frank H. Koch,
Forest Service (USDA), United States
Johanna Witzell,
Linnaeus University, Sweden

*CORRESPONDENCE
Isabel Alvarez Munck
✉ isabel.munck@usda.gov

†These authors have contributed equally to this work and share first authorship

RECEIVED 14 June 2023
ACCEPTED 08 September 2023
PUBLISHED 22 September 2023

CITATION
Munck IA, Yamasaki M and Janelle J (2023) Silvicultural treatments improve pest and disease conditions of white pine (*Pinus strobus*) residual trees and regeneration.
Front. For. Glob. Change 6:1239835.
doi: 10.3389/ffgc.2023.1239835

Silvicultural treatments improve pest and disease conditions of white pine (*Pinus strobus*) residual trees and regeneration

Isabel Alvarez Munck[1*†], Mariko Yamasaki[2†] and Jon Janelle[1,2]

[1]Forest Health Protection, State, Private, and Tribal Forestry, USDA Forest Service, Durham, NH, United States, [2]Northern Research Station, USDA Forest Service, Durham, NH, United States

Managing multiple forest insect pests and diseases is challenging. For example, in eastern white pine (*Pinus strobus*) stands whereas partial shading and high seedling density is encouraged to reduce damage by white pine blister rust (*Cronartium ribicola*) and white pine weevil (*Pissodes strobi*), dense conditions in the understory may increase damage by foliar diseases such as brown spot needle blight (*Lecanosticta acicola*) and Caliciopsis canker (*Caliciopsis pinea*). We evaluated the effect of silvicultural treatments, shelterwoods (residual basal area < 18 m^2 ha^{-1}), low density thinnings (residual basal area ≤ 14 m^2 ha^{-1}), patch cuts (1.2 ha openings), and untreated controls on damage by these insect pest and diseases in residual overstory trees and regeneration. Shelterwoods and low density thinnings provided a good balance of some shading and reduced stem density, which resulted in less weevil damage and foliar disease severity. Crown condition and quality of regeneration was better in all treatments compared to unmanaged controls. Shelterwoods, low density thinnings and patch cuts have the added benefit on increasing seral habitat, resulting in greater songbird diversity.

KEYWORDS

forest management, invasive forest pathogens, host density, white pine weevil, forest diseases

1. Introduction

Eastern white pine (*Pinus strobus*) is an ecologically and commercially important species in Eastern North America (Costanza et al., 2018). For example, more than 150 vertebrate wildlife species use white pine stands for habitat in Eastern USA (Yamasaki, 2003; DeGraaf et al., 2006; Leak et al., 2020). White pine stands are maintained with silvicultural treatments such as shelterwoods, crown thinnings, or patch cuts (Lancaster and Leak, 1978; Seymour, 2007; Ostry et al., 2010; Leak and Yamasaki, 2013). Shelterwoods are a series of forest cuttings to remove overstory trees and promote seedling establishment by scarifying the soil and providing partial shade before the final and complete removal of the overstory (Table 1; Figure 1) (Lancaster and Leak, 1978). Thinnings are like shelterwoods because overstory trees are removed. However, the objective of a thinning is to increase growth of residual trees, whereas the objective of a shelterwood is to regenerate the stand. Patch cuts are small clearcuts where the overstory is completely removed in 1.2 ha (Table 1; Figure 1). These silvicultural treatments also create ephemeral early successional habitat needed by some bird species (Costello et al., 2000; Thompson and DeGraaf, 2001; DeGraaf and Yamasaki, 2003; Yamasaki et al., 2014).

10.3389/ffgc.2023.1239835

TABLE 1 Description of study sites and silvicultural treatments.

Site	Treatment (no. of stands)	Stand size (ha)	Time of treatment	Latitude	Longitude	Tree species present other than eastern white pine (*Pinus strobus*)
Massabesic Experimental Forest Northern Unit, Lyman, Maine	Patch cut-1.2 ha opening (3)	1.2	2007	43.5674	−70.6391	*Acer rubrum, Quercus rubra, Q. alba*
	Low-medium thinning to basal area of 14 m^2 ha^{-1} (2)	6–11	2007	43.5599	−70.6264	*A. rubrum, Picea rubens, Pinus resinosa, Q. rubra*
	Low density thinning to 7 m^2 ha^{-1} (2)	6–11	2007	43.5595	−70.6321	*Abies balsamea, Betula* spp., *Q. vetulina*
	Shelterwood-residual basal area 18 m^2 ha^{-1} (1)	8	2007	43.5679	−70.6438	*A. rubrum, Fagus grandifolia, Q. rubra*
	No treatment-control (1)	10	N/A	43.5627	−70.6318	*A. rubrum, B. populifolia, Prunus serotina, Q. rubra, Q. alba*
Bear Brook State Park, Allentown, New Hampshire	Shelterwood-residual basal area 18 m^2 ha^{-1} (2)	10–23	2009–2011	43.135	−71.3379	*F. grandifolia, B. populifolia, Q. alba*
	No treatment-control (1)	>10	N/A	43.1305	−71.3355	*A. rubrum, F. grandifolia, Q. rubra, Tsuga canadensis*

FIGURE 1
Silvicultural treatments: **(A)** top left patch cut (1.2 ha opening) at the Massabesic Experimental Forest in Lyman, Maine, **(B)** bottom left shelterwood, and **(C)** shaded overstory conditions in an untreated control in Bear Brook State Park, Allentown, New Hampshire.

White pine is also commercially valuable for timber products and aesthetic values for recreational purposes, providing billions of dollars in revenue to local economies (Costanza et al., 2018). However, it is susceptible to a variety of pathogen and insect pests which include, but are not limited to, white pine weevil (*Pissodes strobi*), white pine blister rust (WPBR, *Cronartium ribicola*), Caliciopsis canker (*Caliciopsis pinea*), and foliar diseases such as needle casts and brown spot needle blight (*Lecanosticta acicola*) (Costanza et al., 2018). White pine weevil is a native insect pest to North America, where it damages *Picea* and *Pinus* species by killing the terminal leader, resulting in multi-stemmed growth form and serious lumber defects (Major et al., 2009; Ostry et al., 2010). Vigorously growing trees in full sunlight are more susceptible to damage compared to trees growing in partial shade because weevils attack succulent shoots with thicker bark produced in open conditions (Hamid et al., 1995). In addition, more open conditions increase light and temperature which stimulate the weevils (Hamid et al., 1995). White pine blister rust (WPBR) is lethal to five needle pines in North America and other parts of the world where it has been introduced (Kim et al., 2010). Partial shade and dense stands are also recommended for WPBR management because these conditions lead to self-pruning of lower branches, which are infection courts for the causal agent *Cronartium ribicola* (Ostry et al., 2010). A two-cut shelterwood is one of the most frequently recommended regeneration methods to avoid weevil and WPBR damage (Lancaster and Leak, 1978; Ostry et al., 2010). The first cut coincides with an abundant seed year removing 40%–60% of the overstory. Abundant seed crops (~4,429 thousand seed per hectare) may occur every three to five years, sometimes seven years (Leak et al., 2020). The second cut takes place 5–10 years later when the seedlings are growing rapidly (Lancaster and Leak, 1978).

Prior to 2010, eastern white pine was managed to reduce losses from white pine blister rust and weevil (Lancaster and Leak, 1978; Ostry et al., 2010). Since then, other native pests and diseases such as brown spot needle blight, Caliciopsis canker, and eastern white pine bast scale have caused unprecedented damage (Mech et al., 2013; Broders et al., 2015; Munck et al., 2015; Schulz et al., 2018a,b; Wyka et al., 2018; Costanza et al., 2019; Cram and Fraedrich, 2022). Although the impacts of silvicultural treatments on residual trees in stands damaged by these diseases have been evaluated (McIntire et al., 2018a,b; Costanza et al., 2019, 2020), the impact of these pests and diseases to regeneration following silvicultural treatments is less understood. For example, reducing stand density by thinning improves residual tree growth and symptom severity in stands affected by Caliciopsis canker and foliar diseases (McIntire et al., 2018a; Costanza et al., 2020). Partial shading and high seedling density recommended to control WPBR and weevil damage (Ostry et al., 2010) may increase humidity in the understory, creating conditions favorable to the reproduction and dispersal of foliar and canker fungal pathogens. In addition, inoculum from overstory trees may exacerbate foliar disease severity of understory seedlings (Wyka et al., 2018). Consequently, our objectives were to evaluate the incidence and severity of insect pests and diseases in white pine stands subjected to the following silvicultural treatments: low density thinnings, patch cuts, shelterwoods, and unmanaged or control stands. Understanding the effects of frequently recommended and implemented silvicultural treatments on insect pest and disease incidence and severity is important to maintain valuable white pine forests.

2. Methods

2.1. Study sites and silvicultural treatments

We evaluated the condition of eastern white pine overstory trees and regeneration in stands under different silvicultural regimes at the Northern Unit of the Massabesic Experimental Forest (MEF) in Lyman, Maine, and Bear Brook State Park (BBSP) in Allenstown, New Hampshire (Table 1). In both sites, white pine stands grow in excessively drained glacial outwash soils where soil moisture is too limited for favorable hardwood growth. These two sites, 90 km apart, are abundantly forested with white pine established in 1940s resulting from natural (BBSP) and artificial regeneration (MEF) methods following agricultural abandonment, fire (MEF), or a hurricane (BBSP). Artificial regeneration involved planting and early removal of hardwoods. At the MEF, patch cuts, a shelterwood, and low-density thinning examples cut in 2007–2008 exist on the Northern unit embedded in a forested landscape matrix created following the 1947 fires. The treatments were accomplished through a timber sale administered by the White Mountain National Forest in the fall of 2007 and 2008 before snow fall when the soil was exposed. White pine regeneration (seedlings and saplings) was achieved by timing harvests coinciding with good white pine seed years and heavy soil scarification from harvesting activities. For example, at the MEF the logging contractor whole-tree harvested the sale area using a tracked feller buncher to drop the trees; and rubber-tired skidder to collect the cut stems and haul them to the landing for processing into logs, pulpwood, and chip products. This practice scarifies the ground surface sufficiently to bury white pine seed that germinates the following spring. Other practices that minimally scarify the ground surface leave white pine seed on the ground exposed to seed predation by foraging birds, squirrels, and small mammals. Experimental forests, such as the MEF, provide the unique infrastructure to conduct long term research where results can be demonstrated to cooperators and stakeholders (Wells et al., 2009).

We visually inspected the health of white pines in stands under different silvicultural regimes: shelterwood (residual basal area of 18 m^2 ha^{-1}), patches (1.2 ha openings), low density thinnings (residual basal area of 7 and 14 m^2 ha^{-1}, respectively), and no treatment control (>2 ha) (Leak and Lamson, 1999; Leak and Yamasaki, 2013). Patch cuts and low density thinnings were replicated twice at the MEF, but the shelterwood was not. Thus, two additional shelterwoods and an untreated control stand at BBSP were included in the study (Table 1; Figure 1). Lastly, the presence of foliar pathogens, Caliciopsis canker, white pine weevil and blister rust has been documented in both sites allowing us to quantify the effects of silvicultural treatments on damage caused by these agents (Table 1; Figures 1, 2) [McConkey and Smith, 1958; Munck et al., 2016; Wyka et al., 2018; Leak et al., 2020; State of New Hampshire Department of Natural and Cultural Resources (NHDNCR), 2021].

2.2. Field measurements

At least two stands per treatment were sampled during the summer of 2020. At each stand, three circular fixed area plots were established per stand with methods like those described by Heuss et al. (2019). To determine plot placement, a map was created using ArcGIS by overlaying a 50 m x 50 m grid on the polygon delineating the stand. A random sampling point within the grid was selected representing the center of the first plot and subsequent plots were selected using the map so that they were at least 50 m apart and well within the stand. At each plot, all trees (≥10 cm dbh = diameter at breast height 1.37 m) within a circular plot with a 10 m radius (314 m^2) were evaluated. Tree species and dbh were recorded for each tree. Additionally, for every white pine (*P. strobus*) the following variables were noted: live crown ratio, crown density, white pine foliar disease rating, incidence (presence) of Caliciopsis canker (fruiting bodies in regeneration or resinosis in trees), WPBR, white pine weevil, and other insects or diseases (Table 2). Tree crown condition is an important indicator of forest health because trees with vigorous crown have more photosynthetic capacity to grow (Randolph et al., 2010). Crown density measures the amount of sunlight blocked by all biomass produced by the tree (Randolph et al., 2010). Live crown ratio (LCR) is the ratio of crown length to total height of the tree (USDA Forest Service Forest inventory and analyses National Program, 2011).

To evaluate regeneration, two subplots 5 m and at 120 or 240 degrees from plot center relative to north, respectively. At each subplot, canopy cover was measured with the CanopyApp (UNH Earth Systems Research Center), and the total number of seedlings and saplings were tallied within a circular plot with a 2.5 m radius (20 m^2). The following additional data was collected for the 10 white pine saplings (2.5 cm > dbh < 10 cm) or seedlings (dbh < 2.5 cm and height > 30 cm) closest to subplot center: dbh, height, live crown ratio (LCR), crown density, white pine foliar disease (WPND) rating, incidence of Caliciopsis canker, WPBR, weevil, and other insects or diseases (Table 2; Figure 2). White pine foliar diseases were assessed on a rating scale from 0 to 3 representing the proportion of the crown

TABLE 2 Criteria used to evaluate health of eastern white pine trees (dbh > 10 cm) and regeneration (dbh < 10 cm and height > 30 cm).

Variable	Criteria	Reference
Live crown ratio	The ratio of crown length to total height of the tree (0–100% in 10% increments)	USDA Forest Service Forest inventory and analyses National Program, 2011
Crown density	Amount of sunlight blocked by all biomass produced by the tree (0–100% in 5% increments)	USDA Forest Service Forest inventory and analyses National Program, 2011
White pine foliar disease rating	0: crown not affected by defoliation or chlorosis 1: <1/3 crown affected 2: 1/3 to 2/3 of crown affected 3: >2/3 of crown affected	Broders et al. (2015) Costanza et al. (2018) Livingston et al. (2019)
Caliciopsis canker incidence	Presence (1) or absence (0) of sunken lesions, cankers, resinosis throughout the bole, or black 1–3 mm fruiting bodies in branch whorls	Costanza et al. (2018) Livingston et al. (2019)
White pine blister rust incidence	Presence (1) or absence (0) of resinosis from a single source, spindle shaped cankers, aecial scars, flagging, or bark and crown discoloration	Livingston et al. (2019)
White pine weevil incidence	Presence (1) or absence (0) of death of first leader, discoloration of leader and first whorl, resin droplets from punctures, loss of apical dominance and multi-stemmed pines	Hamid et al. (1995) Livingston et al. (2019)

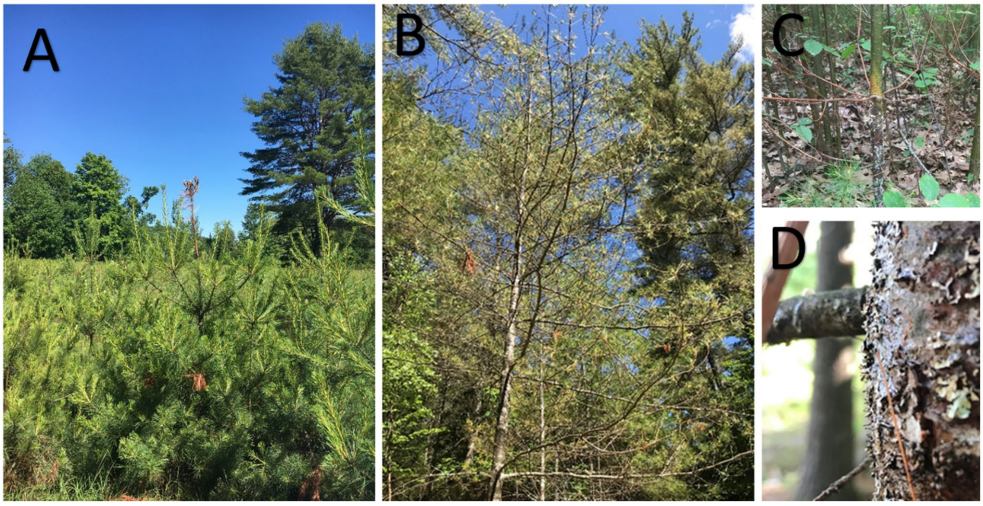

FIGURE 2
Eastern white pine regeneration in southern Maine and New Hampshire with signs and symptoms of insects and **(A)** white pine weevil (*Pissodes strobi*), **(B)** chlorosis and defoliation caused by *Lecanosticta acicola*, **(C)** white pine blister rust stem canker caused by *Cronartium ribicola*, and **(D)** fruiting bodies of *Caliciopsis pinea* protruding from a branch whorl.

in thirds affected (Table 2) (Broders et al., 2015). Symptomatic needles were collected from each stand to confirm presence of foliar pathogens. Needles were stored at 4°C until they were they were incubated in a moist chamber overnight and fruiting structures were inspected under a light microscope (Broders et al., 2015). Only *Lecanosticta acicola* pycnidia and conidia were observed from samples collected at each site.

2.3. Statistical analyses

One-way analyses of variance (ANOVA) were performed using the GLIMMIX procedure (Statistical Analyses Software v. 9.4, SAS Institute Inc., Cary, NC) to investigate main effects of silvicultural treatments on response variables associated with tree condition listed in the first column of Tables 2, 3: dbh (cm), height of regeneration, live crown ratio, crown density, disease severity of foliar pathogens (WPND severity), and incidence of other diseases and weevil damage. When main effects of treatment were significant ($\alpha = 0.05$), a Tukey–Kramer test was used to identify differences between means.

3. Results

We evaluated and measured eastern white pine trees (262) and regeneration (>500 seedlings and saplings) in 36 plots, three per stand, for 12 stands, at least 2 stands per silvicultural treatment (Table 1). Other tree species present in our plots included: *Abies balsamea, Acer rubrum, Betula* spp., *Fagus grandifolia, Prunus serotina, Picea rubens, Pinus resinosa, Quercus rubra, Q. alba*, and *Tsuga canadensis*. Of these, *A. rubrum* and *Q. rubra* were most common (Table 1).

10.3389/ffgc.2023.1239835

TABLE 3 Eastern white pine (*Pinus strobus*) overstory response variables in relation to silvicultural treatments in Maine and New Hampshire.

Response variables	Silvicultural treatments								
	No treatment-control[a]	Patch cut 1.2 ha	Shelterwood 18 m^2 ha^{-1}	Thinning to 7 m^2 ha^{-1}	Thinning to 14 m^2 ha^{-1}	Num DF	N	*F* Value	Pr > *F*
Canopy cover	59 ± 9a	25 ± 7b	40 ± 7ab	42 ± 9ab	69 ± 9a	4	31	4.69	**0.005**
Percentage of EWP stems	61 ± 11a	0 ± 9b	70 ± 9a	72 ± 11a	49 ± 11a	4	31	10.65	**<0.0001**
Stem density (trees ha^{-1})	631 ± 35a	31 ± 29c	177 ± 29b	69 ± 35bc	133 ± 35bc	4	31	50	**<0.0001**
DBH (cm)	33 ± 4a	N/A	33 ± 4a	35 ± 4a	40 ± 5a	3	21	0.51	0.679
Live crown ratio (%)	24 ± 7b	N/A	53 ± 6a	36 ± 7ab	44 ± 8ab	3	21	4.03	**0.021**
Crown density (%)	33 ± 13b	N/A	75 ± 10a	81 ± 13a	81 ± 13a	3	21	10.03	**<0.001**
Foliar disease severity (%)	47 ± 8a	N/A	10 ± 7b	14 ± 8b	25 ± 10ab	3	21	4.68	**0.012**
Resinosis incidence	17 ± 8a	N/A	2 ± 6a	24 ± 8a	5 ± 6a	3	23	1.95	0.149

[a]Means ± standard errors (S.E.) of plots in each treatment. Values followed by the same letter within the same row are not significantly different (α = 0.05).
Effect of response variable in bold are statistically significant α<0.05.

Silvicultural treatments in white pine stands had the intended effects in overstory white pines. These were completely removed from patch cuts, and partially removed from other treatments, thus, stem density was more than four times greater for untreated controls compared to the treated stands (Table 3). Overall, crown condition improved in treated stands compared to controls. For example, crown density of white pines in untreated control stands was significantly less (33%) compared to that in treated stands (>75%) ($p < 0.001$). Conversely, severity of foliar pathogens was greater for trees in untreated stands (47% crown affected) compared to that in treated stands (<25% crown affected) ($p = 0.012$). Resinosis, a symptom of WPBR, Caliciopsis canker and other insects and diseases, was low in all treatments (<17% trees affected) and not statistically significant among treatments.

Compared to untreated control stands, treated stands had more and generally larger regeneration (dbh and height) with better crown condition (LCR, crown density, and WPND severity) (Table 4). The untreated controls produced in average 3,042 ha^{-1} white pine saplings and seedlings compared to >16,000 ha^{-1} saplings and seedlings for treated stands. The dbh and height of seedlings and saplings in untreated control stands was 0.6 cm and 0.9 m, respectively compared to dbh > 1 cm and height > 1.8 m in treated stands (Table 4). The main effect of some treatments was only marginally (dbh, $p = 0.08$) or not statistically significant (height, LCR, and crown density) for least square means comparisons among treatments. However, most treatment values were significantly different than the control value in single pair-wise comparisons (α = 0.05) (Table 4).

As expected, patch cuts and thinning to 7 m^2 ha^{-1}, the treatments with least canopy cover (25 and 42%, respectively) or shade, had the greatest proportion of white pine seedlings with weevil damage (27 and 34%, respectively) compared to untreated control stands where regeneration did not have any weevil damage due to heavy shading (Tables 3, 4). Despite the weevil damaged regeneration, patch cuts in this study produced in average > 10,000 white pine seedlings ha^{-1} without weevil or other pest or insect damage (Figure 3). Similarly, despite more damage from Caliciopsis canker (14%) in thinned stands compared to untreated controls (0%), because regeneration was so abundant in thinned stands (>25,000 seedlings and saplings h^{-1}) compared to untreated stands (3,042 seedlings and saplings h^{-1}), more undamaged regeneration was present in treated stands (Figure 3). White pine blister rust incidence was <6% and not statistically significant among treatments.

4. Discussion

Host density may facilitate or slow down the development of disease epidemics or pest outbreaks (Asaro et al., 2023) and understanding effects of host density is therefore critical to management of resilient forests. Shelterwoods and low-density thinnings are the most prescribed silvicultural treatments for management of eastern white pine insect pests and diseases (Ostry et al., 2010; Livingston et al., 2019). These treatments can reduce disease incidence and severity at the stand level by improving condition of residual trees and removal of the weakest trees during harvesting operations (McIntire et al., 2018a; Costanza et al., 2020). Harvesting operations to implement these treatments can result in abundant white pine regeneration (Leak and Yamasaki, 2013).

Compared to overstory trees, the relationship between high stem density in regeneration and foliar diseases or Caliciopsis canker is not as well understood. In a previous study, stem density was associated with greater Caliciopsis canker disease severity in white pine overstory trees and regeneration (Munck et al., 2016). Similarly, in this study the thinnings to 14 m^2 ha^{-1} had the greatest Caliciopsis canker incidence and the most abundant regeneration. In this study, both overstory and understory white pines across all silvicultural treatments exhibited less foliar disease severity compared to untreated controls. This finding is consistent with a study by McIntire et al. (2018a) that evaluated crown condition of overstory trees before and after thinning stands.

Foresters and land managers are reluctant to implement clear cuts and patch cuts because white pine weevil preferentially attacks regeneration growing in open conditions. Shading provided by residual trees in shelterwoods reduces white pine weevil damage in the understory (Ostry et al., 2010). In this study, patch cuts and low density thinnings had the least canopy cover and consequently, greatest incidence of weevil damage (Tables 3, 4). Both these treatments, however, yielded abundant white pine regeneration with >10,000 seedlings and sampling per hectare. Defective regeneration could be removed in precommercial thinnings when saplings are 6 m tall to a recommended stem density of 490–740 stem per hectare (Livingston et al., 2019), thus plenty of healthy stems would be available in treated stands evaluated in this study. These low-density treatments have the added benefit of creating early successional habitat preferred by some songbirds.

TABLE 4 Eastern white pine (*Pinus strobus*) regeneration response variables in relation to silvicultural treatments in Maine and New Hampshire.

Response variables	Means for silvicultural treatments (± SE)								
	No treatment-control[a]	Patch cut 1.2 ha	Shelterwood 18 m^2 ha^{-1}	Thinning to 7 m^2 ha^{-1}	Thinning to 14 m^2 ha^{-1}	Num DF	*N*	*F* Value	Pr > *F*
Stem density (seedlings & saplings ha^{-1})	3,042 ± 5,314b	16,028 ± 4,339ab	23,083 ± 4,339a	25,000 ± 5,314a	32,667 ± 5,314a	4	30	4.52	**<0.01**
DBH (cm)	0 ± 0.62a	1.97 ± 0.29a*	1.31 ± 0.29a*	1.38 ± 0.36a*	1.06 ± 0.36a*	4	27	2.36	*0.08*
Height (m)	0.9 ± 0.5a	2.1 ± 0.2a*	1.8 ± 0.2a	2 ± 0.3a*	1.9 ± 0.3a*	4	27	1.16	0.35
Live crown ratio (%)	58 ± 11a	79 ± 5a*	65 ± 5a	65 ± 8a*	69 ± 8a*	4	27	1.5	0.23
Crown density (%)	28 ± 13a	59 ± 6a*	56 ± 6a	65 ± 15a*	52 ± 11a*	4	27	2.09	0.11
Foliar disease severity (%)	46 ± 7a	6 ± 5b	6 ± 5b	5 ± 6b	10 ± 6b	4	27	3.84	**0.01**
Weevil incidence[b]	0 ± 10b	27 ± 5ab	12 ± 5b	34 ± 6a	20 ± 6ab	4	27	3.47	**0.02**
Caliciopsis incidence	0 ± 6a	8 ± 3a	4 ± 3a	4 ± 3a	14 ± 3a*	4	27	1.79	1.6
White pine blister rust incidence	0 ± 4	1 ± 2	2 ± 2	6 ± 2	2 ± 2	4	27	0.9	0.48

[a]Means ± standard errors (S.E.) of plots in each treatment. Values followed by the same letter within the same row are not significantly different (α = 0.05). Values followed by asterisk (*) within a row are statistically different to the control in single pairwise comparison using the TTEST in SAS.
[b]Incidence is expressed as the percentage of damaged eastern white pine (*Pinus strobus*) regeneration (seedlings and saplings).
Effect of response variable in bold are statistically significant α<0.05.

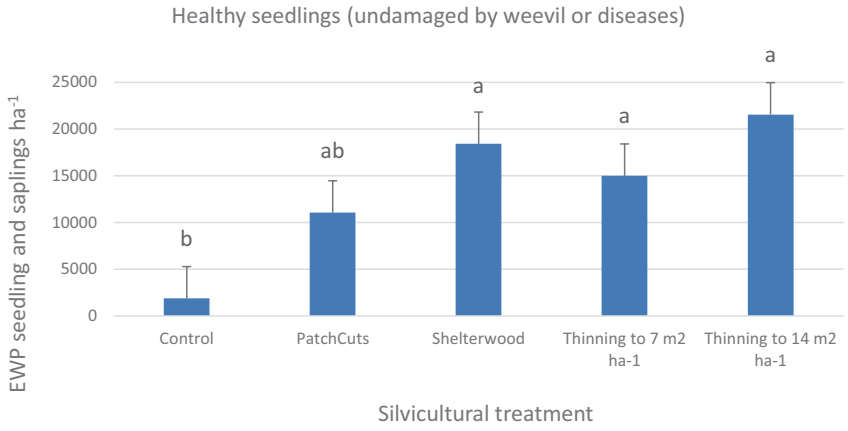

FIGURE 3
Density of undamaged eastern white pine regeneration in different treatments. Bars represent the mean and standard error for plots within each treatment. Values with the same letter are not statistically different (α = 0.05).

In Eastern USA, forested land is mostly privately owned. Obtaining support for silvicultural treatments to improve forest health is challenging because private landowners are not solely interested in commercial value of their trees. However, many are interested in wildlife management. Following treatment, shelterwoods and patch cuts produce greater average species richness of birds than unmanaged forest (Goodale et al., 2009; Duguid et al., 2016). These silvicultural treatments create early successional habitat needed by birds using young forests (Costello et al., 2000; Thompson and DeGraaf, 2001; DeGraaf and Yamasaki, 2003; Yamasaki et al., 2014). Thus, shelterwood and patch cut treatments may both increase biodiversity and improve forest production and regeneration.

In conclusion, silvicultural treatments that reduced stem density in the overstory and scarified the soil during harvesting operations resulted in better conditions of residual trees and plenty of healthy white pine regeneration compared to unmanaged stands. Our study emphasizes the importance of considering a realistic spectrum of natural enemies when designing silvicultural operations. Our findings are consistent with management current recommendations for white pine (Livingston et al., 2019; Leak et al., 2020). Given the economic and ecological value of eastern white pine, the effects of silvicultural treatments on insect and pest conditions merit further study. Results could vary in locations where insect pest and disease pressures are greater. This study was conducted in Northeastern USA, but the insect pest and diseases we evaluated have worldwide distribution. For example, white pine blister rust damages pine in Asia, Europe and North America (Geils et al., 2010). *Lecanosticta acicola* has a global distribution and is a threat to plantations and naturally regenerated stands (van der Nest et al., 2019; Tubby et al., 2023). Pathogenic *Caliciopsis* spp. damage conifer species in Europe, North America, and Eucalyptus spp. in Australia

(Pascoe et al., 2018; Migliorini et al., 2020). Consequently, our findings could be useful to the management of other patho-systems.

Data availability statement

The raw data supporting the conclusions of this article will be made available by the authors, without undue reservation.

Author contributions

MY and JJ designed and implemented silvicultural treatments, respectively. IM and JJ conceived and designed the data collection. IM analyzed the data and prepared the manuscript. All authors contributed to the article and approved the submitted version.

Funding

This project was funded by the USDA Forest Service.

Acknowledgments

We thank the USDA Northern Research Station and State of New Hampshire Department of Natural and Cultural Resources (NHDNCR) for access to the Massabesic Experimental Forest and Bear Brook State Park, respectively. We are thankful for field assistance and hard work from Tyler Brodie, Owen Price, River Mathieu and Kevin Dodds. We are grateful for the assistance of NHDNCR staff specially William Guinn, Kyle Lombard, Billy Kunelius, Scott Rolfe, and Robert Spoerl. We greatly appreciate guidance from Bill Leak, Ken Desmarais, and Rebecca Lilja (USFS), and Mark Ducey (UNH). Thank you for the comments and edits of two reviewers and the editor that have improved the quality of the manuscript.

Conflict of interest

The authors declare that the research was conducted in the absence of any commercial or financial relationships that could be construed as a potential conflict of interest.

Publisher's note

All claims expressed in this article are solely those of the authors and do not necessarily represent those of their affiliated organizations, or those of the publisher, the editors and the reviewers. Any product that may be evaluated in this article, or claim that may be made by its manufacturer, is not guaranteed or endorsed by the publisher.

References

Asaro, C., Koch, F. H., and Potter, K. M. (2023). Denser forests across the USA experience more damage from insects and pathogens. *Sci. Rep.* 13:3666. doi: 10.1038/s41598-023-30675-z

Broders, K., Munck, I., Wyka, S., Iriarte, G., and Beaudoin, E. (2015). Characterization of fungal pathogens associated with white pine needle damage (WPND) in northeastern North America. *Forests* 6, 4088–4104. doi: 10.3390/f6114088

Costanza, K. K. L., Crandall, M. S., Rice, R. W., Livingston, W. H., Munck, I. A., and Lombard, K. (2019). Economic implications of a native tree disease, Caliciopsis canker, on the white pine (*Pinus strobus*) lumber industry in the northeastern United States. *Can. J. For. Res.* 49, 521–530. doi: 10.1139/cjfr-2018-0380

Costanza, K. K. L., Livingston, W. H., Fraver, S., and Munck, I. A. (2020). Dendrochronological analyses and whole-tree dissections reveal Caliciopsis canker (Caliciopsis pinea) damage associated with the declining growth and climatic stressors of eastern white pine (*Pinus strobus*). *Forests* 11:347. doi: 10.3390/f11030347

Costanza, K. K. L., Whitney, T. D., McIntire, C. D., Livingston, W. H., and Gandhi, K. J. K. (2018). A synthesis of emerging health issues of eastern white pine (*Pinus strobus*) in eastern North America. *For. Ecol. Manag.* 423, 3–17. doi: 10.1016/j.foreco.2018.02.049

Costello, C. A., Yamasaki, M., Pekins, P. J., Leak, W. B., and Neefus, C. D. (2000). Songbird response to group selection harvests and clearcuts in a New Hampshire northern hardwood forest. *For. Ecol. Manag.* 127, 41–54. doi: 10.1016/S0378-1127(99)00131-0

Cram, M. M., and Fraedrich, S. W. (2022). Effects of *Caliciopsis pinea* inoculation with and without wounding on *Pinus strobus*. *For. Pathol.* 52:e12733. doi: 10.1111/efp.12733

DeGraaf, R. M., and Yamasaki, M. (2003). Options for managing early-successional forest and shrubland habits in the northeastern United States. *For. Ecol. Manag.* 185, 179–191. doi: 10.1016/S0378-1127(03)00254-8

DeGraaf, R. M., Yamasaki, M., Leak, W. B., and Lester, A. M. (2006). *Technical guide to Forest wildlife habitat Management in new England*. Burlington, VT: University of Vermont Press. 305 p.

Duguid, M. C., Morrell, E. H., Goodale, E., and Ashton, M. S. (2016). Changes in breeding bird abundance and species composition over a 20-year chronosequence following shelterwood harvest in oak hardwood forests. *For. Ecol. Manag.* 376, 221–230. doi: 10.1016/j.foreco.2016.06.010

Geils, B. W., Hummer, K. E., and Hunt, R. S. (2010). White pines, Ribes, and blister rust: a review and synthesis. *For. Pathol.* 40, 147–185. doi: 10.1111/j.1439-0329.2010.00654.x

Goodale, E., Lalbhai, P., Goodale, U. M., and Ashton, P. M. S. (2009). The relationship between shelterwood cuts and crown thinnings and the abundance and distribution of birds in a southern New England forest. *For. Ecol. Manag.* 258, 314–322. doi: 10.1016/j.foreco.2009.04.020

Hamid, A., O'Dell, T. M., and Katovich, S. (1995). "White pine weevil" in *Forest insect and disease leaflet 21*. ed. USDA Forest Service. (Broomall (PA): U.S. Department of Agriculture, Forest Service. Northern Area State & Private Forestry)

Heuss, M., D'Amato, A. W., and Dodds, K. J. (2019). Northward expansion of southern pine beetle generates significant alterations to forest structure and composition of globally rare *Pinus rigida* forests. *For. Ecol. Manag.* 434, 119–130. doi: 10.1016/j.foreco.2018.12.015

Kim, M.-S., Klopfenstein, N. B., Ota, Y., Lee, S. K., Woo, K.-S., and Kaneko, S. (2010). White pine blister rust in Korea, Japan and other Asian regions: comparisons and implications for North America. *For. Pathol.* 40, 382–401. doi: 10.1111/j.1439-0329.2010.00664.x

Lancaster, K. F., and Leak, W. B. (1978). *A silvicultural guide for white pine in the northeast*. USDA For. Serv. Gen. Tech. Rep. Broomall, PA: USDA Forest Service, Northern Research Station NE-41, –13.

Leak, W. B., and Lamson, N. I. (1999). *Revised white pine stocking guide for managed stands*. Na-TP-01-99. Newtown Square, PA: U.S. Department of Agriculture, Forest Service, Northeastern Area State and Private Forestry, 2.

Leak, W. B., and Yamasaki, M. (2013). *Effects of low-density thinning in a declining white pine stand in Maine*. Res. Note NRS-170. Newtown Square, PA: U.S. Department of Agriculture, Forest Service, Northern Research Station. p.6

Leak, W. B., Yamasaki, M., Bennett, K. P., Desmarais, K., Pohl, P., Costello, C., et al. (2020). *White pine silviculture for timber and wildlife habitat in New England*. University of New Hampshire Cooperative Extension, Durham, NH. 34 p.

Livingston, W. H., Munck, I., Lombard, K., Weimer, J., Bergdahl, A., Kenefic, L. S., et al. (2019). *Field manual for managing eastern white pine health in New England* University of Maine, Maine Agric. And for. Exp. Sta., Orono ME: Misc. pub. 764, 20.

Major, J. E., Mosseler, A., Barsi, D. C., Clouthier, A., and Campbell, M. (2009). Impact of three silvicultural treatments on weevil incidence, growth, phenology, and branch-leveldynamics of *Pinus strobus* from large and small populations. *Can. J. For. Res.* 39, 12–25. doi: 10.1139/X08-153

McConkey, T. W., and Smith, W. E. (1958). *The Massabesic experimental Forest*. Station paper NE-108. Upper Darby, PA: U.S. Department of Agriculture, Forest Service, Northeastern Forest Experiment Station. p 19

McIntire, C. D., Munck, I. A., Ducey, M. J., and Asbjornsen, H. (2018a). Thinning treatments reduce severity of foliar pathogens in eastern white pine. *For. Ecol. Manag.* 423, 106–113. doi: 10.1016/j.foreco.2018.03.032

McIntire, C. D., Munck, I. A., Vadeboncoeur, M. A., Livingston, W. H., and Asbjornsen, H. (2018b). Impacts of white pine needle damage on seasonal litterfall dynamics and wood growth of eastern white pine (*Pinus strobus*) in northern New England. *For. Ecol. Manag.* 423, 27–36. doi: 10.1016/j.foreco.2018.02.034

Mech, A. M., Asaro, C., Cram, M. M., Coyle, D. R., Gullan, P. J., Cook, L. G., et al. (2013). *Matsucoccus macrocicatrices* (Hemiptera: Matsucoccidae): first report, distribution, and association with symptomatic eastern white pine in the southeastern United States. *J. Econ. Entomol.* 106, 2391–2398. doi: 10.1603/EC13251

Migliorini, D., Luchi, N., Pepori, A. L., Pecori, F., Aglietti, C., Maccioni, F., et al. (2020). *Caliciopsis moriondi*, a new species for a fungus long confused with the pine pathogen *C. pinea*. *Mycokeys* 73, 87–108. doi: 10.3897/mycokeys.73.53028

Munck, I., Livingston, W., Lombard, K., Luther, T., Ostrofsky, W., Weimer, J., et al. (2015). Extent and severity of Caliciopsis canker. *An emerging disease of eastern white pine (Pinus strobus L.). Forests* 6, 4360–4373. doi: 10.3390/f6114360

Munck, I. A., Luther, T., Wyka, S., Keirstead, D., McCracken, K., Ostrofsky, W., et al. (2016). Soil and stocking effects on Caliciopsis canker of *Pinus strobus* L. *Forests* 7:269. doi: 10.3390/f7110269

Ostry, M. E., Laflamme, G., and Katovich, S. A. (2010). Silvicultural approaches for management of eastern white pine to minimize impacts of damaging agents. *For. Pathol.* 40, 332–346. doi: 10.1111/j.1439-0329.2010.00661.x

Pascoe, I. G., McGee, P. A., Smith, I. W., Dinh, S. Q., and Edwards, J. (2018). *Caliciopsis pleomorpha* sp. nov. (Ascomycota: Coryneliales) causing a severe canker disease of *Eucalyptus cladocalyx* and other eucalypt species in Australia. *Fungal Syst Evol* 5, 197–281. doi: 10.3114/fuse.2020.05.13

Randolph, K. C., Morin, R. S., and Steinman, J. (2010). *Descriptive statistics of tree crown condition in the northeastern United States*. Gen. Tech. Rep. SRS-124. Asheville, NC: U.S. Department of Agriculture, Forest Service, southern Research Station. 21 p.

Schulz, A. N., Mech, A. M., Asaro, C., Coyle, D. R., Cram, M. M., Lucardi, R. D., et al. (2018a). Assessment of abiotic and biotic factors associated with eastern white pine (*Pinus strobus* L.) dieback in the southern Appalachian Mountains. *For. Ecol. Manag.* 423, 59–69. doi: 10.1016/j.foreco.2018.02.021

Schulz, A. N., Mech, A. M., Cram, M. M., Asaro, C., Coyle, D. R., Lucardi, R. D., et al. (2018b). Association of *Caliciopsis pinea* peck and *Matsucoccus macrocicatrices* Richards with eastern white pine (*Pinus strobus* L.) seedling dieback. *For. Ecol. Manag.* 423, 70–83. doi: 10.1016/j.foreco.2018.03.013

Seymour, R. S. (2007). Low-density management of white pine crop trees: a primer and early research results. *North. J. Appl. For.* 24, 301–306. doi: 10.1093/njaf/24.4.301

State of New Hampshire Department of Natural and Cultural Resources (NHDNCR). (2021). Bear brook State Park management plan. Available at: https://www.nhstateparks.org/getmedia/e2880baa-0ba5-470c-ab30-43a158d2ca42/Bear-Brook-SP_Mgt-Plan-2021_final.pdf (Accessed 11 June, 2023)

Thompson, F. R., and DeGraaf, R. M. (2001). Conservation approaches for woody, early successional communities in the eastern United States. *Wildl. Soc. Bull.* 29, 483–494.

Tubby, K., Adamčikova, K., Adamson, K., Akiba, M., Barnes, I., Boroń, P., et al. (2023). The increasing threat to European forests from the invasive foliar pine pathogen, Lecanosticta acicola. *For Ecol Manage* 536:120847. doi: 10.1016/j.foreco.2023.120847

USDA Forest Service Forest inventory and analyses National Program, (2011). Phase 3 field guide version 5.1. Available at: https://www.fia.fs.usda.gov/library/field-guides-methods-proc/docs/2012/field_guide_p3_5-1_sec23_10_2011.pdf (Accessed August 30, 2023).

van der Nest, A., Wingfield, M. J., Janoušek, J., and Barnes, I. (2019). *Lecanosticta acicola*: a growing threat to expanding global pine forests and plantations. *Molecular Plant Pathol.* 20, 1327–1364. doi: 10.1111/mpp.12853

Wells, G., Hayes, D., Krause, K., Bartuska, A., LeVan-Green, S., Anderson, J., et al. (2009). *Experimental forests and ranges: 100 years of research success stories*. General Technical Report FPL-GTR-182. Madison, WI: USDA-Forest Service, Forest Products Laboratory, 29

Wyka, S. A., McIntire, C. D., Smith, C., Munck, I. A., Rock, B. N., Asbjornsen, H., et al. (2018). Effect of climatic variables on abundance and dispersal of *Lecanosticta acicola* spores and their impact on defoliation on eastern white pine. *Phytopathology* 108, 374–383. doi: 10.1094/PHYTO-02-17-0065-R

Yamasaki, M. (2003). "White pine as wildlife habitat" in *Managing white pine in a new millennium 2003 workshop proceedings, 2003 October 9–10, Hillsborough, NH*. ed. N. H. Durham (University of New Hampshire Cooperative Extension), 33–36.

Yamasaki, M., Costello, C. A., and Leak, W. B. (2014). *Effects of clearcutting, patch cutting and low-density shelterwoods on breeding birds and tree regeneration in New Hampshire northern hardwoods*. USDA For. Serv. Res. Pap. NRS-26. 15.

frontiers | Frontiers in Forests and Global Change

TYPE Original Research
PUBLISHED 09 October 2023
DOI 10.3389/ffgc.2023.1215701

OPEN ACCESS

EDITED BY
Salvatore Moricca,
University of Florence, Italy

REVIEWED BY
Francisco J. Ruiz-Gomez,
University of Cordoba, Spain
Federico Sebastiani,
National Research Council, Italy

*CORRESPONDENCE
Sergio Diez-Hermano
✉ sergio.diez.hermano@uva.es
Julio Javier Diez
✉ JulioJavier.Diez@uva.es

†These authors have contributed equally to this work

RECEIVED 02 May 2023
ACCEPTED 25 September 2023
PUBLISHED 09 October 2023

CITATION
Diez-Hermano S, Poveda J, Niño-Sanchez J, Bocos-Asenjo IT, Peix Á, Martín-Pinto P and Diez JJ (2023) Rhizosphere mycobiome diversity in four declining Mediterranean tree species.
Front. For. Glob. Change 6:1215701.
doi: 10.3389/ffgc.2023.1215701

Rhizosphere mycobiome diversity in four declining Mediterranean tree species

Sergio Diez-Hermano[1]*†, Jorge Poveda[1†], Jonatan Niño-Sanchez[1], Irene Teresa Bocos-Asenjo[1], Álvaro Peix[2,3], Pablo Martín-Pinto[1] and Julio Javier Diez[1]*

[1]Department of Plant Production and Forest Resources, Sustainable Forest Management Research Institute (iuFOR). Higher Technical School of Agricultural Engineering (ETSIIAA), University of Valladolid, Palencia, Spain, [2]Instituto de Recursos Naturales y Agrobiología, IRNASA-CSIC, Salamanca, Spain, [3]Grupo de Interacción Planta-Microorganismo, USAL, Unidad Asociada al CSIC por el IRNASA, Salamanca, Spain

Introduction: Forests in the Mediterranean basin are currently in decline. Their resilience has been eroded as a result of climate change and anthropogenic impacts, making them vulnerable to increasingly frequent episodes of drought, fire and the spread of pests and diseases. The impact of these natural and anthropogenic events on soil biodiversity is of particular concern, as the soil fungal community plays a key role in ecosystem homeostasis.

Objectives and methods: In order to analyse the relationship between soil health status and fungal diversity, soil samples were collected from declining Mediterranean forests of *Castanea sativa* (chestnut), *Quercus ilex* (holm oak), *Quercus suber* (cork oak) and *Quercus pyrenaica* (Pyrenean oak). A metabarcoding study was carried out by sequencing the ITS genomic region.

Results: A total of 674 fungal genera were found. It has not been possible to explain the differences in health status from the fungal genera found exclusively on declining forest soils, as none of them have been described as pathogenic. Healthy chestnut soils were characterized by a high alpha diversity and a higher abundance of the genus *Metarhizium*. No differentially abundant genera were found in any of the other forest species tested. Declining chestnut soils harbored more abundance of ectomycorrhizae and soil saprotrophs than healthy samples. Ectomycorrhizae were the dominant lifestyle in all oak species regardless of health status, whereas arbuscular mycorrhizae were preferentially found in declining cork oak soils.

Discussion: This work highlights the resilience of fungal communities of soil against decline and highlights the need to further investigate its relationship with the forest's ability to cope with the challenges of climate change.

KEYWORDS

global change, forest declines, metabarcoding, biodiversity, forest pathology, *Quercus*, *Castanea*

1. Introduction

Mediterranean forests are characteristic ecosystems of the Mediterranean Basin, but also present in California, South Africa and Chile. These forests are a hot spot of genetic diversity in the European continent, as they harbor 290 tree species, compared to 135 reported in the rest of Europe (Gauquelin et al., 2018). The organisms that make up the Mediterranean forests are usually adapted to very specific climatic factors, such as the existence of a marked seasonality

characterized by long periods of summer drought, and great variability in the total annual rainfall. In addition, Mediterranean forests have been subjected for millennia to anthropogenic impacts, mainly fragmentation due to land use change toward agriculture and grazing, overexploitation to obtain goods and services and, more recently, abandonment of their use (Fady et al., 2022). These characteristics have confirmed that Mediterranean forests are as vulnerable to management policies as they are to climate change (Morán-Ordóñez et al., 2020).

Some of the main tree species found in Mediterranean forests are chestnut, cork oaks, holm oaks and Pyrenean oaks. Chestnut (*Castanea sativa* Mill.) covers more than 2.5 million hectares in the Mediterranean Basin, being the only species of the genus native to this region. Chestnut has been widely cultivated as a monoculture for centuries and as a source of timber and fruit, although in recent decades it has been progressively felled (Garfì et al., 2022). Cork oak (*Quercus suber* L.) spreads over between 1.7 and 2.7 million ha of the Mediterranean Basin and has been cultivated for 3,000 years for the production of bark, representing the second most important marketable non-timber forest product (Gauquelin et al., 2018). Holm oak (*Quercus ilex* L.) forests comprise 4% of the forests of the Mediterranean Basin, being fully adapted to a wide range of soil and climatic conditions. In spite of the continuous anthropic exploitation of holm oaks during several centuries, the reduction in the use of their wood as fuel in the last 50 years is turning holm oak forests into high forests (Camponi et al., 2023). Pyrenean oak (*Quercus pyrenaica* Willd.) is found only in France, Spain, Portugal and Morocco. Pyrenean oak forests have historically been exploited by man for timber, and still are to this day, and constitute the main ecosystem of the Mediterranean Basin in diversity of hoverfly species (Perez-Luque et al., 2020; Martín-Pinto et al., 2023).

At present, the Mediterranean forest is in a situation of regression and dieback in several areas of the Mediterranean Basin, due to increased periods of drought, overexploitation, fire, soil degradation and the spread of pests and diseases (Peñuelas and Sardans, 2021). The decline of Mediterranean forests is a complex phenomenon due to multiple and very different causes that can occur slowly and over several years, ending with tree death (Gentilesca et al., 2017). In the case of chestnuts, drought (Waldboth and Oberhuber, 2009), or pathogens such as *Cryphonectria parasitica* (Elliott and Swank, 2008; Waldboth and Oberhuber, 2009), or *Phytophthora* sp. (Vettraino et al., 2005; Akıllı et al., 2012) have been reported as causes related to decline. In cork oak, causes include drought (Zribi et al., 2016; Camilo-Alves et al., 2017; El Ahmadi et al., 2022) and fungi such as *Phytophthora* sp. (Smahi et al., 2017). Or in the case of holm oak, drought events (Limousin et al., 2009) or pathogens such as *Phytophthora cinnamomi* (Frisullo et al., 2018) have been associated with decline.

Soil fungi play fundamental roles in the functioning of ecosystems, as decomposers of organic matter and as beneficial and detrimental organisms in interaction with plants (Wardle and Lindahl, 2014; Fernandes et al., 2022). In the study of soil mycobiome diversity, the DNA metabarcoding methodology represents one of the most widely used tools in the last decade (Wardle and Lindahl, 2014; Tedersoo et al., 2021). Precisely, metabarcoding has identified how disturbance events of natural and anthropogenic origin have a significant effect on the soil mycobiome of forests (Bowd et al., 2022; Martín-Pinto et al., 2023). This methodology of mycobiota diversity analysis has already been used in Mediterranean forest, being described as an effective way for the real knowledge of microbial diversity and functionality (Adamo et al., 2021a,b), also in situations of disturbance, such as fire (García-Carmona et al., 2021) or climate change (Diez-Hermano et al., 2022).

In chestnut, the study of soil fungal diversity by metabarcoding has been confirmed as a more comprehensive strategy than the study of fruiting bodies (Baptista et al., 2015). In the presence of the pathogenic oomycete *Phytophthora cambivora*, it has been reported by metabarcoding how soil mycobiota show resilience to the pathogen, and may play a key role in the forest's resistance to the disease (Venice et al., 2021). The use of metabarcoding in the study of rhizospheric mycobiota of cork oaks has revealed the influence of abiotic factors, such as climate, on its composition (Costa et al., 2022). In addition, the diversity of soil mycobiota is closely related to the decline of cork oaks (Maghnia et al., 2019). In this sense, the fungal diversity most studied by metabarcoding in relation to decline is that of the holm oaks of Spanish "dehesas." In this way, it has been possible to identify how pathogens such as *Phytophthora cinnamomi* in combination with others (such as *Fusarium* spp., *Alternaria* spp. or *Pythium spiculum*) and not in isolation are involved in the development of decline, as well as how fungi such as *Trichoderma* spp. or ectomycorrhizae improve the response of trees affected by these pathogens (Ruiz-Gómez et al., 2019a,b). With respect to Pyrenean oak, to our knowledge, the study of its rhizospheric/soil mycobiota by metabarcoding has been little addressed so far. For example, it has been possible to relate how different management strategies have an impact in soil fungal diversity (Martín-Pinto et al., 2023).

Therefore, the aim of this work is to relate soil mycobiota with the health status of Mediterranean forests. To this end, chestnut, cork oak, holm oak and Pyrenean oak have been selected as key forest species, obtaining rhizospheric soil samples from healthy and declining trees in forests with known presence of pests and pathogens. Soil mycobiota was analyzed by metabarcoding using the ITS region of ribosomal DNA.

2. Materials and methods

2.1. Sampling sites and procedure

Soil samples were extracted from the rhizosphere of healthy and declining tree of *Castanea sativa* (chestnut), *Quercus suber* (cork oak), *Quercus ilex* (holm oak) and *Quercus pyrenaica* (pyrenean oak) from Salamanca (Castile and Leon, Spain) forests (Table 1). Each site sampled corresponded to a single tree species. Soil collection was conducted for all four sites in June and July 2020.

For all sampling sites, declining patches were defined as areas with high percentage of declining trees (presence of canker wounds or stem bleeds, >70% of trees with severe dieback and foliage wilting). Health condition was assessed visually from the ground following guidelines from the ICP Forests Manual Part IV "Visual Assessment of Crown Condition and Damaging Agents" (Eichhorn et al., 2016). Stands of healthy trees were primarily composed of asymptomatic trees free of dieback or crown transparency. Data on tree assessment as well as a map of sampling locations can be found in Supplementary Figures S1, S2.

Three circular plots of healthy trees and three with high degree of decline were selected in each site. Distance between sampled trees

TABLE 1 Description of sampling sites.

Location	Size and density	Characteristics	Soil features	Sampled species	Main criteria for decline
La Alamedilla, Spain	60 ha, 49 trees/ha	Elevation: 756 m Rainfall: 600–854 mm	Medium soil with sandy loam texture and high organic matter content	*Quercus ilex*	Dead trees and exudates
Linares de Riofrío, Spain	10 ha, 1,250 trees/ha	Elevation: 956 m Rainfall: 700–900 mm	Gravels in coarse textured areas and very high organic matter content	*Castanea sativa*	Dead trees and cankers
Cubo de Don Sancho, Spain	6,000 ha, 24 trees/ha	Elevation: 736 m Rainfall: 500–700 mm	Gravels in coarse textured areas and medium organic matter content	*Quercus pyrenaica*	Dead trees, dieback and exit holes
Valdelosa, Spain	6,000 ha, 78 trees/ha	Elevation: 842 m Rainfall: 500–700 mm	Gravel and phreatic zones with sandy loam texture and low organic matter content	*Quercus suber*	Dieback and crown transparency

ranged between 10 and 50 m. Soil under the canopy of five live trees was sampled in and pooled per plot. Surface debris was removed and four cores (100 cm^3 each at opposite N, S, W, E cardinal points) of topsoil from underneath the litter layer were collected, around one meter from each tree trunk. Coarse roots and stones were removed. All soil cores from each plot were pooled, resulting in a composite soil sample per plot and totalling 24 samples (4 sampling sites × 3 plots × 2 health conditions). Samples were stored at −20°C prior to processing.

Throughout this paper soil sampled from stands of healthy trees will be referred to as "healthy trees soil" whereas soil from stands of declining trees will be termed "declining trees soil."

2.2. Sample processing and sequencing

Physicochemical analyses of soil samples were performed in triplicate, at the Analysis and Instrumentation Service of IRNASA-CSIC by standard methods. Analyzed soil properties can be found in Supplementary Table S1.

Samples were sent for molecular analysis to Base Clear B.V (Leiden, Netherlands). DNA extraction was performed using the DNeasy PowerLyzer PowerSoil kit (Qiagen). Region 2 of fungal Internal Transcribed Spacer (ITS2) gene was amplified using the following primers: ITS7-F: 5′-GTG ART CAT CGA RTC TTT G-3′, ITS4-R: 5'-TCC TCC GCT TAT TGA TAT GC-3′ (Fujita et al., 2001; Ihrmark et al., 2012). Paired-end sequence reads (2×300 bp) were generated using the Illumina MiSeq V2 system under accreditation according to the scope of BaseClear B.V (L457; NEN-EN-ISO/IEC 17025). FASTQ read sequence files were generated using bcl2fastq2 version 2.18. Initial quality assessment was based on data passing the Illumina Chastity filtering. Subsequently, reads containing PhiX control signal were removed using an in-house filtering protocol. In addition, reads containing (partial) adapters were clipped (up to a minimum read length of 50 bp). The second quality assessment was based on the remaining reads using the FASTQC quality control tool version 0.11.5. ITS2 sequences were processed following the DADA2 pipeline to generate amplicon sequence variants (ASV) (Callahan et al., 2016). Parameters' values were as follows: filtering and trimming (maxN = 0, maxEE = 2, truncQ = 2, minLen = 50, rm.phix = TRUE, compress = TRUE), learning error rates (nbases = 1e+08, nreads = NULL, errorEstimationFunction = loessErrfun, MAX_CONSIST = 10, OMEGA_C = 0), merging paired reads (errorEstimationFunction = loessErrfun, selfConsist = FALSE, pool = FALSE) and removing chimeras (method = "consensus"). Taxonomy assignment and abundance estimation were performed comparing ASVs against UNITE database version 9.0 (Abarenkov et al., 2022). Rarefaction curves were used to evaluate the relationship between sequencing depth and the number of ASVs.

2.3. Statistical analysis

Prior to the analysis, taking into consideration that only ITS2 marker was used, ASVs' raw reads were aggregated at genus level to have better confidence, and to avoid misidentification of closely-related species (Yang et al., 2018).

Differences between mycobiome communities were evaluated in terms of alpha and beta diversity. Alpha diversity was assessed using Hill diversity indexes according to the equation

$$D = \left(\sum_{i=1}^{S} p_i \left(r_i \right)^l \right)^{\frac{1}{l}}$$

where D is diversity, S is the number of taxa, p_i is the proportion of all individuals that belong to taxa i, r_i is the rarity of taxa i, defined as $1/p_i$, and l is the exponent that determines the rarity scale and corresponds to richness ($l = 1$) or equivalence-corrected versions of Shannon ($l = 0$) and Simpson indexes ($l = -1$) (Roswell et al., 2021). Differences between health conditions per tree species at $l = [-1, 0, 1]$ were contrasted using Wilcoxon's rank test.

Beta diversity was evaluated in terms of differential abundance by taking into account that high-throughput sequencing counts should be considered compositional data (Gloor et al., 2017). Analyses followed the ZicoSeq procedure, which has been shown to be overall more robust and powerful than other existing methods in recent benchmarks (Yang and Chen, 2022). Compositional effects were addressed by adopting a reference-based approach (selecting close-to-invariant taxa as baseline abundances) and association testing was conducted by linear model-based Smith permutation testing [LDM and DACOMP methods in Brill et al. (2022) and Hu and Satten (2020), respectively]. Reference taxa were adjusted for health status (factor with two levels: healthy, declining) as a covariate. Taxa were filtered if their prevalence was less than 20% and their mean relative abundance was less than 0.2%. Percentage of top outliers replaced by

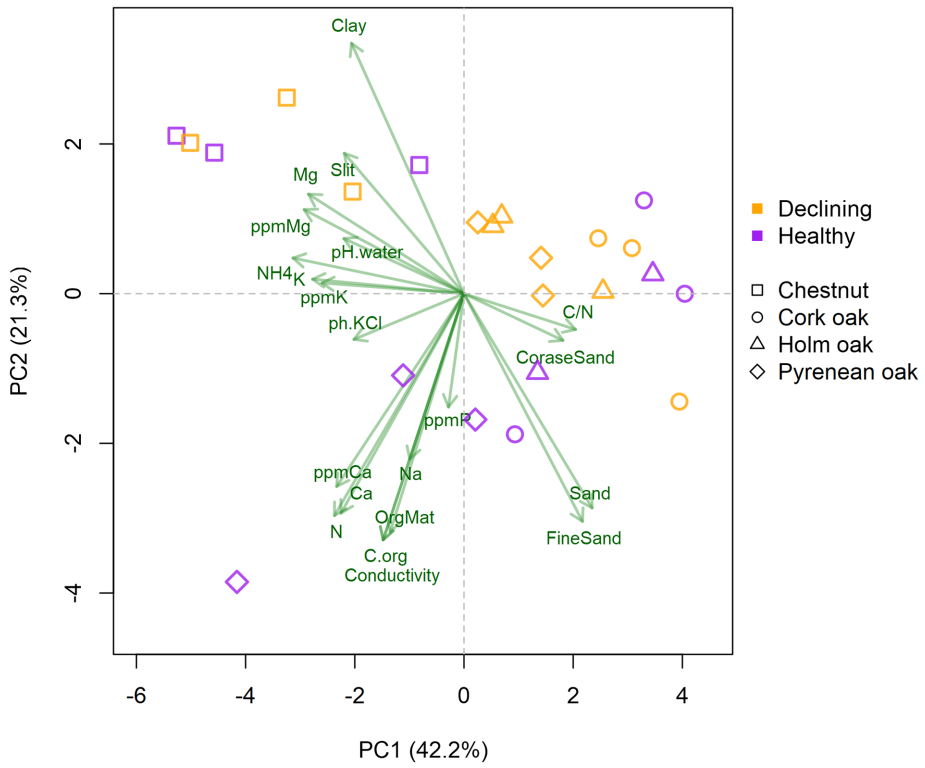

FIGURE 1
Biplot of soil properties, tree species and health status. Green arrows represent soil properties and colored symbols represent soil samples. Axis correspond to the first and second principal components, accounting for 63.5% of total variance. Variables were scaled prior to analysis.

winsorization was 10%. Abundances were square root transformed. Multiple test correction of *p*-values was based on 500 permutation tests.

All fungal genera were included in the functional analyses. Each genus was assigned a functional guild according to the "primary lifestyle" column obtained from FungalTraits database V1.2 (Põlme et al., 2020). Raw read numbers of each guild were summed per tree species and health condition and expressed as $\log_2$(guild abundance/total abundance).

All analyses were performed in R environment 4.1.3 (R Core Team, 2022). Analysis of sequencing data and ASV identification were performed using the packages *Biostrings* (Pagès et al., 2022), *dada2* (Callahan et al., 2016) and *ShortRead* (Morgan et al., 2009). Hill diversity analysis was carried out using the package *MeanRarity* (Roswell and Dushoff, 2022). For compositional analysis the package *GUniFrac* (Chen et al., 2022) was used. Taxonomic information was handled and plotted with the package *metacoder* (Foster et al., 2017).

3. Results

3.1. Soil description

Physico-chemical properties of soils were analyzed and summarized using Principal Component Analysis (Figure 1). Chestnut's soils were characterized by clay and slit texture, higher content of assimilable and free Mg and K and a slight tendency to acidity with high concentration of ionized NH4+. Oak's soils were characterized by sandy textures and a higher C/N ratio, except for soils from declining Pyrenean oaks, which were enriched in Ca, N, P and organic matter. No further associations between health status and soil properties were observed.

3.2. Fungal community description

Sequencing yielded 32,042 (29590–33,305) reads on average (median and P25-75) following quality control (Supplementary Table S2). All samples showed plateauing rarefaction curves (Supplementary Figure S1). The analysis of the fungal communities reported 674 different genera distributed in 15 phyla (Supplementary Table S3). The majority of the phyla were Ascomycota (~66%) and Basidiomycota (~26%) (Figure 2).

To analyse the relationship between the presence/absence of certain fungal genera and forest health status, a comparison was made without considering the plant species. Only those genera that were present in at least 80% of the samples were taken into account. Twenty-two fungal genera (68.8%) were found common to healthy and declining trees soils, while six genera (18.8%) were only present in healthy trees soils and four genera (12.5%) were exclusive to declining forest soils. The genera found in healthy forest soils were *Coleophoma, Geomyces, Podila, Sagenomella, Scytalidium,* and *Varicellaria*. On the other hand, the fungal genera found in declining trees soils, which did not appear in samples of healthy trees, were *Humicola, Meliniomyces, Pleurotus* and *Polyphilus* (Figure 3).

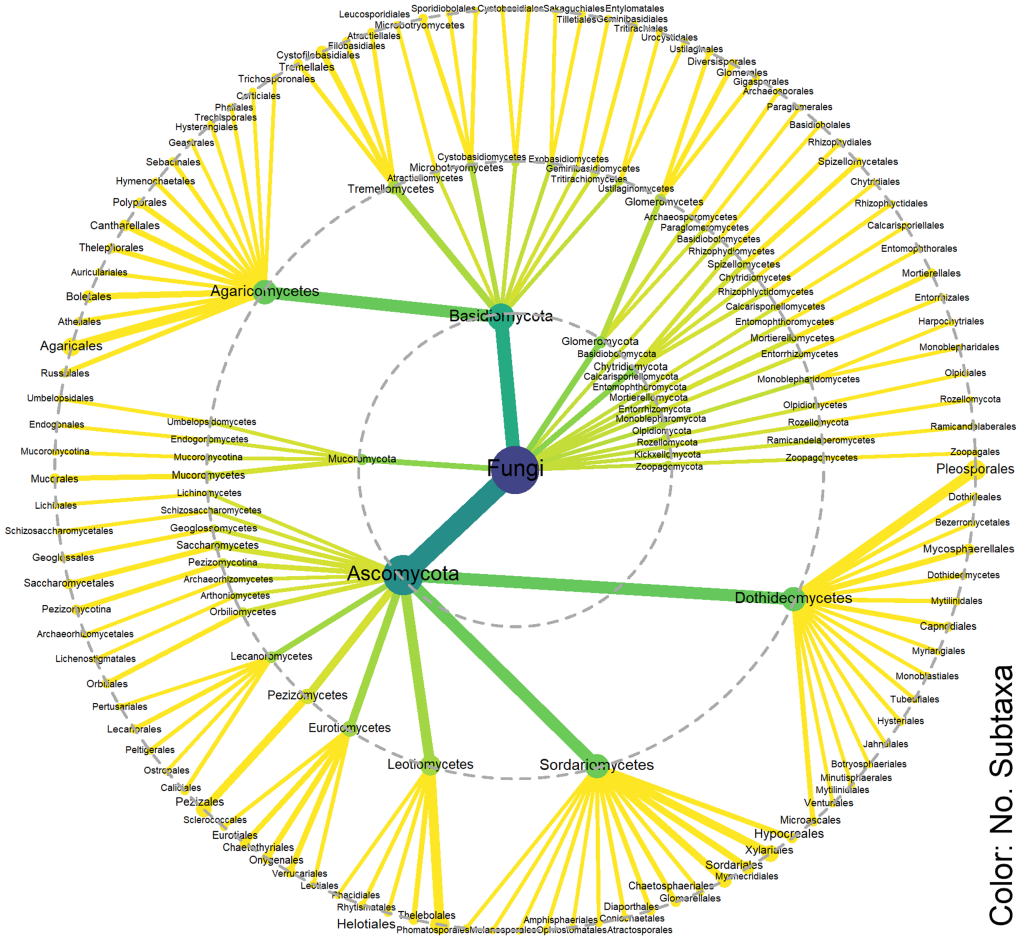

FIGURE 2
Taxonomic heat tree. Node size represents the number of OTUs and color scale represents the number of subtaxa. Dashed grey circles indicate the following taxonomic levels: phylum (inner), class (middle), order (outer). NA: not assigned.

3.3. Diversity analysis

Diversity analysis was performed by comparing the effect of decline in the different tree species. In chestnut there was significantly higher alpha diversity in soil from healthy trees than in soil from declining trees. On the other hand, both cork oak and holm oak reported higher alpha diversity in soil from declining trees than in healthy trees; specifically, the diversity was significantly higher for dominant fungal genera in cork oak (Hill = −1) and for rare genera in holm oak (Hill = 1). In the case of Pyrenean oak, no significant differences were found between fungal genus diversity in soil from healthy and declining trees (Figure 4).

Beta diversity was evaluated in terms of differential abundance (DA) of fungal compositions using square root-transformed values of raw reads. In cork oak, holm oak and Pyrenean oak, no fungal genus was found significantly more abundant in soils of declining trees, nor in healthy trees (Figure 5). Only the genus *Metarhizium* was found to be significantly more abundant in soils of healthy chestnuts (p-val = 0.1 and R2 = 0.2). However, no fungal genus was reported to be significantly more abundant in declining chestnut soils.

3.4. Functional profiles

Primary lifestyle was assigned to each of the fungal genera reported in healthy and declining forest soils per tree species. Most prominent functional niches identified were ectomycorrhizae (EcM) and soil saprophytes, followed by litter/wood saprophytes and plant pathogens, regardless of tree species (Figure 6). Root endophytes were also particularly abundant in soil from holm oak and Pyrenean oak. When taking health status into account, the biggest differences were found in chestnuts and cork oaks, with holm oaks and Pyrenan oaks having similar functional profiles between healthy and declining trees' soil. Fungal genera whose primary function is to form part of the lichen symbiosis were found to be more abundant in healthy chestnut and cork oak soils than in declining soils. Sooty mold fungi in chestnut soils followed the same trend. In cork oaks the largest differences corresponded to arbuscular mycorrhizae (AM), more present in declining than in healthy trees' soil. Some lifestyles were absent from the majority of samples, such as moss symbiont, protistan parasites, epiphytes and algal parasites.

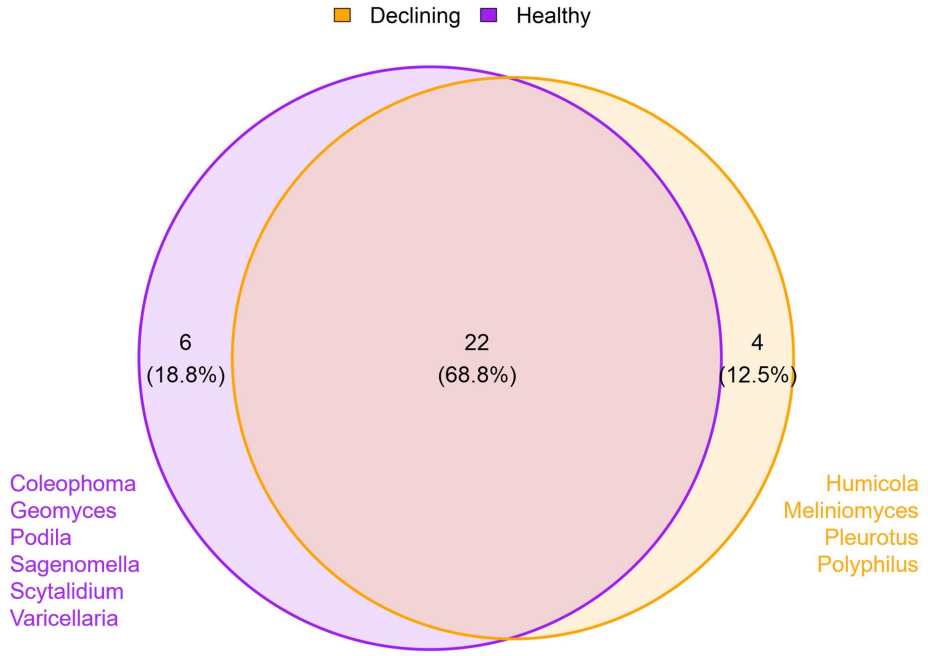

FIGURE 3
Overall effect of health status on mycobiota. Venn's diagram showing the number of common and exclusive genera between samples from healthy ($n = 12$) and declining ($n = 12$) trees. Only genera present in 80% of samples per condition are included, regardless of tree species.

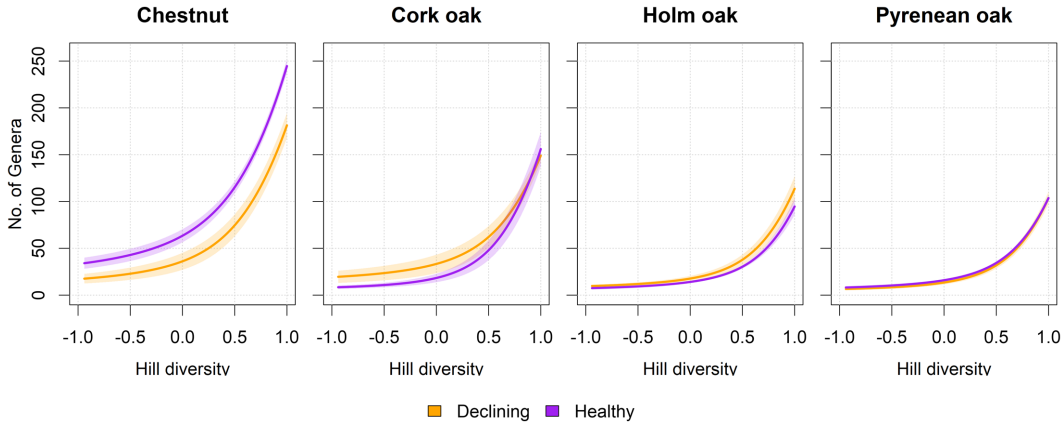

FIGURE 4
Diversity profiles per tree species and health status. Curves represent the average diversity in samples from healthy and declined trees in terms of an imaginary assemblage with that same diversity, but in which all species are equally abundant (Jost, 2006; Roswell et al., 2021). The horizontal axis represents the exponent l of Hill diversity, which can be interpreted as equivalence-corrected versions for richness ($l = 1$), Shannon ($l = 0$) and Simpson ($l = -1$) diversity estimators. Shadowed intervals correspond to standard error. Significant differences were found at $l = [1, 0, -1]$ between declining and healthy chestnut soils (Wilcoxon test, $n = 3$ per tree species and health condition, p-val < 0.05). Raw curves prior to averaging can be found in Supplementary Figure S2.

4. Discussion

Soil mycobiota play a key role in forest functioning and health (Fernandes et al., 2022). Therefore, knowing the fungal diversity of forest soils under different situations and health status is fundamental to understand the role that each component of this diversity plays in the sustainability of the ecosystem, being metabarcoding a proven tool for this purpose (Bowd et al., 2022). In our study, this methodology has allowed us to identify 674 different fungal genera as inhabitants of the rhizosphere of chestnuts, cork oaks, holm oaks and Pyrenean oaks.

Some fungal genera were only present in soils of declining trees. However, none of these genera has been previously described as a forest pathogen, which might be indicative of the soil conditions playing an important role as a predisposing or inciting factor of decline *per se*. *Humicola* is a genus of endophytic fungi of great biotechnological interest in recent years, mainly related to halophytic plants and production of chemical compounds for industrial use (Hosseyni-Moghaddam et al., 2020). *Meliniomyces* is a genus of endophytic fungi and ericoid mycorrhiza (Ohtaka and Narisawa, 2008; Vohnik et al., 2013). *Pleorotus* is a genus of widely known edible

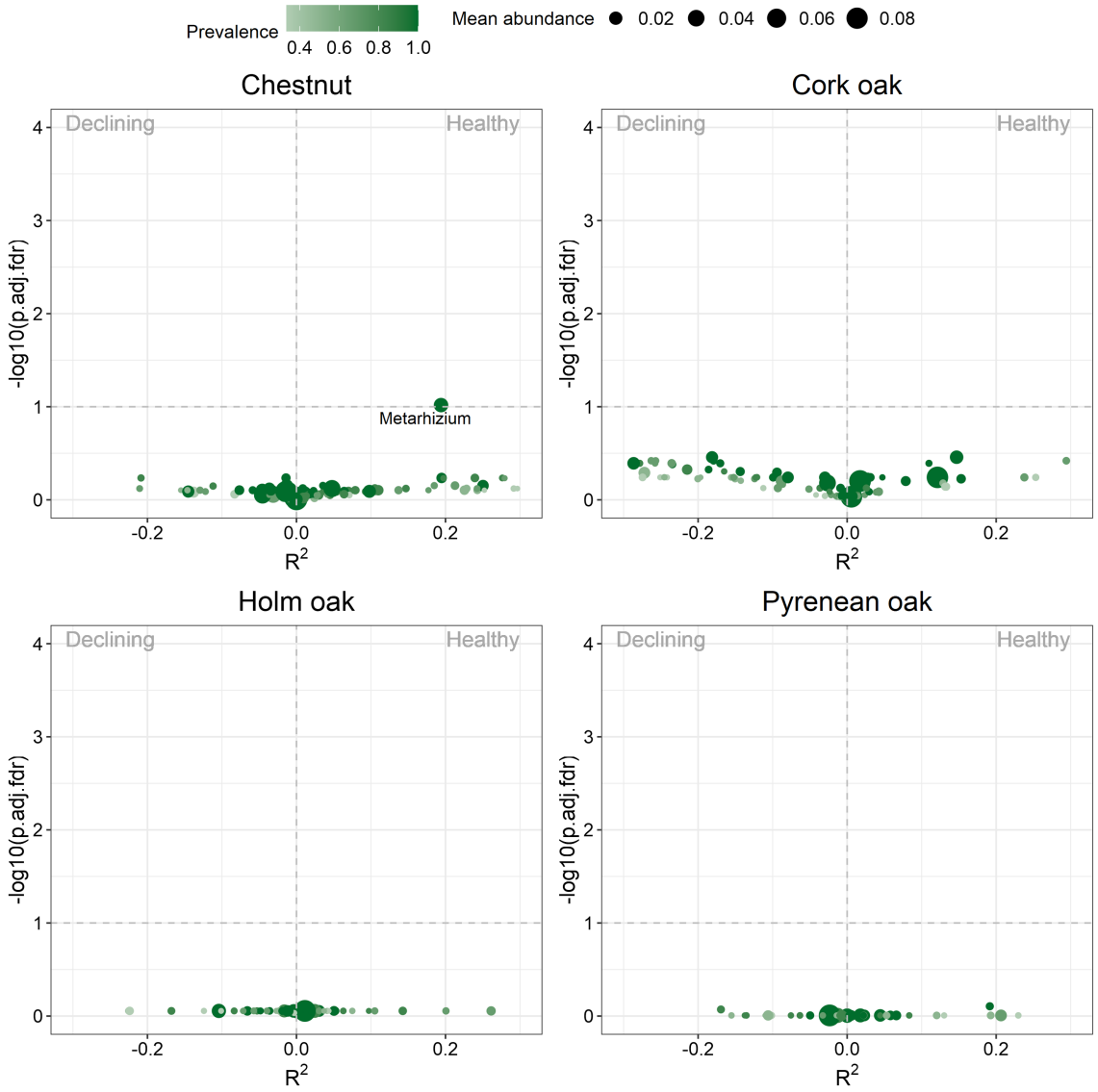

FIGURE 5
Volcano plot of differentially abundant genera detected by ZicoSeq analysis. Each genus is depicted by a dot. Dot size indicates the mean abundance across all samples and color indicates the proportion of samples in which the genus is present. Vertical axis represents value of p adjusted by false discovery rate (FDR) in logarithmic scale (1 = 0.1, 1.30 = 0.05, 2 = 0.01 and so on). Horizontal axis represents the strength of association between abundance and health condition, with the sign indicating the association direction (negative for declining, positive for healthy). Genera that surpass the horizontal dashed line are differentially abundant (p-val < 0.1).

saprophytic fungus (Suwannarach et al., 2020; Doroški et al., 2022) which also includes biological control agents against nematodes (Singh et al., 2019), and its presence is most likely tied to clearings in declining areas. *Polyphilus* is a recently created fungal genus, which includes nematophagous fungi of eggs and cysts of plant-parasitic nematodes (Ashrafi et al., 2018). However, other important microbial communities with putative pathogenic species and capable of exerting direct and indirect effects on these forest species, such as bacteria, oomycetes or nematodes, have not been addressed here. Future work would be interesting in this regard, and could provide important information on their relationship with the health status of the trees as well as their impact on population dynamics of non-pathogenic species.

Similarly, we also found fungal genera exclusive to healthy forest soils, which could be related to control activity of different pathogens. *Varicellaria* is a fungal genus whose life form is algal symbiosis to form lichens (Schmitt et al., 2012) and could be related to the presence of more humidity due to better vegetative condition of the trees. A few species of *Podila* have been described as mycophilic fungi or mycoparasites (Telagathoti et al., 2022), but the absence of specific studies on their potential biocontrol effect prevents associating their presence with the absence of decline. Some genera found can act as animals' pathogens, such as the genus *Geomyces* (Warnecke et al., 2012). The genus *Sagenomella* is widely known to cause systemic illness in animals (Gené et al., 2003), whereas the genus *Scytalidium* includes the causal agent of scytalidiosis and onychomycosis, human skin diseases (Elewski, 1996; Machouart et al., 2013). Interestingly, the genus *Coleophoma*, also absent from declining samples, has been widely described as a forest pathogen (Pehl and Wulf, 2003;

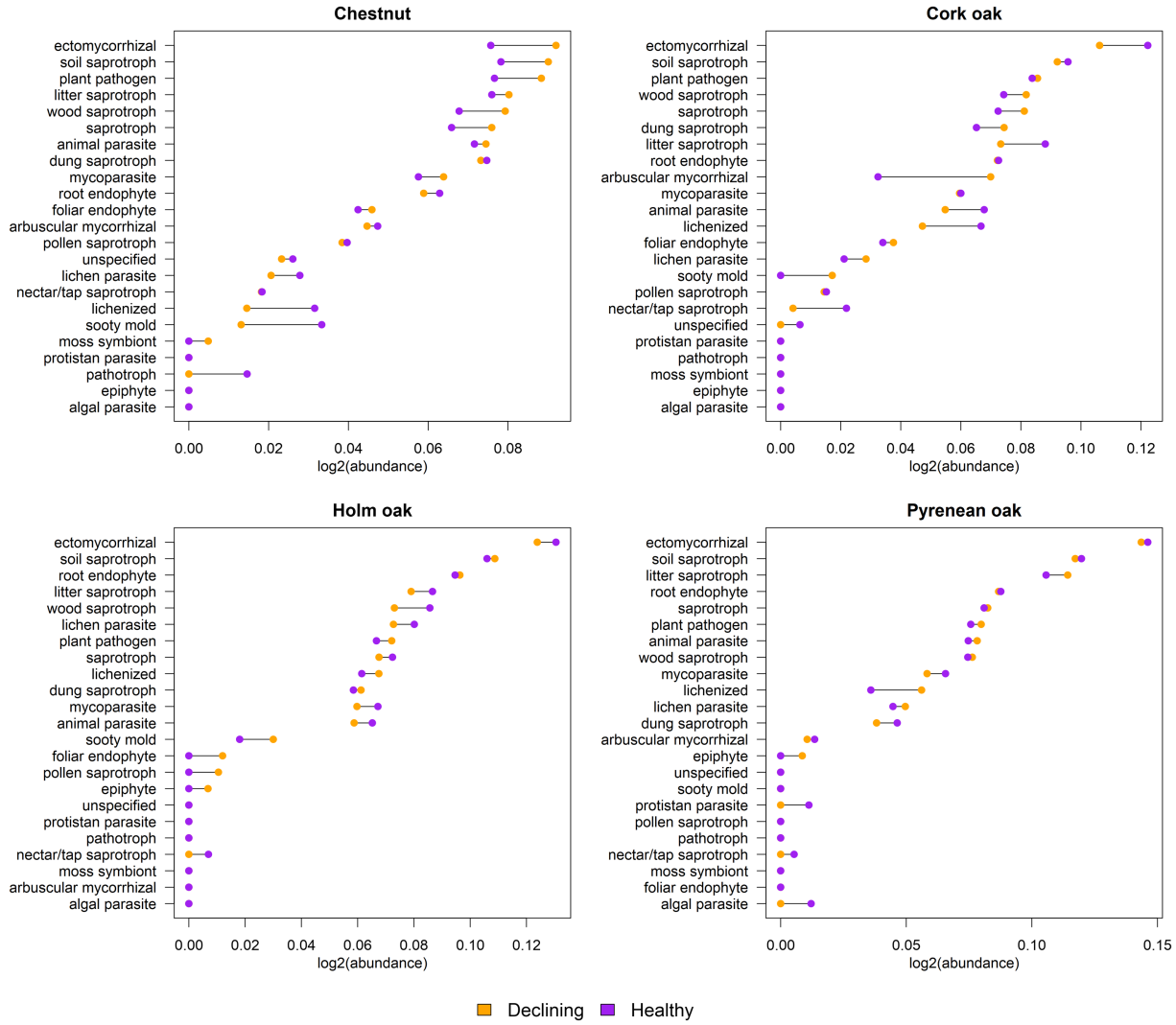

FIGURE 6
Comparison of functional guilds between declined and healthy samples. Horizontal axis represents sum of abundances expressed as $\log_2$ (guild abundance/total abundance). Connecting lines between two dots correspond to the difference between declined and healthy samples.

Bianchinotti and Rajchenberg, 2004). Grazing activities that take place regularly in the sampling sites could offer an explanation to the presence of fungi pathogenic to animals, although their association with healthy trees soils would point to a preference of cattle for such areas that has not been explored.

Regarding biodiversity, a higher alpha diversity was observed in soils of healthy chestnuts than in declining trees. In this sense, other authors have previously described that the rhizosphere of chestnuts has a high diversity, even much higher than that of other forest ecosystems (Kelly et al., 2021). Moreover, this fungal diversity plays a key role in the resistance of trees against pathogens such as the oomycete *Phytophthora cambivora* (Venice et al., 2021). On the other hand, in both cork oak and holm oak, we found a higher fungal diversity in the rhizosphere of declining trees than in healthy ones. Therefore, a higher fungal diversity in these trees may not be related to the biological control of the decline, as has been described by other authors (Gómez-Aparicio et al., 2022). Finally, no differences in alpha diversity were reported between soils of healthy and declining Pyrenean oaks, a novel aspect that requires further studies. Differential abundance analysis indicated that the genus *Metarhizium* is more present in healthy chestnut soils than in declining soils. *Metarhizium* has been widely described as a biological control agent against plant pests and pathogens (Stone and Bidochka, 2020), which might be indicative of this genus playing a significant role in the absence of declining in the selected healthy chestnut stands. Influence of environmental drivers on biodiversity such as slope or elevation has not been evaluated and would be an important confusion factor to be considered in future works.

With respect to the assignment of primary lifestyles, most common functional niches found were EcM and soil saprophytes, very widespread and important functions in fungi that make up the mycobiota of all forest soils (Li et al., 2022). EcM fungi were dominated by some ubiquitous genera such as *Cenococcum, Cortinarius, Inocybe, Laccaria, Russula* and *Tomenteria*, with *Russula* being particularly more abundant in holm oak and Pyrenean oak soils regardless of health status (see complete list in Figure S5). In general, all oak species shared a

predominance of EcM over other functional guilds. Inverse relationship between abundance of EcM and abundance of other guilds has been found before in oaks' soils (Ruiz Gómez et al., 2019b). In contrast, chestnut showed evenness of EcM, saprotrophs and pathogens. We hypothesize that these differences in balance of functional guilds between oaks and chestnuts could be related to oaks' soils being generally poorer and dryer and thus more prone to prevalence of EcM than chestnuts' soils, where water is more readily available to the plant. The aforementioned guilds were also found to be more abundant in declining chestnut soils. Higher presence of opportunistic pathogens is to be expected in the rhizosphere of weakened trees, whereas saprobes might benefit from the excess of dead matter and leaf litter. Declining chestnuts could also have increased generation of roots as an attempt to compensate for compromised water transport, which in turn would allow for more colonization of EcM, however, this phenomenon was not observed in the oak species. Regarding other lifestyles, a significant proportion of AM belonging to 15 genera was found in chestnut and declining cork oak soils, whereas holm oak, Pyrenean oak and healthy cork oak soils showed a remarkable absence of AM (Supplementary Figure S5). In particular, presence of some genera such as *Archaeospora, Entrophospora* and *Dominikia* was tied to health status in cork oak soils, favoring declining samples. The persistence of AM has been reported in dying succulent trees in correlation with $NO3^-$ levels in soil (Vivas et al., 2018), although we found no differences in nitrogen compounds between healthy and declining cork oak soils in our samples.

This work describes the fungal soil mycobiota of four Mediterranean forest species and explores differences between healthy and declining stands. Healthy chestnut soils were characterized by higher alpha diversity and higher abundance of the genus *Metarhizium*, but such relationships were not found in the rest of the forest species included in the study. Finally, with respect to the functional profile, declining chestnut soils harbored more abundance of EcM, saprobic and pathogenic guilds than healthy samples. EcM were the dominant lifestyle in all oak species regardless of health status, whereas AM were preferentially found in healthy cork oak soils. Further experimental validations would be necessary to assess whether functional shifts in soil mycobiota are causally related to trees' health status.

Data availability statement

The datasets presented in this study can be found in online repositories. The names of the repository/repositories and accession number(s) can be found at: https://www.ncbi.nlm.nih.gov/genbank/, PRJNA953856 https://github.com/serbiodh/2023_FrontiersForests_Soil, GitHub.

Author contributions

IB-A collected the data. SD-H analyzed the data. JP, SD-H, and JD wrote the manuscript. IB-A, JN-S, PM-P, AP, and JD designed the sampling scheme. All authors contributed to the article and approved the submitted version.

Funding

This work was supported by the LIFE project MYCORESTORE "Innovative use of mycological resources for resilient and productive mediterranean forests threatened by climate change, LIFE18 CCA/ES/001110," and projects PID2019-110459RB-I00 and PLEC2021-008076 funded by the MICINN (Spain) as well as the project VA208P20 and the Strategic Research Program for Units of Excellence CLU-2019-05 (Unit of Excellence IRNASA/CSIC) both co-funded by the Junta de Castilla y León and European Union (ERDF "Europe drives our growth").

Acknowledgments

The authors would like to thank Álvaro Benito Delgado, Cristina Zamora Ballesteros, and Mariano Rodríguez Rey for their valuable contributions to sampling, laboratory work and troubleshooting.

Conflict of interest

The authors declare that the research was conducted in the absence of any commercial or financial relationships that could be construed as a potential conflict of interest.

Publisher's note

Supplementary material

The Supplementary material for this article can be found online at: https://www.frontiersin.org/articles/10.3389/ffgc.2023.1215701/full#supplementary-material

References

Abarenkov, K., Zirk, A., Piirmann, T., Pöhönen, R., Ivanov, F., Nilsson, R. H., et al. (2022). UNITE general FASTA release for fungi. Version 16.10.2022. *UNITE Commun.* doi: 10.15156/BIO/2483911

Adamo, I., Castano, C., Bonet, J. A., Colinas, C., de Aragon, J. M., and Alday, J. G. (2021b). Soil physico-chemical properties have a greater effect on soil fungi than host species in Mediterranean pure and mixed pine forests. *Soil Biol. Biochem.* 160:108320. doi: 10.1016/j.soilbio.2021.108320

Adamo, I., Piñuela, Y., Bonet, J. A., Castaño, C., Martínez de Aragón, J., Parladé, J., et al. (2021a). Sampling forest soils to describe fungal diversity and composition. Which is the optimal sampling size in mediterranean pure and mixed pine oak forests? *Fungal Biol.* 125, 469–476. doi: 10.1016/j.funbio.2021.01.005

Akıllı, S., Serçe, Ç. U., Katırcıoğlu, Y. Z., and Maden, S. (2012). Involvement of phytophthora spp. in chestnut decline in the Black Sea region of Turkey. *For. Pathol.* 42, 377–386. doi: 10.1111/j.1439-0329.2012.00770.x

Ashrafi, S., Knapp, D. G., Blaudez, D., Chalot, M., Maciá-Vicente, J. G., Zagyva, I., et al. (2018). Inhabiting plant roots, nematodes, and truffles—Polyphilus, a new helotialean genus with two globally distributed species. *Mycologia* 110, 286–299. doi: 10.1080/00275514.2018.1448167

Baptista, P., Reis, F., Pereira, E., Tavares, R. M., Santos, P. M., Richard, F., et al. (2015). Soil DNA pyrosequencing and fruitbody surveys reveal contrasting diversity for various fungal ecological guilds in chestnut orchards. *Environ. Microbiol. Rep.* 7, 946–954. doi: 10.1111/1758-2229.12336

Bianchinotti, V., and Rajchenberg, M. (2004). Coleophoma gevuinae comb. nov., a foliar pathogen on Gevuina avellana (Proteaceae). *Sydowia* 56, 217–221.

Bowd, E. J., Banks, S. C., Bissett, A., May, T. W., and Lindenmayer, D. B. (2022). Disturbance alters the forest soil microbiome. *Mol. Ecol.* 31, 419–447. doi: 10.1111/mec.16242

Brill, B., Amir, A., and Heller, R. (2022). Testing for differential abundance in compositional counts data, with application to microbiome studies. *Ann. Appl. Stat.* 16, 2648–2671. doi: 10.1214/22-AOAS1607

Callahan, B. J., McMurdie, P. J., Rosen, M. J., Han, A. W., Johnson, A. J. A., and Holmes, S. P. (2016). DADA2: high-resolution sample inference from Illumina amplicon data. *Nat. Methods* 13, 581–583. doi: 10.1038/nmeth.3869

Camilo-Alves, C. S., Vaz, M., Da Clara, M. I. E., and Ribeiro, N. M. D. A. (2017). Chronic cork oak decline and water status: new insights. *New For.* 48, 753–772. doi: 10.1007/s11056-017-9595-3

Camponi, L., Cardelli, V., Cocco, S., Serrani, D., Salvucci, A., Cutini, A., et al. (2023). Holm oak (*Quercus ilex* L.) cover: a key soil-forming force in controlling C and nutrient stocks in long-time coppice-managed forests. *J. Environ. Manag.* 330:117181. doi: 10.1016/j.jenvman.2022.117181

Chen, J., Zhang, X., and Yang, L. (2022). GUniFrac: generalized UniFrac distances, distance-based multivariate methods and feature-based univariate methods for microbiome data analysis. R package version 1.7. Available at: https://CRAN.R-project.org/package=GUniFrac

Costa, D., Tavares, R. M., Baptista, P., and Lino-Neto, T. (2022). The influence of bioclimate on soil microbial communities of cork oak. *BMC Microbiol.* 22:163. doi: 10.1186/s12866-022-02574-2

Diez-Hermano, S., Ahmad, F., Niño-Sanchez, J., Benito, A., Hidalgo, E., Escudero, L. M., et al. (2022). Health condition and mycobiome diversity in Mediterranean tree species. *Frontiers in Forests and Global Change* 5:1056980. doi: 10.3389/ffgc.2022.1056980

Doroški, A., Klaus, A., Režek Jambrak, A., and Djekic, I. (2022). Food waste originated material as an alternative substrate used for the cultivation of oyster mushroom (Pleurotus ostreatus): a review. *Sustainability* 14:12509. doi: 10.3390/su141912509

Eichhorn, J., Roskams, P., Potočić, N., Timmermann, V., Ferretti, M., Mues, V., et al. (2016). "Part IV: visual assessment of crown condition and damaging agents. In: UNECE ICP forests programme coordinating Centre" in *Manual on methods and criteria for harmonized sampling, assessment, monitoring and analysis of the effects of air pollution on forests* (Eberswalde, Germany: Thünen Institute of Forest Ecosystems), 49.

El Ahmadi, S., Ramzi, H., Aafi, A., Jmii, N. E., and Aadel, T. (2022). Assessment of Cork oak decline using digital multispectral imagery in relation with in situ crown condition. *Open Journal of Forestry* 13, 145–160. doi: 10.4236/ojf.2023.131010

Elliott, K. J., and Swank, W. T. (2008). Long-term changes in forest composition and diversity following early logging (1919–1923) and the decline of American chestnut (*Castanea dentata*). *Plant Ecol.* 197, 155–172. doi: 10.1007/s11258-007-9352-3

Elewski, B. E. (1996). Onychomycosis caused by Scytalidium dimidiatum. *J. Am. Acad. Dermatol.* 35, 336–338. doi: 10.1016/S0190-9622(96)90664-7

Fady, B., Esposito, E., Abulaila, K., Aleksic, J. M., Alia, R., Alizoti, P., et al. (2022). Forest genetics research in the Mediterranean Basin: bibliometric analysis, knowledge gaps, and perspectives. *Curr. Forest. Rep.* 8, 277–298. doi: 10.1007/s40725-022-00169-8

Fernandes, M. L. P., Bastida, F., Jehmlich, N., Martinović, T., Větrovský, T., Baldrian, P., et al. (2022). Functional soil mycobiome across ecosystems. *J. Proteome* 252:104428. doi: 10.1016/j.jprot.2021.104428

Foster, Z., Sharpton, T., and Grünwald, N. (2017). Metacoder: an R package for visualization and manipulation of community taxonomic diversity data. *PLoS Comput. Biol.* 13, e1005404–e1005415. doi: 10.1371/journal.pcbi.1005404

Frisullo, S., Lima, G., Magnano di San Lio, G., Camele, I., Melissano, L., Puglisi, I., et al. (2018). Phytophthora cinnamomi involved in the decline of holm oak (*Quercus ilex*) stands in southern Italy. *For. Sci.* 64, 290–298. doi: 10.1093/forsci/fxx010

Fujita, S. I., Senda, Y., Nakaguchi, S., and Hashimoto, T. (2001). Multiplex PCR using internal transcribed spacer 1 and 2 regions for rapid detection and identification of yeast strains. *J. Clin. Microbiol.* 39, 3617–3622. doi: 10.1128/JCM.39.10.3617-3622.2001

García-Carmona, M., García-Orenes, F., Mataix-Solera, J., Roldán, A., Pereg, L., and Caravaca, F. (2021). Salvage logging alters microbial community structure and functioning after a wildfire in a Mediterranean forest. *Appl. Soil Ecol.* 168:104130. doi: 10.1016/j.apsoil.2021.104130

Garfì, V., Marziliano, P. A., Chirici, G., Nicolaci, A., and Iovino, F. (2022). Forest management scenarios to reduce the fire risk in chestnut coppices in the Mediterranean area. *Ann. Silvicult. Res.* 47, 63–77. doi: 10.12899/asr-2387

Gauquelin, T., Michon, G., Joffre, R., Duponnois, R., Génin, D., Fady, B., et al. (2018). Mediterranean forests, land use and climate change: a social-ecological perspective. *Reg. Environ. Chang.* 18, 623–636. doi: 10.1007/s10113-016-0994-3

Gené, J., Blanco, J. L., Cano, J., García, M. E., and Guarro, J. (2003). New filamentous fungus Sagenomella chlamydospora responsible for a disseminated infection in a dog. *J. Clin. Microbiol.* 41, 1722–1725. doi: 10.1128/JCM.41.4.1722-1725.2003

Gentilesca, T., Camarero, J. J., Colangelo, M., Nole, A., and Ripullone, F. (2017). Drought-induced oak decline in the western Mediterranean region: an overview on current evidences, mechanisms and management options to improve forest resilience. *iForest-Biogeosci. Forest.* 10, 796–806. doi: 10.3832/ifor2317-010

Gloor, G. B., Macklaim, J. M., Pawlowsky-Glahn, V., and Egozcue, J. J. (2017). Microbiome datasets are compositional: and this is not optional. *Front. Microbiol.* 8:2224. doi: 10.3389/fmicb.2017.02224

Gómez-Aparicio, L., Domínguez-Begines, J., Villa-Sanabria, E., García, L. V., and Muñoz-Pajares, A. J. (2022). Tree decline and mortality following pathogen invasion alters the diversity, composition and network structure of the soil microbiome. *Soil Biol. Biochem.* 166:108560. doi: 10.1016/j.soilbio.2022.108560

Hosseyni-Moghaddam, M. S., Safaie, N., Soltani, J., and Pasdaran, A. (2020). Endophytic association of bioactive and halotolerant *Humicola fuscoatra* with halophytic plants, and its capability of producing anthraquinone and anthranol derivatives. *Antonie Van Leeuwenhoek* 113, 279–291. doi: 10.1007/s10482-019-01336-x

Hu, Y. J., and Satten, G. A. (2020). Testing hypotheses about the microbiome using the linear decomposition model (LDM). *Bioinformatics* 36, 4106–4115. doi: 10.1093/bioinformatics/btaa260

Ihrmark, K., Bödeker, I. T., Cruz-Martinez, K., Friberg, H., Kubartova, A., Schenck, J., et al. (2012). New primers to amplify the fungal ITS2 region–evaluation by 454-sequencing of artificial and natural communities. *FEMS Microbiol. Ecol.* 82, 666–677. doi: 10.1111/j.1574-6941.2012.01437.x

Jost, L. (2006). Entropy and diversity. *Oikos* 113:2. doi: 10.1111/j.2006.0030-1299.14714.x

Kelly, C. N., Schwaner, G. W., Cumming, J. R., and Driscoll, T. P. (2021). Metagenomic reconstruction of nitrogen and carbon cycling pathways in forest soil: influence of different hardwood tree species. *Soil Biol. Biochem.* 156:108226. doi: 10.1016/j.soilbio.2021.108226

Li, X., Qu, Z., Zhang, Y., Ge, Y., and Sun, H. (2022). Soil fungal community and potential function in different Forest ecosystems. *Diversity* 14:520. doi: 10.3390/d14070520

Limousin, J. M., Rambal, S., Ourcival, J. M., Rocheteau, A., Joffre, R., and Rodriguez-Cortina, R. (2009). Long-term transpiration change with rainfall decline in a Mediterranean *Quercus ilex* forest. *Glob. Chang. Biol.* 15, 2163–2175. doi: 10.1111/j.1365-2486.2009.01852.x

Machouart, M., Menir, P., Helenon, R., Quist, D., and Desbois, N. (2013). Scytalidium and scytalidiosis: what's new in 2012? *J. de mycologie médicale* 23, 40–46. doi: 10.1016/j.mycmed.2013.01.002

Maghnia, F. Z., Abbas, Y., Mahé, F., Prin, Y., El Ghachtouli, N., Duponnois, R., et al. (2019). The rhizosphere microbiome: a key component of sustainable cork oak forests in trouble. *For. Ecol. Manag.* 434, 29–39. doi: 10.1016/j.foreco.2018.12.002

Martin-Pinto, P., Sanz-Benito, I., Santos, M., Oria-de-Rueda, J. A., and Geml, J. (2021). Anthropological impacts determine the soil fungal distribution of Mediterranean oak stands. *Ecol. Indic.* 132:108343. doi: 10.1016/j.ecolind.2021.108343

Martín-Pinto, P., Dejene, T., Benucci, G. M. N., Mediavilla, O., Hernández-Rodríguez, M., Geml, J., et al. (2023). Co-responses of bacterial and fungal communities to fire management treatments in Mediterranean pyrophytic ecosystems. *Sci. Total Environ.* 875:162676. doi: 10.1016/j.scitotenv.2023.162676

Morán-Ordóñez, A., Ameztegui, A., De Cáceres, M., De-Miguel, S., Lefèvre, F., Brotons, L., et al. (2020). Future trade-offs and synergies among ecosystem services in Mediterranean forests under global change scenarios. *Ecosyst. Serv.* 45:101174. doi: 10.1016/j.ecoser.2020.101174

Morgan, M., Anders, S., Lawrence, M., Aboyoun, P., Pagès, H., and Gentleman, R. (2009). ShortRead: a bioconductor package for input, quality assessment and exploration of high-throughput sequence data. *Bioinformatics* 25, 2607–2608. doi: 10.1093/bioinformatics/btp450

Ohtaka, N., and Narisawa, K. (2008). Molecular characterization and endophytic nature of the root-associated fungus Meliniomyces variabilis (LtVB3). *J. Gen. Plant Pathol.* 74, 24–31. doi: 10.1007/s10327-007-0046-4

Pagès, H., Aboyoun, P., Gentleman, R., and DebRoy, S. (2022). Biostrings: efficient manipulation of biological strings. R package version 2.64.1. Available at: https://bioconductor.org/packages/Biostrings

Pehl, L., and Wulf, A. (2003). Coleophoma cylindrospora-a new needle fungus of *Tsuga canadensis*. *Nachrichtenblatt des Deutschen Pflanzenschutzdienstes* 55, 110–112.

Peñuelas, J., and Sardans, J. (2021). Global change and forest disturbances in the Mediterranean basin: breakthroughs, knowledge gaps, and recommendations. *Forests* 12:603. doi: 10.3390/f12050603

Perez-Luque, A. J., Benito, B. M., Bonet-Garcia, F. J., and Zamora, R. (2020). Ecological diversity within rear-edge: a case study from Mediterranean Quercus pyrenaica Willd. *Forests* 12:10. doi: 10.3390/f12010010

Põlme, S., Abarenkov, K., Henrik Nilsson, R., Lindahl, B. D., Clemmensen, K. E., Kauserud, H., et al. (2020). FungalTraits: a user-friendly traits database of fungi and fungus-like stramenopiles. *Fung. Divers.* 105, 1–16. doi: 10.1007/s13225-020-00466-2

R Core Team (2022). *R: A Language and Environment for Statistical Computing*. Vienna: R Foundation for Statistical Computing.

Roswell, M., and Dushoff, J. (2022). MeanRarity: hill diversity estimation and visualisation. R package version 0.0.1.0004. Available at: https://github.com/mikeroswell/MeanRarity

Roswell, M., Dushoff, J., and Winfree, R. (2021). A conceptual guide to measuring species diversity. *Oikos* 130, 321–338. doi: 10.1111/oik.07202

Ruiz-Gómez, F. J., Pérez-de-Luque, A., and Navarro-Cerrillo, R. M. (2019a). The involvement of phytophthora root rot and drought stress in holm oak decline: from ecophysiology to microbiome influence. *Curr. Forest. Rep.* 5, 251–266. doi: 10.1007/s40725-019-00105-3

Ruiz Gómez, F. J., Navarro-Cerrillo, R. M., Pérez-de-Luque, A., Oβwald, W., Vannini, A., and Morales-Rodríguez, C. (2019b). Assessment of functional and structural changes of soil fungal and oomycete communities in holm oak declined dehesas through metabarcoding analysis. *Sci. Rep.* 9, 5315–5316. doi: 10.1038/s41598-019-41804-y

Schmitt, I., Otte, J., Parnmen, S., Sadowska-Deś, A., Luecking, R., and Lumbsch, T. (2012). A new circumscription of the genus Varicellaria (Pertusariales, Ascomycota). *MycoKeys* 4, 23–36. doi: 10.3897/mycokeys.4.3545

Singh, R. K., Pandey, S. K., Singh, D., and Masurkar, P. (2019). First report of edible mushroom Pleurotus ostreatus from India with potential to kill plant parasitic nematodes. *Indian Phytopathol.* 72, 173–176. doi: 10.1007/s42360-018-0093-0

Smahi, H., Belhoucine-Guezouli, L., Franceschini, A., and Scanu, B. (2017). Phytophthora species associated with cork oak decline in a Mediterranean forest in western Algeria. *Int. Protect. Oak Forest. IOBC-WPRS Bullet.* 127, 123–129.

Stone, L. B., and Bidochka, M. J. (2020). The multifunctional lifestyles of Metarhizium: evolution and applications. *Appl. Microbiol. Biotechnol.* 104, 9935–9945. doi: 10.1007/s00253-020-10968-3

Suwannarach, N., Kumla, J., Satienperakul, K., Sungpalee, W., Sri-Ngernyuang, K., and Lumyong, S. (2020). Pleurotus sirindhorniae (Pleurotaceae, Agaricales), a new species from northern Thailand. *Phytotaxa* 460, 285–295. doi: 10.11646/phytotaxa.460.4.6

Tedersoo, L., Mikryukov, V., Anslan, S., Bahram, M., Khalid, A. N., Corrales, A., et al. (2021). The global soil mycobiome consortium dataset for boosting fungal diversity research. *Fungal Divers.* 111, 573–588. doi: 10.1007/s13225-021-00493-7

Telagathoti, A., Probst, M., Mandolini, E., and Peintner, U. (2022). Mortierellaceae from subalpine and alpine habitats: new species of Entomortierella, Linnemannia, Mortierella, Podila and Tyroliella gen. Nov. *Stud. Mycol.* 103, 25–58. doi: 10.3114/sim.2022.103.02

Venice, F., Vizzini, A., Frascella, A., Emiliani, G., Danti, R., Della Rocca, G., et al. (2021). Localized reshaping of the fungal community in response to a forest fungal pathogen reveals resilience of Mediterranean mycobiota. *Sci. Total Environ.* 800:149582. doi: 10.1016/j.scitotenv.2021.149582

Vettraino, A. M., Morel, O., Perlerou, C., Robin, C., Diamandis, S., and Vannini, A. (2005). Occurrence and distribution of phytophthora species in European chestnut stands, and their association with ink disease and crown decline. *Eur. J. Plant Pathol.* 111, 169–180. doi: 10.1007/s10658-004-1882-0

Vivas, M., Crous, C. J., Dames, J. F., van der Linde, J. A., Coetzee, M. P. A., and Roux, J. (2018). Arbuscular mycorrhizal fungi persist in dying *Euphorbia ingens* trees. *S. Afr. J. Bot.* 115, 12–17. doi: 10.1016/j.sajb.2017.12.009

Vohnik, M., Mrnka, L., Lukešová, T., Bruzone, M. C., Kohout, P., and Fehrer, J. (2013). The cultivable endophytic community of Norway spruce ectomycorrhizas from microhabitats lacking ericaceous hosts is dominated by ericoid mycorrhizal Meliniomyces variabilis. *Fungal Ecol.* 6, 281–292. doi: 10.1016/j.funeco.2013.03.006

Waldboth, M., and Oberhuber, W. (2009). Synergistic effect of drought and chestnut blight (*Cryphonectria parasitica*) on growth decline of European chestnut (*Castanea sativa*). *For. Pathol.* 39, 43–55. doi: 10.1111/j.1439-0329.2008.00562.x

Wardle, D. A., and Lindahl, B. D. (2014). Disentangling global soil fungal diversity. *Science* 346, 1052–1053. doi: 10.1126/science.aaa1185

Warnecke, L., Turner, J. M., Bollinger, T. K., Lorch, J. M., Misra, V., Cryan, P. M., et al. (2012). Inoculation of bats with European Geomyces destructans supports the novel pathogen hypothesis for the origin of white-nose syndrome. *Proc. Natl. Acad. Sci.* 109, 6999–7003. doi: 10.1073/pnas.1200374109

Yang, L., and Chen, J. (2022). A comprehensive evaluation of microbial differential abundance analysis methods: current status and potential solutions. *Microbiome* 10:130. doi: 10.1186/s40168-022-01320-0

Yang, R. H., Su, J. H., Shang, J. J., Wu, Y. Y., Li, Y., Bao, D. P., et al. (2018). Evaluation of the ribosomal DNA internal transcribed spacer (ITS), specifically ITS1 and ITS2, for the analysis of fungal diversity by deep sequencing. *PLoS One* 13:e0206428. doi: 10.1371/journal.pone.0206428

Zribi, L., Mouillot, F., Guibal, F., Rejeb, S., Rejeb, M. N., and Gharbi, F. (2016). Deep soil conditions make Mediterranean cork oak stem growth vulnerable to autumnal rainfall decline in Tunisia. *Forests* 7:245. doi: 10.3390/f7100245

Frontiers in
Forests and Global Change

Informs and promotes sustainable management of the world's forests

An innovative journal that places forests at the forefront of attention for scientists, policy makers and the public. It advances our understanding of how forests 'work', spanning from molecules to ecosystems to the biosphere.

Discover the latest Research Topics

See more →

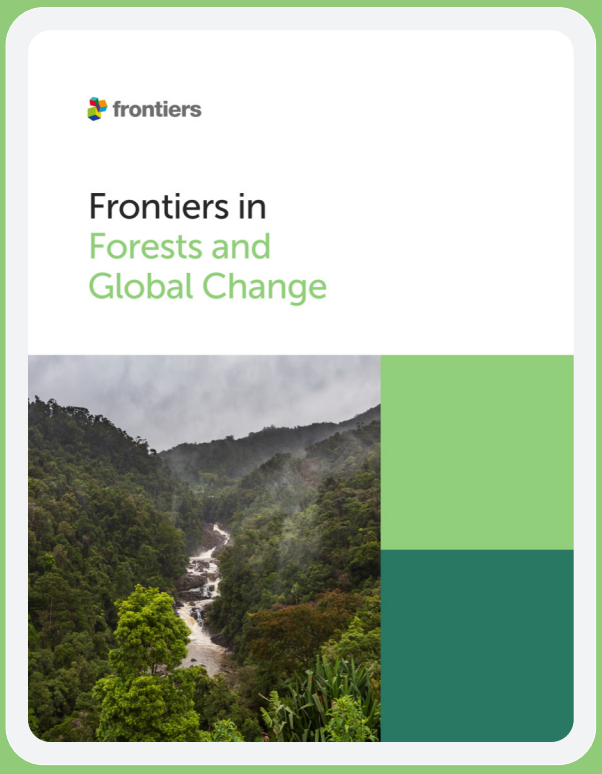

Frontiers

Avenue du Tribunal-Fédéral 34
1005 Lausanne, Switzerland
frontiersin.org

Contact us

+41 (0)21 510 17 00
frontiersin.org/about/contact